MODELLING THE CONTROL STRATEGIES FOR RIDING A MOTORCYCLE

Stuart Rowell, MEng

Thesis submitted to the University of Nottingham
for the degree of Doctor of Philosophy

July 2007

Abstract

Computer simulation models are increasingly necessary as a design tool for modern vehicles, for which a subcategory relates to motorcycles. Simulation models can be employed for a variety of applications, an important area of which relates to the motorcycle's dynamic responses. The response of a motorcycle is heavily dependent on the rider's control actions, and consequently a means of replicating the rider's actions provides an important extension to this area.

The application of mathematical control techniques for replicating the motorcycle rider's control actions is presented in this thesis, detailing specifically the techniques of optimal control and model predictive control. The work begins with modelling the dynamics of the motorcycle using standard procedures. The application of optimal control to a motorcycle rider is not new, but the available results have been extended significantly over those previously available, allowing further insights into the behaviour and therefore applicability of this strategy to modelling a motorcycle rider. Use of the model predictive control approach is new in the field of motorcycle rider modelling, and a similarly extensive parametric study is conducted to evaluate the suitability of this approach, and to highlight the similarities and differences between this and the optimal control approach.

Both controller models were simulated over a standard single lane-change manoeuvre. Comparison of the relative performances of the two control approaches confirmed strong similarities between the techniques, particularly when the modelled rider is permitted an extensive knowledge of the approaching road path to follow. When this knowledge is restricted, differences were apparent between the two, suggesting the predictive control approach is capable of better performance here, and therefore represents a more robust control strategy. An option of the predictive control approach allows more elaborate target paths for the rider to follow to be set. However,

defining the target path for the rider model to follow as the road centreline, and then permitting the controller itself to select the most appropriate course to take, has also been shown to be the more suitable option.

The predictive control technique for motorcycle rider modelling is shown to be a theoretically suitable application. Further work is suggested to validate the results presented here. If it can be confirmed that the model accurately captures a motorcycle rider's actions, this will prove a very useful tool for the understanding of a motorcycle rider's control actions, with potential benefits towards rider safety and furthermore as a design tool for the motorcycle industry.

Acknowledgements

My thanks are extended to my project supervisors, Dr. Atanas Popov and Dr. Jacob Meijaard at the University of Nottingham. Throughout the project they have always been approachable and willing to provide assistance, information and suggestions whenever necessary. Their wealth of knowledge is something to aspire to, and has many times been a source of guidance and insight.

Gratitude must also be given to the Engineering and Physical Sciences Research Council, who provided the funding necessary for this project.

Finally, the support of my fellow students should not go unmentioned; John Coultate, for the instigation of many much needed coffee breaks; Mark Robinson, regular provider of both the afternoon crossword and general humour in the office; Paul Houlston, who has always been willing to share his knowledge to help others on request; and to Chris Larmer, Paul Baalham and Robin Elliot for providing welcome conversations away from the topic in hand.

Contents

List of Figures

List of Tables

Nomenclature

Variables:

a	Distance, perpendicular from steer axis to motorcycle origin
b	Distance, motorcycle origin to rear tyre contact patch
c	Distance, perpendicular from steer axis to front wheel centre
c_b	Generic body damping coefficient
c_δ	Steer damper coefficient
$c_{r,f}$, $c_{r,r}$	Radius, to centre of tyre torus; front, rear tyre
e	Distance, perpendicular from steer axis to front frame mass centre
e_i	Error, predicted controlled output to reference path, i^{th} preview point
$\mathbf{e}$	Error vector, predicted controlled output to reference path, complete preview
f	External force (singular) on a body
$f(x)$	Generic function in terms of generic variable x
$\mathbf{f}$	Tyre forces vector
g	Gravitational constant
h_f, h_r	Height, frame mass centre; front, rear frame
i_p	MPC prediction step number
j	Integer index $1, \ldots, n$
k	Iteration number
$\mathbf{k}$	Controller gain vector for a generic system
k_b	Generic body stiffness coefficient
$k_{s,y}$	Lateral position state gain
l_r	Exponential path relaxation length

m	Number of controlled outputs
m_b	Generic body mass
m_1	Front frame assembly mass (inc. front wheel)
m_2	Rear frame assembly mass (inc. rear wheel)
n	Number of motorcycle states
p	Number of controller inputs
$\mathbf{p}$	Augmented vector state
$\mathbf{q}, \dot{\mathbf{q}}, \ddot{\mathbf{q}}$	Vector of generalised coordinates, velocities, accelerations
q_1	Lateral position cost function weighting parameter
q_2	Yaw angle cost function weighting parameter
r	Steer torque cost function weighting parameter
r_t	Toroidal radius of tyres
s_n	Generic tyre normal spin
s_{lat}	Generic tyre non-dimensional lateral slip ratio
s_{long}	Generic tyre non-dimensional longitudinal slip ratio
s_{tot}	Generic tyre non-dimensional total slip ratio
t	Sample time
u	Control input (single)
$\mathbf{u}$	Control input (vector)
$\tilde{\mathbf{u}}$	Small step change in $\mathbf{u}$
v	Linear forward speed
$\mathbf{v}$	Linear velocity vector
x, $x(t)$	Longitudinal position
$\dot{x}$, $\frac{\partial x(t)}{\partial t}$	Longitudinal velocity
$\mathbf{x}$	Generic system state vector
$\tilde{\mathbf{x}}$	Small step change in $\mathbf{x}$
y, $y(t)$	Lateral position
$\dot{y}$, $\frac{\partial y(t)}{\partial t}$	Lateral velocity
$\mathbf{y}$	Generic system output vector
y_f	Lateral position of MPC reference path
y_g	Motorcycle lateral position in global coordinates
y_{l_i}	Road point lateral position in local coordinates, i^{th} preview point
y_n	New motorcycle lateral position in local coordinates

y_r	Road point lateral position in global coordinates
$\mathbf{y}_f$	Vector of MPC reference path
$\mathbf{y}_g$	Road preview vector, global coordinates
$\mathbf{y}_l$	Road preview vector, local coordinates
$\mathbf{y}_r$	Road preview vector
$\mathbf{y}_{rn}$	Road preview vector, new information into shift register
z	Vertical displacement
$\mathbf{z}$	Combined motorcycle–preview state vector

$\mathbf{A}$	Combined motorcycle–preview A-matrix
$\mathbf{A}_f$	Reference path state space shift-register A-matrix, linear path
$\mathbf{A}_g$	Reference path state space shift-register A-matrix, global coordinates, states component
$\mathbf{A}_l$	Reference path state space shift-register A-matrix, local coordinates, states component
$\mathbf{A}_n$	Reference path state space shift-register A-matrix, local coordinates, global position component
$\mathbf{A}_p$	Preview state space shift-register A-matrix
$\mathbf{A}_r$	Reference path state space shift-register A-matrix, linear error reduction path, set path component
$\mathbf{A}_s$	Reference path state space shift-register A-matrix, linear error reduction path, states component
$\mathbf{B}$	Combined motorcycle–preview B-matrix
$\mathbf{B}_f$	Reference path state space shift-register A-matrix, linear reference path
$\mathbf{B}_p$	Preview state space shift-register B-matrix
$\mathbf{C}$	Combined motorcycle–preview C-matrix
$\mathbf{C}_b$	Damping matrix, generic system
C_α, $C_{\alpha,f}$, $C_{\alpha,r}$	Tyre stiffness, with sideslip; generic, front, rear tyre
C_γ, $C_{\gamma,f}$, $C_{\gamma,r}$	Tyre stiffness, with camber; generic, front, rear tyre

C_l, $C_{l,f}$, $C_{l,r}$	Ratio of tyre stiffness to normal force, with cornering; generic, front, rear tyre
$\mathbf{D}$	Combined motorcycle–preview D-matrix
$\mathbf{E}_M$	Euler Matrix
$\mathbf{F}$	Prediction model state space system matrix relating to system states for a generic system
F_{lat}	Lateral force, generic tyre
F_{long}	Longitudinal force, generic tyre
F_n	Normal force, generic tyre
F_y, $F_{y,f}$, $F_{y,r}$	Lateral tyre force, steady state; generic, front, rear tyre
$\mathbf{G}$	Prediction model state space system matrix relating to system inputs for a generic system
$\mathbf{G}_1$, $\mathbf{G}_2$	Coordinate vector, frame mass centre; front, rear
$\mathbf{H}$	Hamiltonian vector
$\mathbf{I}_i$	Identity matrix, dimension i
I	Moment of Inertia, about single axis
$\mathbf{I}$	Generic inertia matrix
$I_{f,xz}$	Moment of inertia, front frame xy-axes cross couple
$I_{f,x}$	Moment of inertia, front frame about x-axis
$I_{f,y}$	Moment of inertia, front frame about y-axis
$I_{f,z}$	Moment of inertia, front frame about z-axis
$I_{r,x}$	Moment of inertia, rear frame about x-axis
$I_{r,y}$	Moment of inertia, rear frame about y-axis
$I_{r,z}$	Moment of inertia, rear frame about z-axis
$I_{r,xz}$	Moment of inertia, rear frame xy-axes cross couple
$I_{fw,x}$	Moment of inertia, front wheel about x-axis
$I_{fw,y}$	Moment of inertia, front wheel about y-axis
$I_{fw,z}$	Moment of inertia, front wheel about z-axis
$I_{rw,x}$	Moment of inertia, rear wheel about x-axis
$I_{rw,y}$	Moment of inertia, rear wheel about y-axis
$I_{rw,z}$	Moment of inertia, rear wheel about z-axis
J	Cost function value
$\mathbf{J}_{EM}$	Jordan form of Euler matrix
$\mathbf{J}_{ij}$	Partitioned components of J_{EM}

$\mathbf{J}_f$	Jacobian matrix of tyre force equations with respect to the state vector
$\mathbf{J}_s$	Jacobian matrix of motorcycle equations of motion with respect to the state vector
$\mathbf{J}_u$	Jacobian matrix of motorcycle equations of motion with respect to the input vector
$\mathbf{K}$	Gain matrix, generic system
$\mathbf{K}_b$	Stiffness matrix, generic system
$\mathbf{K}_p$, $\mathbf{K}_2$	Preview gains vector
$\mathbf{K}_s$, $\mathbf{K}_1$	State gains vector
$K_{n,f}$, $K_{n,r}$	Tyre Stiffness, normal to surface; front, rear tyre
M	Generic tyre moment about z-axis
$\mathbf{M}$	Prediction model state space outputs matrix relating to system states for a generic system
$\mathbf{M}_b$	Mass matrix, generic system
N_p	Discrete number of preview points
N_u	Discrete number of control points
$\mathbf{N}$	Prediction model state space outputs matrix relating to system inputs for a generic system
N	Number of iterations of full simulation
$\mathbf{P}$	Algebraic Riccati equation solution
$\mathbf{P}_{ij}$	Partitioned components of $\mathbf{P}$
$\mathbf{Q}$	Cost function output weighting matrix
$\mathbf{R}$	Cost function input weighting matrix
R_w, R_f, R_r	Rolling radius; generic, front, rear tyre
$\mathbf{R1}$	Rotation matrix, yaw
$\mathbf{R2}$	Rotation matrix, roll
$\mathbf{R3}$	Rotation matrix, steer
$\mathbf{Reta}$	Rotation matrix, front fork inclination
$\mathbf{S}_Q$	Square root of $\mathbf{Q}$
$\mathbf{S}_R$	Square root of $\mathbf{R}$
T	System kinetic energy
T_p	Preview horizon time
T_u	Control horizon time

T_w	Dead-time horizon time
$\mathbf{T}$	System modal matrix
$\mathbf{T}_{ij}$	Partitioned components of $\mathbf{T}$
$\mathbf{T}^*$	Inverse of $\mathbf{T}$
$\mathbf{T}^*_{ij}$	Partitioned components of $\mathbf{T}^*$
U	Potential energy
$\mathbf{W}$	Virtual power of external forcing
Y_f, Y_r	Dynamic lateral tyre force; front, rear tyre

α	Tyre sideslip angle
γ	Tyre camber angle
δ, $\delta(t)$	Motorcycle steer angle
$\dot{\delta}$, $\frac{\partial \delta(t)}{\partial t}$	Motorcycle steer rate
ϵ_{eq}	Ratio of camber stiffness to cornering stiffness, advanced tyre
$\boldsymbol{\varepsilon}$	Error vector, reference path to predicted uncontrolled output, complete preview
η	Front fork inclination angle
θ	Function of final states and inputs in controller cost function
$\boldsymbol{\kappa}$	Predictive controller gains matrix
$\boldsymbol{\lambda}$	Lagrangian multiplier
μ_w, μ_f, μ_r	Friction coefficient; generic, front, rear tyre
ρ_f, ρ_r	Toroidal tyre radius; front, rear tyre
σ_f, σ_r	Relaxation length; front, rear tyre
ϕ, $\phi(t)$	Motorcycle roll angle
$\dot{\phi}$, $\frac{\partial \phi(t)}{\partial t}$	Motorcycle roll rate
ψ, $\psi(t)$	Motorcycle yaw angle
$\dot{\psi}$, $\frac{\partial \psi(t)}{\partial t}$	Motorcycle yaw rate
ψ_f	Reference path yaw angle
ψ_g	Motorcycle yaw angle, global coordinates
ψ_{l_i}	Road point yaw angle in local coordinates, i^{th} preview point
ψ_n	New motorcycle yaw angle, local coordinates

ψ_r	Road point yaw angle in global coordinates
ω	Angular velocity, single rotation
$\boldsymbol{\omega}$	Angular velocity vector
χ	Vector of predicted future state vectors
φ	Vector of predicted future output vectors

Δ	Small step change in a variable
Θ	Function of states and inputs in controller cost function
Υ	Vector of predicted future input vectors

Abbreviations:

OC	Optimal Control
MPC	Model Predictive Control
ARE	Algebraic Riccati Equation
DOF	Degree(s) of Freedom
ISO	International Standardizations Organization
SAE	Society of Automotive Engineers
VRML	Virtual Reality Modelling Language

General Notations

- $\hat{}$ above a scalar, vector or matrix indicates a predicted value
- subscript v after a scalar, vector or matrix indicates specific reference to the motorcycle model

Chapter 1

Introduction

With increasing frustration due to road traffic congestion and growing concerns over environmental issues, transport remains an area in which alternatives are constantly being sought and questions raised about the viability of large multi-seat motor vehicles, often with only a driver aboard, travelling on the roads everyday. Prototype vehicles using advanced power sources, or employing expensive high-grade materials have been proposed, yet amongst all this concern, there exists already a form of motorised transport which seems much more suitable to single-occupant journeys and could therefore help to alleviate some of the current concerns.

The popularity of motorcycles has seen a steady increase in recent years, with annual sales rising from 93,289 in 1997 to 133,938 at the end of 2004 [55]. In recognition of the increasing relevance of motorcycles as a viable transport option, the Government launched the UK's first National Motorcycle Strategy in 2005, covering topics including environmental issues, infrastructure, and safety. The European Agenda for Motorcycle Safety [30] had covered similar areas a year previously.

The motorcycle as a form of transport has a much smaller impact, both on the road due to dimensional size, and on the environment, due to smaller engines and physical mass. A recent DEFRA (Department for Environment, Food and Rural Affairs) report [22] provided some useful statistics on vehicle CO_2 emissions (Table 1.1), confirming the lower environmental impacts of motorcycles compared with other forms of motorised transport.

Furthermore, the greater manoeuvrability of motorcycles, particularly in traffic, means

less time spent static in queues with the engine still running, and thus a more efficient journey. The vast majority of commuting journeys are made with minimal luggage, and therefore the limited storage space associated with motorcycles should not, in the main, be a hindrance. Despite some impracticalities, the use of motorcycles and scooters is more widespread in mainland Europe (Figure 1.1), quite possibly on account of more conducive weather, though the numbers are still relatively low.

A more important issue that may influence the use of motorcycles concerns safety. Relatively speaking, motorcycles are not a safe form of transport. In the years 1994–2005, they accounted for between 13% and 21% of deaths and serious injuries on UK roads (Table 1.2), despite making up only around 2% of the total traffic by numbers. This is in main due to the fact that when an accident occurs a motorcycle rider lacks the protective structures and safety features afforded to car drivers. Furthermore, the more complicated rider strategy required to control a motorcycle, the relatively greater instabilities, and the smaller visual impact of motorcycles relative to cars mean that motorcycle riders, and in particular inexperienced riders, are, in general, at greater risk of accidents in the first place. Collectively, these have prompted Government action [23], with the safety strategy document setting a target to reduce the number of people killed or seriously injured by 40 % by 2010. A greater understanding of the riding strategy and requirements of motorcycle riders could therefore provide useful information both for rider training, road infrastructure, and also potentially in the development of electronic rider aids that could assist the rider's control.

A range of motivations for computer simulation methods were outlined in [87]. From a more commercial perspective, motorcycle manufacturers, as with any industry, constantly strive to make their product more appealing to the customer, whose decision will be influenced by a number of factors. Some of these will be objective, such as cost or comfort of riding, a greater number may be more subjective, for instance visual styling or riding qualities. In order to develop a better product, it is useful to have some understanding of the more subjective elements, and if possible develop means of quantifying these in a more defined, mathematical way.

Historically, these subjective qualities could only be assessed by the development of physical prototypes which would be extensively assessed by test riders, who would give feedback to the design departments. The development of such prototypes and the necessary testing is both financially and time intensive. Customers will always desire

more for less, and consequently manufacturers must find ways to achieve this if they are to remain in business. Thus, the product must be better, yet the customer does not always expect to pay a premium for this. Furthermore, manufacturers are aiming always to reduce their time-to-market, such that they can respond more readily to either the market needs or potential threats from products offered by their rivals.

The widening use of computer simulation methods has enabled these requirements to be met; modern computer systems are now relatively cheap, can be run all day and every day if needed, negate the need for expensive and time-consuming prototype development, and can generate vast quantities of data in a relatively short time.

There is therefore an increasing need for accurate simulation tools to aid in the motorcycle design process, and indeed these can and have been employed for modelling various aspects of the motorcycle's design. Of the constituent elements of the whole process, the most difficult element to model concerns the rider, and the simulation of his or her control actions.

Compared with a twin-track vehicle such as a car, a motorcycle requires a greater degree of involvement from the rider, requiring control both to guide the motorcycle and to remain upright at low speeds while riding. Furthermore, the control process of the rider involves control via both the steering system and through the influence of body weight movement on the machine. Consequently, this makes the modelling of motorcycle riders a less straight-forward problem. Because the riding process is a more demanding task, it therefore becomes more important to consider the implication of design changes on the ability of a rider to control the machine, and to assess how the rider may need to adjust his control actions in light of the motorcycle's characteristics. Advanced simulation tools will facilitate this process and therefore have also potential commercial benefits.

1.1 Motivation

As a result of the statistics and information provided, the suitability of motorcycles has and will for some time to come be debated by those either in favour or against them, and the aim here is not to fuel the debate further. Rather, the objective here is to consider how engineering research work can be applied to the greater good of

motorcycle knowledge, understanding and design.

The motivation for this research work is to develop motorcycle rider simulation tools. These will enable a simulated motorcycle to be manoeuvred along a set course, that could therefore be employed as a design tool for future motorcycles, or to assist in the modifications of existing machines. Furthermore, development of rider models may provide a useful insight into the control strategies employed by motorcycle riders, which could find use in improving road safety for motorcycle riders.

The last two decades in particular have seen the development of a number of vehicle handling control systems, including anti-lock braking systems, electronic stability control and active suspensions. Almost universally, these systems apply to twin-track vehicles. It is suggested that this, in the most part, is as a result of the relatively simpler control strategy for twin-track vehicles and thus the relatively more simple procedures for developing the necessary computer code to define the strategies of these systems. It is therefore also proposed that the development of motorcycle rider control models may find use in the subsequent development of electronic motorcycle chassis enhancement systems.

1.2 Tables

Vehicle Type	Size Label	gCO_2/km
Petrol Car	Small	159.2
	Medium	188.0
	Large	257.7
Hybrid petrol-electric	Medium	109.7
	Large	194.7
Motorcycle	Small	72.9
	Medium	93.9
	Large	128.6

Table 1.1: Average CO_2 emissions by vehicle type, [22]

	Killed				Killed and Seriously Injured			
	1994-98	2003	2004	2005	1994-98	2003	2004	2005
Car Occupants	49.25	50.43	51.88	52.33	48.80	46.46	47.00	45.46
Motorcyclists	13.05	19.75	18.16	17.78	13.59	20.56	19.35	20.24
Cyclists	5.20	3.25	4.16	4.62	7.83	6.48	6.72	7.34
Pedestrians	28.17	22.06	20.83	20.96	24.49	21.32	21.77	22.17
Others	4.33	4.50	4.97	4.31	5.30	5.18	5.16	4.79
All Road Users	100.00	100.00	100.00	100.00	100.00	100.00	100.00	100.00

Table 1.2: Accident statistics, percentages by road user type, [23]

1.3 Figure

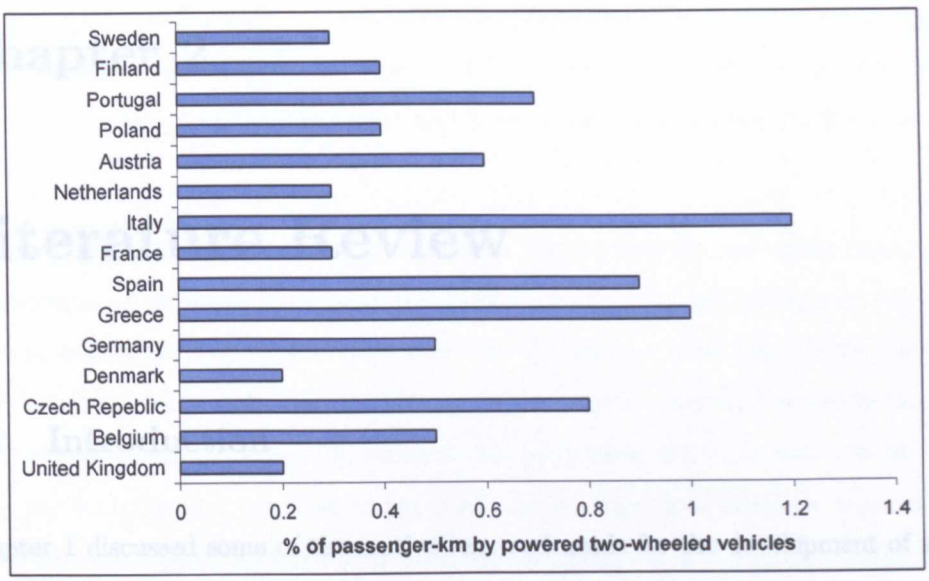

Figure 1.1: Comparative use of motorcycles in the major European countries, [27]

Chapter 2

Literature Review

2.1 Introduction

Chapter 1 discussed some of the motivations and needs for the development of simulation and analysis methods with reference to motorcycles. The ability to replicate realistically a number of physical features, characteristics and phenomena associated with dynamic systems can have significant bearings upon their design, manufacture and understanding to ultimately improve the effectiveness of the modelled system.

With specific reference to a motorcycle and rider, in order to generate a realistic simulation model, the process must be formed by the combination of a number of systems. Broadly, these systems comprise the modelling of the dynamic response of the motorcycle, the correct modelling of the tyre behaviour and the manner in which the rider operates in order to control the motorcycle. These systems themselves consist of a number of smaller subsystems, and thus in total a combined motorcycle–rider simulation model may have a vast array of variables that ultimately affect the performance of the model.

The dynamic response is clearly heavily influenced by the structural properties of the motorcycle. These structural properties include both the geometric dimensions of the motorcycle's construction, and the physical stiffness and damping properties of the motorcycle's components. Additionally a number of other factors may also be relevant, for example the addition of external mass in the form of luggage or a pillion passenger.

The forces acting on the motorcycle will have a significant influence upon the vehicle behaviour, and come from a number of sources. These can include aerodynamic forces, the forces exerted by the rider, but perhaps most fundamentally the forces exerted by the interaction of the tyres with the ground. These forces primarily influence the direction of the motorcycle's motion, but also play a significant role in the stability characteristics of the motorcycle. Additionally, a number of other sources of forcing, such as acceleration or braking forces, will have an impact upon the condition of the vehicle.

Finally the influence that the rider has upon the motorcycle, assuming that limit conditions for tyre forces or stability conditions are not exceeded, ultimately dictates the response of the motorcycle. The rider has influences on the motorcycle due not only to the direct forces that are applied to the motorcycle controls, but also indirectly as a consequence of the structural influence his body mass and body movements have upon the stability and response of the motorcycle. This final influence is far more prevalent for a motorcycle than with a car, for example, where the driver's body mass is virtually static with regard to the vehicle.

The combination and interaction of all these factors determine the stability and handling characteristics of the motorcycle and how the motorcycle may respond to a rider's control actions. As a consequence, a vast array of research work has been conducted in the fields of motorcycle stability, tyre modelling, rider analysis and the combination of all to form advanced motorcycle–rider simulation models, which can ultimately be used to improve the performance of a real motorcycle and rider through better design, manufacture and understanding of the physical characteristics.

This chapter will therefore outline the significant research work conducted in and around these areas, exploring the opportunities that exist for novel research work in the field of motorcycle–rider control. Section 2.2 gives an outline of the historical research into motorcycle behaviour, focusing primarily on the modes of motion and the instabilities of motorcycles, considering both the detailed modelling of motorcycle as a physical structure and how the identified modes of motion are influenced by design features of the motorcycle. Tyre modelling will be covered in Section 2.3, as this has a significant influence upon the motorcycle responses and modes that will be covered in the first section. These two sections provide important background knowledge to the main review in Section 2.4, which will focus on the rider's control of the motorcycle,

and the work that has been conducted previously for both the understanding of a motorcycle rider's control process and subsequently in the modelling of these control actions to form simulation models of motorcycle riders.

2.2 Motorcycle Stability Analysis

The analysis of a motorcycle's response characteristics has been investigated by a number of authors, with ever more complex multi-body dynamics models appearing regularly. The earliest studies considered bicycle models, being simplified motorcycle models without, for example, the inclusion of suspension characteristics.

Whipple was one of the earliest authors to produce stability analysis models of a bicycle [106]. His work resulted in the equations of motion for a bicycle, including rider control inputs, and also identified some of the classic instability modes of bicycles and motorcycles, subsequently to be coined as the weave and capsize modes. Other early authors on the subject, with similar objectives and results, included Bower [8] and Dohring [24]

With more specific reference to motorcycles, being the subject of this thesis, it was not until the early 1970's that the area begin to receive significant attention with the emergence of greater research work. Of these, Sharp was one of the first, producing work of a similar nature to the work of Whipple many years earlier, but focused more specifically on motorcycle research.

Sharp [80] generated the linearised equations of motion for a bicycle model representation of a motorcycle, also exploring the fundamental modes of motion for a motorcycle, which were identified as wobble, weave and capsize modes, terms since adopted almost universally. His inclusion of a tyre model, not a feature in [106], also resulted in the identification of a new mode, termed weave.

Capsize was identified as a non-oscillatory instability related to the tendency of the motorcycle to fall onto its side like an inverted pendulum. Wobble was defined as the high frequency oscillation of the front steering system in a shimmy motion, often compared with that of a shopping trolley wheel. Finally, the weave mode was identified as a combined oscillation involving simultaneous roll and yaw of the motorcycle, such that the motorcycle followed a high-frequency slalom-like trajectory.

A parameter study was conducted using the model as a means of identifying the qualities required to produce stable motorcycles. Sensing the possibilities of the approach as a potential design tool, several research works aimed to develop the techniques used for more advanced motorcycle models, exploring further aspects of motorcycle design and their respective influences upon the motorcycle's behaviour.

Related works by Kane [42] and Sharp [81] investigated the influence of frame flexibility on the stability characteristics, with each author modelling the flexibility in subtly different ways. Both research works found significant influence of frame flexibility upon the stability characteristics of the motorcycle, while Kane also included the influence of mass distribution and front fork trail.

In a similar vein, the effects of front fork flexibilities upon motorcycle behaviour were assessed by Roe [75], leading to the proposal of a new front fork design idea which, following extensive testing, was found to provide superior stability characteristics.

Over subsequent years a number of researchers continued to investigate the influences of various structural elements of the motorcycle, leading to increasingly complex structural models of a motorcycle. Notable authors included Sharp [83, 84, 85], Cossalter and his co-workers [16, 17, 21] and Nishimi [66].

In parallel with research work to investigate further structural aspects of the frame stiffness, it was natural that the most compliant structural element of the motorcycle, namely the suspension, should also be included in the models. Jennings [40] was one of the first to explore this avenue, followed soon after with further work by Sharp [82].

Other aspects influential upon the motorcycle's stability characteristics were also worthy of investigation. The effects of aerodynamic forces on moving bodies were already well appreciated as a result of aerospace research work and physical experiences. Fundamental effects on motorcycles were suspected, but not fully understood, and so at around the same time that structural influences on motorcycle behaviour were being explored, the influence of aerodynamic properties upon the stability modes of motorcycles was investigated by Cooper [12], also later covered in Foale [31] and Hucho [36].

Earlier works had hinted towards the importance of mass distribution with regard to

the stability modes, and the inclusion of accessories such as luggage racks on the rear of a motorcycle could clearly have a significant impact upon this. Research of this area was addressed by Otto [67].

Cornering, acceleration and deceleration were known by experience to change a motorcycle's dynamic characteristics. Koenen [45] completed research work into the dynamic behaviour of motorcycles, for both straight running and cornering conditions. While resonant vibrations of the motorcycle and, in particular the steering system, are undesirable, the impact of vibrational modes is somewhat less dangerous in a straight running situation than in a cornering condition; the steer torques and frequencies associated with such vibrational modes make it very difficult for a rider to overcome them, and in a cornering situation this severely impacts upon a rider's ability to apply any necessary steer control with potentially disastrous consequences.

Since mass distribution was known to have an effect upon the stability of the motorcycle, it seemed logical that acceleration and deceleration would cause a dynamic weight shift and therefore have some impact upon the motorcycle's response. During cornering the tyre contact patch moves significantly around the tyre's cross-section, additional external forces are introduced, and the geometry of the motorcycle is affected due to relative movements of the front and rear frames by the steer angle. Limebeer et al. [48] investigated the acceleration/deceleration case, extending the earlier stability models of Sharp to include these effects, finding theoretical results consistent with riding experiences. The results were also presented in [28].

The braking case was also considered in detail by Meijaard and Popov in [56], and later extended to include suspension deflection, aerodynamic drag and stabilising rider control in [59]. Extensive studies considered the implications on motorcycle stability for varying proportions of front and rear brake force distribution, and the cases of a locked front or rear wheel.

It was already well known that the rider could have a significant influence on the motorcycle by the movement of his body weight on the machine. Early research work had simplified the analysis by considering the rider as a rigidly attached body, but with greater understanding of a motorcycle's principal stability characteristics, it became apparent that this factor ought to be considered in some detail.

A considerably more advanced model was therefore developed by Nishimi et al. [66],

extending earlier models to include flexibilities of the motorcycle rider upon the motorcycle, specifically a lateral freedom of the rider's lower body to move his position on the seat, and a rotation of the upper body relative to the lower body about a longitudinal axis, representative of the rider leaning on the motorcycle.

The influence of the rider's upper body mass upon the stability of the motorcycle was considered further by Sharp and Limebeer [93]. The rider was allowed a roll freedom relative to the rear frame and also a yaw freedom. Roll freedom had already been considered by Katayama et al. [43]. However, it was postulated that when a rider senses excessive levels of steering oscillation, such as the onset of a wobble or weave instability, there is a tendency for the rider's upper body to tense in an attempt to control the oscillations, leading to a yaw motion of the riders upper body fed by the steering oscillations. The responses to initial steer disturbances were modelled, analysing the stability modes that resulted.

The ever-developing capabilities of computer simulations extended the range of possibilities for parameteric investigations further. Consolidating his earlier stability analysis work, Sharp [85] revisited the problem, modelling the motorcycle dynamics through the use of symbolic software programs. The results from these new investigations agreed with findings in earlier work, and reconfirmed that amongst the most important parameters in motorcycle design were the mass centre location of the rear frame and its distance to the front and rear wheels, and the tyre relaxation length.

An eleven degree-of-freedom model was developed by Cossalter and Lot [18], with the model described through the use of direct mathematical modelling as opposed to the use of commercial dynamics analysis software. Reasons for this choice included the ability to more realistically model the complexities unique to motorcycles such as tyre forces at high wheel camber angles. The modelling incorporated a detailed tyre model including a complex shape definition and the consideration of tyre deformation under loads.

Earlier work in motorcycle analysis had been used to study the straight running stability of motorcycles, and the classic instability modes of capsize, wobble and weave considered. Apart from [45], previous works had not included the investigation of cornering modes, with particular difficulties surrounding mainly the question of correctly modelling the tyre characteristics in a cornering condition. Cossalter et al.

[20] therefore also developed his earlier work and used modal analysis to model the stability of the motorcycle for both straight running and cornering behaviour. The modal analysis consisted of calculation of the steady-state conditions, linearisation of the equations, finally the solution of the eigenvalue problem.

While the vast majority of motorcycle simulation work was conducted with regard to road-going machines, James [39] also presented the stability behaviour of an off-road motorcycle through the use of experimentations on an instrumented motorcycle and an analytical simulation model.

Finally, an extensive benchmarking of Whipple's [106] bicycle model was conducted by Meijaard et al. [62], providing both an extensive review of the bicycle stability literature, and the linearised equations of motion of Whipple's model.

This literature review, covering here published work on motorcycle stability characteristics, is by no means exhaustive. The great wealth of work already covered should be apparent, and the extent to which the level of motorcycle stability modelling has now advanced. This review has intended to cover only some of the more relevant findings in this area in order to provide the necessary background information, and to guide the reader toward sources of greater detail in this area.

2.3 Tyre Modelling

Since the tyre forces represent the primary external forcing on the motorcycle–rider system, and therefore play such a fundamental role in the stability characteristics of the motorcycle, a realistic representation of the tyre's characteristics is an essential component of the complete modelling.

Experimental studies of vehicle tyres have highlighted the non-linearity of the forces generated as a function of slip and camber, although within the range of moderate slip ratios, linear models can be used without significant loss of accuracy for the modelling of motorcycle dynamic response. However, with increased complexity of motorcycle models, and with increasing demands to understand the absolute performance characteristics, more realistic non-linear tyre models have been sought.

De Vries and Pacejka [100] considered the impact of tyre modelling upon the stability

of a motorcycle, employing both a relatively simple first-order relaxation model based on lateral velocity and tyre sideslip, and a more complex rigid ring tyre model. Both models were compared against a dynamic tyre test on a rotating drum, and both subsequently applied to a simple bicycle model. For moderate speeds and manoeuvres, the simpler tyre model was seen to give acceptable performance, showing any weakness only at high speeds by not accounting for the gyroscopic effects of the mass of the tyre belt.

Cossalter and his collaborators have presented a number of papers on the detailed modelling of motorcycle tyre geometries and the resulting forces [16, 17, 18]. These led to more detailed definitions of tyre contact patch locations for a cambered tyre, and the forces and moments that are generated as a result, allowing a move away from disc-model tyres that had been used previously.

The significant influence of tyre characteristics in respect of scooter and motorcycle handling was the subject of further investigations by Cossalter et al. [19], comparing the characteristics for a range of different tyre types. The lateral force due to wheel camber was seen to be a more significant lateral force provider than pure sideslip, with the most interesting point to arise from the tests conducted being the observation of the importance of twisting (steer) torques resulting from the cambering of, in particular, the front wheel, and of the effects that this steer torque can have upon the handling characteristics of the motorcycle. This was a factor that had not been considered in previous studies, for example [104], in attempting to assess the requirements of a motorcycle with good handling qualities as perceived by the rider.

An area of particular difficulty yet of great importance concerns the consideration of the tyre forces generated by the parallel processes of lean and side-slip. The "Magic Formula" method [68] had been shown to produce very good analytical representations of the non-linear tyre forces, and so the inclusion of this method into a more complete motorcycle analysis was desirable. However, the complexity of the calculations involved, and the task of determining the formula's parameter values through experimentation, made this task computationally very demanding. Sharp and Bettella [91] therefore looked at a normalisation of parameters approach as a means of reducing the complexity of the task and hence making the integration of the "Magic Formula" method into a complete model more feasible.

The "Magic Formula" tyre model was implemented on a motorcycle simulation model and compared against both a more simple tyre model and experimental data by Tezuka et al. [97]. The simple tyre model comprised a carpet plot model, generating the necessary tyre forces and moments from the interpolation of a data set of experimental tyre test results. The two tyre models were applied to a eight-bodied motorcycle model, simulated in a steady turn. An instrumented motorcycle and rider was tasked with the same manoeuvre, and the results compared. For straight running, the 'Magic Formula' method showed superior correlation to the experimental results, while cornering produced similar results from both methods.

Sharp et al. [92] also combined tyre geometry models by Cossalter and his co-workers [16, 17, 18] with the application of the "Magic Formula" tyre model [68]. The tyre model that resulted was extensively validated against available test data for modern high performance front and rear motorcycle tyres. Furthermore, a monoshock rear suspension arrangement and rider upper body lean freedom was included in the motorcycle dynamics model, resulting in an advanced motorcycle dynamics model.

Meijaard and Popov produced a number of research papers developing advanced tyre simulation models. [58] developed a string model of a motorcycle tyre, allowing for deflections of the string elements both laterally and longitudinally to develop lateral and longitudinal tyre forces with lateral and longitudinal slip and with camber of the tyre. Later tyre models by the same authors [61] defined the tyre contact as a deflected point of the tyre carcass and developed the tyre forces via a simplified representation of the full "Magic Formula", seen to capture the response of the full "Magic Formula" with some accuracy.

A number of research papers have considered the modelling of twin-track vehicle tyres, a good deal fewer consider the greater complexity of a motorcycle tyre with its far more extensive use of camber thrust as a lateral force generator. For a more general understanding of tyre force generation, [31] and [13] also provide an excellent introduction.

2.4 Rider Control

The previous research areas considered were largely concerned with understanding the dynamic response of the motorcycle alone. The aim of this thesis will be focused more towards an understanding and representation of the rider as a controller. However, the rider's control actions will clearly be influenced by the way in which the motorcycle will respond to his control inputs, and so the preceding references all provide vital background knowledge.

The task at hand, however, is the understanding of the rider's control characteristics. This will concern the rider's active control characteristics and the use made of sensory information in selecting a control input, which is clearly a fundamental requirement in the development of a realistic motorcycle–rider model.

2.4.1 Visual Perception

The inputs that a rider applies to the steer controls of a motorcycle are based upon his interpretation of the approaching road that he is tasked with following, and his knowledge and understanding of the motorcycle's response. Clearly the visual perception part is a fundamental requirement in order to accomplish the task, and so a relevant branch of research work concerns the understanding of a motorcycle rider's interpretation of his visual horizon. Observations made by Miyamaru et al. [65] had hinted at the effects that correct modelling of a rider's visual road perception could have upon the ability of a rider control simulation. Identifying the link between visual input and control decision is not an easy task to do; primarily, determining exactly what the rider is looking at, and what proportion of the observed road information is stored and how much is discarded, is not readily obtained.

Donges [25] attempted to address this question, investigating the manner in which the driver perceives the road ahead and uses this information in the control task. The presented theoretical model consisted of a two-mode control strategy, with the future direction of the vehicle influenced by the distant preview (guidance) information and the more immediate preview information, termed stabilisation information, used to stabilise the vehicle motions resulting from the guidance control. Both control strategies were considered to act in parallel.

An experimental simulation was set up, in which drivers were tasked with following a randomly curving track using a driving simulator. A mathematical control strategy to replicate the driver's road perceptions and control actions was compared with the experimental results, comprising an anticipatory open-loop control and a compensatory closed-loop control element. The former represented the guidance information as a feedforward controller, while the latter represented the stabilisation information as a multiple input, single output feedback controller.

Comparisons between the actual drivers and the mathematical control strategy showed similar results, with the control strategy able to anticipate forthcoming changes in roadway curvature and to begin to alter the steering input in advance of that curvature, as would a real driver. The pertinent findings of this research were that a driver's visually-influenced control actions are based on both distant and near preview observations to control fully the heading and attitude of a vehicle.

In a similar study, Land and Horwood [47] also used a simulated road preview, with defined road edges, for experimental drivers to attempt to follow. By varying the extent of the approaching road visible by the test driver, the effect on the driver's control task of the previewed road information suggested, in agreement with [25], that the distant preview was used to determine the curvature of the road, while the near preview information was primarily used for controlling the position-in-lane of the vehicle.

The accuracy of the modelling of a human vehicle controller clearly relies upon the appropriate selection of information input to the driver, and so MacAdam [51] investigated the relative importance of sensory stimuli to the driver to understand which are the more important for the task of driving. The physical attributes of drivers, including the use of visual preview, adaptive control and the presence of an internal vehicle model concept, were also discussed. A control model, combining a number of sensory and physical driver control elements coupled with a vehicle dynamics model, was presented. This model was used to simulate a tyre blow-out while negotiating a double lane-change manoeuvre as an example of the model's ability to represent a human drivers' ability to conduct both planned manoeuvres and also to react to unexpected changes to the task. As a result of such modelling, a number of key features necessary for a realistic representation of a human driver were identified.

2.4.2 Rider Analysis and Modelling

With an appreciation of the complex processes that occur between information input and control output, a far greater quantity of research work has been involved with trying to understand the control procedures of a motorcycle rider and to replicate them effectively. Broadly, the work in this area can be broken into the specifically experimental work, where instrumented equipment was used to gain an insight into the control actions, and the theoretical side, in which some effort is made to replicate the rider's control actions in some computational way. Naturally, a cross-over between the two exists, in which theoretical models are compared with experimental results.

Unlike a twin track vehicle driver who relies primarily on control of the steering system, a motorcycle rider can apply control action to influence the heading direction of the motorcycle either by direct control to the steering system or to the motorcycle itself via forces and torques applied by the body to the seat, footpegs, or by body movement in order to influence the lean condition and hence heading direction of the motorcycle. A number of research works have aimed to understand the use made of these options in the control process applied by a motorcycle rider.

Weir [102] was one of the first authors to study in some detail the control procedures of a motorcycle, investigating the relationships between a number of the motorcycle's states and the principal control inputs available to the rider. The analyses suggested, for a single-loop controller, that roll control was the primary objective of the rider and was best achieved through the steer torque control input. Other good input–output relationships included heading angular rate via rider lean and roll angle via rider body lean. Control of the lateral position, as a means of stabilising the motorcycle, was poor for all control options. The results of the single-loop control strategies were extended to the multiple-loop case, where steer torque to roll angle and upper body lean to heading angle and lateral position was considered to be the most representative control strategy of a motorcycle rider. The influence of the task upon these findings was assessed by parametric variation of the motorcycle model and of the forward speed. By understanding the link between system states and control inputs, and the influence of the design parameters upon this link, the approach had potential application as a design tool to affect the perceived handling of a motorcycle.

In separate studies, Rice [74] and Weir and Zellner [103, 104] also produced useful

research findings in the attempt to understand a rider's control process. Rice experimentally measured a number of motorcycle and rider parameters for four different riders performing a lane change manoeuvre, each having identical equipment but varied levels of riding experience and physical stature. Measured parameters included yaw, roll and steer angles, steer torque and rider lean angle relative to the motorcycle. Weir and Zellner [103] meanwhile modelled the control task theoretically, allowing in a rider model both steer torque and upper body lean torque as control inputs, and using three key control strategies, comparing their theoretical findings with instrumented machines performing similar lane change manoeuvres. Like Rice, they also sought to investigate the specific requirements of a good-handling motorcycle [104], performing experimental results of a similar nature to those of Rice and again taking measurements of motorcycle states and rider control inputs.

The experimental findings of Rice suggested that rider upper body lean was a significant element of the control process, though the author was not able to define to what extent this featured. It was noted that different riders displayed different riding styles; this style included the severity of countersteer to initiate a turn, and the relative amounts of body lean, body lateral movement and steer torque control inputs. It was suggested that the relative use that the rider makes of these control options could be based either on a personal preference or as a consequence of varying levels of riding experience.

These results were mildly contradictory to the findings of Weir and Zellner [104]. As with the work by Rice, the method employed an instrumented motorcycle, here performing a constant radius cornering test and a single lane change manoeuvre, but with subtly different dimensions. Interesting observations made in these experiments suggested that for some riders the upper body lean angles relative to the motorcycle were near zero, implying that the rider remains upright relative to the motorcycle, consequently needing to apply greater levels of steer torque. This goes against the findings of Rice, though it is possible that the length of the lane change manoeuvre and the relative experiences of the rider's may have had some influence upon this. It is reasonable to assume that to complete the manoeuvre over a shorter distance a more severe turn is required, and by leaning the upper body such as to keep the upper body vertical, as Rice found, there will be a force applied to the machine that will tend to help to lean the motorcycle into the turn. It is possible that for the

more gentle manoeuvre such a control input is not required, or in the case of a less experienced rider, may not be a control technique that the rider has developed fully.

Weir and Zellner [103] modelled the theory that a complete manoeuvre consists of three distinct phases, identified previously in [102]. In order to initiate manoeuvres the rider model operated in a precognitive control strategy, whereby the rider executed a manoeuvre using previous experience, instinctively countersteering to initiate a turn for example. A compensatory control was found to be the dominant method for steady state riding, be it in a straight line or negotiating a curve, with the rider establishing the manoeuvre and then reacting to any deviations to this path. Finally, a pursuit control method was suggested, whereby knowledge of the system inputs allowed the rider to apply a feedforward control to the benefit of the motorcycle's performance, including use of either the throttle or brakes for example. At track-racing level, control of the throttle on the exit of turns can be used to increase the rear tyre slip angle and thus help to yaw the motorcycle, in addition to providing accelerative drive out of the corners.

A series of control systems to replicate these features was presented and assessed. Using this model, variations in speed, tyre response and front wheel trail were made, and it was concluded that the resulting equations of motion for the motorcycle–rider system could allow a fuller understanding of what are the criteria for a motorcycle with good handling qualities, and how these may be achieved through parameter variation. The method, it was suggested, may also find use in a rider training role.

The question of controllability of motorcycles and bicycles was considered by Seffen et al. [79]. The concept of controllability is a common descriptor of dynamic systems which determines the ability of the control inputs to exercise control over the system states [38]. Seffen et al. obtained a numerical coefficient, based on the control problem Grammian matrix, which gave an indication of the degree of controllability over the system, and applied this to both a motorcycle model and a bicycle model, conducting a parameter study on both to investigate the effects of design variables upon the ease of control.

Yokomori et al. [108] investigated the ability of a rider to maintain the stability of a motorcycle at low speed with no hands on the handlebars, and thus using only body lean and forces on the footpegs to affect the stability of the motorcycle, comparing

these results with some experimental tests.

Other works of interest to the field of rider control include the work of Miyamaru et al. [65], with the objective of constructing an appropriate real-world motorcycle-riding simulator. The long-term aim was to develop a physical, rather than computer based, simulator for a motorcycle, such that riders can practice the control and riding of a motorcycle without needing to venture on to the highways, with a view to improving rider training and hence safety. The results offer interesting observations into the difficulties that exist in simulating the control tasks applied by a rider on a moving motorcycle.

In studying the control actions required to ride a motorcycle, it was observed that at low speeds the rider actively controls the steer angle, being the primary method of directional control. At higher speeds some steer effort is required to initiate a turn, but thereafter the steer angle is essentially set depending on the roll angle, as it is the balancing of centripetal and weight forces and hence roll angle which governs the turn radius. The distribution of control through steering and roll control then varies accordingly through the speed range from low to high speeds. Further pertinent observations included that in assessing the road ahead of the motorcycle while turning, a rider will tend to look to the inside of that turn, rather than straight ahead. A parameter study was conducted with regard to the rider's head position compared to the motorcycle yaw angle during a slalom manoeuvre, finding that by adding a coefficient of 0.3 multiplied by the yaw rate to the motorcycle yaw angle gave a suitable head angle, leading to improved simulation results.

Detailed works were conducted by Prem and Good [70] and by Katayama et al. [43]. Both groups developed rider control strategies that were tasked with a particular manoeuvre that was later compared with experimental observations. Prem and Good [70] modelled the rider allowing for steer torque and upper body lean; the steer torque inputs were taken to be developed directly as a result of the upper body lean, with the resulting torques developed due to stiffness in the rider's arms. Katayama et al. [43] allowed independent control of steer torque, lower body control torque and upper body control torque.

Prem and Good [70] modelled their proposed system based on previous work by Weir [102]. In this earlier modelling, the rider steer torque was used as the primary means

for stabilising the roll angle of the motorcycle while the rider's upper body roll angle and lower body lateral position were used as the primary means for affecting the yaw angle and lateral position of the motorcycle. The proposal being made and tested by Prem and Good, contradicting with [102], was that the rider's upper body lean angle is the primary control method, and that steer torque is linked to the roll angle; as the upper body is rolled, the stiffness of the arms will naturally apply a steer torque without the rider needing to control the arms independently.

The simple rider control model from [102] was adapted such that the rider steer torque was linked to the rider upper body lean angle. This model would allow roll stabilisation of the motorcycle but not control the path following or yaw of the motorcycle. A more complicated model, based on Weir's multiple loop path control method [102], fed back the lateral position, yaw angle and roll angle outputs in order to control the rider upper body lean and linked steer torque.

Experimental tests were conducted with several riders of varying experience attempting an obstacle avoidance manoeuvre on an instrumented motorcycle. From the tests, key observations made were that a skilled rider will use noticeably more severe amounts of counter-steer to initiate a turn independently of upper body lean angle. However, once the initial counter-steer, turn-in phase of the turn is completed, for both riders the upper body lean angle and steer angle were seen to be closely coupled, supporting the proposed theory of linked body roll and steer torque.

Both of the theoretical control models were found to yield broadly similar responses, with appropriate control gains applied. However the key conclusions drawn were that the unskilled rider can be represented by the simpler single feedback loop controlling the upper body lean, whereas to replicate the skilled rider required the multiple loop feedback model to correctly replicate the rider's actions. This implies that a skilled rider is able to control steer torque and upper body lean angle independently, whereas the less skilled rider cannot achieve this so readily.

By contrast, Katayama et al. [43], considered the rider as a two mass system represented as an upper body and the lower body, treated as upside-down connected pendula; the lower mass pivoted about the longitudinal axis of the motorcycle at ground level with the upper mass then pivoting about the longitudinal axis of the lower body mass. The model itself was an extension of Sharp's model [80] with the

addition of the two rider degrees of freedom. Rider control covered three inputs; steer torque, lower body control torque and upper body control torque, calculated by means of proportionality to motorcycle roll angle and a calculated heading error of the motorcycle based on a simple preview method.

A lane-change manoeuvre at fixed speed was studied with the three control methods considered separately. It was found that steer torque was the most important parameter, the lower body influence was found to be $\frac{1}{12}$ of the steer with the upper-body control influence at $\frac{1}{80}$ of the steer effect for the particular lane-change manoeuvre considered, suggesting that upper body movement is primarily to maintain rider comfort and of limited influence upon the control of the motorcycle attitude. The lower-body movement is considered to assist the steer torque as a means of control.

The modelling method was compared with experiment by using 12 riders on instrumented machines. Different riders were found to employ varying control strategies (riding styles) with regard to magnitudes of initial steer torques for instance, and as such the simulation required the control coefficients to be adjusted appropriately. However, assuming this was done the simulation was capable of replicating the measured motorcycle–rider behaviour with good accuracy. This suggests, however, that a generic motorcycle–rider simulation can have only limited accuracy due to the heavy influence of rider style upon the motorcycles behaviour.

Previous research works, including [104], had sought to provide some means by which to determine the qualities required for a good handling motorcycle. With a similar aim, Cossalter et al. [16] calculated the steer torques necessary to complete a given manoeuvre using an appropriate mathematical model. The model itself was a generic four-body bicycle model, with the influence of suspension movement neglected, as the consideration of a steady turn should result in fixed wheel positions relative to the motorcycle frames. Changes to the physical attributes of both tyres and the motorcycle influence these torques, and so analysis of this type may enable a motorcycle to be designed that exhibits particular characteristics with regard to steer torque felt by the rider, and hence influence the rider's perception of its handling.

2.4.3 Optimised Rider Models

A number of research works have involved analysing the rider's control actions and seeking to replicate these via the use of a mathematical control strategy. Another branch is concerned with the development of rider models that attempt to optimise the mathematically defined riding task and hence replicate the rider's control actions accordingly.

Considering first the approach taken to optimise the vehicle performance based on system dynamics, Cossalter et al. [14] developed a technique termed the Optimal Manoeuvre Method. This approach essentially employed an optimisation strategy with several performance criteria forming the cost function. These elements included maximising the distance travelled over a manoeuvre, trajectory constraints to keep the motorcycle within the road width, costs to ensure the ratio of lateral front wheel force to longitudinal thrust/braking forces were not excessive, and other less significant performance factors. Experimental performance evaluation with respect to handling and manoeuvre capabilities would always be heavily influenced by rider ability and control strategies, and in limit cornering conditions rider style and handling preferences may adversely affect experimental results. The Optimal Manoeuvre Method was therefore developed that would use an optimal preview approach in order to simulate the manoeuvre of a motorcycle, having the advantage of applying, within reason, whatever input controls were necessary, through steer torque, throttle and braking actions, such that the motorcycle performed the required manoeuvre in the most efficient manner specific to that motorcycle. This would therefore give a more appropriate measure of ultimate machine performance, on the assumption that a rider would be able to apply the necessary control strategy to achieve this, reasoning that a highly skilled rider would be able to adapt himself to the particular motorcycle and therefore maximise its performance. Simulations were compared with telemetric data for a motorcycle negotiating an S-bend on a race track, and found to agree well. The findings were also presented by Cossalter in [15].

Cossalter's co-authors Biral and Da Lio applied the Optimal Manoeuvre Method to the modelling of a vehicle driver [6]. The principles of the approach were the same as for the motorcycle case, with similar simulations and results.

A review of driver control models was made by Guo and Guan [33] before presenting

the development of their own optimal preview driver control models. In particular, the broad areas of compensatory and preview tracking models were compared, suggesting that the latter provides a far superior path tracking ability. The optimal preview control model of MacAdam [50] was reviewed, and the concept extended to produce more intricate driver control models considering the lateral accelerations of previewed road position and orientation information. Initially based on a global coordinate system, the model was adapted to local coordinates, displaying good performance. The control of forward speed was discussed, as was the concept of a reference path, being a path that the driver may desire to follow, rather than necessarily the centreline of some constrained road path.

Di Puccio et al. [73] compared three types of driver control model for path tracking of a four-wheeled vehicle; a simple preview tracking model using single point preview, the second a simple fuzzy-logic controller, the third a more detailed fuzzy controller aimed at capturing the driver's behavioural characteristics. The single point preview model represented a very simple prediction model, determining the future position of the vehicle based on the current vehicle states. The fuzzy control models however proved unable to realistically reproduce human behaviour.

A very similar preview-tracking approach was taken by Sharp et al. [86]. Again with application to a twin-track vehicle, Sharp and his co-authors successfully generated a driver control model capable of steering a vehicle model along a road path. The road information was presented to the driver model as a series of discrete road points, and the controller generated a steer control input using PID theory to minimise the lateral errors between the previewed road and a preview arm projected directly ahead of the vehicle, this time using a multiple preview point approach. The theory was later applied to the case of a motorcycle [76], but the application was seen to be inappropriate to the task. The requirement to countersteer a motorcycle was not well catered for by this approach, leading to ineffective path following.

The possibility of a control system to assist in motorcycle stabilisation as an aid to safety was investigated by Kamata and Nishimura [41]. This control system was evaluated through implementation of such a device on a computer simulation of a motorcycle. Use of such a control device was shown to be beneficial in reducing the roll angle of the motorcycle following a disturbance over a range of vehicle speeds. Though the paper covered only theoretical work, it was indicated that subsequent in-

vestigations by the authors would look at adapting such a system to a real motorcycle and evaluating the effects experimentally.

The use of computer-aided methods for motorbike handling and stability analysis was further investigated by Styles [96]. Particular emphasis was placed on the steer torque, and to identification of the important contributors to this torque. Important design parameters for the motorcycle were varied and the effects upon the steer torques re-examined. The important contributors were found to be the moment arising from the normal tyre force, the gyroscopic torque in roll and the aligning moment resulting from the lateral force through mechanical trail.

A method of optimal preview was also investigated, with the aim of assisting future motorcycle development. Manoeuvre simulations were again run and parameter variations made. The stability was analysed by observing the eigenvalues resulting from the state space matrices used in the modelling.

A driver control strategy was also proposed by Antos and Ambrósio [1] for a twin-track vehicle. The vehicle model, with some simplifications made, was combined with a multivariable bilinear control methodology presented elsewhere. The controller used an optimal control strategy, without preview, to force the vehicle to follow a predetermined 'ideal' path, with information on this path input by means of coordinates, section lengths and section curvatures. Essentially, current vehicle position and states relative to the ideal path were combined with an optimal controller that applied a steering control to the vehicle front wheels and rotational torques to all four wheels. The weightings for the controller cost function were user-defined and close path following was achieved, although the lack of any form of visual preview would seem to be in contradiction with the driving tasks employed by a human driver.

Modelling of the control strategies for riding a motorcycle was investigated by Huyge et al. [37] with the use of a multibody motorcycle model coupled with a separate model to replicate the rider's control actions, in this case an applied handlebar torque. The biomechanical information for the rider was included in the multibody motorcycle model, though the movement of the rider's body mass was not used as a direct control input to the motorcycle as had been done by other authors previously. The strategy adopted in regard of the rider's control used a target roll angle to be input to the model, which corresponded to a particular turn radius for a specific motorcycle at a

given speed. The controller of the motorcycle applied a steer torque to the handlebars in order to generate the required roll angle and to correct if the target roll angle was not being met. The presented example of an S-bend manoeuvre showed good path following results. However, it is known that a rider will countersteer prior to commencing a turn, and so will necessarily need to employ some form of preview to initiate the turn. While countersteer is shown in the model, it was not in the form of a preview control to initiate the turn, but appears instead to be applied in a regulatory manner to adopt the target roll angle only once the turn has begun.

Building on earlier works on driver preview control [98], Sharp [94] adapted the optimal control technique to the application of a motorcycle rider's control actions. As with the driver model, the optimal control element related to a visual preview of the road, for which the controller calculated a series of gain values in order to minimise a combined cost of lateral path position error and steer torque input. The control input parameters available to the rider were steer torque applied to the handlebars and an upper body lean torque. The path following performance was seen to be very successful, and with the results suggesting, in agreement with earlier work by Katayama [43] in particular, that the primary control method was through steer torque and with the influence of rider lean torque an order of magnitude less important than the steer torque. By calculating a series of gain values against the previewed road path, this effectively allowed the relative importance of the previewed road to the task of path following to be assessed. In agreement with Land and Horwood [47], the near preview information was seen to be more important in regard of maintaining the position of the motorcycle relative to the road.

Other interesting areas of research into rider control that have recently appeared include the use of predictive control. The mechanics of the method are not dissimilar to an optimal control technique, which has been applied in a number of ways to assess both motorcycle performance [4, 15] and driver/rider performance [51, 94]. However, unlike optimal control, predictive control generates a set of anticipated future states, and by the comparison of predicted future states with target future states, a control input is generated that attempts to find a balance between minimising the state errors and the control input required.

Prokop and Cole, the latter with his co-workers, separately developed predictive control driver models. Prokop [72] developed an extensive application of this technique

in modelling the control actions of a twin-track vehicle driver, allowing control of steer angle, throttle and braking inputs. Using the plant of the vehicle dynamics, the output several seconds ahead of the vehicle could be predicted and coupled with a PID controller in order to guide the system to the targets set by the nature of the road. A number of simulated manoeuvres were compared with experimental manoeuvres, concluding that the method was conceptually capable of replicating a driver's control actions.

The controller developed by Cole et al. [11] was a more representative application of the complete model predictive control technique. As with Prokop's model, a prediction of future output states was made, but in this case the control input determined by minimisation of a quadratic cost function, in a similar manner to the optimal control approaches. The investigations showed encouraging similarity to the conceptually accurate optimal control method, but limited path-tracking results were available against which to judge its applicability to the task of modelling vehicular control.

2.5 Summary

The literature review has covered the wide range of research areas with relevance to motorcycles and motorcycle riders. These have been broadly defined as the areas of motorcycle stability characteristics, tyre modelling and rider control modelling.

The first of these, motorcycle stability analysis, has been extensively studied by a number of researchers over many years. A great deal of the early simulation models have been incorporated into commercial software packages, such that results can be achieved relatively easily via these programs. Extensive work has been conducted into developing ever more complex models to represent further structural characteristics of a motorcycle, to the point where there is limited scope to establish any novel yet constructive avenues of research.

Tyre modelling continues to be an important area for research. The tyre is the principal provider of external forcing to the motorcycle and hence primarily affects its behaviour. The "Magic Formula" is widely regarded as being capable of successfully generating realistic tyre forces and moments, and without access to tyre testing apparatus, the scope for research work into motorcycle tyre behaviour is restricted.

Since high quality dynamic representations of motorcycles are now widely understood and available, and the rider plays such a significant part in this response, the modelling of the dynamic behaviour of the combined motorcycle–rider becomes the next goal. In recent years a number of control strategies have been employed as a means of replicating the control actions of the rider. While some of these proved successful in being capable of applying suitable control to a dynamic model of a motorcycle, the question should be asked whether the goal is to generate an appropriate control input or to replicate the control strategy employed by a human rider. In the latter case, this must include the consideration of how the rider interprets information available to him, and how this information is used in performing his control task.

To date, there are few controller models that have been applied specifically to replicating the control actions of a motorcycle rider, and those that have been demonstrated appear worthy of more detailed investigations. The objective of this thesis will therefore be to replicate the contemporary rider control models and conduct more extensive parameter studies to establish particular strengths or weaknesses of these methods. In particular, the principles of model predictive control strategies, hitherto not applied to the modelling of a motorcycle rider, appear to provide the necessary elements for replicating the complex actions of a motorcycle rider between problem interpretation and control solution.

2.5.1 Objectives and Thesis Outline

In light of the findings outlined in the literature, the goal of this thesis will be to developed the concept of model predictive control for the specific application of a producing a motorcycle rider control model. The motivations for this work are covered in Chapter 1.

The starting point will be the generation of an appropriate basis upon which to assess the control techniques. Chapters 3 and 4 will therefore detail the specifics of modelling the motorcycle dynamics and the rider's preview respectively. Combined, these two elements will form the motorcycle–rider model that will form the basis of the more detailed rider control modelling.

The rider modelling will consider the application of two specific control theories. Chapter 5 will cover the use of optimal control for replicating the rider's control

actions. Both the theory and application will be covered, with an extensive parameter study conducted to evaluate the performance. Subsequently, Chapter 6 will consider the application of predictive control techniques for the same aim, again with detailed theory and parameter studies conducted.

A cautionary note to the reader is needed here. Both optimal control and model predictive control techniques can be considered 'optimal' approaches, since they both aim to minimise a cost function to provide the theoretically best possible control input. However, the distinction in this thesis is made between optimal control and predictive control techniques, which will be more clearly defined by the theory in the relevant chapters (Chapters 5, 6).

For both control techniques, extensive parameter studies, to understand to a suitable extent the behaviour of the control system, will be conducted to assess the applicability of the approaches to the task. The aim is that this will result in a suitable control strategy for replicating the actions of the rider, with good potential for future development and application. A feature of predictive control that is considered to be suitable for the application here is the ability to include constraints on the modelling, which can therefore be used to represent limits in the available road width, the physical limits of steering lock, and any other limitations pertinent to the task.

The two techniques will then be compared and contrasted in Chapter 7, with final conclusions drawn in Chapter 8.

Chapter 3

Motorcycle Modelling

3.1 Introduction

In order to generate a motorcycle–rider simulation tool, an appropriate dynamic model of the motorcycle is required, enabling the response of the motorcycle to internal and external forces to be determined. The response of the dynamic model must correctly replicate the response of the real motorcycle to these forces if the combined controller model is to be assessed correctly. Without a correct dynamic model, any conclusions drawn about the performance of the controller model may be meaningless.

A motorcycle is a complicated piece of machinery, consisting of many thousands of parts, each with its own physical properties. Many of these parts are not completely constrained within the motorcycle as a whole, having freedoms to rotate, translate or a combination of both. The dynamics of the engine and driveline are a complex system, and every structural component on the motorcycle has associated with it some mass, damping and stiffness properties.

In order to develop a simulation tool for the dynamics of a modern motorcycle, the system must be simplified considerably in order to capture the fundamental physical characteristics of the motorcycle with sufficient computational efficiency. The purpose of the research work presented in this thesis is to develop a controller representative of a human rider, and so provided that the dynamic motorcycle model employed replicates the fundamental responses of a motorcycle to forcing, then detailed dynamic models to capture intricate dynamic characteristics are not considered necessary, and

the use of a simplified model can therefore be justified. Computer software can be employed to generate the appropriate equations of motion, which provides the dynamic response of a generic motorcycle model to the dominant internal and external forces.

This chapter will therefore detail the processes and techniques used in order to generate the dynamic response of a simplified motorcycle model. The model itself was generated through direct mathematical methods and based on the much-cited model in [80]. The mathematical procedure will initially be presented, and the resulting model subsequently validated against [80]. A more detailed tyre model than in [80] will be presented, validated and implemented to the motorcycle model, resulting in a model more capable of accurately replicating the motorcycle responses at high tyre slip and camber angles. This model will be used as the motorcycle model to which the rider control strategy will be applied, to enable a path following task to be simulated. The combined motorcycle–rider simulation model using a novel control strategy will form the goal of this thesis, and so this dynamic response model will form the platform on which the control model will be evaluated. The novelty of the work is largely restricted to the control modelling of the rider; the modelling of the motorcycle's dynamics is a tool on which the control model will be applied.

3.2 Coordinate System

Before performing any type of dynamic modelling, it is essential to define a clear coordinate system that is to be used, and ensure that all dimensions, forces and velocities conform to those coordinates. The choice of coordinate system can be arbitrary, provided that this coordinate system remains consistent throughout the modelling.

There are, however, conventions that are commonly used, and for vehicle modelling the typical coordinate systems used are the SAE (Society of Automotive Engineers) or ISO (International Standardization Organization) systems. Both coordinate systems consist of a set of three orthogonal axes, where, with respect to a vehicle, the x-axis is aligned with the direction of travel. The SAE coordinate system has the y-axis aligned positive right and the z-axis positive down (Figure 3.1), while the ISO coordinate system aligns the axes positive left and positive upwards (Figure 3.2).

In both coordinate systems the roll, pitch and yaw rotation directions are right-hand-rule rotations about the x-, y- and z-axes respectively.

For a global coordinate system, the axes remain fixed at the origin of the simulation, while for a moving coordinate system simulation the coordinate system remains fixed to and moves with the vehicle. In a general moving coordinate system the axes translate longitudinally and laterally and yaw, roll etc. with the motorcycle. For ground-based vehicle modelling, the coordinate system rotates only with the yaw rotation of the vehicle such that the x- and y-axes remain constrained to the ground plane, even when the vehicle itself adopts a roll angle.

For the motorcycle model employed here, the SAE coordinate system is used. The motorcycle's origin is defined by the position of the rear frame centre of mass projected vertically down to the ground plane with the motorcycle upright. The x-, y- and z-axes form an orthogonal set of axes, with the x- and y- axes in the ground plane and the z-axis perpendicular to the ground plane projecting vertically down. The x-axis projects ahead of the motorcycle, and the y-axis projects to the right of the motorcycle. A yaw rotation ψ constitutes a rotation of the entire motorcycle about the vertical z-axis to define the yaw frame. A pitch angle θ defines a rotation of the motorcycle about it's y-axis, i.e. in the yaw frame, to define the pitch frame. A roll angle ϕ constitutes a rotation of the motorcycle about the x-axis of the motorcycle in the pitch frame to define the roll frame. Finally, a rotation δ of the front frame about the steer axis of the motorcycle in the roll frame constitutes the steer, and hence defines the steer frame. The motorcycle model used is described in detail in Section 3.4.

Positive lateral tyre forces are in the positive lateral direction for the motorcycle model used here. Hence, positive slip is in the negative lateral direction. Thus, positive tyre camber results in positive lateral forces.

3.3 Tyre Model

Initial modelling work employed a simple linear tyre model,

$$F_y = C_\alpha \alpha + C_\gamma \gamma \tag{3.1}$$

where lateral forces were the sum of the product of sideslip angle α with tyre sideslip stiffness C_α, and the product of camber angle γ with camber stiffness C_γ. The detailed definitions of sideslip, camber angles and other useful definitions can be found in Appendix 1 of [68]. This simple tyre model was used to establish the early motorcycle dynamic models, before a more advanced tyre model was introduced.

The lateral tyre forces generated by this simple tyre model for a range of slip ratios and wheel camber angles of a front tyre are shown in Figure 3.3, for which the tyre parameter values can be found in Appendix A.

The advanced tyre model that has been employed here is based on work by Meijaard and Popov [60], where a non-linear model was developed to capture the behaviour of the lateral and longitudinal forces and moments about the vertical axis of a motorcycle tyre. The work was conducted using a commercial multibody simulation program [3]. Here, the approach is modelled using symbolic mathematical coding [53]. For small angles of sideslip, the response of a tyre can be represented quite well by a linear model, but to capture the response for larger slip angles typically experienced at higher speeds, a more advanced model is required. The tyre model itself is obtained by a simplification of the "Magic Formula" by Pacejka [68]. This section will outline the fundamental steps applied to obtain the tyre model, and the validation of this model against the original work by Meijaard and Popov.

3.3.1 Tyre Force Equations

Full details of the tyre model used can be found in [60]. Here, an overview of the technique will be presented.

Tyre forces are generated by the combination of deformation of the tyre in the contact patch and slip of the tyre's contact patch relative to the ground surface. Both result in slip velocities between the wheel and the ground surface, and therefore the initial steps are concerned with calculating the slip velocities of the wheel and tyre as a rigid body in the lateral and longitudinal directions. This is achieved through vectorial definitions of the wheel centre and contact patch location, and knowledge of the wheel spin velocity and wheel forward speed.

The vector corresponding to the wheel spin axis is obtained by rotating a unit vector in

the positive lateral direction by the yaw, roll and, for the front wheel, fork inclination and steer angle. The component of this vector in the z-direction is equivalent to the sine of the camber angle, and thus the camber angle of the wheel is obtained by taking the arcsine of this component.

The axial spin rate of the wheel is obtained by the division of the forward speed with the nominal undeflected tyre radius. The motorcycle will be assumed to run at a constant forward speed, and thus the axial spin rate is not required as a variable here. This spin rate, being about an axis perpendicular to the wheel plane, is then translated via the rotations of yaw, roll and, if appropriate, fork inclination and steer to define the spin velocity of the wheel in the motorcycle's reference frame.

The tyre contact patch is defined by a single point in the contact patch area, the exact position being the combination of several vectors. The starting point for the definition of a generic tyre can be an arbitrary point in the ground plane. For the more specific application here, the origin will be taken as the origin of the motorcycle coordinate system. This origin is located at the intersection of a projection vertically down from the rear frame's centre of mass with the ground plane when the motorcycle is upright (Figure 3.4). First, the position of the wheel centre in this reference frame is defined. A vector in the plane of the wheel projected down towards the contact patch then defines the centre of the toriodal profile of the tyre, and finally, a vector projection vertically down, with length equal to the toroidal radius of the tyre, defines the undeflected tyre contact point.

The intersection of a vertical line through this undeflected contact point with the road surface is used to define the deflected, actual contact point of the tyre with the road surface. The division of the tyre's vertical stiffness with the vertical displacement of the deflected contact point relative to the undeflected point can provide the vertical force acting on the tyre. For the application here, the tyre forces were calculated from statics.

Tyre forces result from deformation of the tyre carcass as the tyre moves into the contact patch area, coupled with the tyre's stiffness properties. This distortion of the tyre effectively results in a higher axial spin rate for a given forward wheel speed than would be experienced for a solid wheel with the same rolling radius. The wheel in the contact patch area can therefore appear to move relative to the road surface,

leading to the definition of a tyre slip velocity.

This slip velocity can be obtained numerically by considering an increased effective wheel radius, with the wheel rotating at the same angular velocity as for a solid wheel with the actual tyre rolling radius. A new effective radius is therefore defined, being part way between the undeflected and deflected tyre contact points.

The angular velocity of the wheel is obtained from the forward speed of the wheel and the actual rolling radius of the tyre. Thus, use of this angular velocity with the increased effective rolling radius leads to an increased effective contact patch speed relative to the wheel centre. The summation of this contact patch speed with the speed of the wheel centre results in the effective slip velocity in the contact patch.

This process is done independently for the longitudinal and lateral tyre contact patch velocities to independently control the behaviour of the tyre's lateral and longitudinal force properties with slip. Dimensionless slip quantities are then obtained by the division of the tyre contact point slip velocities with the velocity of the wheel centre in the plane parallel to the ground plane.

The lateral and longitudinal tyre forces and tyre moment about the vertical axis are obtained by a simplified version of the "Magic Formula". Specifically, the expressions are [60]

$$F_{lat} = \frac{C_l F_n (s_{lat} - \epsilon_{eq} s_n / \sqrt{1 - (C_l/\mu_w)^2 s_{tot}^2})}{\sqrt{1 + (C_l/\mu_w)^2 s_{tot}^2}} \tag{3.2a}$$

$$F_{long} = \frac{C_l F_n s_{long}}{\sqrt{1 + (C_l/\mu_w)^2 s_{tot}^2}} \tag{3.2b}$$

$$M = \frac{\epsilon_{eq} R_w C_l F_n s_{lat}}{1 + (C_l/\mu_w)^2 s_{tot}^2} \tag{3.2c}$$

where C_l is the ratio of the cornering stiffness to normal force, μ_w is the generic tyre friction coefficient, ϵ_{eq} is equivalent to the ratio of camber stiffness to cornering stiffness, F_n is the normal force, s_{lat} and s_{long} are the dimensionless lateral and longitudinal slip quantities, s_{tot} is the dimensionless uni-directional slip quantity, s_n is the normal wheel spin, and finally R_w is the nominal wheel radius.

In this application, the longitudinal tyre force is not required, since the motorcycle modelling will be conducted at a constant forward speed.

3.3.2 Validation of Tyre Model

The tyre model, described in the preceding section, was coded using Maple symbolic software [53] and validated against the original tyre model in [60], itself validated against the full Magic Tyre Formula in [68]. The original validation of the model considered the lateral tyre forces generated for a representative range of tyre camber angles and sideslip ratios. All parameters for the motorcycle tyre in this application were as in [60], allowing a direct comparison of the results to ensure the correct implementation of the approach, and can be found in Appendix A.

First, however, a reminder about sign conventions is required. The referenced paper considers positive lateral slip to be in the positive lateral direction. The lateral force generated by slip is directed so as to oppose the slip direction, and thus positive lateral tyre force is in a direction opposite to positive slip, and hence in a direction opposite to positive lateral displacement. This convention is adopted temporarily to validate the tyre model against the original paper.

The lateral tyre forces were obtained for a range of tyre camber angles from 0^o to 50^o, typical of the operating range of a road-going motorcycle tyre, with the lateral slip ratio in the range -0.3 to $+0.3$, and for the tyre parameter values in Appendix A. The lateral tyre forces and moments are presented in Figure 3.5, where the non-linear response, characteristic of pneumatic rubber tyre, is clearly apparent.

Considering first the tyre operating at zero camber angle, i.e. in the upright position, it is seen that in the slip range -0.05 to $+0.05$ the response of the tyre lateral force is close to linear. Models that employed a linear tyre model would therefore show reasonable accuracy within these operating ranges. Outside this range, the ratio of lateral tyre force to lateral slip diminishes as tyre force saturation begins, at which point a linear model would give rise to incorrect results, and at slips approaching $+/-0.3$ for zero tyre camber angle the tyre is close to fully saturated with the maximum lateral force obtained. The tyre moments about the vertical axis show similar responses, with a small linear operating range about zero slip, in the range approximately -0.05 to $+0.05$. The tyre moments peak somewhat earlier than for the lateral forces, at lateral slips of approximately $+/-0.08$, with the moments then decaying away as tyre saturation sets in with increasing lateral slip.

As a motorcycle tyre is cambered, a lateral force is generated in the direction of the tyre's lean, a characteristic known as camber thrust. The camber thrust force acts in the direction in which the tyre is cambered such that a positive camber angle, in which the top of the tyre is deflected in the positive lateral direction relative to the contact patch, results in a lateral tyre force in the positive lateral direction. It was noted previously that positive slip is considered to be in the positive lateral displacement direction, and thus positive lateral tyre force is in the negative lateral displacement direction. Thus, a positive tyre camber should result in a negative lateral tyre force.

The effect of camber on the lateral forces generated by the tyre are again apparent in Figure 3.5. Considering first the case for zero lateral sideslip, it is seen that as the camber of the tyre is increased, the tyre lateral forces become increasingly negative, as expected, i.e the effect of camber is to generate a lateral tyre force in the direction of the lean of the tyre. As the tyre camber increases, the cumulative gains in lateral force with each additional 10^o of camber diminish. Expected lateral tyre force properties can be found from experimental studies of tyres, carried out by both tyre manufacturers and by research institutions. Results from the former are well-guarded. However, detailed information on typical tyre behaviour can be found in [68], while other references of a broader nature include [13, 31]. Further combinations of sideslip and camber give results that would be expected of a motorcycle tyre, showing the combined effects of lateral force generation through sideslip and camber thrust that have been outlined previously.

As a final point of interest, and to give justification for the use of this advanced tyre model, the lateral force generated by the simple and linear tyre models are compared, here for the 0^o camber angle condition of the front tyre (Figure 3.6) and the 50^o camber condition of the rear tyre (Figure 3.7). The responses of the linear tyre model are seen to be a good approximation to more realistic tyre forces over only a narrow range of sideslip ratios, and outside this narrow range the tyre forces generated by the linear tyre would not be representative of a real motorcycle tyre.

This advanced tyre model, coded using Maple symbolic software [53] has therefore been validated against the original model in [60], itself originally validated against [68], giving confidence that the advanced tyre model employed here gives a realistic representation of a motorcycle tyre across a broad range of operating conditions for lateral slip and tyre camber angle. This advanced tyre model was therefore employed

in modelling the dynamic response of the motorcycle to control inputs subsequently used in the motorcycle–rider simulations.

3.4 Motorcycle Model

The modelling of the motorcycle itself is considered here. A motorcycle is a machine formed from many smaller subassemblies and parts, each of which has its own characteristic dynamic behaviour, and when combined, the response of the whole motorcycle is influenced by the interaction of all subcomponents with each other. For ultimate accuracy of the dynamic behaviour of the motorcycle, it would be necessary to consider the individual contributions of all such subassemblies. To perform such a calculation would, however, require extensive numerical calculation, and thus a simplified motorcycle model was employed here.

The fundamental characteristic response of the motorcycle is dictated by the interaction of the principal bodies of the motorcycle and their movement relative to each other, and so in the interests of computational efficiency, the motorcycle has been modelled as a simplified four-bodied bicycle. This implies that the motorcycle is represented to consist of front frame, rear frame, front wheel and rear wheel, without the inclusion of suspension freedoms. The front frame refers to the front forks, brake calipers, handlebars and any fixtures that move with the steering, such as lighting assemblies or mudguards. The rear frame is taken to represent the combined structural and geometric properties of the rear chassis structure, engine and drivetrain assembly, seat structure, fuel tank and any other rigidly attached fittings to this combined structure. The front and rear wheel bodies consist of all rotating wheel parts, namely the wheel itself, the tyre and all rotating brake components.

This simplified motorcycle model is depicted in Figure 3.4, with a coordinate system as described in Section 3.2. The front frame attaches to the rear frame via a revolute joint inclined through the steering inclination angle η, with rotational velocity restrained by the use of a steering damper. The wheels similarly attach via revolute joints along their spin axes. Suspension deflections are not accounted for in the model used here, and hence motions of pitch and heave are not included. In principle, some pitch motion will result from the geometry of the tyres and steer system whenever the steer angle is non-zero, and also through deformation of the tyres. In practice, the

effects of this on the pitch angle of the motorcycle are small, and considered to have a negligible impact upon the dynamic behaviour of the motorcycle. The wheels are axi-symmetric, and thus it is not necessary to include the rotation angles of the wheels as specific system states. The actual rotational angles of the wheels are unimportant; only the angular velocities are required which can be readily obtained with knowledge of the forward speed and rolling radius of the tyres. The non-linear characteristics of the tyre's lateral forces are obtained using the simplified "Magic Formula" approach presented in [60], and described in Section 3.3.

The geometric and physical properties of the motorcycle are taken from [80]. The values used for the motorcycle were typical for a contemporary motorcycle at the time of publication of the referenced paper. The fundamental designs of motorcycles have not changed dramatically since the publication of the cited paper, and hence use of the data is still considered valid in modelling the response of a typical motorcycle, and the model used here is therefore essentially an extension of the original motorcycle model presented in [80]. Many more advanced motorcycle models have been developed in the literature [81], consisting of additional flexures of the motorcycle's structure in particular. However, the object of the work presented in this thesis is concerned with the modelling of the rider, and so the exact details of the motorcycle model used for the simulation process are not a primary consideration, provided that the fundamental response and primary modes of the motorcycle are captured. The motorcycle model developed in [80] has been used extensively for both academic and non-academic applications, and can therefore justifiably be used as a reference model on which to base the development of a rider control strategy that is the goal of this thesis.

3.4.1 Motorcycle Equations of Motion

This section will outline the basic theory that was used to obtain the simplified motorcycle model's equations of motion.

An array of commercial computer programs are available that are capable of modelling the dynamic response of physical systems. Popular codes include generic dynamics programs such as MD Solutions [63] or Virtual.Lab [99], and more specific programs, for example CarSim [10] and BikeSim [5]. Such programs typically require the definition of the principal structural characteristics of the bodies of the systems and

information regarding the coupling between the bodies. The programs build up the complete structure from knowledge of the sub-bodies and their interactions to obtain the dynamic response of the entire combined assembly.

The approach taken here develops the dynamic response of the motorcycle from fundamental mathematical principles. The equations of motion are developed symbolically, using a symbolic software code Maple [53], and derived using Lagrange's theory. Fundamentally, the positions, motions and physical properties of the system's bodies are defined, and then by consideration of the energy of the system as a function of the system's degrees of freedom, the equations of motion are obtained.

These equations of motion are initially obtained symbolically, and are then exported to Matlab [54] where the numerical responses and motion simulation of the motorcycle are performed. The reasons why the equations are initially developed symbolically will become clear in subsequent sections of this thesis.

The theory of Lagrange can be broken down into a few fundamental steps. The first step involves the definition of the physical properties of the motorcycle's main bodies and the definition of the principal degrees of freedom allowing the energy of the system, both kinetic and potential, to be obtained. The external forces acting on the system are then defined, and the instantaneous virtual power of these forces obtained. The combination of internal energies and the external energies as a result of external forces are then used to obtain the dynamic response of the entire motorcycle assembly.

Theory

The Lagrangian method for deriving the equations of motion can be found in many dynamics textbooks [64, 101]. The method involves calculating the kinetic and potential energy of a system and using these functions to generate the equations of motion. Explicitly, for an unforced system the Lagrange's equations are defined by:

$$\frac{d}{dt}\left(\frac{\partial T}{\partial \dot{\mathbf{q}}}\right) - \frac{\partial T}{\partial \mathbf{q}} + \frac{\partial U}{\partial \mathbf{q}} = 0 \tag{3.3a}$$

where T is the kinetic energy of the system, U is the potential energy, and $\mathbf{q}$ is the vector containing the degrees of freedom. Extending this to include the influence of

external forcing on the system, the Lagrange's equations become

$$\frac{d}{dt}\left(\frac{\partial T}{\partial \dot{\mathbf{q}}}\right) - \frac{\partial T}{\partial \mathbf{q}} + \frac{\partial U}{\partial \mathbf{q}} = \mathbf{W} \tag{3.3b}$$

where $\mathbf{W}$ is the sum of the virtual powers of any external forcing on the system. Specifically, these powers can include aerodynamic forces and tyre contact patch forces.

The kinetic and potential energies of the motorcycle system are broken down into the individual contributions made by the front and rear frames and the front and rear wheels. The kinetic energy comes from two sources: a translational component resulting from linear velocities and a rotational component from angular velocities of the bodies. The generic linear and angular kinetic energies of an object can be defined by $\frac{1}{2}m_b v^2$ in a single direction, where m_b is the body mass and v is the velocity of the body, and $\frac{1}{2}I\omega^2$ for a single rotation direction, where I is the object's moment of inertia and ω is the angular velocity of the body. For the more general case of translation and rotations in a six degrees of freedom system (3 linear, 3 angular), these expressions extend to $\frac{1}{2}\mathbf{v}^T m_b \mathbf{v}$, where $\mathbf{v}$ is the vector of linear velocities of a body, and the rotational kinetic energy is defined by $\frac{1}{2}\boldsymbol{\omega}^T \mathbf{I}\boldsymbol{\omega}$ where $\boldsymbol{\omega}$ is the vector of angular velocities of a body and $\mathbf{I}$ is the inertia matrix of the body in three dimensions. Since the body is moving in three-dimensional space, the energy terms should account for motion in all three dimensions.

The derivatives of the energy terms with respect to the degrees of freedom of the motorcycle are obtained from the Jacobian matrix of the energies of the motorcycle in all six directions (3 orthogonal linear directions and 3 orthogonal angular directions) with the degrees of freedom of the motorcycle system.

In a similar way, the first term in the Lagrange's equations (3.3b) is obtained from the time derivative of the Jacobian of the kinetic energy terms with respect to the time derivatives of the motorcycle degrees of freedom.

The virtual powers result from the product of the magnitudes of the forces and moments, taken in the 3 principal orthogonal directions and the 3 principal orthogonal rotations, with the velocities of the corresponding points of application of forces and moments, again in the 3 principal directions and rotations. In this application, these

are the tyre contact forces, acting at the tyre contact patches.

The motorcycle model considered here has five degrees of freedom, detailed in Section 3.4; longitudinal and lateral displacement of the motorcycle, yaw and roll rotations of the motorcycle and steer rotation of the front frame relative to the rear frame. Consequently, the application of Lagrange's equations results in five second-order equations of motion.

Implementation in Maple

The fundamental principle of the Lagrange's equation has been outlined. Further details, if required, can readily be obtained from the referenced texts [64, 101]. Here, the application of the theory using Maple symbolic software [53] will be outlined. To fully detail every line of code would be both tedious to the reader and an uneconomical use of space within this thesis, and so only the key inputs and steps required to obtain the desired equations of motion are presented. While automatic modelling codes are readily available, the equations of motion were developed in Maple using Lagrange's theory explicitly in order to retain more complete control of the modelling detail. This does not therefore represent any significant novelty to the literature; the model developed will provide a tool for the subsequent work on rider control.

Fundamentally, the coding of Lagrange's theory can be broken down into several broad processes:

1. Define preliminary vectors and matrices necessary for the calculations.
2. Define the body positions and rotations, and hence linear and angular velocities.
3. Calculate the total kinetic and potential energies.
4. Calculate all applied forces and velocities of points of application to obtain total virtual power.
5. Form the Lagrange's equation.
6. Manipulate into the state space format and export to Matlab.

The preliminary vectors and matrices included the definition of the state vector and the definition of rotation matrices corresponding to the yaw, roll, steer and front frame inclination angles. The vector **q** of the system degrees of freedom, consisting of global longitudinal x and lateral position y, global yaw angle ψ, roll angle ϕ and steer angle δ, together with their first and second derivatives were input as

```
          q  := <x, y, psi, phi, delta>;
      q_dot  := <dxdt, dydt, dpsidt, dphidt, ddeltadt>;
  q_dot_dot  := <d2xdt2, d2ydt2, d2psidt2, d2phidt2, d2deltadt2>;
```
(3.4)

It should be noted in this instance that the degrees of freedom are not specifically defined as functions of time, even though they are taken to be so. Similarly, the derivatives are not expressed as functions of time as far as the computer code is concerned. During the coding, it was at times necessary to take derivatives with respect to time t, and sometimes with respect to the states, which are functions of time themselves. Maple cannot perform differentiation with respect to functions, only with respect to variables, and so it became necessary during coding to change definitions of variables between explicit functions of time and independent variables, for instance substituting $\frac{\partial x(t)}{\partial t}$ with *dxdt* and *vice versa*, so that the derivative of an expression with respect to the time derivative of $x(t)$, i.e. *dxdt*, could be taken.

Definitions of the rotation matrices concerning the yaw angle ψ, roll angle ϕ, front frame inclination angle η and steer angle δ are required. These matrices were used to orientate the coordinate system as necessary to define the positions of the bodies and positions of key features of the motorcycle in the arbitrary displaced state. Using as an example the matrix **R1**, corresponding to a yaw rotation, the matrix and its transpose are input as

```
     R1  := << cos(psi(t)) | -sin(psi(t)) | 0 >,
            < sin(psi(t)) | cos(psi(t)) | 0 >,
            < 0 | 0 | 1 >>;
  tr_R1  := transpose(R1);
```
(3.5)

leading to

$$
\begin{aligned}
\texttt{R1} &= \begin{bmatrix} \cos(\psi(t)) & -\sin(\psi(t)) & 0 \\ \sin(\psi(t)) & \cos(\psi(t)) & 0 \\ 0 & 0 & 1 \end{bmatrix} \\
\texttt{tr\_R1} &= \begin{bmatrix} \cos(\psi(t)) & \sin(\psi(t)) & 0 \\ -\sin(\psi(t)) & \cos(\psi(t)) & 0 \\ 0 & 0 & 1 \end{bmatrix}
\end{aligned}
\tag{3.6}
$$

With the degrees of freedom of the motorcycle and the corresponding rotation matrices defined, the physical dimensions and orientations of the motorcycle assembly can be fully defined in space. To define the position of a body within a moving coordinate system it is necessary to fix a rotation convention. By changing the order of rotations and translations, the final position of a body is changed significantly, as demonstrated in Figure 3.8, and so a single convention must be used consistently. The convention used here, in common with the general practice of vehicle dynamics, is yaw rotation first, followed by pitch rotation then roll rotation. The front frame is then defined by a rotation for the steer axis inclination followed by the steer rotation itself. For the application here, suspension deflection of the motorcycle is not permitted, the small influence of the steering geometry on the pitch of the motorcycle has been neglected, and hence no pitching motion of the motorcycle is considered.

The following code example defines the location of the front frame mass centre. The starting point is the origin of the global coordinate system. In the displaced coordinate system the location of the front frame mass centre can be defined by [32]:

```
G1  :=  <x(t), y(t), 0>
            + R1.(<0, rt*tan(phi(t)), -rt>
               + R2.(<c1, 0, -(h1-rt)>
                  + (Reta.R3.<e, 0, 0>)));
```
(3.7)

In this expression the first vector defines the position of the motorcycle's origin within the global coordinate system (Point a, Figure 3.9). In the second expression, the coordinate system is rotated by the yaw angle using the vector R1, and in this intermediate coordinate system the intermediate origin is displaced to the centre of the toroidal

tyre profile (Point b, Figure 3.9). The third expression rotates the coordinate system by the roll angle (matrix R2), in which a translation moves the coordinate system to the front frame steering joint (Point c, Figure 3.9). Finally, the last expression rotates by the front frame inclination angle (matrix Reta), then by the steer angle of the front frame (matrix R3), followed finally by the location of the front frame mass centre relative to the front frame steering joint (Point d, Figure 3.9).

In order to calculate the kinetic energy of the motorcycle, it is necessary to know the velocities of the centres of mass. Having defined the locations in space of these points, defined now as specific functions of time, it is a simple procedure to obtain the velocities of the points. These are simply the time-derivatives of the position vectors, and can be readily obtained using the derivative function `diff` in Maple:

```
G1_dot  :=  map(diff,G1,t);                                    (3.8)
```

In a similar manner, the angular velocities of the bodies are calculated. The individual angular velocities resulting from yaw, roll and steer were defined earlier, and so the angular velocity of the bodies is simply the combined effect of all these rotations, paying specific attention to the order in which the rotations are applied. Using again the front frame as an example, the angular velocity may be defined as:

```
omega_1  :=  evalm( Steer_Rate
                  + ( tr_R3.tr_Reta.Roll_Rate                  (3.9)
                      + ( tr_R3.tr_Reta.tr_R2.Yaw_Rate)))
```

Similar expressions for the rear frame and the wheels are derived. It should be noted here that the angular velocities of the wheels will be the combination of rotations due to yaw and roll, plus the contribution of their spin velocities about their spin axes.

The energy expressions necessary in the derivation of the Lagrange's equation can now be obtained. The kinetic energies of the bodies are comprised of the individual bodies translational and rotational energies, calculated by $\frac{1}{2}\mathbf{v}^T m_b \mathbf{v}$ and $\frac{1}{2}\boldsymbol{\omega}^T \mathbf{I} \boldsymbol{\omega}$ respectively.

For the front frame, this is coded with

```
T1_Linear := evalm((1/2)*(m1*transpose(G1_dot).G1_dot));
T1_Rotational := evalm((1/2)*(transpose(omega_1).I1.omega_1));
```
(3.10)

where `m1` is the mass of the front frame. Similar terms express the kinetic energies of the rear frame, and the rotational kinetic energy of the wheels.

With regard to the angular velocities of the front and rear wheels, as explained in [80], the kinetic energy of the wheels needs to be included since they form a substantial part of the overall vehicle mass. The masses of the front and rear frames includes the wheels, and so their contribution to the energies of the system by their linear motion and rotation with the frames is accounted for. However, the wheels have additional energy due to rotations about their spin axes, and so this must also be accounted for. Thus, the rotational kinetic energy for the wheels alone, assuming no spin relative to the frames, is calculated. The rotational kinetic energy with the spin included was then calculated and subtraction of the former from the later leaves only the rotational kinetic energy contribution from the wheel spin speed, which is then added to the rotational kinetic energy of the appropriate frame.

The potential energy of the motorcycle is calculated next, and is simply the summation of the front and rear energies, with the wheel masses included in the frame masses. This is obtained from the mass multiplied by gravitational constant g and by the height above ground, which is simply the z-axis component of the body position vector in three dimensional space:

```
Potential := < m1*g*<0 | 0 | -1>.G1 + m2*g*<0 | 0 | -1>.G2 >;
```
(3.11)

To form the necessary components of the Lagrange's equations (3.3b), the energy terms must be differentiated with respect to the state vector $\mathbf{q}$. Again this can be achieved by taking the Jacobian matrix which can be readily implemented in Maple. At this point it is necessary to remove any specific definition of variables as functions of time, such that the energy expressions can be differentiated with respect to the

states. Applying the `jacobian` command, the necessary derivative expression of the kinetic energy is obtained:

```
dT_dq  :=jacobian(Kinetic, q);
```
(3.12)

where **q** is the vector of the degrees of freedom, as seen earlier. The third term in (3.3b) is similarly obtained by taking the Jacobian matrix of the potential energy expression with respect to the state vector.

The first term in (3.3b) requires subtle manipulation of the expressions. As before, the Jacobian matrix of the kinetic energy term, with specific references to functions of time replaced, is taken with respect now to the time-derivative of the state vector. To complete the first term, the time derivative of this new expression must be obtained. However, at this point the terms in the expression are not specific functions of time, and so the time derivative of this expression would result in a zero matrix. Thus, the specific time-dependencies of the terms must first be reinstated, and once done the time derivative of this new expression can then be sought.

There is also one additional term which is included at this point concerning the Rayleigh dissipation energy of the steering damper. This energy is calculated from $\frac{1}{2}c_\delta(\frac{\partial\delta(t)}{\partial t})^2$ where c_δ is the steer damping coefficient, and again the `jacobian` function is used to evaluate the derivatives of this energy with respect to the system degrees of freedom:

```
dR_dqdot  :=  jacobian(Rayleigh_Dissipation, q_dot);
```
(3.13)

The Rayleigh dissipation term is added to the left hand side of equation (3.3b) to obtain the unforced system dynamic response. To complete the modelling, the effects of external forcing on the motorcycle must be accounted for. The virtual power is calculated by the multiplication of the forces by the virtual velocities of the points of application of the force, both linearly and rotationally as appropriate. The positions of the points of application are therefore calculated first, in a process very similar to that used to establish the mass centres of the bodies of the motorcycle (3.7). The variables within these expressions are given as functions of time, enabling the linear velocities of the points to be once again obtained by simply taking the derivative of

the expression with respect to time. The rotations of the points and hence the angular velocities are obtained in a similar process, and combined with the linear velocities to form 6×1 velocity vectors of the linear and angular velocities, where the order of the elements is the x-, y- and z-lateral velocities, and x-, y- and z-axis angular velocities.

The last step in calculating the virtual power is to create a vector of the actual forces and moments acting at the point, with the order of these forces and moments corresponding to the order of the velocities in the 6×1 velocity vector. In the case of the model used here, this refers only to the external tyre contact patch forces. The virtual power is then simply the product of the force and moment vector with the linear and angular velocity vector. By multiplying the velocity vector with the transpose of the force and moment vector, each velocity element is multiplied by the corresponding force/moment element to obtain the single total virtual power for that point. If this point corresponded to the front tyre contact patch, for instance, the same process would also be required for the velocities, forces, moments and resulting virtual power of the rear contact patch.

Summating all the virtual power terms relating to the external forces then allows their inclusion in (3.3b) and hence the formation of the equations of motion for the forced dynamic response of the motorcycle. This equation will be in terms of all degrees of freedom and the associated derivatives.

State Space formulation

Thus far, the equations of motion for the motorcycle are expressed as a 5×1 vector of second-order symbolic equations where each element corresponds to each of the degrees of freedom, and also as a 2×1 vector consisting of two first-order equations relating to the dynamic forces of the front and rear tyres. For the subsequent numerical operations to model the response of the motorcycle, these equations will be formed into a combined state space representation. The five second-order equations will therefore be formed into ten first-order equations, combined with the two first-order tyre equations to result in twelve first-order equations of motion.

Fundamentally, the form of a second-order equation of motion for a generic single degree of freedom system is

$$m_b\ddot{x} + c_b\dot{x} + k_b x = f \tag{3.14}$$

which, when extended to the multiple degrees of freedom case, becomes

$$\mathbf{M}_b\ddot{\mathbf{q}} + \mathbf{C}_b\dot{\mathbf{q}} + \mathbf{K}_b\mathbf{q} = \mathbf{J}_u\mathbf{u} \tag{3.15}$$

where the matrices $\mathbf{M}_b$, $\mathbf{C}_b$ and $\mathbf{K}_b$ are the mass, damping and stiffness matrices of the dynamic system response, the vector $\mathbf{q}$ is the vector of generalised coordinates, and matrix $\mathbf{J}_u$ is the matrix relating the system inputs vector $\mathbf{u}$ to the generalised coordinates of the system.

The first-order state space model is obtained by defining a new state vector, consisting of the states and their first derivatives:

$$\mathbf{x} = \begin{bmatrix} \mathbf{q} \\ \dot{\mathbf{q}} \end{bmatrix} \tag{3.16}$$

Making this substitution, the second order system (3.15) is converted to a first-order system by forming the standard state space model:

$$\begin{bmatrix} \dot{\mathbf{q}} \\ \ddot{\mathbf{q}} \end{bmatrix} = \begin{bmatrix} \mathbf{0} & \mathbf{I} \\ -\mathbf{M}_b^{-1}\mathbf{K}_b & -\mathbf{M}_b^{-1}\mathbf{C}_b \end{bmatrix} \begin{bmatrix} \mathbf{q} \\ \dot{\mathbf{q}} \end{bmatrix} + \begin{bmatrix} \mathbf{0} \\ \mathbf{M}_b^{-1}\mathbf{J}_u \end{bmatrix} \mathbf{u} \tag{3.17}$$

For the problem here, rather than forming individually the matrices $\mathbf{M}_b$, $\mathbf{C}_b$ and $\mathbf{K}_b$, the Jacobian matrix approach can be taken to obtain the equivalent of these more readily. Thus the Jacobian matrix of the 4×1 vector of the equations of motion with respect to the states vector $[\mathbf{q}^T \ \dot{\mathbf{q}}^T]^T$ is taken, resulting in a Jacobian matrix, termed $\mathbf{J}_s$, equivalent in form to $[\mathbf{K}_b \ \mathbf{C}_b]$. Similarly, the Jacobian matrix of the equations of motion with respect to the input vector $\mathbf{u}$ can be taken, to give $\mathbf{J}_u$.

To complete the formation of the state space matrix form, the matrix $\mathbf{M}_b$ is required. This is again readily obtained by taking the Jacobian matrix of the 5×1 equations

of motion with respect to the second-order terms of the generalised coordinates, $\ddot{\mathbf{q}}$. Multiplying the negative inverse of this matrix with the previous Jacobian results in $-\mathbf{M}_b^{-1}\mathbf{J}_s$, a matrix form equivalent to $[-\mathbf{M}_b^{-1}\mathbf{K}_b \ -\mathbf{M}_b^{-1}\mathbf{C}_b]$. The complete state space model can then be formed as

$$\begin{bmatrix} \dot{\mathbf{q}} \\ \ddot{\mathbf{q}} \end{bmatrix} = \begin{bmatrix} \mathbf{0} & \mathbf{I} \\ [\ -\mathbf{M}_b^{-1}\mathbf{J}_s\ ] & \end{bmatrix} \begin{bmatrix} \mathbf{q} \\ \dot{\mathbf{q}} \end{bmatrix} + \begin{bmatrix} \mathbf{0} \\ \mathbf{M}_b^{-1}\mathbf{J}_u \end{bmatrix} \mathbf{u} \tag{3.18}$$

For the case here, the complete problem consists of the five second-order equations of motion and two first-order equations relating to the tyre lateral force responses, and these equations must be solved jointly.

The two additional states relate to the front and rear dynamic lateral tyre forces, and are given as

$$\mathbf{f} = \begin{bmatrix} Y_r \\ Y_f \end{bmatrix} \tag{3.19}$$

Thus, when combined with the previous zero- and first-order terms of the generalised coordinates, the extended state space vector of the motorcycle becomes

$$\mathbf{x}_v = \begin{bmatrix} \mathbf{q} \\ \mathbf{f} \\ \dot{\mathbf{q}} \end{bmatrix} \tag{3.20}$$

The state space model of the combined first- and second-order equations of motion can be solved in the same manner as previously. The Jacobian matrix $\mathbf{J}_s$ of the second-order equations of motion is taken with respect to the now extended state vector $\mathbf{x}_v$, and similarly the Jacobian matrix of the first-order tyre forces equations of motion is taken with respect to $\mathbf{x}_v$ to give $\mathbf{J}_f$

Thus, the complete state space representation of the motorcycle model is achieved with

$$\begin{bmatrix} \dot{\mathbf{q}} \\ \dot{\mathbf{f}} \\ \ddot{\mathbf{q}} \end{bmatrix} = \begin{bmatrix} \mathbf{0}_{5\times7} & \mathbf{I}_{5\times5} \\ \begin{bmatrix} \mathbf{J}_f \end{bmatrix} & \\ \begin{bmatrix} \mathbf{M}_b^{-1}\mathbf{J}_s \end{bmatrix} & \end{bmatrix} \begin{bmatrix} \mathbf{q} \\ \mathbf{f} \\ \dot{\mathbf{q}} \end{bmatrix} + \begin{bmatrix} \mathbf{0} \\ \mathbf{0} \\ \mathbf{M}_b^{-1}\mathbf{J}_u \end{bmatrix} \mathbf{u} \tag{3.21}$$

which is then equivalent to the continuous-time dynamic response model of the motorcycle,

$$\dot{\mathbf{x}}_v = \mathbf{A}_v\mathbf{x}_v + \mathbf{B}_v\mathbf{u} \tag{3.22}$$

where $\mathbf{x}_v$ is the vector of vehicle states, $\mathbf{A}_v$ is the state space dynamic response matrix, $\mathbf{B}_v$ is the state space input response vector and $\mathbf{u}$ is the actual vehicle control input, all in continuous-time.

By modelling the process in this symbolic way, the non-linearity of the equations of motion is retained. The linearisation only occurs once the numerical values of the motorcycle's states are input, which, in subsequent motion simulation, will be conducted at each discrete step of the simulation. Thus, at each simulation step, a new valid linear state space model will be obtained.

Obtaining the symbolic model using the steps outlined above was not entirely straightforward however. For the mass matrix $\mathbf{M}_b$, the inverse is required, and due to the complexity of the equations of motion, the expressions contains many thousands of terms. To find the symbolic inverse of the mass matrix is therefore an incredibly demanding problem from a computational perspective. Consequently, it was found necessary to apply some simplification procedures to assist with this problem.

Specifically, before forming the mass matrix $\mathbf{M}_b$, a vector of the second order terms from the equations of motion vector was extracted. The `expand` operation in Maple was used first, in order to expand any compound or embedded expressions. The `combine` operation was used next, with the trigonometric extension `trig` used, to combine together the trigonometric expressions and thus simplify the number of terms within each element of the vector. The final operation consisted of a Taylor series expansion, to the fourth-order, to further reduce the size of the second-order ex-

pressions, before the Jacobian operation was used on this new vector to obtain the simplified mass matrix $\mathbf{M}_b$. With the reduced size of the elements in the mass matrix, obtaining the inverse of the matrix as required became a task that was achievable within the computational abilities of the software [53] and personal computer used.

Finally, the necessary expressions are exported to Matlab [54], where the numerical operations were conducted to calculate the system's response and hence validate the model generated. Within Matlab, the numerical values for the states, which vary during the simulation, were substituted. As the values would be constantly changing, then obtaining the state space equations symbolically meant that the complicated operation of solving the Lagrange's equations was only required once. The numerical forms could then readily be obtained by substitution of the appropriate state values.

The differential equations resulting from the Lagrange's equations are of a continuous nature, having the form of (3.22). While a motorcycle rider would almost certainly operate in a continuous-time manner, for the purpose of modelling what could be a random road path a discrete-time approach brings useful simplification to the modelling process. Thus, the symbolic continuous-time state space matrices were exported to Matlab [54], the numeric values substituted, and the state space model then converted to discrete-time using the function command `c2dm` built in to Matlab to convert the state space model from continuous- to discrete-time, thus adopting the form

$$\mathbf{x}_v(k+1) = \mathbf{A}_v(k)\mathbf{x}_v(k) + \mathbf{B}_v(k)\mathbf{u}(k) \tag{3.23}$$

where $\mathbf{x}_v(k)$ is the vector of vehicle states, $\mathbf{A}_v(k)$ is the state space dynamic response matrix, $\mathbf{B}_v(k)$ is the state space input response vector and $\mathbf{u}(k)$ is the actual vehicle control input, all at the k^{th} step. The time-step set for this discretisation was $\frac{1}{50}$ s, therefore able to capture oscillations with frequencies up to 25 Hz. The objective of the work was not to investigate the vibrational characteristics of the motorcycle, but to develop a model on which to apply a control strategy. The omission of higher-frequency modes brought about by this frequency threshold was not therefore considered important in the context of the work.

3.4.2 Validation of the Equations of Motion

The model generated was based on a simplified motorcycle model using the application of well-proven principles of Lagrange's theory. However, the execution of these principles, using symbolic software programming, leaves open the potential for errors to creep in, both in the way that the computer code may deal with the mathematical procedures required, and from the possibility for programming errors to have arisen during the model generation. Thus it becomes necessary to ensure that the behaviour of these mathematical models is consistent with expectations, and that any subsequent modelling work conducted will have an accurate base from which to build.

The simplified motorcycle model used (Figure 3.4) was taken from [80]. This work identified the principal vibrational modes of the motorcycle, showing both the frequency and damping of these modes across the typical speed range of the motorcycle. The starting point for the modelling was therefore to replicate the model in [80], employing initially the simple linear tyre model, as in the original work. To compare the model here with the original model by Sharp, the stability modes of the motorcycle were assessed by obtaining the damping and, where appropriate, the frequencies of the principal vibration modes, namely for the wobble, weave and capsize modes originally identified by Sharp. These damping ratios and frequencies are obtained from the eigenvalues of $\mathbf{A}_v$ in the state space equations of motion of the motorcycle.

The real parts of the eigenvalues, representing the damping ratios of the modes, are presented in Figure 3.10. With the advances in computing power since the original work of Sharp, the analysis of the modes over the full speed range with a high resolution can readily be obtained quickly using even a modest personal computer. The results in Figure 3.10 therefore cover the speed range from 2 m/s up to 50 m/s at a resolution of 0.1 m/s, enabling the behaviour of the results to be examined in detail. The response closely resembles the original results in [80], with the capsize, weave and wobble modes readily identified. The root locus plot of the eigenvalues is shown in Figure 3.11. This also replicates the results of Sharp's model, presented in [28].

The capsize mode appears mildly stable at low speeds; the real part of the eigenvalue at 2 m/s is approximately -3.5 and is non-oscillatory. As the speed increases the mode becomes marginally unstable at a speed of approximately 10 m/s and above,

remaining of the order of 0.08 for speeds from 10 m/s and upwards, but is easily stabilised by the rider's control.

The weave mode is mildly unstable at low speed, with real part 2.6 and imaginary part of 1.3 rad/s. The imaginary parts of the modes, indicative of the oscillation frequencies, are shown in Figure 3.11. The weave mode becomes stable at approximately 6 m/s, with increasing stability reaching a maximum at just over 15 m/s of -6.6 with frequency of approximately 11.6 rad/s, before decaying gradually as the speed increases, but remaining still stable.

The wobble mode is stable over the full speed range considered. At 2 m/s the real part of the eigenvalue corresponding to this mode is -5.0 and with frequency of 56.0 rad/s. As the speed increases, the real part reaches a minimum of -6.9 with corresponding frequency of approximately 55.2 rad/s at 13 m/s. The stability of the mode decreases almost linearly as the speed increases further, with a stability margin of -0.8 and frequency 57.9 rad/s at 50 m/s.

Confirmation of these principal modes is obtained by components of the modal plots. Figures 3.12, 3.13 and 3.14 show the magnitudes of the eigenvectors corresponding to the three key modes of capsize, wobble and weave at a forward speed of 25 m/s respectively.

At the forward speed of 25 m/s, the capsize mode (Figure 3.12) is marginally stable and non-oscillatory. The mode results in small angles of roll and steer, and greater levels of yaw angle as the motorcycle gradually veers off to one side from the straight running as a result of this stability mode. Lateral tyre forces and lateral accelerations are low.

The wobble mode (Figure 3.13) is associated with significant oscillation of the front frame relative to the rear frame, while the rear frame remains relatively unaffected, and the motorcycle continues along a straight path, resulting in significant front tyre forces, steer angles and steer rates. Any changes to the yaw and roll angles are therefore small and with rear tyre forces low, features which are all apparent in the modal plot.

The weave mode (Figure 3.14) consists of oscillations of both the front and rear frames in anti-phase, leading to significant variation of both roll and yaw states as

the motorcycle performs a slalom-like progress along a straight path, and significant lateral forces from both the front and rear tyres. The rear tyre force is naturally larger due to the rear weight bias of the motorcycle. The variations in the motorcycle states expected from this mode are apparent in the modal plot.

The results here all correspond very closely to the original results in [80], giving confidence in the correct modelling of the motorcycle when employing the simple tyre model. Having confirmed the correct behaviour of the motorcycle model with the simple tyre, the model was extended by the application of the advanced tyre model.

3.4.3 Validation of the Advanced Tyre Motorcycle Model

With confidence in the programming of the motorcycle model using the simple tyre model and of the coding of the advanced tyre model, the two elements were combined together.

Again, the stability of the model in the speed range 2 to 50 m/s was analysed by considering the eigenvalues of the state space model of the motorcycle's equations of motion, presented in Figure 3.15. The frequency response of the motorcycle model is shown by the root locus plot (Figure 3.16). The identified modes are again confirmed by modal analysis (Figures 3.17, 3.18, 3.19). It is apparent that the results of the eigenvalue analysis differ from the results when the simple tyre model was employed, however the basic traits of the modes are still identifiable and are not dissimilar.

The capsize mode is relatively unchanged with the introduction of the advanced tyre model. The mode shows greater stability at lower speed, with an eigenvalue real part of -4.4 at 2 m/s, compared with -3.5 when employing the simple tyre model. Again, the mode becomes mildly unstable at approximately 10 m/s.

The wobble mode can again be identified, showing a similar trend to the simple tyre model, but with notable differences. This mode was seen to be stable over the full speed range when the simple tyre model was employed, but with the introduction of the advanced tyre model it is unstable at low speeds, rapidly becoming stable as the speed is increased, crossing into the stable range at approximately 6 m/s, then becoming unstable again at approximately 39 m/s. Although the simple tyre model wobble mode did not become unstable again over the speed range considered, it is

apparent from the stability plot (Figure 3.10) that this seems likely to happen at speeds not significantly greater than 50 m/s. The frequency of this oscillatory mode with the advanced tyre model ranges from 50.6 rad/s at 2 m/s, to 49.9 rad/s at the peak stability at 15 m/s, to 54.0 rad/s at 50 m/s.

The behaviour of the weave mode is not dissimilar when the advanced tyre model is employed, though the changes to the stability of the mode are more dramatic over the speed range than with the simple tyre model. The mode is again unstable at low speed, with eigenvalue real part 2.6 and frequency 1.6 rad/s at 2 m/s. The mode becomes stable at just over 5 m/s, with peak stability of the mode at 12 m/s, with corresponding frequency of 12.7 rad/s. The stability of the mode decreases again to reach a stable value of approximately -0.7 with a corresponding frequency of approximately 22.0 rad/s.

Comparing the capsize mode for the simple and advanced tyre models, it is seen that the advanced tyre model shows slightly greater magnitude of the lateral state and slightly lower roll angle state, suggesting slightly larger lateral tyre force generation with roll.

Although the model now presented cannot directly be validated against previous literature, both the original motorcycle model with the simple tyre and the independent advanced tyre model have been separately validated against expected behaviour. The combination of the two would therefore also be expected to show correct representation of the real behaviour of a motorcycle.

3.5 Motorcycle Model Conclusions

This chapter has presented the mathematical model of the motorcycle dynamics that will subsequently be combined with the rider control model. The simplified motorcycle model and the theory used to generate the equations of motion has been presented. The theory for both a simple and an advanced tyre model have also been shown, with the motivation for the advanced model discussed.

Validation of the advanced tyre model was carried out against the original source of the model [60] to confirm the correct implementation of the procedure.

The much-cited model from [80], employing the simple tyre model, was reproduced and validated to ensure initially that the mathematical procedure used was correct. With confidence of the correct response, the validated advanced tyre model was incorporated into the motorcycle model, and the response of the new hybrid model analysed. The net effect of this analysis suggested that, while the dynamic response of the motorcycle model was changed by the introduction of the advanced tyre model, the response is fundamentally changed only subtly from the simple tyre model version. Thus, the motorcycle model generated here utilising the advanced tyre method can justifiably be employed with confidence that the response of the model is suitably representative of a real motorcycle.

Subsequent chapters will present the theory of the rider model and the control strategies that will be employed for this task. The suitability of the control strategies will be assessed by their ability to guide and control a motorcycle model, which will be the model presented here. The results shown in this chapter give confidence of the correct dynamic response of the model, and so the control actions to be generated will therefore be based upon an accurate model of the motorcycle's behaviour, and this control can be applied to the model in the knowledge that the subsequent response will be consistent with what may be expected for a real motorcycle and rider combination.

3.6 Figures

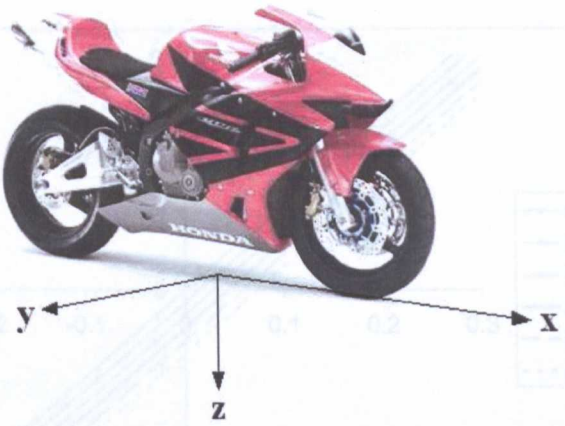

Figure 3.1: SAE coordinate system, motorcycle image from [34]

Figure 3.2: ISO coordinate system, motorcycle image from [34]

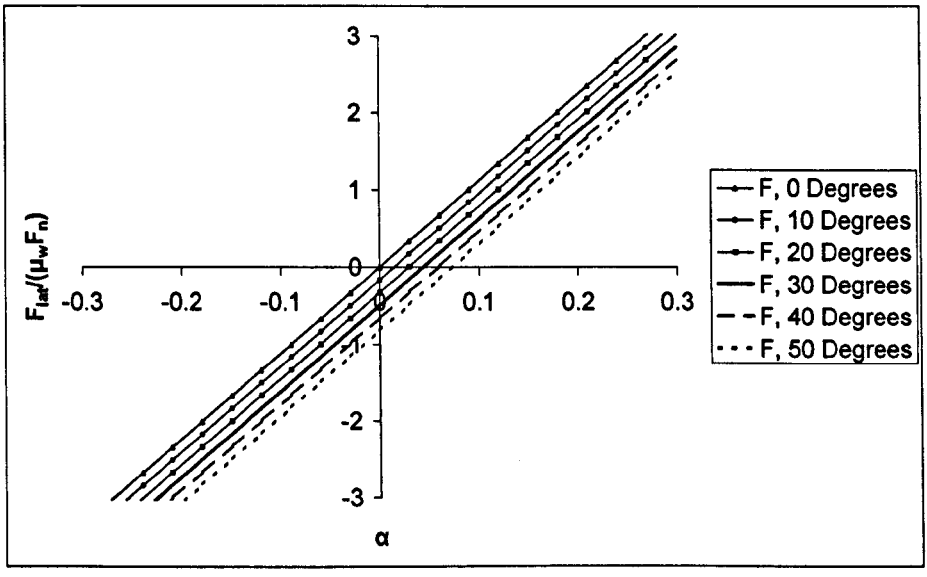

Figure 3.3: Normalised lateral tyre forces with slip ratio and wheel camber, simple tyre model, parameter values as in Appendix A

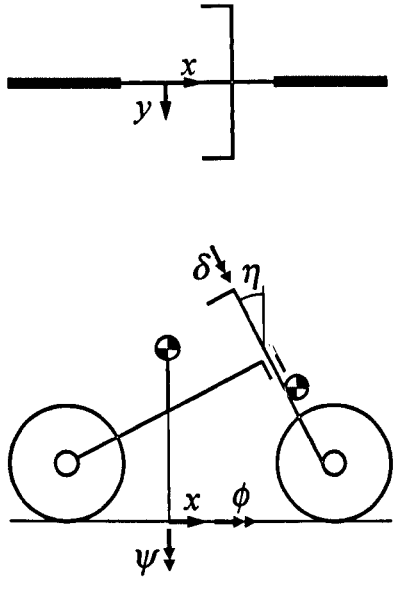

Figure 3.4: Simplified 'bicycle' model of the motorcycle

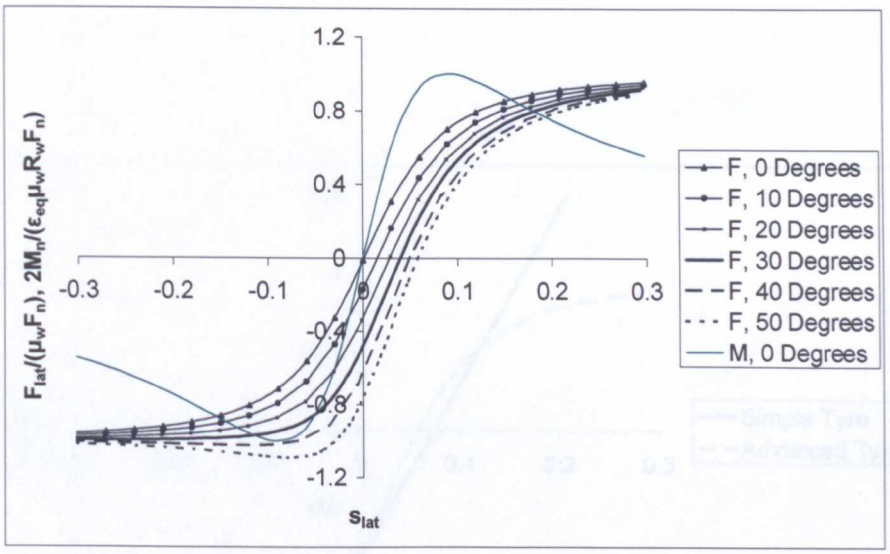

Figure 3.5: Normalised lateral tyre forces with slip ratio and wheel camber, advanced tyre model, parameter values as in Appendix A

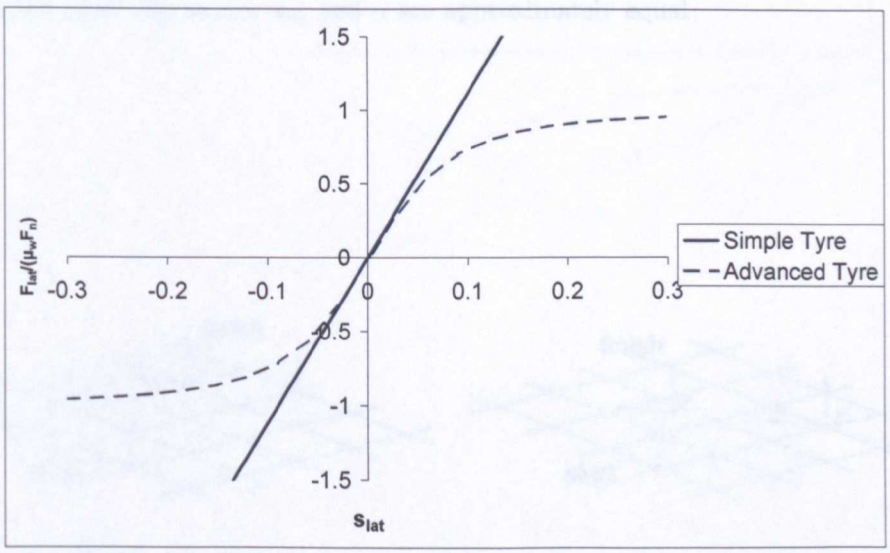

Figure 3.6: Normalised lateral tyre forces comparison, 0^o wheel camber, front tyre, where for small slip angles s_{lat} and α are approximately equal

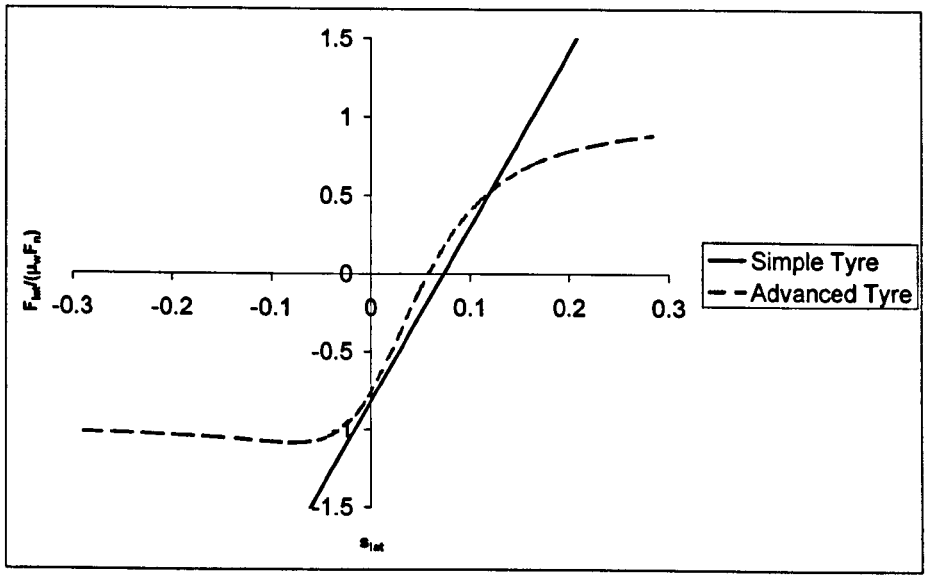

Figure 3.7: Normalised lateral tyre forces comparison, 50° wheel camber, rear tyre, where for small slip angles s_{lat} and α are approximately equal

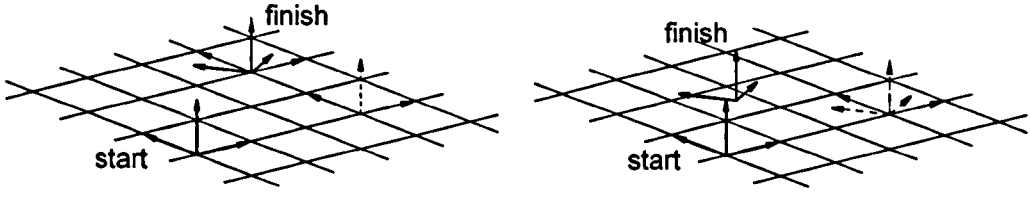

Figure 3.8: Difference in final orientation following translation, translation, rotation (left), and translation, rotation, translation (right)

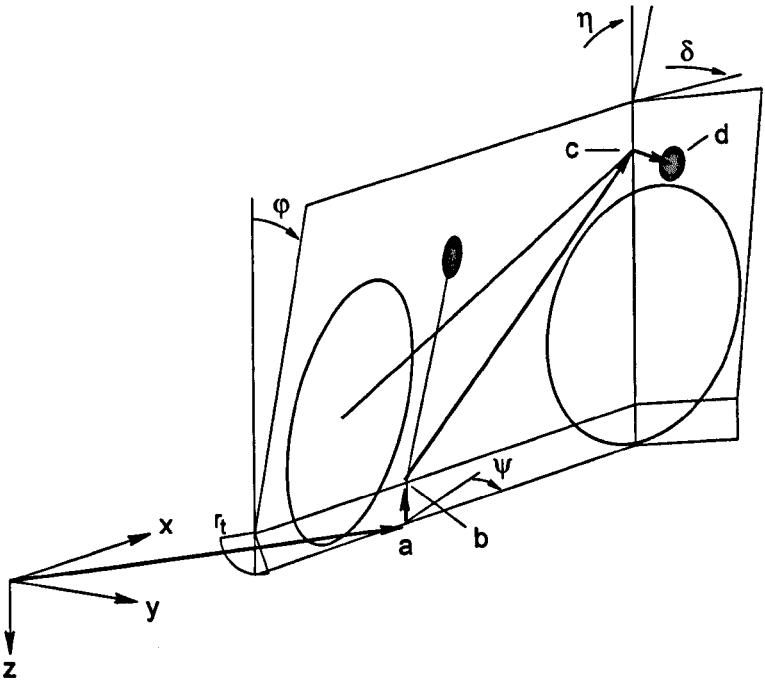

Figure 3.9: Vectorial definition of front frame mass centre in displaced coordinates

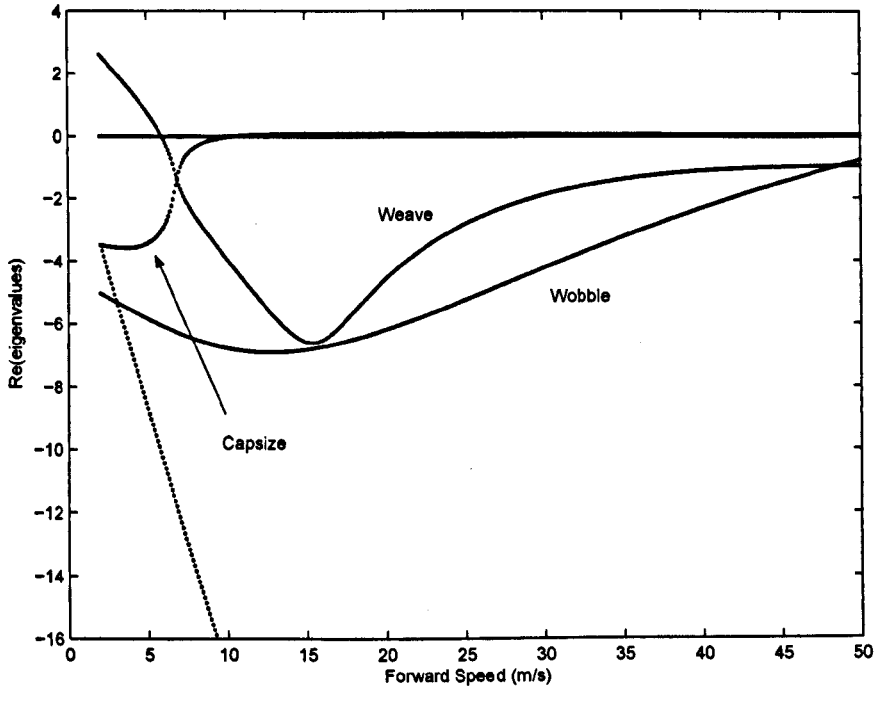

Figure 3.10: Real parts of the system matrix eigenvalues, simple tyre motorcycle model

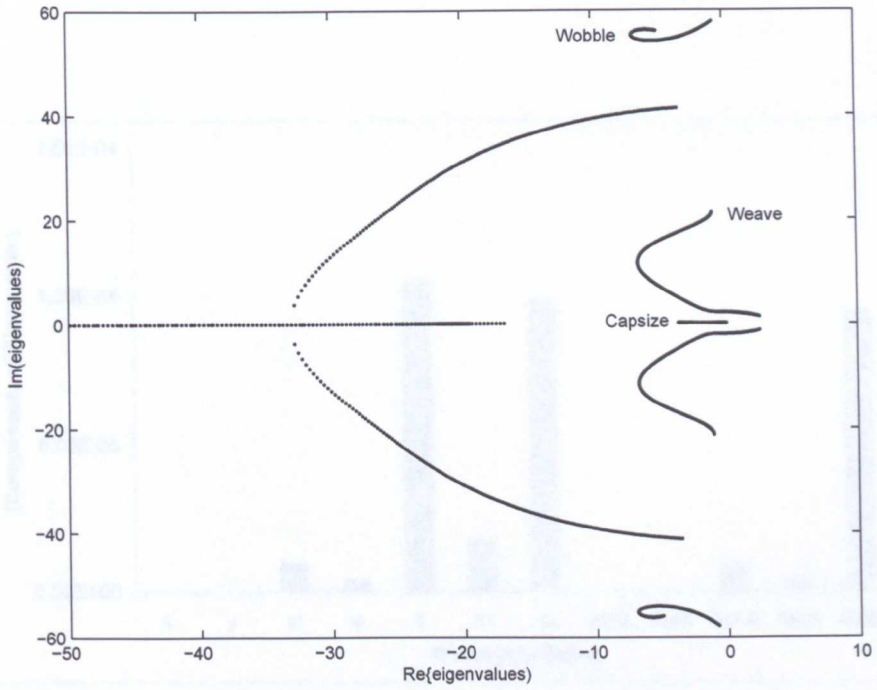

Figure 3.11: Root locus plot of the system matrix eigenvalues, simple tyre motorcycle model

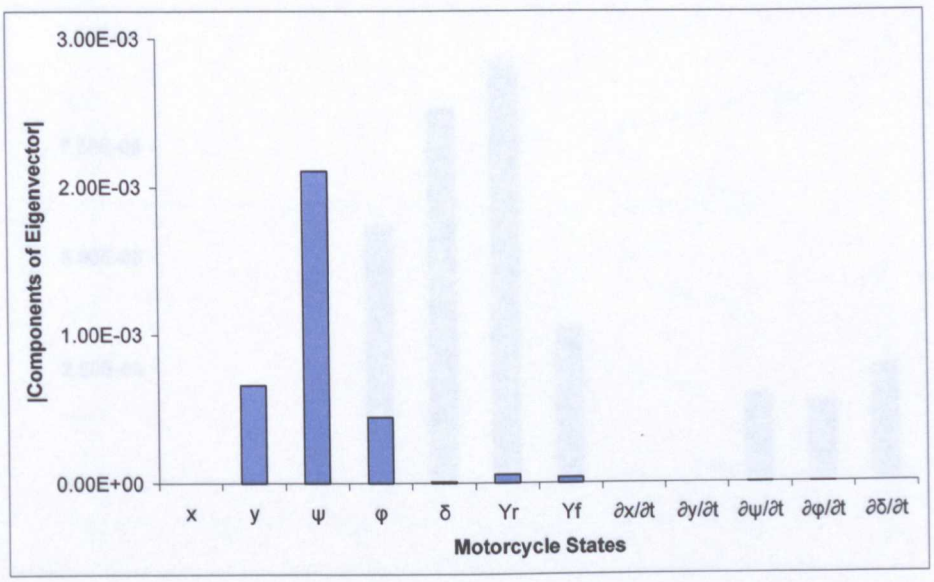

Figure 3.12: Capsize mode, simple tyre. Eigenvalue = 0.079733

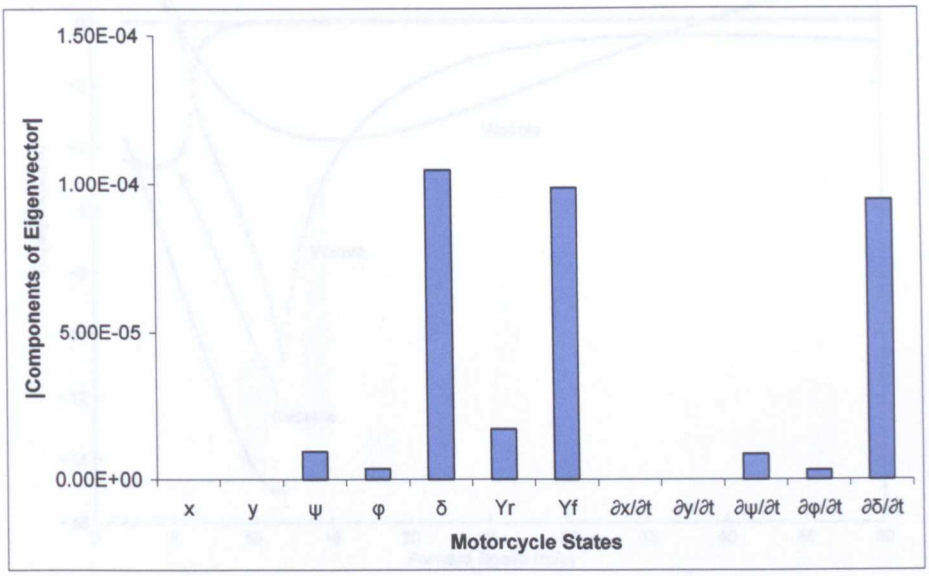

Figure 3.13: Wobble mode, simple tyre. Eigenvalue $= -5.2281 \pm 54.061i$

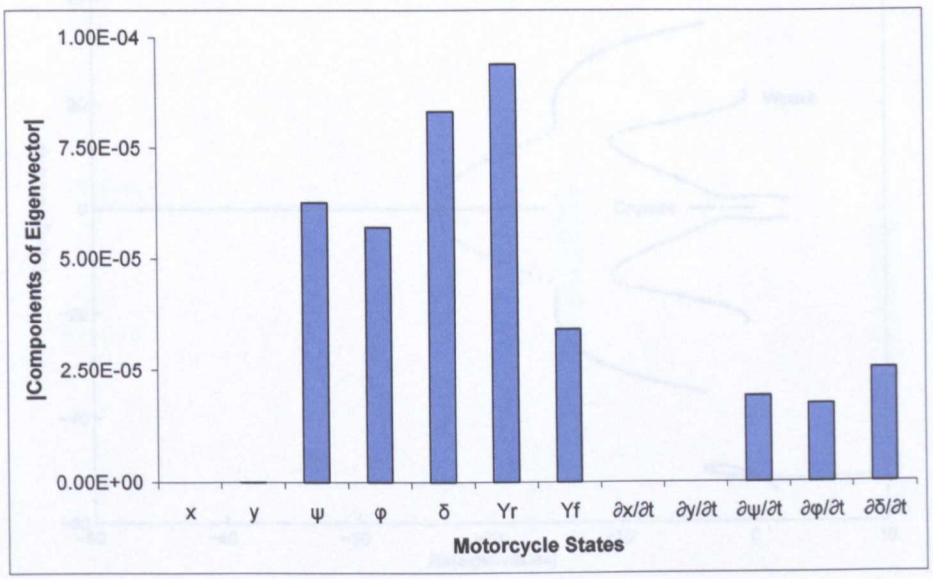

Figure 3.14: Weave mode, simple tyre. Eigenvalue $= -2.8095 \pm 18.067i$

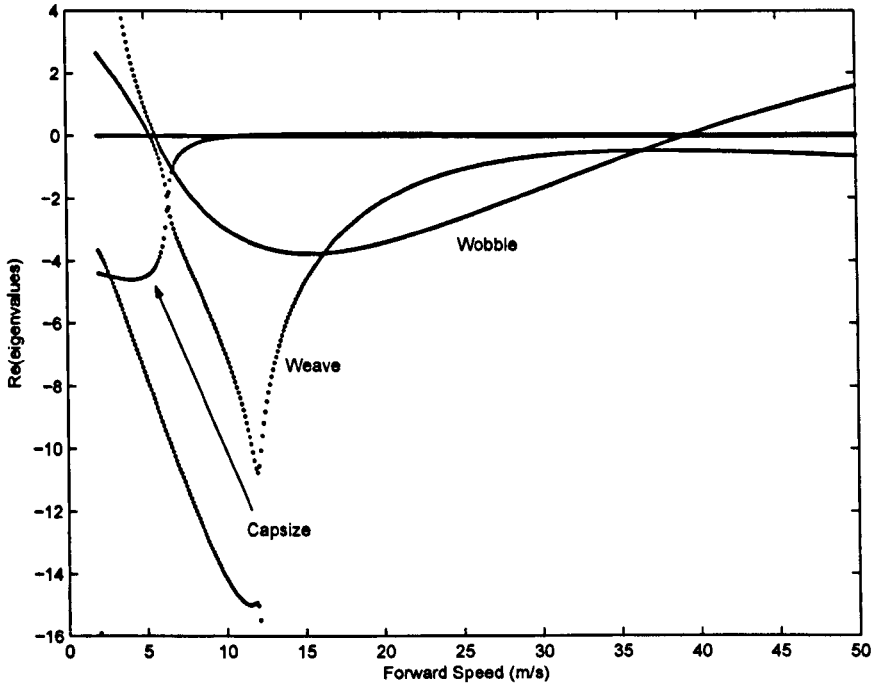

Figure 3.15: Real parts of the system matrix eigenvalues, advanced tyre motorcycle model

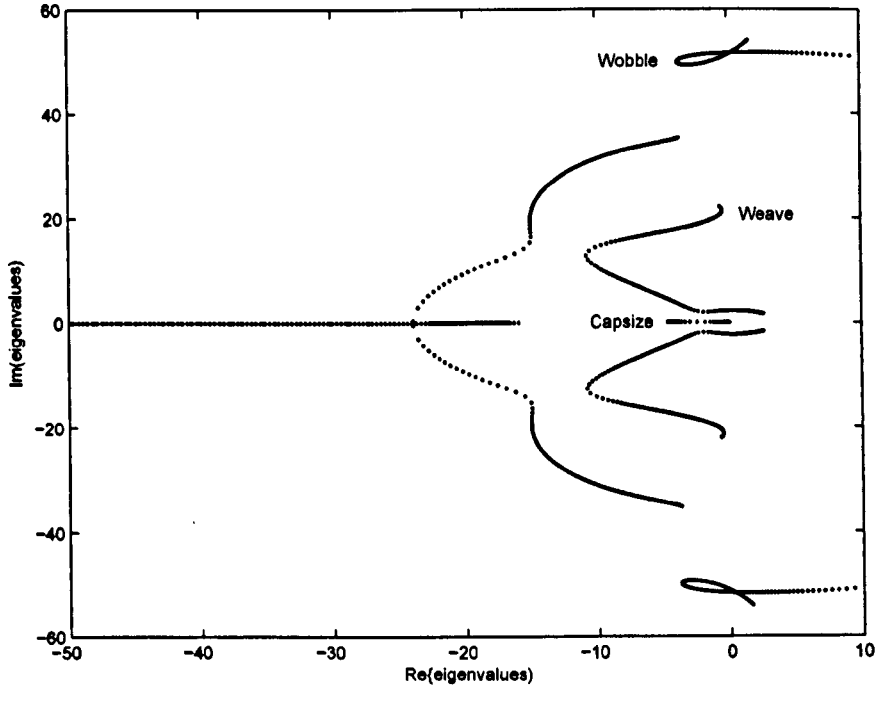

Figure 3.16: Root locus plot of the system matrix eigenvalues, advanced tyre motorcycle model

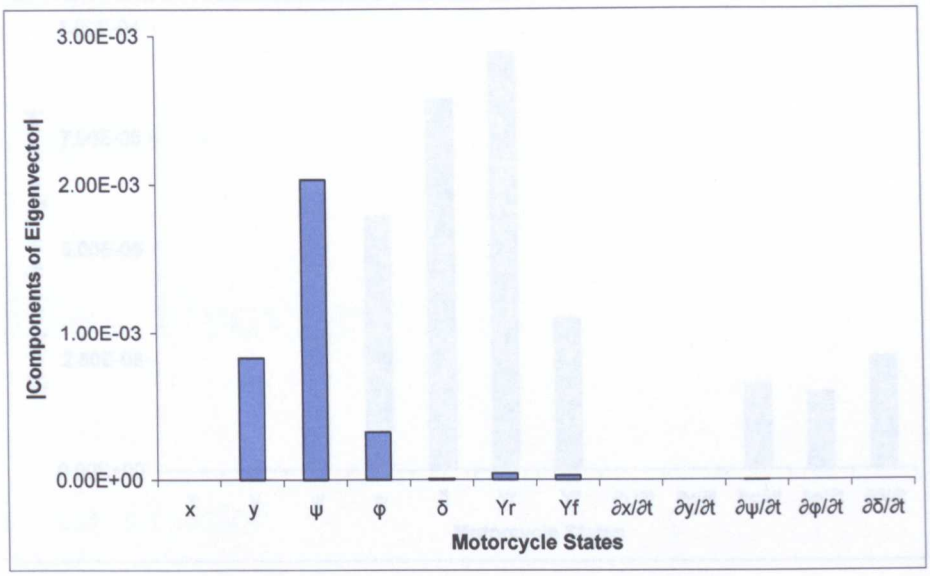

Figure 3.17: Capsize mode, advanced tyre. Eigenvalue = 0.060997

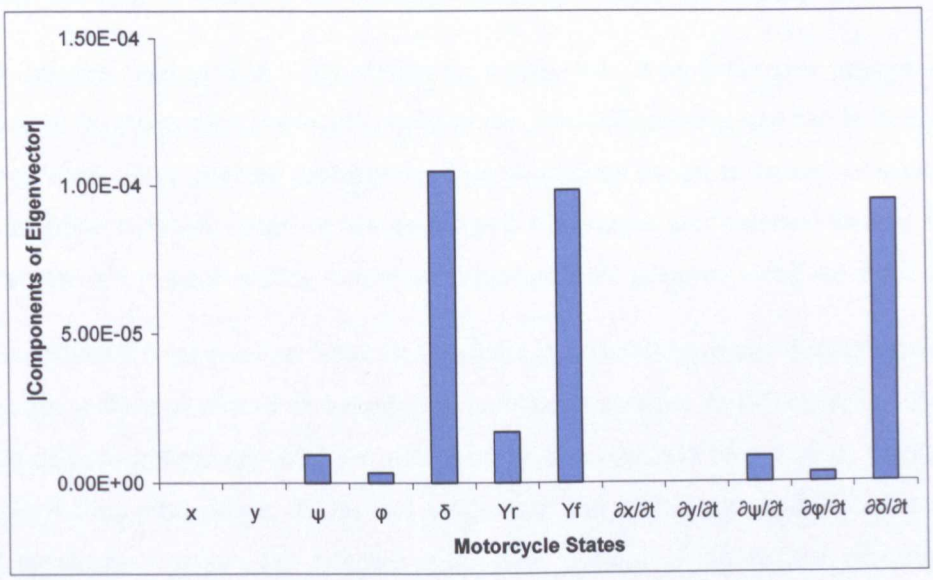

Figure 3.18: Wobble mode, advanced tyre. Eigenvalue = $-2.6314 \pm 49.419i$

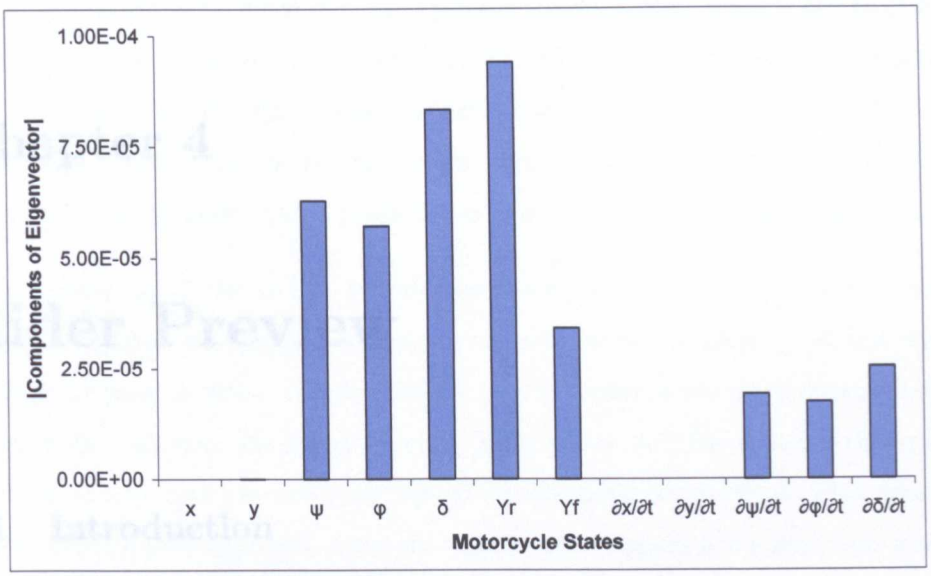

Figure 3.19: Weave mode, advanced tyre. Eigenvalue $= -1.0804 \pm 19.934i$

Chapter 4

Rider Preview

4.1 Introduction

A human rider operates by observing the road ahead and taking in information about the motorcycle's condition. Knowledge of the road information gives him a path to follow, and knowledge of the motorcycle's condition then informs him of his position relative to the intended path, the lean angle, steer angle, yaw angle and associated rates. This information is used to decide what control input to apply in order to achieve the task of following the intended path and control the motorcycle.

It is therefore logical that a simulation controller should replicate this process and thus take in information pertaining to both the road information and the motorcycle states. Thus, the combined motorcycle–rider simulation model is formed to combine the dynamic response model of the motorcycle to internal and external forcing with knowledge of the approaching road path, updated with progress along the road.

A fundamental consideration when undertaking the modelling of any dynamic system of bodies is the selection of an appropriate coordinate system. In principle, the choice of coordinate system should have no effect on the outcome of a system response, provided that dimensions, forces and motions of the bodies are modelled correctly and consistently within the selected coordinate system. With careful selection of a coordinate system, however, the dynamic modelling can, in some cases, be made simpler and more appropriate to the system being represented.

For the case of modelling vehicle drivers, the choice of coordinate system is an interesting question. On the one hand, the task being undertaken by a simulated driver is to follow a chosen road path. The road path is a fixed, global feature, and so it may seem appropriate to model the motorcycle and road preview using global coordinates. This will make the definition of the road path simple and straightforward, and at any time during a simulation the position of the vehicle relative to the globally fixed road path, and thus the performance of the driver control model, can be determined easily.

On the other hand, the task is to simulate the driver's actions. The driver moves within the global coordinates, without necessarily having knowledge of the layout of the road path in global coordinates. It may therefore seem more appropriate to consider the task from the driver's moving perspective and thus consider the motorcycle states and road preview path relative to the driver at all times. This becomes a more complicated approach, since throughout the simulation the road information interpreted by the driver must be continuously redefined into the moving coordinate system, and in addition the global position of the vehicle must be obtained in order to assess the performance of the controller in achieving the overall global path following task. Although the latter approach appears the more complicated, it intuitively seems the more correct method of modelling a vehicle driver.

This chapter will outline the steps necessary to generate a discrete-time state space vehicle model with road preview operating in both a fixed, global coordinate system, and a moving, vehicle-fixed local coordinate system. It will be seen in subsequent analysis of controller methods that the local approach can, in certain circumstances, be necessary for correct performance of the controller.

4.2 Road Preview Shift Register

4.2.1 Global Coordinates Preview

Initially, the rider model operating in global coordinates is considered. This method is the relatively more simple approach and will outline the fundamental principles of the shift-register process used to update the rider's preview information, initially presented in [98] and also later employed in [94].

In driving a vehicle or riding a motorcycle, a driver will base his control actions on knowledge of the vehicle conditions and the requirements of the task, in this case following the road path he can see. It is therefore logical that the system state vector $\mathbf{z}(k)$ should comprise information pertaining to both the vehicle states and the road states. The vehicle state vector $\mathbf{x}_v(k)$ is therefore augmented by the addition of the vector of road preview information, $\mathbf{y}_r(k)$. [98] and [94] included only the lateral deviation of the road path, calculating the yaw angles trigonometrically. Here, the road preview consists of both the lateral position and yaw angle of previewed discrete road information points in global coordinates, such that

$$\mathbf{z}(k) = \begin{bmatrix} \mathbf{x}_v(k) \\ \mathbf{y}_r(k) \end{bmatrix} \tag{4.1a}$$

with

$$\mathbf{y}_r(k) = \begin{bmatrix} y_{r_1}(k) & \psi_{r_1}(k) & y_{r_2}(k) & \psi_{r_2}(k) & \dots & y_{r_{N_p}}(k) & \psi_{r_{N_p}}(k) \end{bmatrix}^T \tag{4.1b}$$

where $y_{r_i}(k)$ and $\psi_{r_i}(k)$ are the lateral positions and yaw angles of the i^{th} road preview point at the k^{th} simulation iteration step (Figure 4.1). The states in the vehicle state vector $\mathbf{x}_v$ are here defined in global coordinates.

The rider's road information is therefore stored as lateral positions of the road and the yaw angle of the road at discrete points along the path, and at the start of the simulation the first N_p road information points are loaded, where N_p is the number of preview points selected.

As the motorcycle progresses along the road in the simulated motion, the road information must be updated in light of the rider's new viewpoint relative to the road, and the new information that has come into his limited preview horizon at the forward limit of this horizon. The spacing of the discrete road points in the initial road preview vector $\mathbf{y}_r$ is such that following one iteration step the road information point y_{r_1} is the road information point y_{r_2} at the previous iteration step, and likewise the previous ψ_{r_2} becomes the new ψ_{r_1}, as depicted in Figure 4.2. Here, the dots represent the discrete points of the road path. Filled dots imply that these road points are stored in the rider model's road preview information vector $\mathbf{y}_r$. At each step, as the road preview is updated the 'old' values of y_{r_1} and ψ_{r_1} are discarded, such that at any simulation iteration step k the rider model has only the preview information for

the N_p road points ahead of him at that step.

A simple shift-register matrix can therefore be used that will perform this change in the vector $\mathbf{y}_r$, such that all the road information is moved up by one position in the vector $\mathbf{y}_r$ with each successive discrete iteration step of the motorcycle simulation. At each step, the previous road information y_{r_1} and ψ_{r_1} are discarded, and the new road information point $y_{r_{N_p}}$ and $\psi_{r_{N_p}}$ must be introduced to the vector $\mathbf{y}_r$. The process is represented by a discrete-time state space expression, formed as

$$\mathbf{y}_r(k+1) = \mathbf{A}_p\mathbf{y}_r(k) + \mathbf{B}_p\mathbf{y}_{rn}(k) \tag{4.2a}$$

where

$$\mathbf{A}_p = \begin{bmatrix} \mathbf{0} & \mathbf{I}_m & \mathbf{0} & \mathbf{0} & & \mathbf{0} \\ \mathbf{0} & \mathbf{0} & \mathbf{I}_m & \mathbf{0} & & \mathbf{0} \\ \mathbf{0} & \mathbf{0} & \mathbf{0} & \mathbf{I}_m & \cdots & \mathbf{0} \\ \mathbf{0} & \mathbf{0} & \mathbf{0} & \mathbf{0} & & \mathbf{0} \\ & & \vdots & & & \vdots \\ \mathbf{0} & \mathbf{0} & \mathbf{0} & \mathbf{0} & & \mathbf{I}_m \\ \mathbf{0} & \mathbf{0} & \mathbf{0} & \mathbf{0} & \cdots & \mathbf{0} \end{bmatrix}_{(N_p m \times N_p m)} \tag{4.2b}$$

$$\mathbf{B}_p = \begin{bmatrix} \mathbf{0} \\ \mathbf{0} \\ \mathbf{0} \\ \mathbf{0} \\ \vdots \\ \mathbf{I}_m \end{bmatrix}_{(N_p m \times m)} \tag{4.2c}$$

$$\mathbf{y}_{rn} = \begin{bmatrix} y_{r_{N_p+1}}(k) \\ \psi_{r_{N_p+1}}(k) \end{bmatrix} \tag{4.2d}$$

and m is the number of parameters in each discrete road preview point, in this case 2. The updating of the road preview points in a global coordinate system is a relatively straight-forward process, since the numerical values of the global coordinates do not change with the motion of the motorcycle, only their location within the road preview information vector will need changing.

Thus, both the motorcycle dynamics model (3.23) and the rider's road preview information (4.2) are now represented by simple discrete-time state space models. In line with the aim to form a single combined motorcycle–preview representation of the riding task, these can now be readily formed into a simple combined rider-preview state space model having the following structure:

$$\begin{bmatrix} \mathbf{x}_v(k+1) \\ \mathbf{y}_r(k+1) \end{bmatrix} = \begin{bmatrix} \mathbf{A}_v(k) & \mathbf{0} \\ \mathbf{0} & \mathbf{A}_p \end{bmatrix} \begin{bmatrix} \mathbf{x}_v(k) \\ \mathbf{y}_r(k) \end{bmatrix} + \begin{bmatrix} \mathbf{B}_v(k) \\ \mathbf{0} \end{bmatrix} \mathbf{u}(k) + \begin{bmatrix} \mathbf{0} \\ \mathbf{B}_p \end{bmatrix} \mathbf{y}_{rn}(k) \tag{4.3}$$

The states of a combined motorcycle–rider model should include both the information the rider has of the vehicle conditions and also of the road conditions, and the combination therefore of both the vehicle state space model and the road preview state space model is a logical and justified approach. The control that the rider applies will be based on both vehicle and road information, and so a control strategy will be developed in order to achieve this condition. This was the approach presented in Sharp [94].

Controller gains will subsequently be calculated that are applied to the states of both vehicle and road preview, thus developing a realistic representation of the control actions of a motorcycle rider.

4.2.2 Local Coordinates Preview

The modelling of the rider's preview in global coordinates, taken from [94], is an elegant and simple way of updating the rider's visual preview. However, it will be seen that it can at times be advantageous to represent the rider's preview in a local coordinate system, and thus the combined rider-preview model will now be converted to operate in a vehicle-fixed coordinate system. It is suggested that this representation of the combined motorcycle–rider system is a more accurate assessment of the manner in which a rider would operate. A similar observation was made by Cole et al. [11], and necessary modelling modifications to a driver preview model were made to accomplish the task. The goal here is the same, though the details of the process are subtly different. Fundamentally, the processes required to achieve the rider-preview model in vehicle-fixed coordinates are not dissimilar to the globally fixed coordinates,

though the details of the process differ.

It should be noted here that the following theory and subsequent simulations relate to a path which is close to straight running, such that small angle theories are assumed without significant loss of accuracy. To extend to a more general model, the x-coordinate of the motorcycle would also be required as a generalised coordinate in the road preview information.

Previously, the motorcycle state vector was combined with the vector of previewed road information to generate the combined motorcycle–preview vector (4.1a). If the motorcycle is set to start from the global origin, then the initial local road preview information is the same as the initial global road preview information. For subsequent iterations, the values $y_{r_i}(k)$ and $\psi_{r_i}(k)$ for $i = 1 \ldots N_p$ in the road preview vector and the motorcycle's state vector $x_v(k)$ will be replaced by the equivalent information in local coordinates, i.e.

$$\mathbf{z}(k) = \begin{bmatrix} \mathbf{x}_l(k) \\ \mathbf{y}_l(k) \end{bmatrix} \tag{4.4a}$$

with

$$\mathbf{y}_l(k) = \begin{bmatrix} y_{l_1}(k) & \psi_{l_1}(k) & y_{l_2}(k) & \psi_{l_2}(k) & \ldots & y_{l_{N_p}}(k) & \psi_{l_{N_p}}(k) \end{bmatrix}^T \tag{4.4b}$$

The order of the elements in the state vector $\mathbf{x}_l(k)$ is unchanged compared with $\mathbf{x}_v(k)$. However, the states in $\mathbf{x}_l$ are now defined relative to the moving coordinate system. The state space model remains essentially the same, but now at each step of the simulation the lateral position and yaw angle states are reset to zero when the new local coordinate system is defined with each iteration step. The steer and roll angles are unchanged.

In the global coordinates system, the road preview information was updated by a simple shift register process (4.2). It is desirable if possible to retain this simple structure, but modify it in such a way that the state vector gives the road preview information in local rather than global coordinates and updates it accordingly.

At the k^{th} step, the rider has preview of N_p points ahead of him, defined in his local coordinate frame at step k. As the motorcycle advances one step to $k+1$, the road preview information must be updated to account for his motion and defined in the

new local coordinate frame at $k+1$.

From step k to step $k+1$, the local coordinates frame will move both laterally and as a rotation due to yaw of the motorcycle. There is also longitudinal motion, accounted for by the shifting of the road preview information in the preview vector. Thus, the shift-register process must move the road preview information in the preview vector as before, but also take account of the change in the preview information on account of the lateral and yaw shifts of the coordinate system with each successive simulation step.

Figure 4.3 shows a diagrammatic representation of the road preview information being updated from step k to $k+1$. When the motorcycle is at the origin of the local coordinates system for step k, both the yaw angle and lateral position are zero in the local coordinates. In the coordinate system of step k, the new lateral position and yaw angle over the step k to $k+1$ are defined as $y_n(k)$ and $\psi_n(k)$. When the motorcycle has moved to step $k+1$, the motorcycle lateral position and yaw angle will be reset to zero, being then at the origin of the local coordinate frame at $k+1$.

Thus, the preview information of the i^{th} preview point for the $(k+1)^{th}$ step (which was the $(i+1)^{th}$ point at the step k) can be calculated as

$$\begin{aligned} y_{l_i}(k+1) &= y_{l_{i+1}}(k) - y_n(k) - \psi_n(k)d_i \\ \psi_{l_i}(k+1) &= \psi_{l_{i+1}}(k) - \psi_n(k) \end{aligned} \tag{4.5}$$

where $d_i = (i-1)vt$, where v is the forward speed, assumed constant, t is the discrete time step, and hence (vt) is the distance travelled in one iteration step.

The equivalent expressions for the global coordinate system were

$$\begin{aligned} y_{r_i}(k+1) &= y_{r_{i+1}}(k) \\ \psi_{r_i}(k+1) &= \psi_{r_{i+1}}(k) \end{aligned} \tag{4.6}$$

Thus, the aim is to modify the state space representation of the combined motorcycle–preview model to perform this calculation for all the previewed road information points and thus modify the shift-register to operate in local coordinates.

The vehicle state vector already includes both the lateral displacement and yaw angles of the motorcycle, and so the obvious way in which to achieve this would be a simple

modification to the lower part of the state space matrix **A** to use these values and hence modify the road preview. This could be achieved with

$$\begin{bmatrix} \mathbf{x}_l(k+1) \\ \mathbf{y}_l(k+1) \end{bmatrix} = \begin{bmatrix} \mathbf{A}_v(k) & \mathbf{0} \\ \mathbf{A}_l(k) & \mathbf{A}_p \end{bmatrix} \begin{bmatrix} \mathbf{x}_l(k) \\ \mathbf{y}_l(k) \end{bmatrix} \tag{4.7a}$$

The states $y_n(k)$ and $\psi_n(k)$ are calculated by the discrete-time state space model over the iteration step from k to $k+1$. Strictly, they should perhaps be defined as terms at $k+1$, but defining them as terms at k avoids the confusion as to which reference frame they are in. For confirmation, $y_n(k)$ and $\psi_n(k)$ are the lateral displacement and yaw angle of the motorcycle achieved over the step k to $k+1$, but in the reference frame of step k, before the states are reset to local values (zero) in the new local frame at $k+1$. The matrix $\mathbf{A}_l(k)$ that will update the local road preview in accordance with (4.5) and for $j = 1,..,n$, where n is the number of vehicle states, is

$$\mathbf{A}_l(k) = \begin{bmatrix} -\mathbf{A}_v(k)(1,j) \\ -\mathbf{A}_v(k)(2,j) \\ -\mathbf{A}_v(k)(1,j) - vt\mathbf{A}_v(k)(2,j) \\ -\mathbf{A}_v(k)(2,j) \\ \vdots \\ -\mathbf{A}_v(k)(1,j) - (N_p-2)vt\mathbf{A}_v(k)(2,j) \\ -\mathbf{A}_v(k)(2,j) \\ -\mathbf{A}_v(k)(1,j) - (N_p-1)vt\mathbf{A}_v(k)(2,j) \\ -\mathbf{A}_v(k)(2,j) \end{bmatrix}_{(N_p m \times n)} \tag{4.7b}$$

Thus $\mathbf{A}_v(k)(1,j)$ and $\mathbf{A}_v(k)(2,j)$ refer to the rows in the $\mathbf{A}_v(k)$ matrix calculating the lateral position (row 1) and yaw angle (row 2) respectively. The matrix $\mathbf{A}_p$ is unchanged. This then correctly updates the road preview information in local coordinates following one iterative vehicle step to achieve the structure of (4.5).

Following the iteration step, the vehicle states relating to the vehicle position must then be reset in local coordinates, and are therefore set to zero. This refers only to the lateral position and yaw angle states of the motorcycle; all other states (roll angle, steer angle, tyre forces and velocities) must not be reset. This does not imply that the corresponding rows of the state space matrices are also zero: the elements in these rows consists of terms relating to all the generalised coordinates, not all of

which are set to zero.

To complete the iteration step, the new road information point as a result of the rider's forward motion must be included at the forward limit of his preview horizon. In the same manner that the information in the combined vehicle-state vector is modified, the new information point must also be converted to the new coordinate system.

The preview points within the rider's preview are, with each successive iteration step, converted from one set of local coordinates to the new coordinate system and need only be adjusted to account for the changes in lateral position and yaw angle over that iteration step. The new preview information fed into the rider's preview at the limit of the horizon must however be converted from the global coordinates to the new local coordinate system. This requires a similar calculation to that employed on the rest of the preview information, but making use of the global lateral position and global yaw angle of the motorcycle in the adjustment made to the road information.

Assuming that the trajectory is close to straight running such that small angle theory can be assumed without significant loss of accuracy, the new global lateral position y_g and yaw angle ψ_g of the motorcycle at the step $k+1$ can be achieved from the values at k, i.e. $y_g(k)$, plus the change in the local values over the iteration step k to $k+1$ which, as before, are termed $y_l(k)$ and $\psi_l(k)$. Strictly, they are the state values when the motorcycle is at the position $k+1$, but in the reference frame of k, before they are reset to zero again in the new local coordinate frame at step $k+1$ (Figure 4.4), such that

$$\begin{aligned} y_g(k+1) &= y_l(k) + y_g(k) + \psi_g(k)vt \\ \psi_g(k+1) &= \psi_l(k) + \psi_g(k) \end{aligned} \tag{4.8}$$

Thus, the new preview information point fed in to the rider's preview at the limit of the horizon at the step $k+1$ must be transferred from the global coordinates to the local coordinates at the step $k+1$ (Figure 4.5), achieved with

$$\begin{bmatrix} y_{l_{N_p}}(k+1) \\ \psi_{l_{N_p}}(k+1) \end{bmatrix} = \begin{bmatrix} y_{r_{N_p}}(k+1) - y_g(k+1) - vT_p\psi_g(k+1) \\ \psi_{r_{N_p}}(k+1) - \psi_g(k+1) \end{bmatrix} \tag{4.9a}$$

which, by substitution of (4.8), results in

$$\begin{bmatrix} y_{l_{N_p}}(k+1) \\ \psi_{l_{N_p}}(k+1) \end{bmatrix} = \begin{bmatrix} y_{r_{N_p}}(k+1) - \{y_{l_1}(k+1) + y_g(k)\} - N_p v t\{\psi_{l_1}(k+1) + \psi_g(k)\} \\ \psi_{r_{N_p}}(k+1) - \{\psi_{l_1}(k+1) + \psi_g(k)\} \end{bmatrix} \tag{4.9b}$$

The global position and yaw angles are appended onto the end of the rider-preview state vector, such that

$$\begin{bmatrix} \mathbf{x}_v(k) \\ \mathbf{y}_l(k) \\ \mathbf{y}_g(k) \end{bmatrix} = \begin{bmatrix} y(k) & \psi(k) & y_{l_1}(k) & \psi_{l_1}(k) & \dots & y_{l_{N_p}}(k) & \psi_{l_{N_p}}(k) & y_g(k) & \psi_g(k) \end{bmatrix}^T, \tag{4.9c}$$

and thus the complete discrete-time matrix structure for operating in local coordinates is achieved with

$$\begin{bmatrix} \mathbf{x}_v(k+1) \\ \mathbf{y}_l(k+1) \\ \mathbf{y}_g(k+1) \end{bmatrix} = \begin{bmatrix} \mathbf{A}_v(k) & \mathbf{0} & \mathbf{0} \\ \mathbf{A}_l(k) & \mathbf{A}_p & \mathbf{A}_n \\ \mathbf{A}_g(k) & \mathbf{0} & \mathbf{I}_m \end{bmatrix} \begin{bmatrix} \mathbf{x}_v(k) \\ \mathbf{y}_l(k) \\ \mathbf{y}_g(k) \end{bmatrix} + \begin{bmatrix} \mathbf{B}_v(k) \\ \mathbf{0} \\ \mathbf{0} \end{bmatrix} u(k) + \begin{bmatrix} \mathbf{0} \\ \mathbf{B}_n \\ \mathbf{0} \end{bmatrix} \mathbf{y}_{rn}(k) \tag{4.10a}$$

where $\mathbf{A}_v(k)$ is the vehicle discrete-time dynamics matrix, $\mathbf{B}_v(k)$ is the discrete-time dynamics input vector. Matrices $\mathbf{A}_l(k)$ and $\mathbf{A}_p(k)$ are as defined previously, and, with $j = 1, .., n$ as before,

$$\mathbf{A}_n = \begin{bmatrix} 0 & 0 \\ 0 & 0 \\ 0 & 0 \\ 0 & 0 \\ \vdots & \\ 0 & 0 \\ 0 & 0 \\ -1 & -vN_pt \\ 0 & -1 \end{bmatrix}_{(N_p m \times m)} \tag{4.10b}$$

,

$$\mathbf{A}_g(k) = \begin{bmatrix} \mathbf{A}_v(k)(1,j) + N_p v t \mathbf{A}_v(k)(2,j) \\ \mathbf{A}_v(k)(2,j) \end{bmatrix}_{(m \times n)} \tag{4.10c}$$

,

$$\mathbf{B}_n = \begin{bmatrix} 0 & 0 & 0 & 0 & \cdots & 0 & 0 & 0 & 1 \\ 0 & 0 & 0 & 0 & & 0 & 0 & 1 & 0 \end{bmatrix}^T_{(N_p m \times m)} \tag{4.10d}$$

4.3 Rider Preview Conclusions

This chapter has covered the detail regarding the rider's road preview, and the manner in which it is formulated into a discrete-time state space model in line with the motorcycle dynamics (Chapter 3). The theory of this shift-register process and the combination with a vehicle dynamics model was detailed in [98] and considered the global coordinates system. The inputs to the combined motorcycle–rider system considered here consist of the road information and the rider's steer torque control input.

The steer torque control input will be determined by the use of a control strategy, representing the control process of the motorcycle rider. Two control theories will be analysed; optimal control, covered in Chapter 5, and predictive control, detailed in Chapter 6. Thus, the combined motorcycle–preview model presented in this chapter will be the platform on which the two control strategies will be modelled and evaluated.

The rider's road preview has also been presented in a local coordinates form. A similar local-coordinates approach was taken in [11], where the road preview information was retained in a global coordinates system, but converted to local coordinates when being used to calculate the control inputs. Thus, the approach used here, for which the road information itself is in local coordinates, represents a departure from the previous literature.

The majority of the modelling will be conducted in a global coordinates system, as

this represents the simpler of the two approaches. In principle the choice of coordinate system should have no effect on the performance of the system, provided that any measurements or calculations made are consistent with the choice of coordinate system. However, it will be seen in Chapter 5 that the use of a local coordinates road preview system can have significant benefits to the path following accuracy of a limited-preview optimal control strategy due to assumptions made in the modelling of the controller, and so the inclusion of a local coordinates model is included here for subsequent use.

4.4 Figures

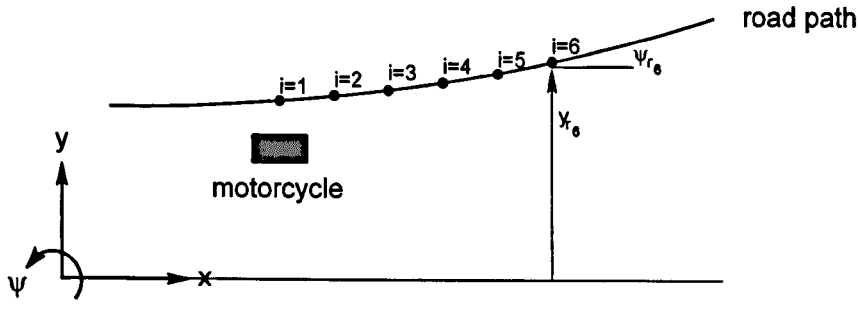

Figure 4.1: Road preview information in discrete steps for $N_p = 6$

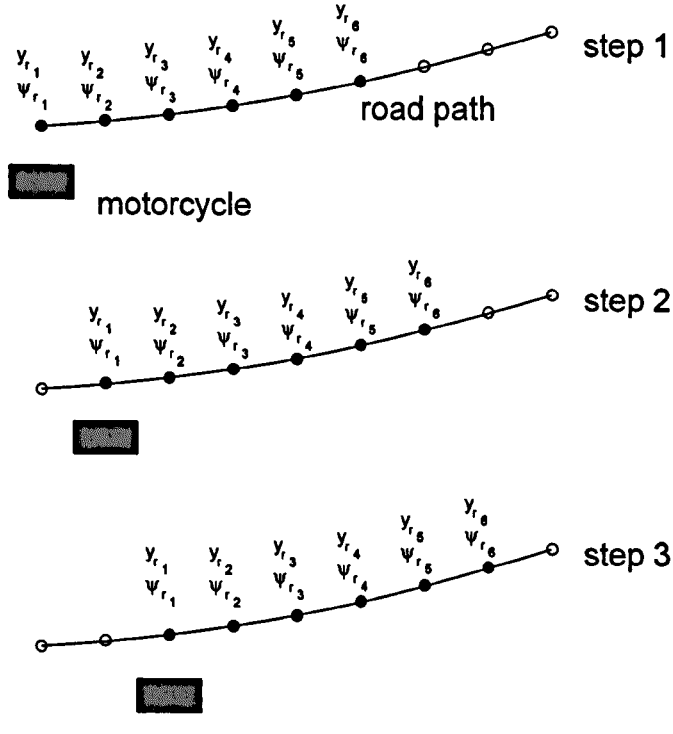

Figure 4.2: Update of road preview information in discrete steps for $N_p = 6$

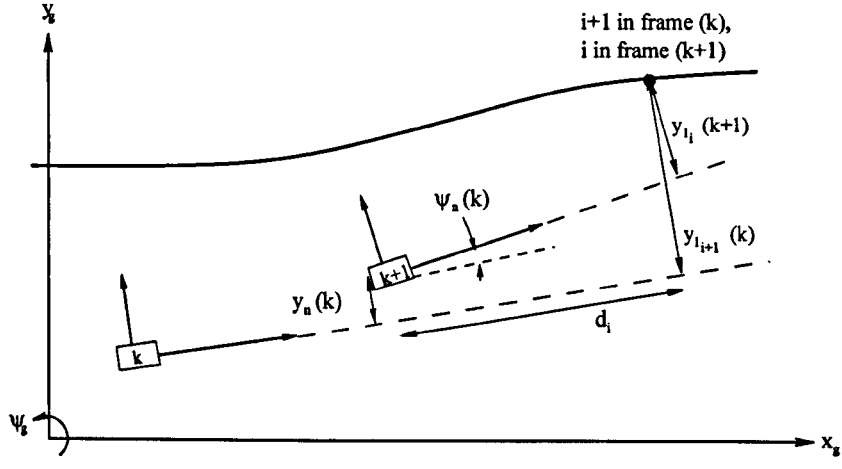

Figure 4.3: Update of road preview in local coordinates

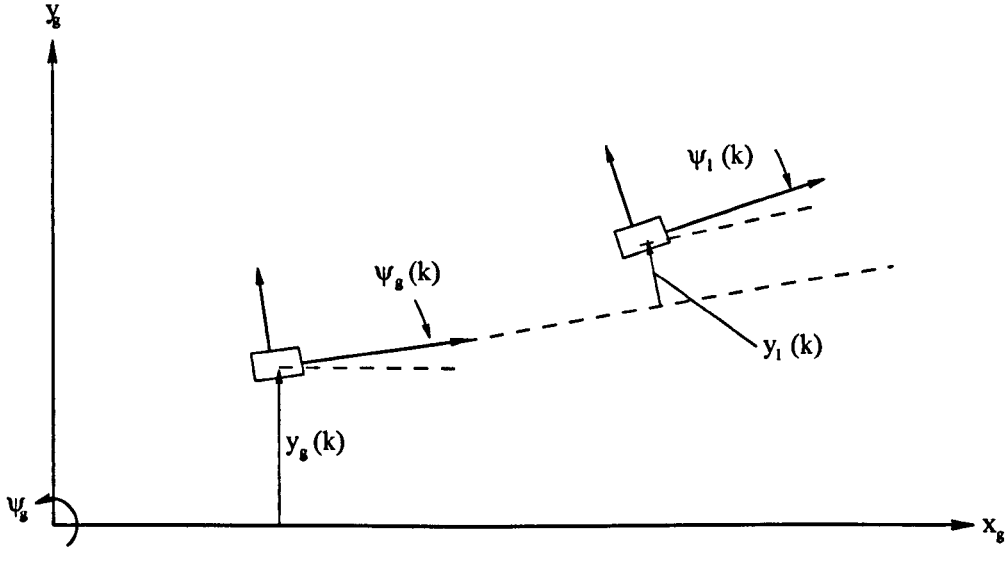

Figure 4.4: Update of motorcycle global position when moving one step ahead in reference frame of step k using a local coordinates approach

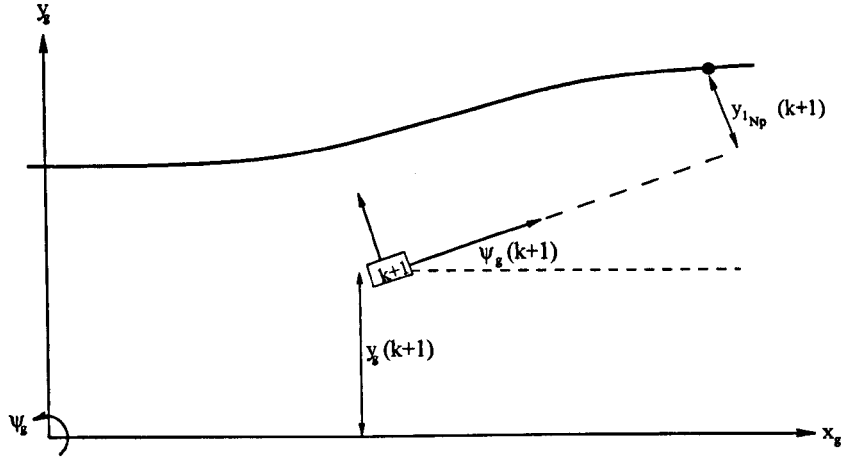

Figure 4.5: Conversion of new preview point information from global to local coordinates

Chapter 5

Optimal Control Rider Model

5.1 Introduction

The application of optimal control techniques is widespread in the field of control engineering and for good reason. Optimal control is a control strategy capable of balancing a number of performance requirements in order to generate a system input that will strike the best balance between the often conflicting requirements of the controlled system.

Typically, an optimal control technique can be used to balance the requirements of system accuracy against control effort required. These two factors commonly act against each other, with more accurate control requiring a greater control force. Weighting parameters are applied to the output and input variables to permit tuning of the control system, enabling the controller to be biased towards high performance accuracy or conversely to minimise the control inputs. Furthermore, if a number of performance parameters are present, the relative importance of these can be tuned using the weighting factors, and likewise for multiple control inputs.

These features make optimal control a suitable approach for the modelling of a vehicle driver. A vehicle driver has broadly two choices. On the one hand, he can follow the road path very accurately, though this may be at a high cost with regard to his steer control inputs. Conversely, he may elect to cut corners of the road path, simplifying his control inputs but at a cost to the accuracy of his path following. Thus, the optimal control strategy for this application will aim to balance path following

accuracy against steer effort input.

The chapter will begin by introducing the theory of the optimal control approach, including both the generation of the cost function and associated relevance to the control problem, and how the optimal controller gains are calculated in order to provide the theoretically optimal control input. An extensive parameter study is conducted to extend the work of Sharp [94] and to obtain a fuller insight into the behaviour and suitability of the optimal control approach for a range of situations, including variations of the preview horizon length, the forward speed and the cost function error weighting parameters. The results that are presented will form a benchmark against which the predictive control approach, to be covered in Chapter 6, can be compared. At the time of writing the predictive control approach has not specifically been applied to the modelling of a motorcycle rider, and will therefore form the main area of interest in this thesis. The direct comparisons between the optimal control approach presented in this chapter, and the predictive control approach, detailed in Chapter 6, will be drawn in Chapter 7, and will ultimately aim to determine the more effective control strategy for modelling a motorcycle rider.

5.2 Optimal Control Theory

An optimal controller is a mathematical means of generating a controlling input to a system that will balance the requirements of system accuracy against control effort input. This balance is achieved by generating a cost function, consisting of accuracy and input effort components, which is to be minimised by the controller. Weighting factors applied to both the output and input variables allow the contribution in the cost function of the individual elements to be varied, thus affecting the relative contribution of output and input variables to the overall cost. Consequently, a greater bias can be applied to inputs or outputs with appropriate selection of weighting parameters.

This chapter begins by presenting the optimal control theory for an arbitrary dynamic system. The specific application to the motorcycle riding task will be detailed in Section 5.2.3.

For a general discrete-time system at the k^{th} iteration step with states $\mathbf{x}(k)$ and

control input $\mathbf{u}(k)$, the calculated system outputs $\mathbf{y}(k)$ and system states $\mathbf{x}(k+1)$ following one iteration step can be expressed as [95]

$$\begin{aligned} \mathbf{x}(k+1) &= f[\mathbf{x}(k), \mathbf{u}(k), k] \\ \mathbf{y}(k) &= \Phi[\mathbf{x}(k), \mathbf{u}(k), k] \end{aligned} \tag{5.1}$$

The equations of motion can be represented by a linearised state space expression which will capture the system dynamics and provide the required system outputs, having the form

$$\mathbf{x}(k+1) = \mathbf{A}(k)\mathbf{x}(k) + \mathbf{B}(k)\mathbf{u}(k) \tag{5.2a}$$

$$\mathbf{y}(k) = \mathbf{C}(k)\mathbf{x}(k) + \mathbf{D}(k)\mathbf{u}(k) \tag{5.2b}$$

where the matrices $\mathbf{A}(k)$, $\mathbf{B}(k)$, $\mathbf{C}(k)$ and $\mathbf{D}(k)$ represent the discrete-time state space matrices at the k^{th} step as shown in Chapter 3.

In general control terms, accurate system performance is usually achieved with a high control cost; accurate control of a robot arm, for instance, would require large actuator forces if rapid but accurate movement is required. Similarly, in following a curving road path significant steer inputs may be required if the path is to be followed accurately. In the case of twin-track vehicles, the steering is achieved by control of the steer angle, whereas for the case of a motorcycle the directional control is achieved via the control of the steer torque applied to the handlebars. These torque inputs however can be reduced if some element of corner-cutting is made in order to reduce the complexity of the path to be followed, and the optimal control technique therefore seeks to calculate an appropriate system input $\mathbf{u}(k)$ that will provide a suitable compromise between the conflicts of system accuracy and control effort, based on weighting values to define the relative importance of system performance characteristics.

The standard approach used, taken from [95], is to define a cost function incorporating the sum of the weighted squares of calculated system outputs and measured system inputs, expressed as

$$J(k) = \frac{1}{2}\Big(\mathbf{y}^T(k)\mathbf{Q}(k)\mathbf{y}(k) + \mathbf{u}^T(k)\mathbf{R}(k)\mathbf{u}(k)\Big) \tag{5.3}$$

where $J(k)$ is the cost function, $\mathbf{y}(k)$ is the vector of measured system outputs, $\mathbf{u}(k)$ is the vector of system inputs, and $\mathbf{Q}(k)$ and $\mathbf{R}(k)$ are the weighting matrices on $\mathbf{y}(k)$ and $\mathbf{u}(k)$ respectively, all at the k^{th} iteration step. In the general case, both $\mathbf{Q}(k)$ and $\mathbf{R}(k)$ are symmetric positive semi-definite matrices. In the applications that will follow, they are diagonal matrices with the elements on the diagonal corresponding to the weightings on the states and control inputs, q_1, q_2 ... q_m and r_1, r_2 ... r_p respectively, with m the number of controlled outputs and p the number of control inputs in the cost function.

With $\mathbf{D}(k) = \mathbf{0}$, since the required output information is contained solely within the system states, and making the substitution $\mathbf{y}(k) = \mathbf{C}(k)\mathbf{x}(k)$, the cost function can be expressed as

$$J(k) = \frac{1}{2}\Big(\mathbf{x}^T(k)\{\mathbf{C}^T(k)\mathbf{Q}(k)\mathbf{C}(k)\}\mathbf{x}(k) + \mathbf{u}^T(k)\mathbf{R}(k)\mathbf{u}(k)\Big) \tag{5.4}$$

The output matrix $\mathbf{C}(k)$ and weighting matrices $\mathbf{Q}(k)$ and $\mathbf{R}(k)$ remain constant in this application, and so the identifier (k) can be omitted for clarity. Over a predetermined number of iterations, the optimum performance is sought that minimises the cost over the sum of all the iterations, and so the cost function becomes

$$J = \frac{1}{2}\sum_{k=0}^{N-1}\Big(\mathbf{x}^T(k)\{\mathbf{C}^T\mathbf{Q}\mathbf{C}\}\mathbf{x}(k) + \mathbf{u}^T(k)\mathbf{R}\mathbf{u}(k)\Big) \tag{5.5}$$

which can be expressed as

$$J = \sum_{k=0}^{N-1}\Theta[\mathbf{x}(k), \mathbf{u}(k), k] \tag{5.6}$$

In the general case, a cost can be placed on the final system states after a predetermined number N of iterations, such that the cost function is extended to

$$J = \theta[\mathbf{x}(N), \mathbf{u}(N), N] + \sum_{k=0}^{N-1}\Theta[\mathbf{x}(k), \mathbf{u}(k), k] \tag{5.7}$$

Due to constraints within a system, the minimum cost and therefore the theoretical optimal solution may not be a feasible option for that system, and therefore some

constraint must be placed upon the calculation of the optimal gains to account for these. The main physical constraints on a system are the equations of motion; the response of a system cannot violate the equations of motion, and thus the optimal control solution must therefore take account of these constraints. These are included by appending the equations of motion into the cost function, multiplied by an appropriate factor, the Lagrangian multiplier vector $\boldsymbol{\lambda}(k)$. The complete cost function, combining costs on system states, system input and the dynamics of the system, is thus given by the extension of (5.7):

$$J = \theta[\mathbf{x}(N), \mathbf{u}(N), N] + \sum_{k=0}^{N-1} \Big(\Theta[\mathbf{x}(k), \mathbf{u}(k), k] - \boldsymbol{\lambda}^T(k+1)[\mathbf{x}(k+1) - f(\mathbf{x}(k), \mathbf{u}(k), k)] \Big) \tag{5.8}$$

This then represents a cost function consisting of final system states cost, control input cost and measured system output. For the purpose of modelling a motorcycle rider, the simulation is continuous and the final system states $\mathbf{x}(N)$ are not achieved, and so this element can be omitted from the cost function in this application, leading to

$$J = \sum_{k=0}^{N-1} \Big(\Theta[\mathbf{x}(k), \mathbf{u}(k), k] - \boldsymbol{\lambda}^T(k+1)[\mathbf{x}(k+1) - f(\mathbf{x}(k), \mathbf{u}(k), k)] \Big) \tag{5.9}$$

At this stage, we introduce the concept of the Hamiltonian, which is defined by

$$\mathbf{H}(k) = \Theta[\mathbf{x}(k), \mathbf{u}(k), k] + \boldsymbol{\lambda}^T(k+1) f[\mathbf{x}(k), \mathbf{u}(k), k] \tag{5.10}$$

This therefore simplifies (5.9) to

$$J = \sum_{k=0}^{N-1} \Big(\mathbf{H}(k) - \boldsymbol{\lambda}^T(k+1)\mathbf{x}(k+1) \Big) \tag{5.11}$$

This expression still represents the constrained cost function, and so the optimum solution is obtained by minimisation of this function. Applying the method of perturbations using the concept of small variations in the state and input vectors. The theory presented here is taken from [95].

$$\mathbf{x}(k) = \tilde{\mathbf{x}}(k) + \Delta\delta(k) \tag{5.12a}$$

$$\mathbf{u}(k) = \tilde{\mathbf{u}}(k) + \Delta\eta(k) \tag{5.12b}$$

where Δ represents a small change of the variable. These expressions are substituted into the cost function (5.11). Since the optimal solution is sought, then the aim is to minimise the cost function, and, to find the minimum of the function, the following two conditions must be satisfied:

$$\lim_{\Delta \to 0} \frac{\partial J}{\partial \Delta} = 0 \quad \text{and} \quad \lim_{\Delta \to 0} \frac{\partial^2 J}{\partial \Delta^2} > 0 \tag{5.13}$$

These requirements lead to the Euler equations, defined as

$$\frac{\partial \mathbf{H}(k)}{\partial \mathbf{x}(k)} = \mathbf{C}^T(k)\mathbf{Q}(k)\mathbf{C}(k)\mathbf{x}(k) + \mathbf{A}^T(k)\boldsymbol{\lambda}(k+1) = \boldsymbol{\lambda}(k) \tag{5.14a}$$

$$\frac{\partial \mathbf{H}(k)}{\partial \mathbf{u}(k)} = \mathbf{R}(k)\mathbf{u}(k) + \mathbf{B}^T(k)\boldsymbol{\lambda}(k+1) = \mathbf{0} \tag{5.14b}$$

In order to obtain $\boldsymbol{\lambda}(k+1)$ and hence $\mathbf{u}(k)$ from (5.14b), the solution to (5.14a) must be sought. $\boldsymbol{\lambda}(k)$ is unknown at this stage, and so an initial estimate of its solution is made, setting

$$\boldsymbol{\lambda}(k) = \mathbf{P}(k)\mathbf{x}(k) \tag{5.15}$$

Where $\mathbf{P}(k)$ is an unknown matrix that could be viewed as systems of coupled quadratic equations [107]. Making use of (5.15) and (5.2a), (5.14b) can be rearranged to give

$$\mathbf{u}(k) = -[\mathbf{B}^T(k)\mathbf{P}(k+1)\mathbf{B}(k) + \mathbf{R}(k)]^{-1}\mathbf{B}^T(k)\mathbf{P}(k+1)\mathbf{A}(k)\mathbf{x}(k) \tag{5.16}$$

To obtain the optimal control input $\mathbf{u}(k)$ therefore requires $\mathbf{P}(k+1)$ to be calculated. Assuming the weighting matrices $\mathbf{Q}(k)$ and $\mathbf{R}(k)$ to be invariant as before, the iteration step identifier k can be omitted for clarity. Combining (5.14a), (5.15), (5.16) with (5.2a) leads to

$$\mathbf{P}(k)\mathbf{x}(k) = \mathbf{C}^T(k)\mathbf{Q}\mathbf{C}(k)\mathbf{x}(k) + \mathbf{A}^T(k)\mathbf{P}(k+1)\Big(\mathbf{A}(k)\mathbf{x}(k) - \mathbf{B}(k)[\mathbf{B}^T(k)\mathbf{P}(k+1)\mathbf{B}(k) + \mathbf{R}]^{-1}\mathbf{B}^T(k)\mathbf{P}(k+1)\mathbf{A}(k)\mathbf{x}(k)\Big) \tag{5.17}$$

The term $\mathbf{x}(k)$ in (5.17) can be cancelled to simplify the expression to the Algebraic Riccati Equation:

$$\mathbf{P}(k)=\mathbf{A}^T(k)\mathbf{P}(k+1)\mathbf{A}(k) - \mathbf{A}^T(k)\mathbf{P}(k+1)\mathbf{B}(k)[\mathbf{B}^T(k)\mathbf{P}(k+1)\mathbf{B}(k)+\mathbf{R}]^{-1}\mathbf{B}^T(k)\mathbf{P}(k+1)\mathbf{A}(k)+\mathbf{C}^T(k)\mathbf{Q}\mathbf{C}(k) \tag{5.18}$$

If $\mathbf{P}(k+1)$ can be obtained, then from (5.16) the optimal input $\mathbf{u}(k)$ can be found. This can be re-expressed as $\mathbf{u}(k) = -\mathbf{K}\mathbf{x}(k)$, where the optimal control gain $\mathbf{K}$ is given by

$$\mathbf{K} = [\mathbf{B}^T(k)\mathbf{P}(k+1)\mathbf{B}(k) + \mathbf{R}]^{-1}\mathbf{B}^T(k)\mathbf{P}(k+1)\mathbf{A}(k) \tag{5.19}$$

5.2.1 Algebraic Riccati Equation Solution: Numerical Method

Two techniques exist for the solution of the Algebraic Riccati Equation (ARE) for $\mathbf{P}(k+1)$, being the numerical or analytical. The simpler method is the numerical iterative method. For this approach, an initial value for $\mathbf{P}(k+1)$ is selected and, using equation (5.18), a value for $\mathbf{P}(k)$ can be obtained. This, however, will not be the correct result, as an initial estimate for $\mathbf{P}(k+1)$ was made. Thus, a new value of $\mathbf{P}(k+1)$, equal to the value of $\mathbf{P}(k)$ just obtained, is taken as the new initial estimate and the process repeated. With each successive iteration, the estimate of $\mathbf{P}(k+1)$ will become closer to the real value of $\mathbf{P}(k+1)$. When the estimated value $\mathbf{P}(k+1)$ and the value of $\mathbf{P}(k)$ that results from (5.18) become equal within a desired accuracy level, then the matrix $\mathbf{P}(k+1)$ can be used to obtain the optimal controller gain and

hence input.

The choice of initial value for $\mathbf{P}(k+1)$ at the start of the iterative process is arbitrary; the closer the initial estimate is to the final solution, then the sooner the iterative process will obtain the result, but by the very nature of the process the final solution will gradually and eventually be obtained. Typically however, the initial value $\mathbf{P}(k+1)$ is chosen as the eigenvalues of the matrix $\mathbf{A}(k)$.

Convergence of the Riccati equation via numerical methods, and hence the solution, is not always guaranteed however. More details of the theory can be found in [38, 46], where it is shown that convergence is guaranteed provided that the system is controllable and observable, or is exponentially stable.

Although this iterative process is fundamentally straight-forward, one notable disadvantage is the potentially high processing time required to solve a problem in this way. This factor will depend to some extent on the accuracy of the initial estimate to the final solution, and the accuracy tolerances that are applied to the iterative process. Depending on the application, this potentially high processing time may be considered important.

5.2.2 Algebraic Riccati Equation Solution: Analytical Method

The alternative approach is the analytical method. Mathematically this is a more complex process, but can have the advantage of being computationally more efficient, calculating the solution to $\mathbf{P}(k)$ in a single calculation.

Calculating $\mathbf{u}(k)$ from (5.14b) and substituting into (5.2a) gives

$$\mathbf{x}(k+1) = \mathbf{A}(k)\mathbf{x}(k) - \mathbf{B}(k)\mathbf{R}^{-1}\mathbf{B}(k)^T\boldsymbol{\lambda}(k+1) \tag{5.20}$$

and rearrangement of (5.14a) results in

$$\boldsymbol{\lambda}(k+1) = -\mathbf{A}^{-T}(k)\mathbf{Q}\mathbf{x}(k) + \mathbf{A}^{-T}(k)\boldsymbol{\lambda}(k) \tag{5.21}$$

The combination of (5.20) and (5.21) therefore results in

$$\mathbf{x}(k+1) = \Big(\mathbf{A}(k) + \mathbf{B}(k)\mathbf{R}^{-1}\mathbf{B}^{T}(k)\mathbf{A}^{-T}(k)\mathbf{Q}\Big)\mathbf{x}(k) - \mathbf{B}(k)\mathbf{R}^{-1}\mathbf{B}^{T}(k)\mathbf{A}^{-T}(k)\boldsymbol{\lambda}(k) \tag{5.22}$$

The matrices $\mathbf{A}(k)$ and $\mathbf{B}(k)$ will change with each iteration step, but with the iteration identifiers k omitted for clarity, the expressions (5.21) and (5.22) can be written as a single discrete-step matrix expression:

$$\begin{bmatrix} \mathbf{x}(k+1) \\ \boldsymbol{\lambda}(k+1) \end{bmatrix} = \begin{bmatrix} \mathbf{A} + \mathbf{B}\mathbf{R}^{-1}\mathbf{B}^{T}\mathbf{A}^{-T}\mathbf{Q} & -\mathbf{B}\mathbf{R}^{-1}\mathbf{B}^{T}\mathbf{A}^{-T} \\ -\mathbf{A}^{-T}\mathbf{Q} & \mathbf{A}^{-T} \end{bmatrix} \begin{bmatrix} \mathbf{x}(k) \\ \boldsymbol{\lambda}(k) \end{bmatrix} \tag{5.23}$$

This relationship can be represented by introducing the augmented vector $\mathbf{p}(k) = [\mathbf{x}(k), \boldsymbol{\lambda}(k)]^{T}$, and defining the Euler Matrix $\mathbf{E}_{M}$, such that

$$\mathbf{p}(k+1) = \mathbf{E}_{M}\mathbf{p}(k) \tag{5.24}$$

The general solution to (5.24) can be represented by

$$\mathbf{p}(k) = \mathbf{E}_{M}^{k}\mathbf{p}(0) = \mathbf{T}\mathbf{J}_{EM}^{k}\mathbf{T}^{-1}\mathbf{p}(0) \tag{5.25}$$

where $\mathbf{J}_{EM}$ is the Jordan matrix of the Euler matrix (5.23) and $\mathbf{T}$ the modal matrix of the system, whose columns are the eigenvectors of the Euler matrix, arranged with the matrices partitioned into the n stable and n unstable eigenvalues and eigenvectors [95] such that

$$\mathbf{J}_{EM} = \begin{bmatrix} \mathbf{J}_{11} & \mathbf{0} \\ \mathbf{0} & \mathbf{J}_{22} \end{bmatrix} \tag{5.26a}$$

$$\mathbf{T} = \begin{bmatrix} \mathbf{T}_{11} & \mathbf{T}_{12} \\ \mathbf{T}_{21} & \mathbf{T}_{22} \end{bmatrix} \tag{5.26b}$$

$$\mathbf{T}^{-1} = \mathbf{T}^{*} = \begin{bmatrix} \mathbf{T}_{11}^{*} & \mathbf{T}_{12}^{*} \\ \mathbf{T}_{21}^{*} & \mathbf{T}_{22}^{*} \end{bmatrix} \tag{5.26c}$$

where the components $\mathbf{T}^*_{11}$, $\mathbf{T}^*_{12}$ etc. represent the partitioned components of the inverse of the matrix $\mathbf{T}$, and are not equal to $\mathbf{T}^{-1}_{11}$, $\mathbf{T}^{-1}_{12}$ etc.

The first n columns are the eigenvectors of the stable roots, and the second n columns refer to the eigenvectors of the unstable roots. Using this partitioned structure of the matrices, (5.25) can be formed into a vector-matrix expression:

$$\begin{bmatrix} \mathbf{x}(k) \\ \boldsymbol{\lambda}(k) \end{bmatrix} = \begin{bmatrix} \mathbf{T}_{11} & \mathbf{T}_{12} \\ \mathbf{T}_{21} & \mathbf{T}_{22} \end{bmatrix} \begin{bmatrix} \mathbf{J}^k_{11} & \mathbf{0} \\ \mathbf{0} & \mathbf{J}^k_{22} \end{bmatrix} \begin{bmatrix} \mathbf{T}^*_{11} & \mathbf{T}^*_{12} \\ \mathbf{T}^*_{21} & \mathbf{T}^*_{22} \end{bmatrix} \begin{bmatrix} \mathbf{x}(0) \\ \boldsymbol{\lambda}(0) \end{bmatrix} \tag{5.27}$$

which can be expanded to give

$$\mathbf{x}(k) = \left(\mathbf{T}_{11}\mathbf{J}^k_{11}\mathbf{T}^*_{11} + \mathbf{T}_{12}\mathbf{J}^k_{22}\mathbf{T}^*_{21}\right)\mathbf{x}(0) + \left(\mathbf{T}_{11}\mathbf{J}^k_{11}\mathbf{T}^*_{12} + \mathbf{T}_{12}\mathbf{J}^k_{22}\mathbf{T}^*_{22}\right)\boldsymbol{\lambda}(0) \tag{5.28a}$$

$$\boldsymbol{\lambda}(k) = \left(\mathbf{T}_{21}\mathbf{J}^k_{11}\mathbf{T}^*_{11} + \mathbf{T}_{22}\mathbf{J}^k_{22}\mathbf{T}^*_{21}\right)\mathbf{x}(0) + \left(\mathbf{T}_{21}\mathbf{J}^k_{11}\mathbf{T}^*_{12} + \mathbf{T}_{22}\mathbf{J}^k_{22}\mathbf{T}^*_{22}\right)\boldsymbol{\lambda}(0) \tag{5.28b}$$

Since a stable solution is required, we must therefore eliminate from (5.28) any instance of the unstable matrix $\mathbf{J}^k_{22}$. Thus, it must be the case that for both (5.28a) and (5.28b),

$$\left(\mathbf{T}_{12}\mathbf{J}^k_{22}\mathbf{T}^*_{21}\right)\mathbf{x}(0) + \left(\mathbf{T}_{12}\mathbf{J}^k_{22}\mathbf{T}^*_{22}\right)\boldsymbol{\lambda}(0) = \mathbf{0} \tag{5.29}$$

and therefore

$$\mathbf{T}^*_{21}\mathbf{x}(0) + \mathbf{T}^*_{22}\boldsymbol{\lambda}(0) = \mathbf{0} \tag{5.30a}$$

$$\boldsymbol{\lambda}(0) = -(\mathbf{T}^*_{22})^{-1}\mathbf{T}^*_{21}\mathbf{x}(0) \tag{5.30b}$$

By elimination of the unstable terms matrix $\mathbf{J}^k_{22}$, the expressions (5.28a) and (5.28b) simplify to

$$\mathbf{x}(k) = \mathbf{T}_{11}\mathbf{J}^k_{11}\mathbf{T}^*_{11}\mathbf{x}(0) + \mathbf{T}_{11}\mathbf{J}^k_{11}\mathbf{T}^*_{12}\boldsymbol{\lambda}(0) \tag{5.31a}$$

$$\boldsymbol{\lambda}(k) = \mathbf{T}_{21}\mathbf{J}^k_{11}\mathbf{T}^*_{11}\mathbf{x}(0) + \mathbf{T}_{21}\mathbf{J}^k_{11}\mathbf{T}^*_{12}\boldsymbol{\lambda}(0) \tag{5.31b}$$

The substitution of (5.30b) into (5.31a) and (5.31b) results in

$$\mathbf{x}(k) = \mathbf{T}_{11}\mathbf{J}_{11}^{k}[\mathbf{T}_{11}^{*} - \mathbf{T}_{12}^{*}(\mathbf{T}_{22}^{*})^{-1}\mathbf{T}_{21}^{*}]\mathbf{x}(0) \tag{5.32a}$$

$$\boldsymbol{\lambda}(k) = \mathbf{T}_{21}\mathbf{J}_{11}^{k}[\mathbf{T}_{11}^{*} - \mathbf{T}_{12}^{*}(\mathbf{T}_{22}^{*})^{-1}\mathbf{T}_{21}^{*}]\mathbf{x}(0) \tag{5.32b}$$

Making the temporary substitution $\mathbf{J}_{11}^{k}[\mathbf{T}_{11}^{*} - \mathbf{T}_{12}^{*}(\mathbf{T}_{22}^{*})^{-1}\mathbf{T}_{21}^{*}]\mathbf{x}(0) = \boldsymbol{\beta}$, expressions (5.32a) and (5.32b) can be simplified to

$$\mathbf{x}(k) = \mathbf{T}_{11}\boldsymbol{\beta} \tag{5.33a}$$

$$\boldsymbol{\lambda}(k) = \mathbf{T}_{21}\boldsymbol{\beta} \tag{5.33b}$$

Referring back to (5.15), we can therefore now express the Riccati equation solution as

$$\mathbf{P}(k) = \mathbf{T}_{21}\mathbf{T}_{11}^{-1} \tag{5.34}$$

Recall that the columns of the matrix $\mathbf{T}$ consist of the eigenvectors of the Euler matrix $\mathbf{E}_M$, arranged such that the leftmost columns contain the stable eigenvectors. The upper half of these, i.e. the quadrant $\mathbf{T}_{11}$, corresponds to the stable roots of the system, while the lower half, the element $\mathbf{T}_{21}$, consists of the eigenvectors associated with the eigenvalues of the Lagrangian multiplier.

The eigenvectors can be sorted based on the magnitudes of the eigenvalues [98], such that the n stable eigenvalues, associated with magnitudes less than unity, are selected, forming the elements $[\mathbf{T}_{11}^{T}\ \mathbf{T}_{12}^{T}]^{T}$. Thus, $\mathbf{T}_{21}$ and $\mathbf{T}_{11}^{-1}$ can be obtained, and (5.34) solved to obtain the Riccati equation solution and hence generate the optimal controller gains.

Therefore, via this approach the Riccati equation solution can be obtained simply from the eigenvalues of the Euler matrix in a single step, assuming that the eigenvalues of the Euler matrix are symmetrically distributed with respect to the imaginary axis in the complex z-plane, with half stable and half unstable, and with no eigenvalues equal to zero.

The eigenvalue-eigenvector method was found to be a suitable approach for the modelling of a car driver using a similar optimal control strategy [98], and so was initially adopted here due to the relatively lower computational demand with respect to processing time of the method compared with the numerical approach.

However, as is often the case with iterative processes, small errors can quickly develop into much larger errors. While the eigenvalue-eigenvector method proved acceptable for relatively gentle manoeuvres for which state values such as roll angle and state accelerations were low, more severe manoeuvres led to numerical errors in the code which ultimately caused the program to fail. While this problem was not explored in great detail, it is suspected that this is a result of the numerical limitations in computing. The method requires the inverse of the matrix element $\mathbf{T}_{11}$ to be obtained, and if the elements in this matrix become such that the problem is ill-conditioned, then this would result in the computational problems experienced.

If the solution were obtained by using the numerical iterative method to solve the Riccati equation then this problem could be avoided, and so the code was therefore adapted to use the iterative solution method instead where necessary.

5.2.3 Application to the Riding Task

The theory for obtaining optimal controller gains for a generic dynamic system has been covered in the preceding sections. The specific application to the motorcycle rider modelling task is now outlined here.

Chapter 4 detailed the shift-register procedure that is used to provide the road preview information element, leading to the combined motorcycle–preview model, having the form

$$\begin{bmatrix} \mathbf{x}_v(k+1) \\ \mathbf{y}_r(k+1) \end{bmatrix} = \begin{bmatrix} \mathbf{A}_v(k) & \mathbf{0} \\ \mathbf{0} & \mathbf{A}_p \end{bmatrix} \begin{bmatrix} \mathbf{x}_v(k) \\ \mathbf{y}_r(k) \end{bmatrix} + \begin{bmatrix} \mathbf{B}_v(k) \\ \mathbf{0} \end{bmatrix} \mathbf{u}(k) + \begin{bmatrix} \mathbf{0} \\ \mathbf{B}_p \end{bmatrix} \mathbf{y}_{rn}(k) \tag{5.35}$$

In principle therefore, the solution method for the optimal control input follows the theory outlined for a generic dynamic system outlined in preceding sections, replacing the matrices for the generic system with the matrix forms given in (5.35).

Since the objective of the model is to follow the previewed road path, the output element of the cost function (5.4) can be set to provide the errors between the lateral path following and the path heading angle by appropriate selection of the output matrix $\mathbf{C}(k)$:

$$\mathbf{C}(k) = \begin{bmatrix} 0 & 1 & 0 & \dots & -1 & 0 & \dots & 0 \\ 0 & 0 & 1 & \dots & 0 & -1 & \dots & 0 \end{bmatrix}_{m \times n+N_p m} \tag{5.36}$$

where the road preview information consists of both lateral positions and heading angles of the road path in global coordinates. The lateral motorcycle position and yaw angle are the 2^{nd} and 3^{rd} elements in the motorcycle state vector, thus multiplying by 1, while the lateral position and heading angle of the target path at the first preview point (corresponding to the motorcycle's target position on the path) are the elements at $n+1$ and $n+2$ in the combined motorcycle–preview vector $z(k)$, multiplied by -1. When only the lateral position information is known, the target heading angle can still be deduced by simple trigonometry [98].

The corresponding matrix $\mathbf{Q}(k)$ is

$$\mathbf{Q}(k) = \begin{bmatrix} q_1 & 0 \\ 0 & q_2 \end{bmatrix} \tag{5.37}$$

where the elements q_1 and q_2 respectively weight the lateral path following error and heading angle error of the motorcycle relative to the target road path.

The vector of control inputs $\mathbf{u}(k)$ consists only of a steer torque input, and is therefore represented as $u(k)$. The corresponding weighting matrix $\mathbf{R}(k)$ consists therefore only of a single element, r, weighting the steer torque control input.

The number N_p of preview points in the road information vector is determined by the length (in time) of the preview horizon T_p and the discrete sampling time t, i.e $N_p = T_p/t$

5.2.4 Optimal Gains

A necessary condition for the analytical method presented previously is for the system state matrix $\mathbf{A}(k)$ to be non-singular, and for the case of the motorcycle dynamics alone ($\mathbf{A}_v(k)$), this condition is satisfied. However, when the road preview is appended to the state space representation of the motorcycle–rider as in (5.35), the augmented system state matrix then becomes singular. The problem is still solvable, finding the solution to the Riccati equation and subsequently the optimal gains, but requires a manipulation process developed in [71] and also later for a car–driver application in [98].

Essentially, this requires that the state space representation of the combined motorcycle–preview model is partitioned into smaller sub-matrices that represent the motorcycle dynamics and the road preview separately, i.e

$$\mathbf{K} = \begin{bmatrix} \mathbf{K}_1(k) & \mathbf{K}_2(k) \end{bmatrix} \quad \text{and} \quad \mathbf{P} = \begin{bmatrix} \mathbf{P}_{11}(k) & \mathbf{P}_{12}(k) \\ \mathbf{P}_{21}(k) & \mathbf{P}_{22}(k) \end{bmatrix} \tag{5.38}$$

where the subscript 1 relates to the motorcycle dynamics and the subscript 2 to the road preview. Thus, $\mathbf{K}_1(k)$ would be the element of the gain vector $\mathbf{K}(k)$ applied to the motorcycle states, and $\mathbf{K}_2(k)$, the elements corresponding to the preview element. The matrix $\mathbf{A}_v(k)$ in (4.3) is non-singular, and so for the case with no preview included (i.e. $\mathbf{K}(k) = \mathbf{K}_1(k)$ and $\mathbf{P}(k) = \mathbf{P}_{11}(k)$) the analytical method can be used to solve the optimal control problem without difficulty. Manipulation of the ARE, shown in detail in [98], shows that by solving first the non-preview case to obtain $\mathbf{K}_1(k)$ and $\mathbf{P}_{11}(k)$ the matrix $\mathbf{P}_{12}(k)$ can be obtained, and that with these matrices it is then possible to obtain $\mathbf{K}_2(k)$, the element of the optimal preview gain relating to the previewed road path. Forthwith therefore, the matrices $\mathbf{K}_1(k)$ and $\mathbf{K}_2(k)$ will be referred to as $\mathbf{K}_s$, the state gains, and $\mathbf{K}_p$, the preview gains, respectively.

Thus the controller gains for the combined rider-preview model were obtained which then enabled the simulated model to perform the path following task. The simulation itself was run as a discrete time iterative model, and thus at each step of the discrete time simulation the control problem using the preceding theory was solved to generate the required steer input and hence follow the target path.

5.3 Optimal Control Rider Model Results

The work covered here and the model developed aim to replicate and extend the work conducted by Sharp [94]. There, the model employed the same optimal control strategy and was applied to a broadly similar motorcycle model. However, the model used here has what is believed to represent a more advanced and realistic tyre model, and additionally with the non-linearity of the motorcycle dynamics accounted for by continuously re-evaluated linearisations of the motorcycle state space equations of motion during the simulated motion. The results presented in [94] appeared to represent well the actions of a motorcycle rider, and the technique will therefore be used as a benchmark against which to assess the performance of a model predictive control technique that was subsequently applied to the rider model. Direct comparisons and conclusions of the two techniques are drawn in Chapter 7.

The optimally-controlled motorcycle rider model is tasked with a simple path following exercise, involving a simple single lane change consisting of a lateral shift of 3.5 m over a forwards distance of 20 m (Figure 5.1). This is an ISO standard manoeuvre commonly used in the assessment of vehicle manoeuvre performance.

The optimal control strategy has several variables that are set to define the operating characteristics of the controller, including weighting factors on the system outputs, weighting factors on the system inputs, the preview horizon and more fundamental parameters such as the sampling time of the discrete model.

The specific application of the optimal control theory and the relevant terms were covered in Section 5.2.3. The weighting parameters in the cost function will provide the primary means of varying the system's performance; the weighting factor q_1 applied to the lateral path error, q_2 weighting the yaw angle error, and r on the steer torque control input. In addition, the preview horizon time T_p will be varied to change the distance to which the rider is able to see ahead. Division of the preview horizon T_p by the discrete time interval t will then give the number of discrete preview points.

Details relating to the nature of the manoeuvre task itself can be varied. This can include both the nature of the road path and the forward velocity v at which the rider attempts the manoeuvre. In order to maintain some consistency and thus allow

the characteristics of the controller alone to be assessed, the road path will remain fixed for the purpose of these investigations, remaining as a 3.5 m lateral shift over a forward distance of 20 m. The speed v at which the rider attempts this manoeuvre however will be changed, to account for low and high speed conditions.

The presented results will consider the implications on the control task of variation of the principal variables outlined above, independently of each other. This will permit clear observations to be drawn on the effects of parameter variation on the control task. Furthermore, these observations will permit conclusions to be made regarding the applicability of the control strategy to the modelling of a human motorcycle rider.

5.3.1 Low Speed Optimal Control Model

Initially, a baseline model will be evaluated that will provide a model against which changes to the controller settings can be assessed. This baseline model will aim to provide a system with a moderate performance and balance between accuracy and effort, with sufficient but not excessive preview, and the speed will be relatively low. Subsequently, parameters will be varied individually to assess the implications that they have upon the performance characteristics of the controller. The full range of parameter sets for low speed are presented in Table 5.1.

Baseline Parameter Set

The ability of the model to track the path is assessed first. Figure 5.2 presents the path followed by the model using the initial baseline parameters (Set 1), where it is observed that the model is able to successfully negotiate the manoeuvre and tracks the path well after the manoeuvre phase is complete. Additionally, the countersteer associated with riding a motorcycle is evidenced by a slight deviation away from the turn direction before the lane change begins.

The controller's gains are considered next, where the magnitudes of the gains may be thought of as representative of the importance placed the state elements by the rider for the control task. Due to variation of the state space model on account of the model's non-linearity, some variation of the gains occurs over the manoeuvre. The gain values that will be presented are for the motorcycle approximately one quarter

of the way through the lane-change, at the point where the roll angle on the initial left turn is the greatest.

The controller state gains that give rise to the control are presented in Figure 5.3, appearing to suggest that the highest gain value is associated with the yaw angle state. The gain in the roll angle state is the next largest, with all other state gains of significantly lower magnitude.

However, the significance of the magnitudes of the state gains needs to be clarified due to the different units and magnitudes of the states. The gains are therefore compared by the contributions that they individually make to the complete control input, the steer torque. The total steer torque, overlaid with the motorcycle's roll angle, is presented in Figure 5.4, showing the expected pattern of a main (negative torque) countersteer to initiate the manoeuvre, increasing to a positive peak to stabilise the resulting roll and eventually reduce this roll, decaying as the roll angle then reduces followed by a negative torque to stabilise the motorcycle once it is upright again. The contribution made to this total torque by each state is the sum of the state gain value and the state value itself, and therefore it is more representative to consider the controller in these terms. The use of global coordinates here complicates the analysis somewhat, as the significant torque contribution from the lateral position is offset by the significant but opposite contribution made by the road preview. These are therefore removed from the analysis, together with a number of additional states that have a much more insignificant contribution to the overall steer torque, to leave only the contributions made by the yaw angle, roll angle and their respective velocities, and the lateral velocity of the motorcycle. Figure 5.5 shows the contributions to the total steer torque of the states and state gains over the path following simulation. From this plot, it is apparent that the contribution to the steer torque resulting from the yaw angle gain is still the most significant, followed by that resulting from the roll angle.

The same analysis was also made for the motorcycle operating in a local coordinate manner. In local coordinates, the situation where the motorcycle lateral position and road preview information contribute equal and opposite non-zero steer torque contributions in straight running does not arise, and thus the steer torque contributions made by the individual states are much more easily understood. Figure 5.6 shows again the steer torque contributions arising from the yaw angle, roll angle and

their respective velocities, and the lateral velocity of the motorcycle. The pattern is similar, however the roll angle and road preview information now provide the largest contributions to the overall steer torque, while the contribution made by the yaw angle component is virtually nil and is therefore not shown in the figure.

These findings suggest two things. Firstly, the local coordinates approach would appear to suggest that roll angle control is the primary objective, followed by control of the lateral position of the motorcycle. These statements are in strong agreement with Weir [102], who suggested that roll control was the primary objective of the steer torque control, and lateral position and yaw angle control were slightly weaker objectives met by movement of the rider's upper body. Secondly, the observation that, in local coordinates, the locally observed yaw angle of the motorcycle has a much smaller significance on the future path of the motorcycle is in strong agreement with the observations of Cole et al. [11]. In a local coordinate system, the yaw angle will, in general, always be relatively small, and so this result may not be surprising.

Considering now the preview gains (Figure 5.7), these also show fundamental characteristics. The gains are initially zero, rising to a peak in the middle preview distance before decaying gradually towards zero, implying minimal influence on the control task of the road information at this distance ahead. Thus, it appears that the rider model places no importance on the road observed directly in front of the motorcycle, with the road in the middle preview being of most influence to the control task, and with the distant previewed information being of reducing importance as the preview distance increases much beyond 20 m ahead.

In attempting to optimise the path following exercise, the controller steers the motorcycle in order to stay on course. For road errors perceived directly in front of the motorcycle, there is nothing that can be done about these errors; the motorcycle would need to stop and be physically moved in order to correct any errors here. A short distance ahead of the motorcycle, the rider will have some opportunity to correct any path errors by steering, but may not be completely successful due to the limited forward distance available and limited steering capabilities (Figure 5.8). As the distance ahead of the motorcycle at which lateral deviations are observed increases, so the rider begins to have sufficient opportunity to correct any path following errors that are detected in the visual preview, and this may explain the increase in the preview gains as the preview distance increases. At greater preview distances, the rider

has an excess of time available to take any necessary control actions. The correction of these potential path-tracking errors are of lower importance than those for which the available time is limited and, consequently, as the preview distance increases further, the preview gains begin to diminish away towards zero. By considering the capabilities of a motorcycle rider in this manner, then the preview gains achieved by the controller would appear to offer a good representation of the process.

The steer torque that results from the controller gains and that leads to the path following performance seen is shown in Figure 5.9. The steer torque shows the expected characteristics, with a countersteer in advance of the turn to initiate the manoeuvre, leading to a peak torque as the rider begins to bring the motorcycle back upright to change the turn direction, reducing again and finishing with another countersteer torque to arrest the roll movement as the motorcycle is brought back upright.

These initial observations on the performance of the optimal control strategy appear encouraging; the path following task is successfully accomplished, achieved with realistic steer torques and with controller gains that would appear to fit well intuitively with the expected control characteristics of a motorcycle rider. These results were also originally found by Sharp [94]. This therefore gives some confidence in extending the parameter set to further investigate the performance of the control strategy.

Cost Function Weighting Influence

The weighting parameter associated with the lateral path error q_1 is now varied. The initial value for q_1 was 5000 m^{-2}, and additionally, 1000 m^{-2} and 10000 m^{-2} are now used. The lower value should lead to a less accurate path following performance, the higher value a closer following of the path due to their influence on the optimal control cost function.

The path following errors for the three weighting parameters are presented in Figure 5.10. In line with expectations, the increase and decrease in the values for q_1 have a direct influence on the path-tracking accuracy achieved, with the controller displaying less accurate path following and therefore greater path errors termed 'loose' control, with the more accurate path following performance resulting from higher values of q_1 referred to as 'tight' control [94].

The changes in the path following performance stem from the change in steer torques generated by the controller model. It is seen (Figure 5.11) that the loose control is associated with early initiation of the manoeuvre, leading ultimately to lower peak torque values, and in this manner, the rider model is sacrificing path-tracking accuracy in order to reduce the magnitude of the steer torques he must apply. This is to be expected, since the optimal control cost function comprises elements relating to both the output performance and the control input effort. An increased bias to either performance or effort optimisation, achieved via increased weighting parameters, would naturally be expected to reduce the emphasis on the other cost function element, and *vice versa*. So it is then that a decrease in the output performance bias appears to result in an increase in the control effort bias. Similarly, tight control, indicative of low path errors, leads to correspondingly higher peak steer torques applied over a much shorter duration.

These steer torques arise from the controller gains, with variation of the controller settings naturally affecting the controller gains. Figures 5.12 and 5.13 show the state and preview gains for all three error weighting values. Increases in q_1 are seen to produce increases in all the state gains; the ratios between them however remain constant. The effect on the preview gains is also to increase them, but more interesting is the shift that is observed in the distribution of the gain values. With increased q_1, indicative of tighter control, the bias in the preview gains moves closer to the motorcycle. In other words, the distance ahead of the rider corresponding to his most important road information point moves closer to him. This implies that the rider is focusing on the road closer to him, which would seem like an expected result.

Loose control is associated with minimisation of control effort, and to achieve this a rider may be expected to select the most efficient path from an initial point 'A' to a final point 'B', travelling as directly as possible to minimise the control effort required (Figure 5.14). In order to select the most efficient path, a complete knowledge of the road path is desirable, and so the rider would be expected to be looking further down the road and considering a distant target as being more important in deciding his control strategy. Consequently it might be expected that the preview gains would be more evenly distributed, and extending to a greater distance ahead.

Conversely, tight control is associated with accurate path tracking, where the rider will attempt to position his motorcycle on the target path at all times during the

motion, irrespective of the path some distance ahead. The focus is on ensuring that throughout the simulation, where the motorcycle is immediately about to move to still accurately follows the path, regardless of the path some greater distance ahead. Thus the rider would be expected to focus more attention on the near-preview information, and less on the far-preview distance (Figure 5.14).

Thus, the expected actions of a human rider with a change in path following strategy appear to be represented well by the optimal control technique. The changes in the preview gains observed with the change in q_1 appear to be an acceptable representation of a human rider's control actions, adding credibility to the applicability of the approach.

Preview Horizon Effects

The preview horizon time T_p available to the rider is now varied to assess the impact that this parameter has upon the control performance of the optimal control strategy. The preview horizon is set to 4.5 s and 1.5 s to represent excessive and limited preview respectively (Sets 4 & 5, Table 5.1).

The rider model was initially allowed 3.0 s of visual road preview. At a forward speed of 10 m/s, this was seen to be sufficient to allow the preview gains to diminish to zero (Figure 5.7), suggesting that the rider had enough preview information to make the necessary control actions for complete control. It might therefore be expected that further additional preview information would have minimal impact upon his control actions.

The controller gains and resulting steer torques and path following error (Figures 5.15, 5.16, 5.17, 5.18) largely seem to support this view. There is seen to be minimal difference between the plots as the allowable preview is increased from 3.0 s to 4.5 s, suggesting minimal impact on the controller performance as a result of the increased preview horizon.

A rider generates a control action based on the knowledge that he has of the road and of the motorcycle. If the rider were presented with new road information which had minimal impact upon his required control actions, it is reasonable that no attention would be paid to this new information, and therefore the attention paid to

the original information would not change. Hence, if the rider's preview knowledge is already sufficient to determine an appropriate control strategy, then the preview gain distribution would be expected to show minimal difference.

However, if the rider were presented with new information that would influence his control problem, it seems likely that the rider's control would be expected to adjust in light of this; some of the rider's attention would additionally be focused on this new information, and consequently the level of attention paid to the rest of the road information reduced slightly, modifying the preview gains. By a similar token, it would seem equally likely that the reverse would be true, and that if relevant road information regarding the control task were removed, then the attention paid to the remaining road information would be changed.

The state gains (Figure 5.15) show identical gains for all three preview horizon lengths considered.

The reduction in the available preview information available to the rider appears to have minimal effect on the distribution of the preview gains (Figure 5.16), at least for the 10 m/s forward speed case. Irrespective of the horizon length, the preview gains are identical; the only change resulting from a reduction of the horizon is that the preview gains are simply truncated, and thus the preview gain curves overlap each other when plotted together.

The steer torque control input that results from a change in the preview horizon is shown in Figure 5.17. For preview horizons of 3.0 s and 4.5 s, the control inputs are virtually identical. For the reduced horizon of 1.5 s, the resulting torque is seen to be modified slightly, which may appear to agree with the expected modification of control resulting from the change in road information available.

However, the effect of this preview limitation and modified steer torque input on the path following performance of the motorcycle is seen to be detrimental. The broad characteristic is unchanged, with initial countersteer leading the motorcycle to follow the lane change before straightening up after the turn to follow the straight-running road section. Figure 5.18 shows the path errors that result from the change in allowable preview horizon, with the cases for $T_p = 3.0$ s and 4.5 s being so similar that the traces follow each other almost identically. Whereas previously the motorcycle accurately tracked the straight section, it is noted that the limited preview case

now results in a path tracking error, essentially a steady-state error in pure control terms, following the manoeuvre. The controller gains, notably the preview gains, have not been recalculated to account for the reduction in available preview information, but have merely been truncated, and evidently this can lead to poor path tracking performance if the gains are reduced too far.

An initial thought, in order to in some way compensate for these lost gains terms, may be to introduce some form of scale factor to compensate for the lost terms. However, without knowledge of the full set of gains, it is not possible to determine what the scaling factor should be in order to obtain equivalency of the sums of the gains, and so any scaling factor chosen could not be accurately determined.

It is not unreasonable to expect a human motorcycle rider to still be able to track a path, even with limited preview. The transient performance may well suffer, but if given only, say, 1.0 m of visual preview, the rider would still have knowledge of whether his final steady state road position were on the path that he should be following or offset from it, and would therefore, given sufficient time, be able to track back across the road to recover the target path.

This control characteristic would appear to be a limitation of the optimal control technique in modelling a human motorcycle rider operating in a global coordinate system. The limitation is worthy of further investigation, and is therefore considered mathematically.

The control input $u(k)$, in this case the steer torque, that ultimately dictates the trajectory of the motorcycle is generated by the combination of torques resulting from the multiplication of states and state gains, and of road lateral preview and preview gains:

$$u(k) = \mathbf{K}_s \mathbf{x}_v(k) + \mathbf{K}_p \mathbf{y}_r(k), \tag{5.39a}$$

where $\mathbf{K}_s$ is the vector of state gains, $\mathbf{x}_v(k)$ is the state vector, $\mathbf{K}_p$ the vector of preview gains and $\mathbf{y}_r(k)$ is the vector of the previewed road path. At the exit of the turn and return to straight running, the vehicle states $\mathbf{x}_v(k)$ all tend to zero, apart from the state representing the vehicle lateral position, y, and thus at the exit of a turn,

$$u(k) = k_{s,y}y(k) + \mathbf{K}_p\mathbf{y}_r(k) \tag{5.39b}$$

where $k_{s,y}$ is the state gain corresponding to the lateral position $y(k)$ of the motorcycle

In the steady state following the manoeuvre, $u(k)$ is zero, and thus

$$k_{s,y}y(k) = -\mathbf{K}_p\mathbf{y}_r(k) \tag{5.39c}$$

$$\Rightarrow k_{s,y}y(k) = -\sum_{i=1}^{Np} K_{p_i}y_{r_i}(k) \tag{5.39d}$$

With sufficient preview horizon $N_p \rightarrow \infty$, this condition is achieved with $y(k) = y_{r_1}(k)$, and the motorcycle accurately tracks the path. Similar observations were in [90] for the case where the preview horizon is sufficiently long such that the controllers gains tend to zero, in which case the controller's performance is independent of the coordinate system. The case is now explored for the condition of limited preview, such that the gains have not necessarily reached minimal values.

With limited preview, in steady state the steer torque still becomes zero, and the above condition given in (5.39d) will still hold. Although the preview gain values remain the same in magnitude, the gain vector itself becomes truncated as a consequence of the limited horizon, and hence

$$\sum_{i=1}^{Np} K_{p_i} \neq \sum_{i=1}^{\infty} K_{p_i} \tag{5.39e}$$

The vector $\mathbf{y}_r(k)$ and state gain $\mathbf{K}_s$ are unchanged, and thus it must be the case that

$$y(k)\,|_{Np<\infty} \neq y(k)|_{Np\rightarrow\infty} \tag{5.39f}$$

and hence,

$$y(k) \neq y_{r_1}(k) \tag{5.39g}$$

Thus for any finite preview distance, there will be a steady-state error in the path-tracking performance when the rider is modelled in this way. An infinite preview

horizon is not a practical option, so the significance of the reduction must be analysed. The significance of this error effect can be assessed by the value of $(\sum_{i=1}^{\infty} K_{p_i} - \sum_{i=1}^{Np} K_{p_i})$; the smaller this difference, the smaller will be the steady state error in the controller. Thus, provided that the controller gains omitted are insignificantly small, the reduction in preview horizon should have an insignificant impact upon the accuracy of the controller model. If the preview horizon is so short that the preview gains have not reached close to zero values at the limit of the preview horizon, then the value of $(\sum_{i=1}^{\infty} K_{p_i} - \sum_{i=1}^{Np} K_{p_i})$ will not be insignificantly small and thus significant steady-state path following errors are likely to result.

Thus it would appear that reductions in the preview distance available to the rider model can have detrimental effects on the performance of the controller, and this needs to be considered when such a control technique is applied to control tasks of this nature.

Low Speed Modelling Conclusions

Optimal control appears to be a useful technique for the representation of a human motorcycle rider, with the ability to replicate realistic control actions in order to complete a path following task. The nature of the controller gains, which are indicative of the use made of available information in generating the control actions, appear realistic of the human rider.

The effects of control variables, namely related to the path following accuracy variables, are capable of influencing the balance that a rider makes between accuracy and control effort. However, the technique is not without limitations as seen when the preview horizon is reduced.

5.3.2 High Speed Baseline Parameter Set

The speed of the motorcycle model is now increased to 40 m/s. This will enable any changes in the control task as a result of forward speed to be analysed. The parameter sets are as for the lower speed case, but with $v = 40$ m/s (Table 5.2).

The performance of the controller at higher speed is fundamentally similar to that seen at the lower speed, with the path following performance (Figure 5.19) displaying

similar traits but with greater levels of corner cutting. The nature of the gains that lead to these control inputs are similar to those seen at lower speed, but notably have higher magnitudes. Steer torques are also significantly increased with the increase in forward speed (Figure 5.20).

Fundamentally, it is believed that the increase in forward speed leads to increases in the gyroscopic torques provided by the rotating wheels. The increased gyroscopic torques mean that, for a given steer input, a greater steer torque is required to overcome these gyroscopics, and the result of this is seen in all aspects of the controller's performance.

At higher speeds, the ratio of the steer torque to the steer angle increases. In order to minimise the combined cost function of path following (dictated by steer angle) and steer torque, then as speeds increase the emphasis shifts in favour of minimising steer torque rather than steer angle. Consequently, the path chosen by the rider tends towards a greater level of corner-cutting as speeds increase.

It has been seen before that a looser control strategy, involving greater levels of corner cutting, is associated with an increased use of the full preview information, where peak preview gains may be reduced, but the distribution of gains is extended to a greater preview distance. The increase in speed shows this characteristic (Figure 5.21), a characteristic which is not unlike the switch from tight to loose control strategies (Figure 5.13). In other words, at higher speeds but with identical controller parameter settings, the corner cutting characteristics of the motorcycle rider's control actions are seen to be greater than for the lower speed case. Figure 5.21 also shows a significant oscillatory pattern in the preview gains. This arises due to the minimal damping of the wobble mode at this forward speed (see also Figure 3.15).

5.3.3 Local Coordinate Preview

The initial motivation for modifying the controller to operate in local coordinates was partly because this is arguably the way that a motorcycle rider would operate, but more importantly in an attempt to eliminate the steady-state tracking errors that can occur using global coordinates with a limited preview horizon. In principle, a change of coordinates should not have an impact upon the results of a robust control strategy. However, the path-following errors that result are a consequence of using theory that

assumes an infinite horizon. When the horizon is long, terms that are lost from the preview gains are zero and therefore not significant. When the preview horizon is much shorter, more significant terms are lost, leading to errors in the controllers' performance. It is now investigated whether these errors are overcome through the use of a local coordinate system.

The controller strategy remains essentially unchanged, with the controller operating on a preview road in his local coordinate frame. This, in principle, is no different to the motorcycle beginning from the origin of a global coordinates frame. However, with each iterative step the road preview is updated as local coordinates information (4.9c). The final two points on the preview vector track the global position and yaw one step ahead of the preview horizon and are not included in the control problem.

As before, the steady-state is achieved when the steer torque is reduced to zero, arising when

$$u(k) = \mathbf{K}_s \mathbf{x}_v(k) + \mathbf{K}_p \mathbf{y}_r(k) = 0 \tag{5.40a}$$

which, when the all states bar the lateral position settle to zero, simplifies to

$$k_{s,y} y(k) = -\mathbf{K}_p \mathbf{y}_r(k) \tag{5.40b}$$

In global coordinates the left hand side was not equal to zero following a manoeuvre, and thus the right hand side would be required to be equal and opposite. Limited $\mathbf{K}_p$ meant that this was achieved when $y(k) \neq y_{r_1}(k)$ in the global case, and thus a steady state error arose in the straight-path path-tracking following the manoeuvre part of the task.

By using local coordinates, the target $y_{r_1}(k)$ is zero when the rider regains the target path. The right hand side will tend to zero, as will the left hand side and thus $y(k)$. Although the reduction in $\mathbf{K}_p$ will affect the transient performance of the controller, the steady state local lateral position of the motorcycle should not be affected by the limited vector $\mathbf{K}_p$, thus forming a more robust optimal control rider model.

This is confirmed by comparison of two simulations run to identical parameters. One simulation is set to operate using the original global coordinate system, the other in

local coordinates. The model is intentionally run with limited preview horizon, such that the effect of the modified coordinate system is more clearly seen.

The vehicle parameters are: $v = 10$ m/s, $q_1 = 5000$ m^{-2}, $q_2 = 0$ rad^{-2}, $r = 1$, $T_p = 1.0$ s. The path following results, shown in Figure 5.22, clearly demonstrates the beneficial effect of modelling the road using local coordinates.

Although the transient response of the global coordinates model appears better, the large steady state error in the path tracking ability of the model is both undesirable and unrealistic of the actions of a human rider. If a rider had only limited forward vision, due possibly to weather conditions, night-time riding or obstructions from other vehicles ahead of him, the transient response may justifiably be compromised, but the rider would still be able to see sufficient road path to know whether he is on target (position-in-lane control), or displaced to one side or the other, and consequently would eventually be able to track back onto the target path if needed.

This represents a notable and important weakness of the optimal control approach for more general rider-control modelling. While it has been shown that these limitations can be corrected through the use of a local coordinate system, the local approach, covered in Section 4.2.2, is a more complex approach than global coordinates. Regardless of the coordinate system used, the rider still has a knowledge of both the motorcycle's position and heading, and the position and heading of the road. He can therefore deduce the relative difference between the two to determine whether he is off the target path and therefore is required to exercise some control in order to regain the target path.

Thus, a controller that is capable of accurate performance regardless of the coordinate system used would provide a more robust and representative control strategy, and therefore be more suitable for the task at hand. For the optimal control approach, this appears to be achieved only when a local coordinates approach is employed.

5.4 Optimal Control Conclusions

The application of optimal control theory has been made to the modelling of a motorcycle rider, initially developed by Sharp [94]. The work here has aimed to generate a more extensive set of results to gain further insight into the characteristics of the

method, and to highlight any strengths or weaknesses that may transpire from the more extensive analysis.

The findings of the work here agree well with those in [94], giving confidence that the results here are correct. As before, the characteristics of the controller appear to provide a good representation of a motorcycle rider, showing strong suitability of the application. State gain results were not presented in [94], and thus no conclusions could be drawn on the relevance of the control of the motorcycle's states. The findings presented here have shown that for all cases the pattern of the state gains remains consistent, with the yaw angle and roll angle gains having the largest magnitudes. The more relevant question of how these relate to the physical control applied to the motorcycle show subtly different results. For the global coordinate system, the contribution arising from the yaw gain is again the largest, followed by the roll angle contribution. However when the coordinate system is switched to local, the results are notably changed, with the roll angle contribution being the most significant, followed by the lateral position contribution, and with the yaw angle providing a much smaller overall contribution.

Since the local coordinate system is arguably more representative of the way that a human rider operates and interprets information, this would tend to suggest that roll angle and lateral position control are the more important considerations for a motorcycle rider. Encouragingly, these findings are in strong agreement with Weir [102], where the links between a number of information inputs and possible control outputs found the roll angle to steer torque contribution to be the most important, followed by lateral position control, which was best controlled by movement of the rider's body mass.

The analysis of the preview gains again shows agreement with the results of Sharp [94], and also to the wider results provided by Donges [25] and by Land and Horwood [47], where the important aspects of a car driver's preview were discussed. The results had suggested the distinction between guidance control, biasing the distant preview, and the position-in-lane control provided by the near preview information. Changing the riding strategy required through the cost function weighting parameters was seen to change the influence of the near and far preview information in accordance with either guidance or position-in-lane riding approaches, thus agreeing with the theories of the referenced papers.

The technique is not, however, without its limitations. Notably, the use of a global coordinate system, particularly when combined with limited road preview, appears to result in a poor representation of the rider's actions. Although it was found that this problem could be overcome if the simulations were conducted in a moving coordinate system, it remains a fact that for anything other than an infinite horizon there will be some steady-state errors resulting, though provided that sufficient preview is permitted, these errors can be reduced to insignificant values.

Useful analysis relating to the global versus local coordinates problem was made by Cole et al. [11], who noted, in agreement with earlier results by Sharp and Valtetsiotis [90] and the results here, that the question of global versus lateral coordinates has no impact upon the path following abilities of the controller when sufficient preview is allowed. The sufficiency of the preview is defined as the preview gains reaching zero as before. This is because the change in the previewed lateral displacements brought about by a change of reference origin and multiplied by the preview gains is compensated for by the change in the corresponding state multiplied by its state gain, the two effectively being equal and opposite. As the theory assumes an infinite horizon, then this change of reference frame will work provided that the preview gains diminish to zero such that no significant terms are omitted.

In the case where the preview gains are reduced significantly, the theoretical calculation is still based on the assumption of an infinite horizon, and consequently there appears no reason why the calculated gain values should differ, as is the case. However, with the loss of significant terms from the preview gains, the contributions from the state gain multiplied by the state and the preview gains multiplied by the states are no longer equal and opposite when the vehicle is on the target path, and consequently the steady state errors that were observed result when a non-local reference frame is used. For a local coordinates approach and accurate path following, both the state contribution and the preview contribution should, strictly, still be equal and opposite for correct path following. However, this occurs now with both contributions equal to zero, since the local lateral and yaw displacements are zero for steady running and the local road preview for a steady path, when on that target path, is also zero. The loss of zero terms in the preview resulting from a short preview horizon therefore has no effect on the numerical result and hence the performance of the local coordinates controller.

Cole et al.'s results suggested that, even with the road path in the state vector defined by global coordinates, the truncation of the preview horizon could be compensated for by a change in the state gains that would correspond to the 'lost' contribution from the shortened preview and therefore still result in accurate path following. Their model employed a conversion matrix that would effectively recalculate the global road information into a local picture as observed in the moving vehicle, and in this way the controller was effectively set to operate in a local coordinates manner, even though the road path in the state vector was still defined in a global reference frame. Thus, the control problem was effectively being solved for a local coordinates problem, but using global road information.

To retain accurate path following for a shortened preview horizon, the loss of significant road preview terms in the control problem can be overcome in two ways. Either the controller gains are calculated in such a way as to compensate for these, as was the case in [11], where the road preview was global but the controller modified to operate in a local manner, or the road preview information converted directly into the local coordinates and the controller structure kept the same, as was the case here. Either way, both controllers effectively operate using a local picture of the road, and should therefore generate comparable path-following performances.

Thus the statement is again made that for accurate path following using this approach, the problem must be solved for a local coordinates approach for accurate results with short horizons. Whether this is achieved by conversion of the preview gains or by conversion of the road information may be a question of preference, however both should produce the same results.

The results presented here using optimal control methodology have extended the understanding of the technique for this application. Chapter 6 will present the predictive control technique for modelling the rider, an approach which has some significant similarities to the optimal approach presented in this chapter, but also some notable and possibly significant differences. The predictive control rider model will be presented with the same tasks as for the optimal approach here, and so the optimal control results shown here will be used as a measure against which the performance of a model predictive control rider model can be compared. Some weaknesses of the optimal control approach have been highlighted here, and so the goal the predictive control method will be to replicate the positive features while also aiming to correct

the limitations found. Finally, the direct comparisons of the optimal control results and the predictive control results will then be drawn in Chapter 7.

5.5 Tables

Parameter	Set 1 Baseline	Set 2 Loose Control	Set 3 Tight Control	Set 4 Long Preview	Set 5 Short Preview
v [ms^{-1}]	10	10	10	10	10
T_p [s]	3	3	3	4.5	1.5
q_1 [m^{-2}]	5000	1000	10000	5000	5000
q_2 [rad^{-2}]	0	0	0	0	0
r [(Nm)$^{-2}$]	1	1	1	1	1

Table 5.1: Low speed controller parameter sets, optimal control

Parameter	Set 6 Baseline	Set 7 Loose Control	Set 8 Tight Control	Set 9 Long Preview	Set 10 Short Preview
v [ms^{-1}]	40	40	40	40	40
T_p [s]	3	3	3	4.5	1.5
q_1 [m^{-2}]	5000	1000	10000	5000	5000
q_2 [rad^{-2}]	0	0	0	0	0
r [(Nm)$^{-2}$]	1	1	1	1	1

Table 5.2: High speed controller parameter sets, optimal control

5.6 Figures

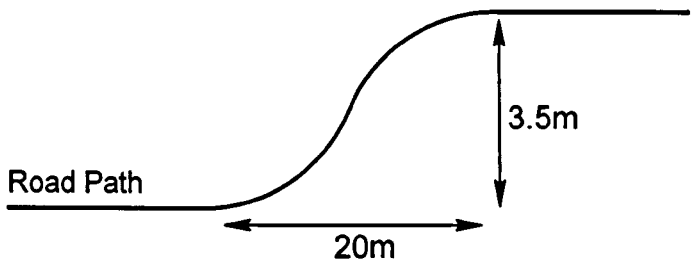

Figure 5.1: Single lane change path, not to scale

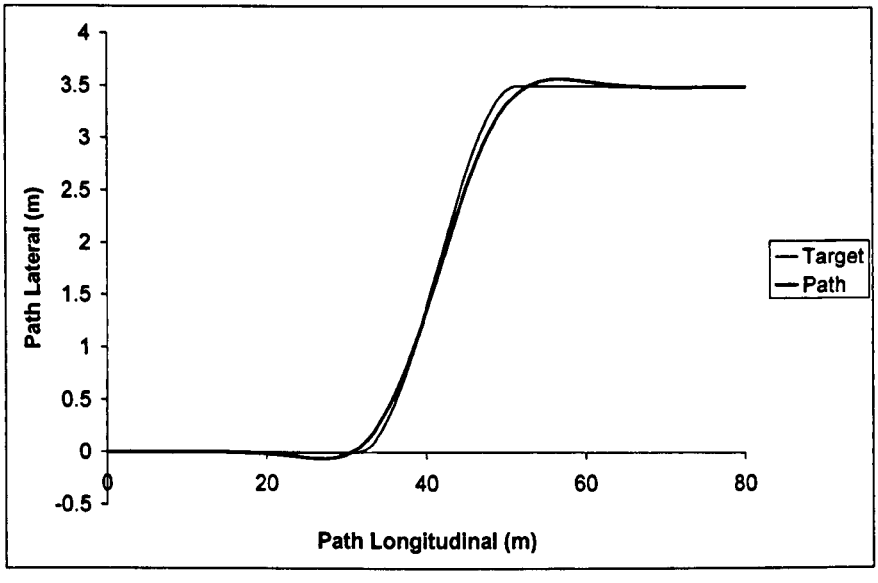

Figure 5.2: Path following, $v = 10$ m/s, $T_p = 3.0$ s, $q_1 = 5000$ m^{-2}

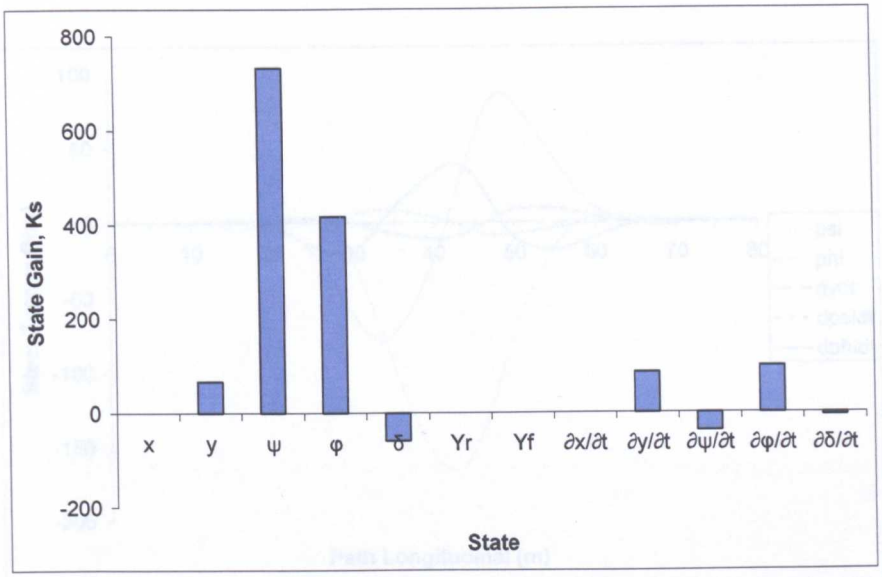

Figure 5.3: State gains, $v = 10$ m/s, $T_p = 3.0$ s, $q_1 = 5000$ m^{-2}

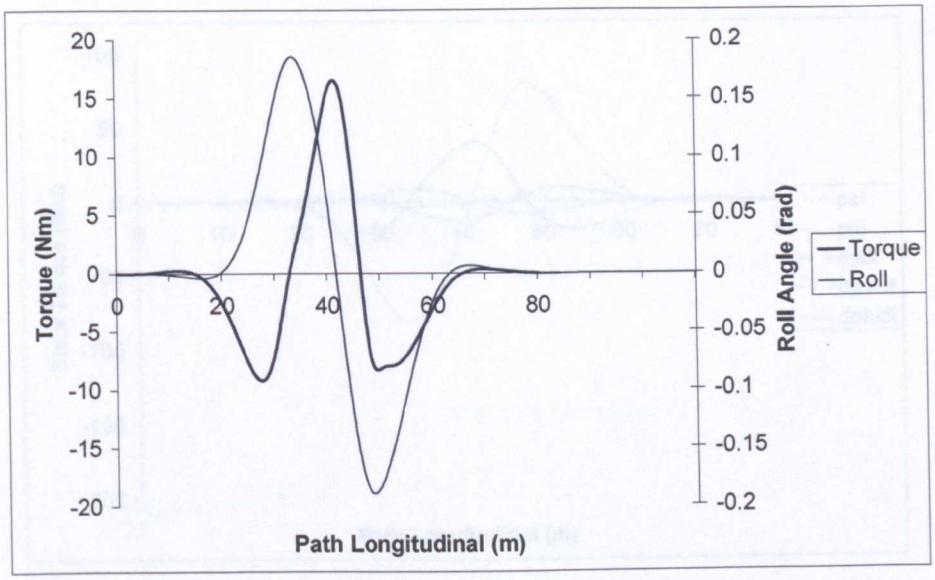

Figure 5.4: Steer torque and roll angle, $v = 10$ m/s, $T_p = 3.0$ s, $q_1 = 5000$ m^{-2}

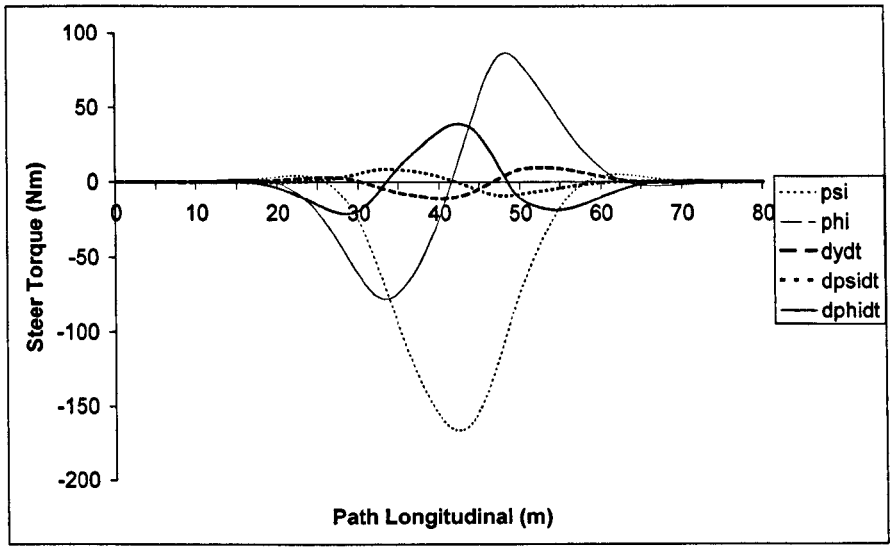

Figure 5.5: Principal individual state torque contributors, $v = 10$ m/s, $T_p = 3.0$ s, $q_1 = 5000$ m^{-2}, global coordinates

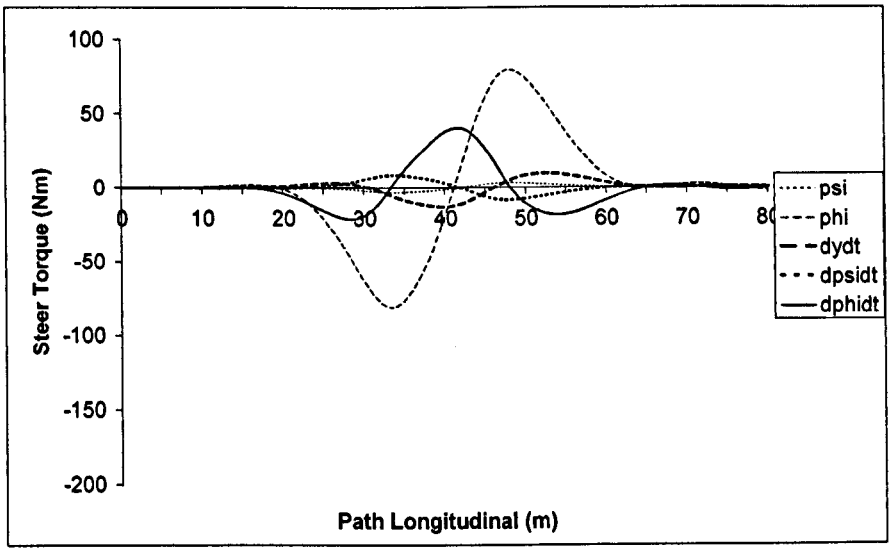

Figure 5.6: Principal individual state torque contributors, $v = 10$ m/s, $T_p = 3.0$ s, $q_1 = 5000$ m^{-2}, local coordinates

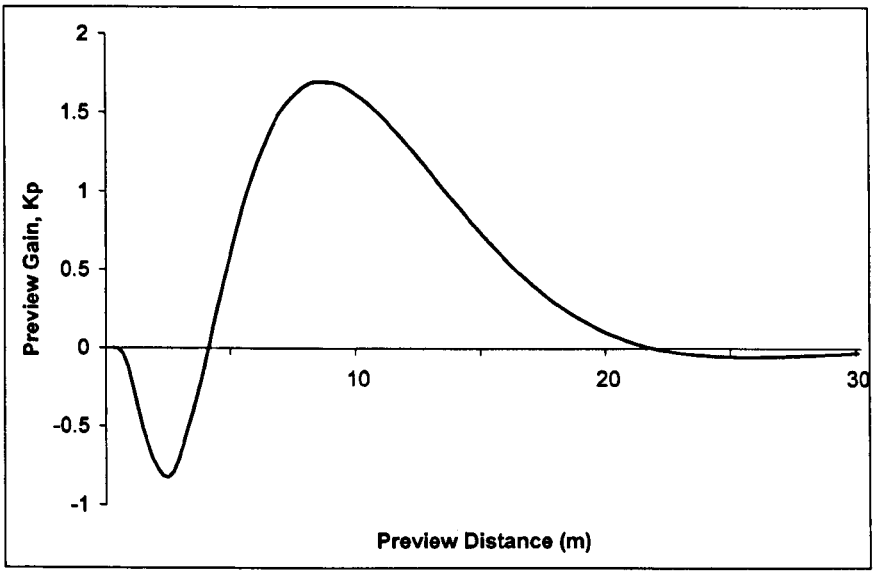

Figure 5.7: Preview gains, $v = 10$ m/s, $T_p = 3.0$ s, $q_1 = 5000$ m^{-2}

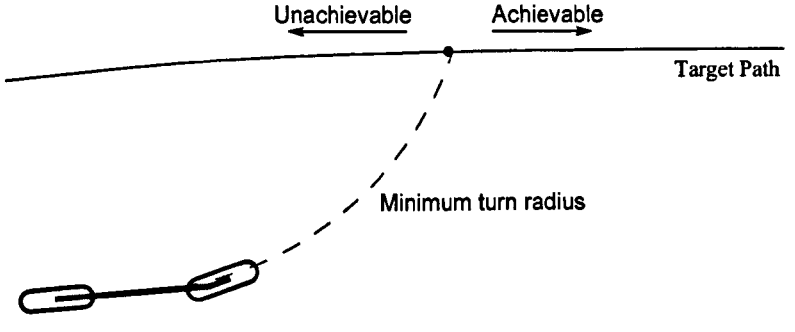

Figure 5.8: Path error correction capabilites of a motorcycle

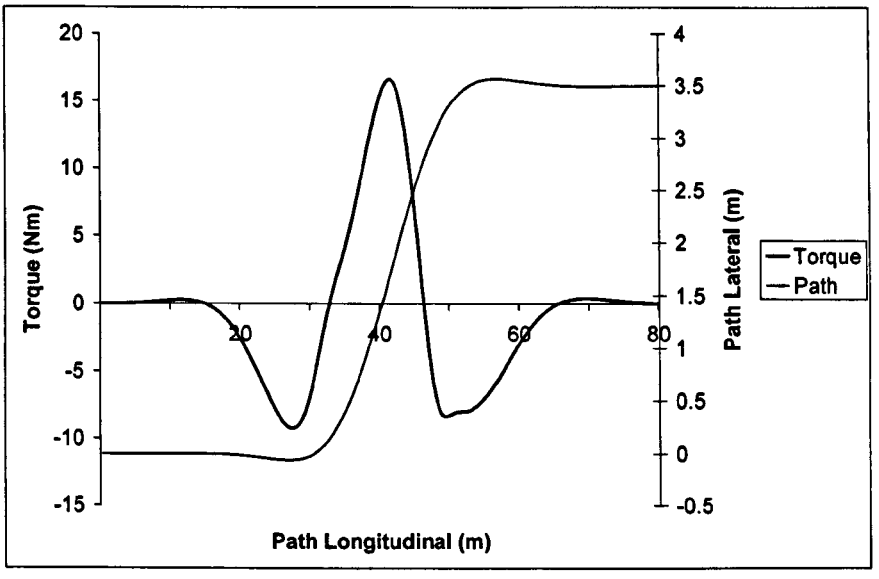

Figure 5.9: Steer torque, $v = 10$ m/s, $T_p = 3.0$ s, $q_1 = 5000$ m^{-2}

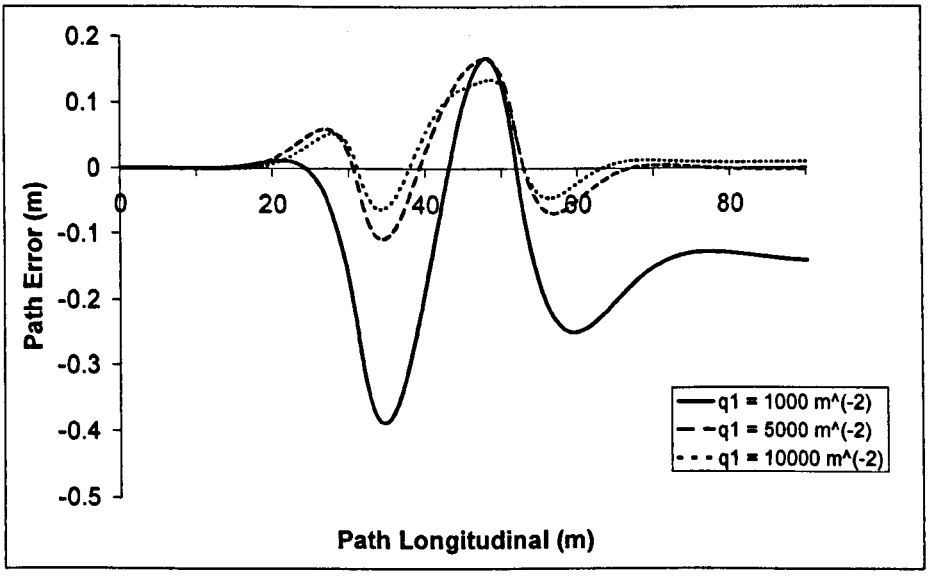

Figure 5.10: Path errors, $v = 10$ m/s, $T_p = 3.0$ s, $q_1 = 1000$, 5000 & 10000 m^{-2}

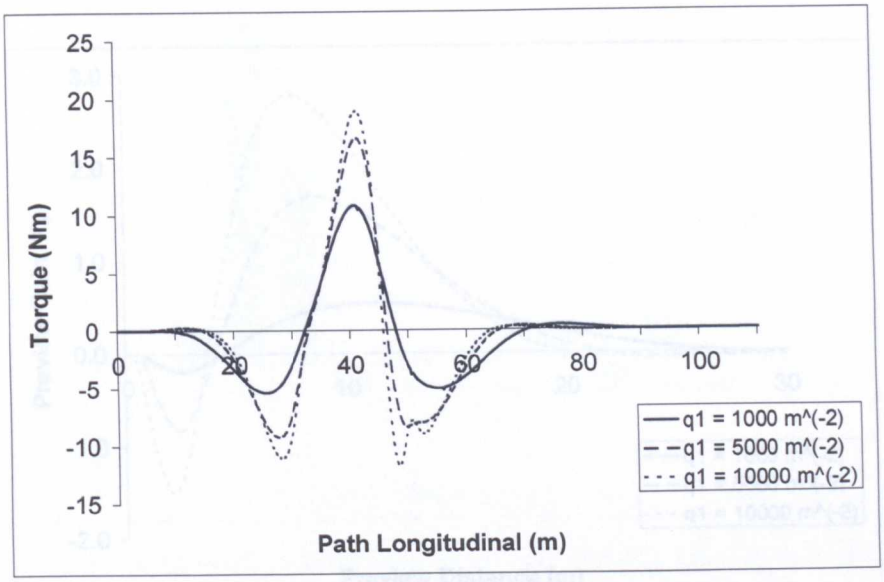

Figure 5.11: Steer torque, $v = 10$ m/s, $T_p = 3.0$ s, $q_1 = 1000$, 5000 & 10000 m^{-2}

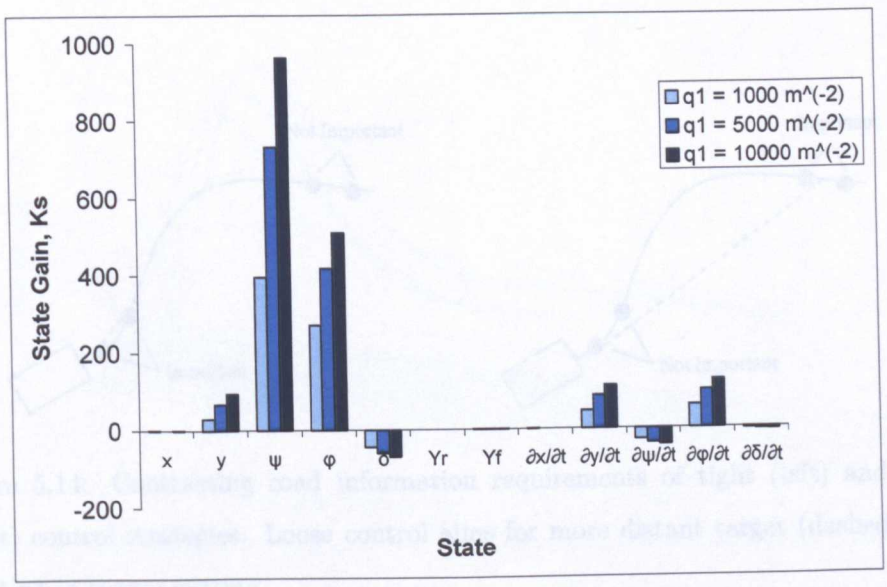

Figure 5.12: State gains, $v = 10$ m/s, $T_p = 3.0$ s, $q_1 = 1000$, 5000 & 10000 m^{-2}

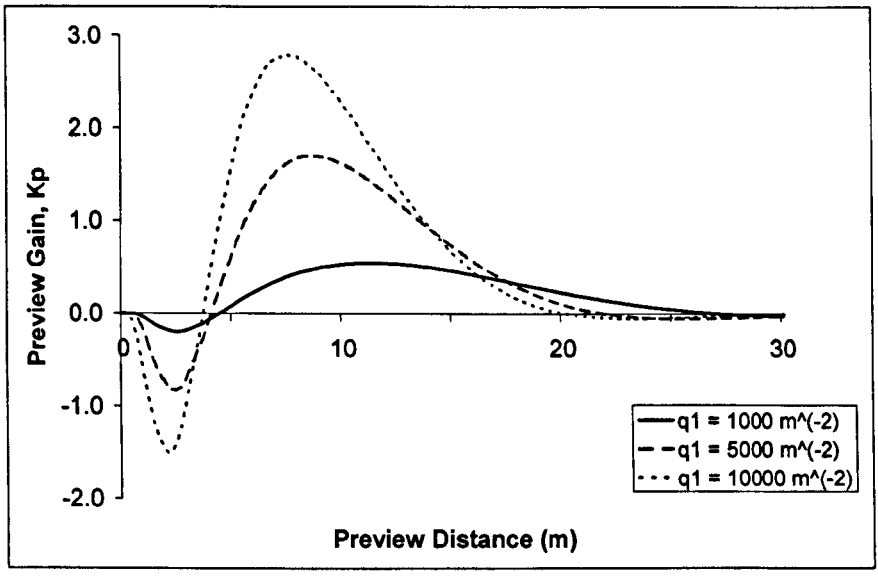

Figure 5.13: Preview Gains, $v = 10$ m/s, $T_p = 3.0$ s, $q_1 = 1000$, 5000 & 10000 m^{-2}

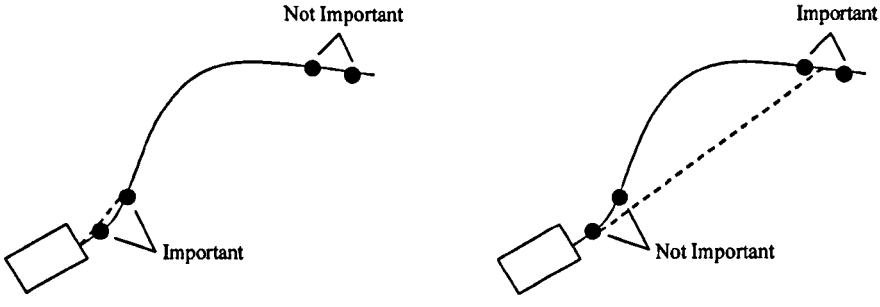

Figure 5.14: Contrasting road information requirements of tight (left) and loose (right) control strategies. Loose control aims for more distant target (dashed line), resulting in corner cutting

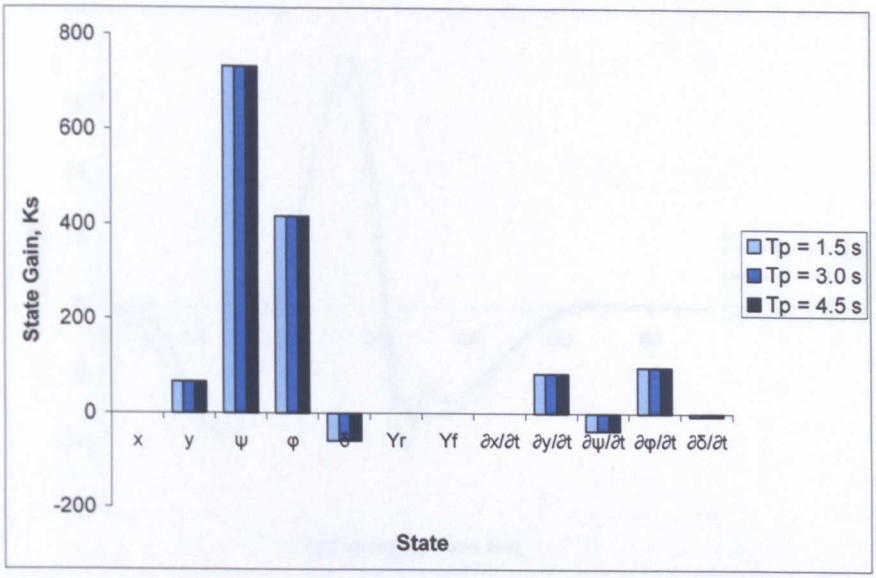

Figure 5.15: State gains, $v = 10$ m/s, $T_p = 1.5$ s, 3.0 s & 4.5 s, $q_1 = 5000$ m^{-2}

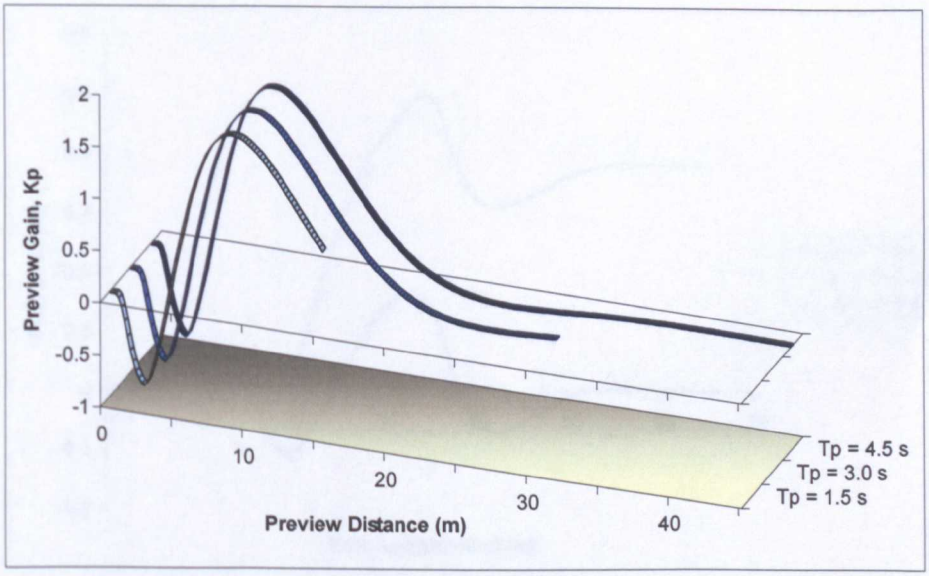

Figure 5.16: Preview gains, $v = 10$ m/s, $T_p = 1.5$ s, 3.0 s & 4.5 s, $q_1 = 5000$ m^{-2}

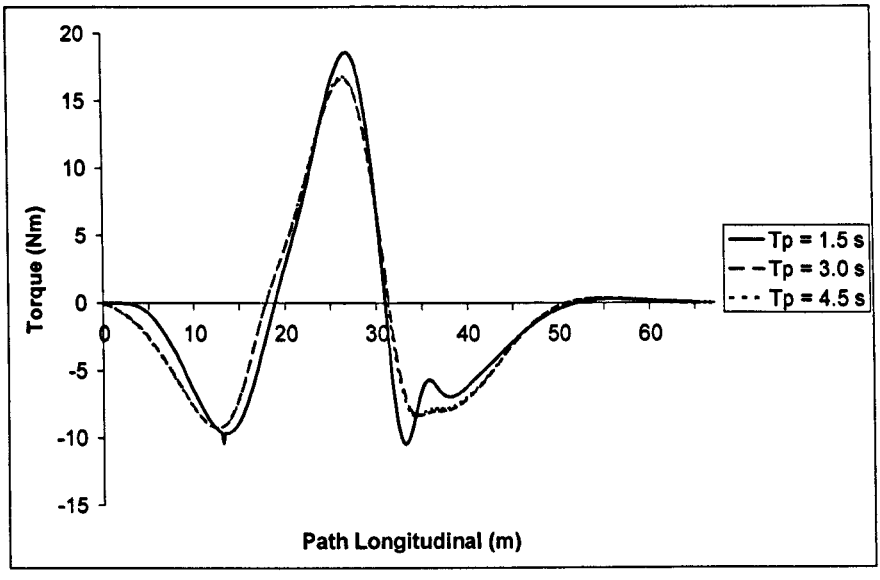

Figure 5.17: Steer torque, $v = 10$ m/s, $T_p = 1.5$ s, 3.0 s & 4.5 s, $q_1 = 5000$ m^{-2}

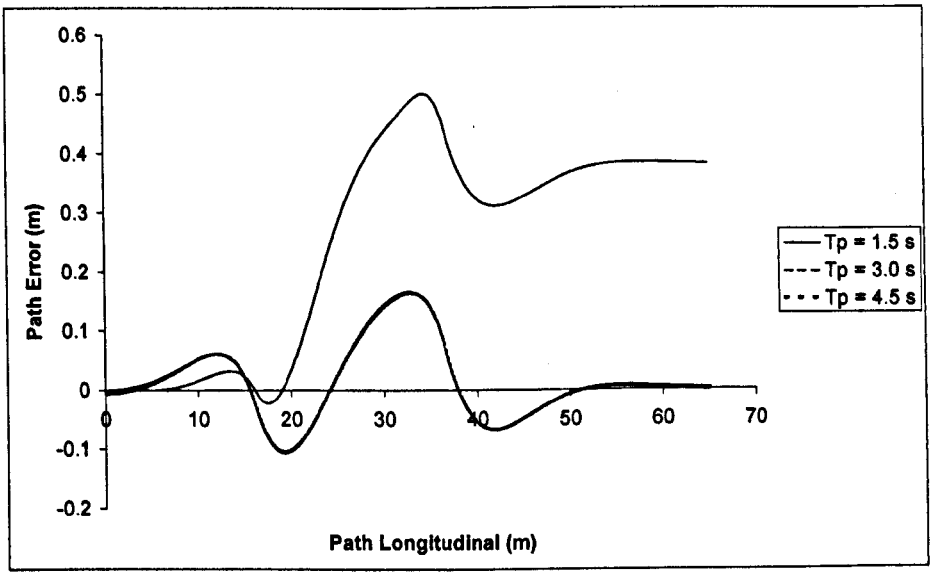

Figure 5.18: Path errors, $v = 10$ m/s, $T_p = 1.5$ s, 3.0 s & 4.5 s, $q_1 = 5000$ m^{-2}

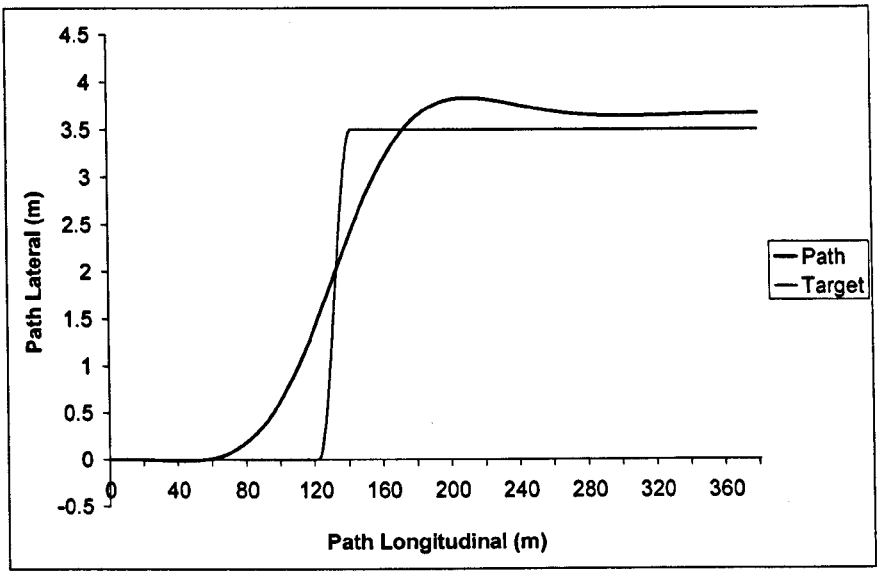

Figure 5.19: Path following, $v = 40$ m/s, $T_p = 3.0$ s, $q_1 = 5000$ m^{-2}

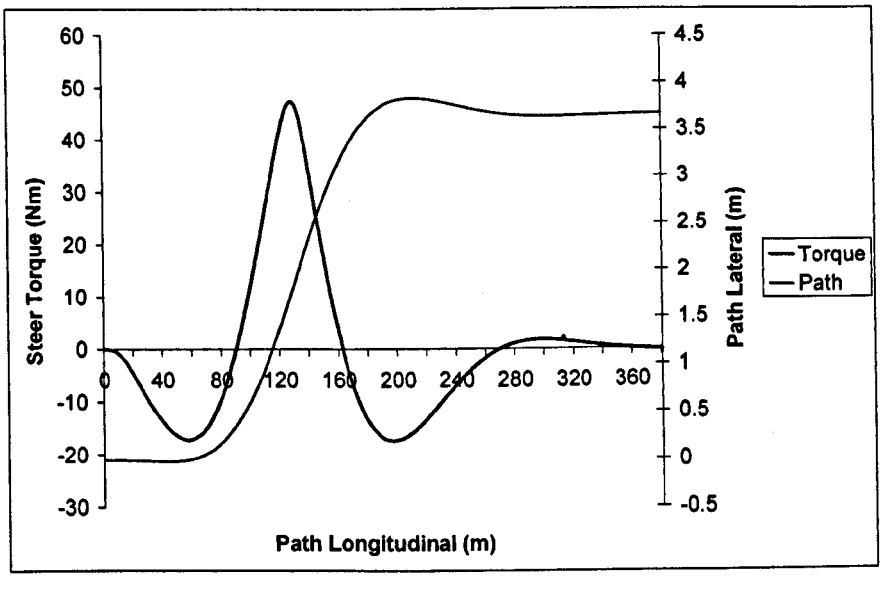

Figure 5.20: Steer torque, $v = 40$ m/s, $T_p = 3.0$ s, $q_1 = 5000$ m^{-2}

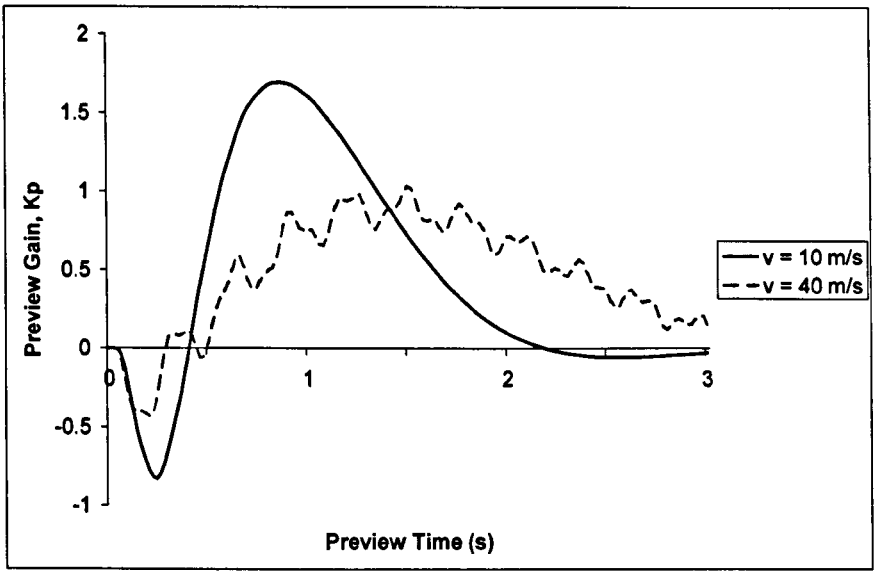

Figure 5.21: Preview gains, $v = 10$ m/s & 40 m/s, $T_p = 3.0$ s, $q_1 = 5000$ m^{-2}

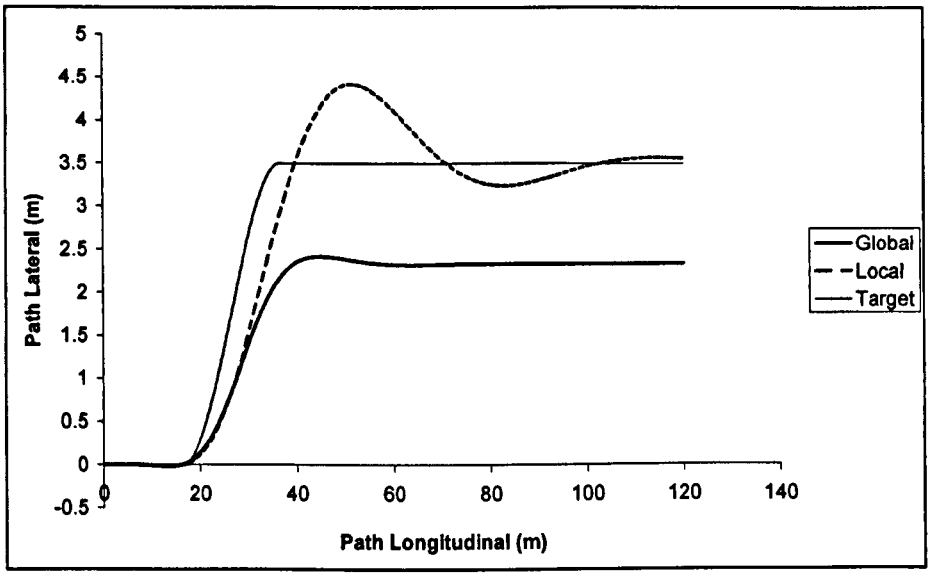

Figure 5.22: Path comparison, global vs. local coordinate system, $v = 10$ m/s, $T_p = 1.5$ s, $q_1 = 5000$ m^{-2}

Chapter 6

Model Predictive Control Rider Model

6.1 Introduction

As the name suggests, Model Predictive Control (MPC) is a technique in which a prediction of a system's behaviour is made in order to generate some form of optimised control input. The prediction is based on knowledge of the system's dynamic response characteristics and the calculation of a set of future control inputs. The predicted future system states can be compared against a set of future target states, with the set of future control inputs continuously re-evaluated, if necessary, in an attempt to ensure that the predicted future states match the target future states [35].

Widespread use of predictive control has been applied to the chemical engineering industry, where the need to predict the future behaviour of chemical reactors and other similar delayed-response systems was answered through the use of predictive control techniques. In recent years use has been made of MPC techniques in numerous other areas, including the modelling of human controllers for the task of driving [11, 72].

The application of predictive control methods to the simulation of a vehicle driver seems an entirely appropriate choice. In driving/riding a vehicle, the pilot has previewed information of the approaching road path to follow and knowledge of the vehicle's condition. A motorcycle rider will also have knowledge of how the machine is likely to respond to certain control inputs as a result of previous riding experience,

and can therefore subconsciously plan his future control actions in order to follow the road path he sees ahead of him. This process of evaluating the road and vehicle and forming the necessary future control strategy is evaluated in a continuous manner throughout the riding task.

With riding experience, for instance, a motorcycle rider will know that to change his path heading to, say, the left, he will be required to countersteer to the right at some distance prior to the point at which he wishes to start the left turn. While this may not be a conscious process, the rider has to some extent predicted the future response of the motorcycle to his initial countersteer to the right based on his knowledge of typical system response. Similarly, if he were wanting to stop, he would know that a certain braking distance is required to achieve this, and therefore makes a subconscious prediction for how long it will take to slow down in choosing the point at which he will start to brake, and balances this knowledge against the severity of braking that he is prepared to tolerate.

The riding task that the rider is presented with will change continuously due to changes in both the road path as he progresses along a path, and due to the changing vehicle states during motion of the motorcycle. The predicted future control actions that the rider has will therefore also be continually updated in light of the ever-changing task. The changes in the task may be gradual, such as the changing direction of the approaching road path, or quite sudden, such as a sudden loss of road traction as a result of water, debris or oil on the road, causing the vehicle to respond in an unexpected manner.

Breaking the riding task into small discrete time-steps, although at an instant the rider may have control predictions for the full picture of his riding task, he will only ever make use of and apply his first control prediction, before re-evaluating the control problem and at the next instant using the next first control prediction in a continuous process.

This chapter covers the theory of MPC techniques and the application to the modelling of a motorcycle rider. The chapter begins with the detailed theory of the prediction model, for both a linear prediction model and the more realistic non-linear prediction model that will account for changes to the motorcycle states over the course of the prediction horizon. The opportunities available for the definition of

a reference path for the motorcycle to attempt to follow are considered, presenting the theory for the application of different reference path definitions. The theory for predictive controller gains is outlined before the strategy is applied to the motorcycle model attempting a lane change manoeuvre. A wide range of controller parameters is considered, including preview and control horizons, forward speed and cost function weighting parameters, together with the effects of different reference path definitions. Hence the applicability of the technique in replicating the actions of a motorcycle rider and the detailed characteristics of the controller will be ascertained. Subsequently, in Chapter 7, the comparisons between this approach and the previous optimal control approach detailed in Chapter 5 will be made, in order to present the potential advantages that may be found when using the predictive control approach.

6.2 MPC Theory

The MPC approach [52] consists of two fundamental parameters that differentiate it from other similar techniques such as optimal control, namely the prediction model and the reference path definition that the controller attempts to follow.

Model predictive control, as suggested by the name, forms a prediction model to anticipate the future response of the system using a known set of future control inputs, and by making use of the known system response to controlling inputs. A motorcycle rider, for example, will have a reasonably accurate knowledge of how the motorcycle will respond to his controlling inputs, and therefore it can be said that he has knowledge of the system response to control inputs. In riding a motorcycle, the rider will be looking ahead at the road and subconsciously will have anticipated his future control inputs in response to the road path he sees ahead of him, and consequently he may have anticipated a set of predicted future control inputs. This is the primary difference between an MPC approach and an optimal control approach (Chapter 5), where a control input is generated only for the motorcycle's current position and based on the current motorcycle states only.

The second fundamental difference concerns the system output that the rider is aiming to follow. The MPC technique is defined with two output paths, known as the set path and the reference path. The set path is the absolute target of the system which it ultimately aims to follow, in this case the road centreline. It is unlikely that the

system will follow exactly the set path. In the case of the motorcycle, as seen with the optimal control approach in Chapter 5, there is always some element of corner cutting. The reference path is therefore a newly defined path that takes the system from some position displaced from the set path, and that returns to the set path over some time and distance. This condition is depicted in Figure 6.1.

The reference path itself can be defined in any manner chosen. It can be a simple step, such that the reference path *is* the set path, it can be defined by a linear path from the current system states to target system states over a finite time, or indeed can be an exponential, quadratic or any other chosen path definition. The reference path, as its name suggests, is simply a reference which the system aims to follow.

It is accepted that the motorcycle will not follow the road path exactly, with some corner-cutting likely. A motorcycle is not capable of correcting a lateral path error instantaneously; the rider must steer, and with forward motion the lateral position of the motorcycle on the road can be changed, and thus any lateral path errors resolved. A rider will therefore aim to follow a path that will take him from his current, possibly displaced, position to his target path position at some point in his future.

Another feature of predictive control, which is of less use for the application here, includes the capacity to deal with system response lag. Such control is widely used in the chemical engineering industry, where the response to control is often not realised until some time in the future, and is in general known as the dead-time or dead-zone. Thus, the prediction element of the control strategy can take account of the delay that will exist between control input and output response and can therefore predict the need to apply the necessary control in advance. The ability to replicate this lag in the control strategy can, for some applications, be a vital component.

These features of MPC make the application to modelling a motorcycle rider potentially more suitable than the optimal control technique. For simplicity, the system is initially defined with the reference path and set path equal, such that the effects of the prediction model can be more closely compared with the results of the optimal control technique. Subsequently, some analysis is made into the effects of different reference path definitions on the performance of a rider model simulated using MPC techniques.

It is necessary, at this point, to clarify some of the terminology that will subsequently

be used, primarily concerning the distinction between the simulation and the prediction.

The goal here is to create a model that replicates a motorcycle rider negotiating a path manoeuvre. The complete representation of the motorcycle following the path is the simulation model. Thus, the simulation is the actual path that the motorcycle model follows as a result of the rider model's control actions. The simulation model, using optimal control techniques, was also presented in Chapter 5.

In addition to this, the MPC approach has a prediction model. The simulation model used here is a discrete sample simulation. At each discrete step of the simulation, the control strategy forms a prediction model, itself formed as series of discrete steps, which will predict the future path of the motorcycle up to a finite horizon, from that particular discrete simulation step. The prediction model for that simulation step will be used to calculate the required control input for that one simulation step. Once the control has been applied, and the motorcycle simulation moves to the next discrete step, a new prediction model will be formed up to the finite horizon from the new discrete simulation step, the new control input calculated, and the simulation model moved to the next simulation step.

The principles of the simulation and prediction models are, in fact, almost identical, however the distinction between the simulation and the prediction model is important to be aware of.

6.2.1 Linear Prediction Model

MPC techniques develop a prediction model that aims to anticipate the future response of the controlled system based on a set of future control inputs. Comparison between the predicted future outputs and the required future outputs defined by the reference path result in a set of errors. The controller forms a cost function combining these errors with the control input cost and, in a similar manner to the optimal control approach (Chapter 5), determines the best set of future control inputs to balance output error minimisation against control input effort.

As with the optimal control approach, the starting point in the analysis of MPC techniques is with the equations of motion for the dynamic system response, formed

into the convenient linearised discrete-time state space system model, as presented in Section 3.4.1. For a generic system at the k^{th} step, this takes the form

$$\mathbf{x}(k+1) = \mathbf{A}(k)\mathbf{x}(k) + \mathbf{B}(k)\mathbf{u}(k) \tag{6.1a}$$

$$\mathbf{y}(k) = \mathbf{C}(k)\mathbf{x}(k) + \mathbf{D}(k)\mathbf{u}(k) \tag{6.1b}$$

where the vectors $\mathbf{x}(k)$, $\mathbf{y}(k)$ and $\mathbf{u}(k)$ represent respectively the system states, system output and system input, and the matrices $\mathbf{A}(k)$, $\mathbf{B}(k)$, $\mathbf{C}(k)$ and $\mathbf{D}(k)$ are the discrete-time state space matrices, all at the k^{th} step.

The distinction between the prediction and the simulation is emphasised again here. The expression given in (6.1), when used with the actual state values and control inputs, generates the actual system output and the states of the system at the next step. This therefore represents a discrete step in the simulation. Here, we use the dynamic response model of the system (based on the predicted states $\hat{\mathbf{x}}(k)$) given by this expression to determine a predicted future set of states and a predicted future system output using predicted future states and control input:

$$\hat{\mathbf{x}}(k+1) = \hat{\mathbf{A}}(k)\hat{\mathbf{x}}(k) + \hat{\mathbf{B}}(k)\hat{\mathbf{u}}(k) \tag{6.2a}$$

$$\hat{\mathbf{y}}(k+1) = \hat{\mathbf{C}}(k+1)\hat{\mathbf{x}}(k+1) + \hat{\mathbf{D}}(k+1)\hat{\mathbf{u}}(k+1) \tag{6.2b}$$

Since the state space matrices $\mathbf{A}(k)$, $\mathbf{B}(k)$, $\mathbf{C}(k)$ and $\mathbf{D}(k)$ are dependent on the system states $\mathbf{x}(k)$, they too will be predicted when $\hat{\mathbf{x}}(k)$ is used, and hence are given here as $\hat{\mathbf{A}}(k)$, $\hat{\mathbf{B}}(k)$, $\hat{\mathbf{C}}(k)$ and $\hat{\mathbf{D}}(k)$.

At step k, the state vector $\hat{\mathbf{x}}(k+1)$ is not available directly in (6.2b), but can be obtained by substitution of (6.2a):

$$\hat{\mathbf{x}}(k+1) = \hat{\mathbf{A}}(k)\hat{\mathbf{x}}(k) + \hat{\mathbf{B}}(k)\hat{\mathbf{u}}(k) \tag{6.3a}$$

$$\hat{\mathbf{y}}(k+1) = \hat{\mathbf{C}}(k+1)[\hat{\mathbf{A}}(k)\hat{\mathbf{x}}(k) + \hat{\mathbf{B}}(k)\hat{\mathbf{u}}(k)] + \hat{\mathbf{D}}(k+1)\hat{\mathbf{u}}(k+1) \tag{6.3b}$$

The distinction here is drawn between the optimal control output, where the system output relates to the system's current states, and predictive control where in effect the output is the predicted future path. The error that the controller aims to minimise is between the states of the system at the current k^{th} step, and the target states at the k^{th} step. For the optimal control approach, the first preview point is the system information relative to the system's current position i.e. the road information for the motorcycle's current discrete simulation point. The rider preview element and corresponding state space formualtion for this condition was given in Chapter 4.

For the predictive control approach, the output considered is the future predicted output $\hat{\mathbf{y}}(k+1)$, and the subsequent minimisation of this predicted future output against a future target. The preview horizon is therefore subtly different. The preview horizon for the predictive controller will begin at the first prediction point in the rider's horizon, in other words one step ahead of the motorcycle's current position, i.e. at $k+1$. The theory for the state space modelling of this predictive control rider preview is no different from the approach given in Chapter 4. Provided that the initial information fed into the rider's road preview vector corresponds to the information one step ahead, and the new information fed into the preview vector similarly accounts for the correct new information point, the shift-register matrix form is no different.

The discrete-time state space representation of the system dynamics given in (6.3) can be used to predict the output of the system to some predetermined number of iteration steps in the future [11]. The prediction begins from the current simulation point, for which the vector $\hat{\mathbf{x}}(k)$, and the matrices $\hat{\mathbf{A}}(k)$, $\hat{\mathbf{B}}(k)$, $\hat{\mathbf{C}}(k)$ and $\hat{\mathbf{D}}(k)$ are known, and are $\mathbf{x}(k)$, $\mathbf{A}(k)$, $\mathbf{B}(k)$, $\mathbf{C}(k)$ and $\mathbf{D}(k)$. The input vector $\hat{\mathbf{u}}(k)$ is, at this point, a predicted input still, but will subsequently be recalculated as $\mathbf{u}(k)$, which will be used for the simulation step. Thus, the system information at step k is used to predict the first output in the rider's preview horizon, $\hat{\mathbf{y}}(k+1)$

With knowledge or prediction of the second control input $\hat{\mathbf{u}}(k+1)$, a similar process can be applied to determine the system output after the second iteration:

$$\hat{\mathbf{x}}(k+2) = \hat{\mathbf{A}}(k+1)\hat{\mathbf{x}}(k+1) + \hat{\mathbf{B}}(k+1)\hat{\mathbf{u}}(k+1) \quad (6.4a)$$

$$\hat{\mathbf{y}}(k+2) = \hat{\mathbf{C}}(k+2)\hat{\mathbf{x}}(k+2) + \hat{\mathbf{D}}(k+2)\hat{\mathbf{u}}(k+2) \quad (6.4b)$$

Only the current states $\mathbf{x}(k)$ and state space matrices $\mathbf{A}(k)$, $\mathbf{B}(k)$, $\mathbf{C}(k)$ and $\mathbf{D}(k)$, for the current step, are exactly known, and therefore the solution to (6.4) cannot be solved directly. However the result from (6.3) can be employed here, and, substituted appropriately in (6.4), will result in the predicted system response at $k+2$ as:

$$\hat{\mathbf{x}}(k+2) = \hat{\mathbf{A}}(k+1)[\mathbf{A}(k)\mathbf{x}(k)+\mathbf{B}(k)\hat{\mathbf{u}}(k)]+\hat{\mathbf{B}}(k+1)\hat{\mathbf{u}}(k+1) \tag{6.5a}$$

$$\begin{aligned}\hat{\mathbf{y}}(k+2) = {} & \hat{\mathbf{C}}(k+2)\{\hat{\mathbf{A}}(k+1)[\mathbf{A}(k)\mathbf{x}(k)+\mathbf{B}(k)\hat{\mathbf{u}}(k)]+\hat{\mathbf{B}}(k+1)\hat{\mathbf{u}}(k+1)\} \\ & +\hat{\mathbf{D}}(k+2)\hat{\mathbf{u}}(k+2)\end{aligned} \tag{6.5b}$$

For a linear prediction model, it is assumed that the state space matrices $\hat{\mathbf{A}}(k+i_p)$, $\hat{\mathbf{B}}(k+i_p)$, $\hat{\mathbf{C}}(k)(k+i_p)$ and $\hat{\mathbf{D}}(k)(k+i_p)$, where i_p is the number of the prediction step, are invariant over the full prediction, defining them now simply as **A**, **B**, **C** and **D**. That is to say that at the k^{th} iteration step, the linear state space matrices are obtained and it is assumed that these matrices are valid over the full prediction at the k^{th} step. However, when the controller gains are calculated and the simulation moved to the next step, the state space matrices are re-evaluated, and these new matrices used for the full prediction horizon at that next simulation step.

gain changes

Furthermore, the system output is assumed to be based solely on the system states, and not the control input. Thus, the matrix **D** is set to zero and can therefore be removed from the expressions.

With the simplifications of the predicted state space matrices made, the expressions (6.2) and (6.4) can be redefined as

$$\begin{aligned}
\hat{\mathbf{x}}(k+1) &= \mathbf{A}\mathbf{x}(k) + \mathbf{B}\hat{\mathbf{u}}(k) \\
\\
\hat{\mathbf{y}}(k+1) &= \mathbf{C}\mathbf{x}(k+1) \\
&= \mathbf{C}[\mathbf{A}\mathbf{x}(k) + \mathbf{B}\hat{\mathbf{u}}(k)] \\
&= \mathbf{C}\mathbf{A}\mathbf{x}(k) + \mathbf{C}\mathbf{B}\hat{\mathbf{u}}(k) \\
\\
\hat{\mathbf{x}}(k+2) &= \mathbf{A}\hat{\mathbf{x}}(k+1) + \mathbf{B}\hat{\mathbf{u}}(k+1) \\
&= \mathbf{A}[\mathbf{A}\mathbf{x}(k) + \mathbf{B}\hat{\mathbf{u}}(k)] + \mathbf{B}\hat{\mathbf{u}}(k+1) \\
&= \mathbf{A}^2\mathbf{x}(k) + \mathbf{A}\mathbf{B}\hat{\mathbf{u}}(k) + \mathbf{B}\hat{\mathbf{u}}(k+1) \\
\\
\hat{\mathbf{y}}(k+2) &= \mathbf{C}\hat{\mathbf{x}}(k+2) \\
&= \mathbf{C}[\mathbf{A}\mathbf{x}(k+1) + \mathbf{B}\hat{\mathbf{u}}(k+1)] \\
&= \mathbf{C}\mathbf{A}\mathbf{x}(k+1) + \mathbf{C}\mathbf{B}\hat{\mathbf{u}}(k+1)
\end{aligned} \tag{6.6}$$

It is seen from the above expressions that a pattern is starting to emerge for the prediction of the future states and outputs using the initial vehicle states $\mathbf{x}(k)$ and the predicted future control inputs $\hat{\mathbf{u}}(k), \hat{\mathbf{u}}(k+1)$.... This pattern can readily be formed into a state space expression, calculating all future system states and system outputs using the initial states $\mathbf{x}(k)$ and vector of predicted future control inputs $\hat{\mathbf{u}}(k)$, $\hat{\mathbf{u}}(k+1)$, etc.:

$$\begin{bmatrix} \hat{\mathbf{x}}(k+1) \\ \hat{\mathbf{x}}(k+2) \\ \hat{\mathbf{x}}(k+3) \\ \vdots \\ \hat{\mathbf{x}}(k+N_p) \end{bmatrix} = \begin{bmatrix} \mathbf{A} \\ \mathbf{A}^2 \\ \mathbf{A}^3 \\ \vdots \\ \mathbf{A}^{N_p} \end{bmatrix} \mathbf{x}(k) + \begin{bmatrix} \mathbf{B} & \mathbf{0} & . & \mathbf{0} \\ \mathbf{A}\mathbf{B} & \mathbf{B} & . & \mathbf{0} \\ \mathbf{A}^2\mathbf{B} & \mathbf{A}\mathbf{B} & . & \mathbf{0} \\ . & . & . & . \\ \mathbf{A}^{N_p-1}\mathbf{B} & \mathbf{A}^{N_p-2}\mathbf{B} & . & \mathbf{B} \end{bmatrix} \begin{bmatrix} \hat{\mathbf{u}}(k) \\ \hat{\mathbf{u}}(k+1) \\ \hat{\mathbf{u}}(k+2) \\ \vdots \\ \hat{\mathbf{u}}(k+(N_p-1)) \end{bmatrix} \tag{6.7a}$$

and similarly for the system output

$$\begin{bmatrix} \hat{y}(k+1) \\ \hat{y}(k+2) \\ \hat{y}(k+3) \\ \vdots \\ \hat{y}(k+N_p) \end{bmatrix} = \begin{bmatrix} \mathbf{CA} \\ \mathbf{CA}^2 \\ \mathbf{CA}^3 \\ \vdots \\ \mathbf{CA}^{N_p} \end{bmatrix} \mathbf{x}(k) + \begin{bmatrix} \mathbf{CB} & \mathbf{0} & . & \mathbf{0} \\ \mathbf{CAB} & \mathbf{CB} & . & \mathbf{0} \\ \mathbf{CA}^2\mathbf{B} & \mathbf{CAB} & . & \mathbf{0} \\ . & . & . & . \\ \mathbf{CA}^{N_p-1}\mathbf{B} & \mathbf{CA}^{N_p-2}\mathbf{B} & . & \mathbf{CB} \end{bmatrix} \begin{bmatrix} \hat{u}(k) \\ \hat{u}(k+1) \\ \hat{u}(k+2) \\ \vdots \\ \hat{u}(k+(N_p-1)) \end{bmatrix} \tag{6.7b}$$

which can be represented by

$$\chi(k) = \mathbf{F}(k)\mathbf{x}(k) + \mathbf{G}(k)\Upsilon(k) \tag{6.8a}$$

$$\varphi(k) = \mathbf{M}(k)\mathbf{x}(k) + \mathbf{N}(k)\Upsilon(k) \tag{6.8b}$$

where $\chi(k)$, $\varphi(k)$ and $\Upsilon(k)$ represent the full vectors of all predicted future states vectors, the vectors of predicted future outputs and the vectors of predicted future inputs at the k^{th} step respectively.

The matrices $\mathbf{F}(k)$, $\mathbf{G}(k)$, $\mathbf{M}(k)$ and $\mathbf{N}(k)$ have been defined here specifically for a particular iteration step k, while the constitutive elements given in (6.7b) do not show such time-dependency. A reminder is made to the elements of the matrices $\mathbf{F}(k)$, $\mathbf{G}(k)$, $\mathbf{M}(k)$ and $\mathbf{N}(k)$: at the simulation step k for a linear prediction model, the system state space matrices $\mathbf{A}(k)$, $\mathbf{B}(k)$, $\mathbf{C}(k)$ and $\mathbf{D}(k)$ are used to form all of the elements in (6.7), assumed invariant over the prediction horizon, and, only for clarity, are defined as $\mathbf{A}$, $\mathbf{B}$, $\mathbf{C}$ and $\mathbf{D}$ in (6.7).

To this point, the assumption has been made that the preview horizon and the control horizon are equal, and that there are consequently an equal number N_p of future road

preview points and future control inputs. Details relating to the discrete preview horizon can be found in Chapter 4.

This condition is not strictly necessary, and it is possible that the control horizon can be set shorter than the preview horizon. Defining the number of control inputs in the control horizon as N_u, where N_u is the control horizon time T_u divided by the discrete time step interval t, the control inputs can be held constant from the control horizon up to the prediction horizon, such that the future control input vector is defined as

$$\Upsilon(k) = \begin{bmatrix} \hat{\mathbf{u}}^T(k) & \hat{\mathbf{u}}^T(k+1) & \dots & \hat{\mathbf{u}}^T(k+(N_u-1)) & \dots & \hat{\mathbf{u}}^T(k+(N_u-1)) \end{bmatrix}^T \tag{6.9}$$

In this case, columns N_u to N_p of the matrices $\mathbf{G}(k)$ and $\mathbf{N}(k)$ are all multiplied by the control input $\hat{\mathbf{u}}(k+(N_u-1))$, and thus these columns can be summed such that the expressions (6.7a) and (6.7b) become

$$\begin{bmatrix} \hat{\mathbf{x}}(k+1) \\ \hat{\mathbf{x}}(k+2) \\ \hat{\mathbf{x}}(k+2) \\ \vdots \\ \hat{\mathbf{x}}(k+N_p) \end{bmatrix} = \begin{bmatrix} \mathbf{A} \\ \mathbf{A}^2 \\ \mathbf{A}^3 \\ \vdots \\ \mathbf{A}^{N_p} \end{bmatrix} \mathbf{x}(k) + \begin{bmatrix} \mathbf{B} & \mathbf{0} & . & \mathbf{0} \\ \mathbf{AB} & \mathbf{B} & . & \mathbf{0} \\ \mathbf{A}^2\mathbf{B} & \mathbf{AB} & . & \mathbf{0} \\ . & . & . & . \\ \mathbf{A}^{N_p-1}\mathbf{B} & \mathbf{A}^{N_p-2}\mathbf{B} & . & \sum_{i=0}^{N_p-N_u} \mathbf{A}^i\mathbf{B} \end{bmatrix} \begin{bmatrix} \hat{\mathbf{u}}(k) \\ \hat{\mathbf{u}}(k+1) \\ \hat{\mathbf{u}}(k+2) \\ \vdots \\ \hat{\mathbf{u}}(k+(N_u-1)) \end{bmatrix} \tag{6.10a}$$

and again for the system output

$$\begin{bmatrix} \hat{\mathbf{y}}(k+1) \\ \hat{\mathbf{y}}(k+2) \\ \hat{\mathbf{y}}(k+3) \\ \vdots \\ \hat{\mathbf{y}}(k+N_p) \end{bmatrix} = \begin{bmatrix} \mathbf{CA} \\ \mathbf{CA}^2 \\ \mathbf{CA}^3 \\ \vdots \\ \mathbf{CA}^{N_p} \end{bmatrix} \mathbf{x}(k) + \begin{bmatrix} \mathbf{CB} & \mathbf{0} & . & \mathbf{0} \\ \mathbf{CAB} & \mathbf{CB} & . & \mathbf{0} \\ \mathbf{CA}^2\mathbf{B} & \mathbf{CAB} & . & \mathbf{0} \\ . & . & . & . \\ \mathbf{CA}^{N_p-1}\mathbf{B} & \mathbf{CA}^{N_p-2}\mathbf{B} & . & \mathbf{C}\sum_{i=0}^{N_p-N_u}\mathbf{A}^i\mathbf{B} \end{bmatrix} \begin{bmatrix} \hat{\mathbf{u}}(k) \\ \hat{\mathbf{u}}(k+1) \\ \hat{\mathbf{u}}(k+2) \\ \vdots \\ \hat{\mathbf{u}}(k+(N_u-1)) \end{bmatrix} \tag{6.10b}$$

and the matrices $\mathbf{F}(k)$, $\mathbf{G}(k)$, $\mathbf{M}(k)$, and $\mathbf{N}(k)$ are now redefined using the modified expressions (6.10a) and (6.10b).

This therefore results in a state space representation of the predicted future states and future outputs of a modelled system allowing for different control and prediction horizons. Replacing the generic state space matrices $\mathbf{A}, \mathbf{B}$ and $\mathbf{C}$ with the motorcycle state space matrices $\mathbf{A}_v(k), \mathbf{B}_v(k)$ and $\mathbf{C}_v(k)$, the prediction model can be used in defining a control strategy to control the motorcycle and accomplish the path following task.

6.2.2 Non-Linear Prediction Model

The theory of MPC and the prediction model, used to anticipate the system output at some point in the future, is the characteristic feature of MPC that differentiates it from optimal control techniques. The controller attempts to control the system such that the anticipated future states match the target future states. It should therefore be apparent that a fundamental requirement of an MPC controller is to have an accurate prediction model if useful controller performance is to be obtained.

For the case of time-invariant systems, the theory has already been discussed through

the derivation of equations (6.1) through to (6.10). The time-invariant nature of the state space model presented eased the analysis considerably, as at each iteration step k of the model simulation, the sub-matrix elements of the generic prediction model matrices were multiples of only three fixed matrices, $\mathbf{A}(k)$, $\mathbf{B}(k)$ and $\mathbf{C}(k)$.

Non-linear state space models will have matrices that will vary linearly with changes in the system state vector, and thus may be time-variant. In such cases, it is necessary to linearise the equations of motion for a specific set of states. The model can then be used as a linear model within small variations only of the individual states, before system accuracy degrades excessively. Typically, the model state space matrices will be linearised for a set of system states at each iteration step, and with each subsequent iteration step the model state space matrices will then be re-linearised for the new system states (Figure 6.2). For a system such as a motorcycle, whose states change significantly over time, it is necessary to re-linearise repeatedly the state space model to retain some accuracy of the linearised state space model.

The prediction model described in Section 6.2.1 makes use of the system state space matrices $\mathbf{A}(k)$, $\mathbf{B}(k)$ and $\mathbf{C}(k)$ over the preview horizon, yet the predicted system states may change significantly from the actual model states to the states at another point in the predicted future horizon. Therefore use of a fixed state space representation of the system, applied over the whole prediction horizon, may not be accurate. For technical accuracy, it would be necessary to evaluate and linearise the prediction model at the first step of the prediction horizon, before moving forward to predict the next system response in the predicted horizon, re-evaluating and re-linearising the model, and repeating up to the limit of the prediction horizon.

Specifically, the prediction of the vehicle states one step ahead of the motorcycle will, as before, be given by

$$\hat{\mathbf{x}}(k+1) = \hat{\mathbf{A}}(k)\hat{\mathbf{x}}(k) + \hat{\mathbf{B}}(k)\hat{\mathbf{u}}(k) \tag{6.11a}$$

$$\hat{\mathbf{y}}(k+1) = \hat{\mathbf{C}}(k+1)\hat{\mathbf{x}}(k+1) + \hat{\mathbf{D}}(k+1)\hat{\mathbf{u}}(k+1) \tag{6.11b}$$

The predicted state space equations $\hat{\mathbf{A}}(k)$, $\hat{\mathbf{B}}(k)$, $\hat{\mathbf{C}}(k)$ and $\hat{\mathbf{D}}(k)$, linearised at k, are valid over the step k to $k+1$, and therefore the prediction over this iteration step is also valid.

At the prediction point $k+1$, the system states will be different from at the k^{th} point. The system state space matrices are calculated based on the values of the states, and therefore $\hat{\mathbf{A}}(k) \neq \hat{\mathbf{A}}(k+1)$, $\hat{\mathbf{B}}(k) \neq \hat{\mathbf{B}}(k+1)$ etc. Again, the output will be assumed to have no dependency on the input, and therefore $\mathbf{D}(k)$ is set to zero. Over the prediction iteration $k+1$ to $k+2$, the correct prediction is therefore given by

$$\hat{\mathbf{x}}(k+2) = \hat{\mathbf{A}}(k+1)\hat{\mathbf{x}}(k+1) + \hat{\mathbf{B}}(k+1)\hat{\mathbf{u}}(k+1) \tag{6.12a}$$

$$\hat{\mathbf{y}}(k+2) = \hat{\mathbf{C}}(k+2)\hat{\mathbf{x}}(k+2) \tag{6.12b}$$

Extending this sequence up to the prediction horizon, the appropriate prediction matrices again take the form

$$\boldsymbol{\chi}(k) = \mathbf{F}(k)\mathbf{x}(k) + \mathbf{G}(k)\boldsymbol{\Upsilon}(k) \tag{6.13}$$

$$\boldsymbol{\varphi}(k) = \mathbf{M}(k)\mathbf{x}(k) + \mathbf{N}(k)\boldsymbol{\Upsilon}(k) \tag{6.14}$$

except that this time the appropriate matrices are given by

$$\mathbf{F}(k) = \begin{bmatrix} \hat{\mathbf{A}}(k) \\ \hat{\mathbf{A}}(k+1)\hat{\mathbf{A}}(k) \\ \hat{\mathbf{A}}(k+2)\hat{\mathbf{A}}(k+1)\hat{\mathbf{A}}(k) \\ \vdots \\ \prod_{i=0}^{N_p-1} \hat{\mathbf{A}}(k+i) \end{bmatrix}_{(N_p \times n)} \tag{6.15}$$

$$\mathbf{G}(k) = \begin{bmatrix} \hat{\mathbf{B}}(k) & \mathbf{0} & . & \mathbf{0} \\ \hat{\mathbf{A}}(k+1)\hat{\mathbf{B}}(k) & \hat{\mathbf{B}}(k+1) & . & \mathbf{0} \\ \hat{\mathbf{A}}(k+2)\hat{\mathbf{A}}(k+1)\hat{\mathbf{B}}(k) & \hat{\mathbf{A}}(k+2)\hat{\mathbf{B}}(k+1) & . & \mathbf{0} \\ . & . & . & . \\ \prod_{i=1}^{N_p-1} \hat{\mathbf{A}}(k+i)\hat{\mathbf{B}}(k) & \prod_{i=2}^{N_p-1} \hat{\mathbf{A}}(k+i)\hat{\mathbf{B}}(k+1) & . & \hat{\mathbf{B}}(k+N_p-1) \end{bmatrix}_{(N_p n \times N_p n)} \tag{6.16}$$

$$\mathbf{M}(k)=\begin{bmatrix} \hat{\mathbf{C}}(k+1)\hat{\mathbf{A}}(k) \\ \hat{\mathbf{C}}(k+2)\hat{\mathbf{A}}(k+1)\hat{\mathbf{A}}(k) \\ \hat{\mathbf{C}}(k+3)\hat{\mathbf{A}}(k+2)\hat{\mathbf{A}}(k+1)\hat{\mathbf{A}}(k) \\ \vdots \\ \hat{\mathbf{C}}(k+N_p)\prod_{i=0}^{N_p-1}\hat{\mathbf{A}}(k+i) \end{bmatrix}_{(N_p m \times n)} \tag{6.17}$$

$$\mathbf{N}(k)=\begin{bmatrix} \hat{\mathbf{C}}(k+1)\hat{\mathbf{B}}(k) & \mathbf{0} & . & \mathbf{0} \\ \hat{\mathbf{C}}(k+2)\hat{\mathbf{A}}(k+1)\hat{\mathbf{B}}(k) & \hat{\mathbf{C}}(k+2)\hat{\mathbf{B}}(k+1) & . & \mathbf{0} \\ \hat{\mathbf{C}}(k+3)\hat{\mathbf{A}}(k+2)\hat{\mathbf{A}}(k+1)\hat{\mathbf{A}}(k+1)\hat{\mathbf{B}}(k) & \hat{\mathbf{C}}(k+3)\hat{\mathbf{A}}(k+1)\hat{\mathbf{B}}(k+1) & . & \mathbf{0} \\ . & . & . & . \\ \hat{\mathbf{C}}(k+N_p)\prod_{i=1}^{N_p-1}\hat{\mathbf{A}}(k+i)\hat{\mathbf{B}}(k) & \hat{\mathbf{C}}(k+N_p)\prod_{i=1}^{N_p-2}\hat{\mathbf{A}}(k+i)\hat{\mathbf{B}}(k+1) & . & \hat{\mathbf{C}}(k+N_p)\hat{\mathbf{B}}(k+N_p-1) \end{bmatrix}_{(N_p m \times N_p n)} \tag{6.18}$$

This approach is technically more correct than the method outlined by equations (6.1) to (6.10), although from a computational perspective it is considerably more demanding.

For the simplified approach, at each simulation iteration step, the state space matrices are calculated, and from this the prediction model matrices $\mathbf{F}(k)$, $\mathbf{G}(k)$, $\mathbf{M}(k)$ and $\mathbf{N}(k)$ are calculated once. These are then used to predict the future system output and consequently generate the controller gains and input.

Using the more technically correct approach outlined here, at each iteration step of the simulation model, the prediction of the system states at $(k+1)$, i.e. one step ahead of the motorcycle, are calculated. To achieve this, the predicted state vector $\hat{\mathbf{x}}(k+1)$ is calculated using matrices $\mathbf{A}(k)$, $\mathbf{B}(k)$ and $\mathbf{C}(k)$. Using $\hat{\mathbf{x}}(k+1)$, matrices $\mathbf{A}(k+1)$, $\mathbf{B}(k+1)$ and $\mathbf{C}(k+1)$ are then calculated, allowing the prediction of $\hat{\mathbf{x}}(k+2)$, subsequently $\mathbf{A}(k+2)$, $\mathbf{B}(k+2)$ and $\mathbf{C}(k+2)$, $\hat{\mathbf{x}}(k+2)$, etc., gradually populating the matrices $\mathbf{F}(k)$, $\mathbf{G}(k)$, $\mathbf{M}(k)$ and $\mathbf{N}(k)$, with the necessary terms and thus eventually allowing the necessary controller gains and system input to be obtained for one iteration step of the simulated model's motion (Figure 6.3).

The value of N_p can be large, typically in excess of 100, and consequently, this makes the simulation process using a full non-linear prediction model a considerably more

computationally demanding task. The implications of this will be assessed in the results, to determine how critical it is to the performance of the controller to model the prediction in this way, or whether acceptable performance can be achieved with the relatively more simple prediction model.

6.2.3 Reference Path Definition

A key feature of the MPC technique that differentiates it from optimal control is the use of a reference path. This is a path that the system output attempts to follow in order to take the system from a displaced state to the target state in a defined manner over a defined time step. In the case of a motorcycle model, this constitutes a path that a rider would follow to take him from a position off the ideal, intended road path to regain the target path over a certain forward distance.

The definition of how the system is tasked to get from the displaced state to the target state is open to interpretation and is another control variable that can be introduced into the MPC system. Typically, the system might be tasked with regaining the target path by a linear, exponential or sinusoidal return path, for example. These three conditions are depicted in Figure 6.4.

Two specific definitions are made here relating to the terminology that will be used. For the path information, a subscript 'r' will relate to the actual road, the set path, and the subscript 'f' will relate to the reference path.

The applicability of the various options for defining the reference path is discussed in the results sections. For now, the theory required to define a typical reference path is outlined.

Linear Reference Path

A linear reference path is considered first, and can be achieved with relative ease. With knowledge of the current system state and the final, target state, the intermediate points are simply interpolated linearly based on the difference between the two points (Figure 6.5).

Assuming the current system state to be at zero, the i^{th} reference path point at the k^{th} iteration step $y_{f_i}(k)$, for $i = 1, \ldots, N_p$, is achieved with

$$y_{f_i}(k) = \frac{i}{N_p} y_{r_{N_p}}(k) \tag{6.19}$$

Extending this to the general case of non-zero current motorcycle position $y_v(k)$, results in

$$y_{f_i}(k) = \frac{i}{N_p}\Big(y_{r_{N_p}}(k) - y_v(k)\Big) + y_v(k) \tag{6.20}$$

which simplifies to

$$y_{f_i}(k) = \frac{i}{N_p} y_{r_{N_p}}(k) + \frac{N_p - i}{N_p} y_v(k) \tag{6.21}$$

Writing the expression explicitly for all discrete points in the preview horizon, this becomes

$$\begin{bmatrix} y_{f_1}(k) \\ y_{f_2}(k) \\ y_{f_3}(k) \\ \vdots \\ y_{f_{N_p-1}}(k) \\ y_{f_{N_p}}(k) \end{bmatrix} = \begin{bmatrix} \frac{1}{N_p} y_{r_{N_p}} + \frac{(N_p-1)}{N_p} y_v(k) \\ \frac{2}{N_p} y_{r_{N_p}} + \frac{(N_p-2)}{N_p} y_v(k) \\ \frac{3}{N_p} y_{r_{N_p}} + \frac{(N_p-3)}{N_p} y_v(k) \\ \vdots \\ \frac{N_p-1}{N_p} y_{r_{N_p}} + \frac{1}{N_p} y_v(k) \\ y_{r_{N_p}} \end{bmatrix} \tag{6.22}$$

The required form for the definition of the reference path is as a discrete-time state space model such that it can be combined with the motorcycle model as defined previously (4.2). In the discrete-time state space representation of the system, the system states, which includes the path information, are required to be calculated for the system at the $(k+1)^{th}$ step, not at the k^{th} step as given by (6.22). Thus, in calculating the new reference path for the $(k+1)^{th}$ step, this path should take the motorcycle from the position of the motorcycle at $(k+1)$ to the target road point at $(k+1)$.

The i^{th} reference path point for the iteration step $(k+1)$ that should be generated by the state space model, from (6.21), is therefore given by

$$y_{f_i}(k+1) = \frac{i}{N_p} y_{r_{N_p}}(k+1) + \frac{Np-i}{N_p} y_v(k+1) \tag{6.23}$$

where the position of the motorcycle $y_v(k+1)$ is given by

$$y_v(k+1) = \mathbf{A}_v(k)(2,j)\mathbf{x}_v(k) + \mathbf{B}_v(k)(2,j)\mathbf{u}(k) \tag{6.24}$$

and where the selection of the second rows of the matrices $\mathbf{A}_v(k)$ and $\mathbf{B}_v(k)$ correspond to the location of the lateral position state in the motorcycle state vector and j is the index $1,\ldots,n$, indicating that the whole of the second row is selected.

Using the result from (6.23), the discrete-time state space representation (6.22) becomes

$$\begin{bmatrix} y_{f_1}(k+1) \\ y_{f_2}(k+1) \\ y_{f_3}(k+1) \\ \vdots \\ y_{f_{N_p-1}}(k+1) \\ y_{f_{N_p}}(k+1) \end{bmatrix} = \begin{bmatrix} \frac{1}{N_p} y_{r_{N_p}}(k+1) + \frac{(N_p-1)}{N_p} y_v(k+1) \\ \frac{2}{N_p} y_{r_{N_p}}(k+1) + \frac{(N_p-2)}{N_p} y_v(k+1) \\ \frac{3}{N_p} y_{r_{N_p}}(k+1) + \frac{(N_p-3)}{N_p} y_v(k+1) \\ \vdots \\ \frac{N_p-1}{N_p} y_{r_{N_p}}(k+1) + \frac{1}{N_p} y_v(k+1) \\ y_{r_{N_p}}(k+1) \end{bmatrix}_{(N_p \times 1)} \tag{6.25}$$

If the road preview vector $\mathbf{y}_r(k)$ is extended to include (N_p+1) road information points, then the first terms in the right-hand-side of (6.25) can be readily obtained from $\mathbf{A}_p\mathbf{y}_r(k)$, where

$$\mathbf{A}_p = \begin{bmatrix} 0 & \ldots & 0 & \frac{1}{N_p} \\ 0 & \ldots & 0 & \frac{2}{N_p} \\ 0 & \ldots & 0 & \frac{3}{N_p} \\ \cdot & \cdots & \cdot & \cdot \\ 0 & \ldots & 0 & \frac{Np-1}{N_p} \\ 0 & \ldots & 0 & 1 \\ 0 & \ldots & 0 & 0 \end{bmatrix}_{(N_p+1 \times n)} \tag{6.26}$$

The matrix $\mathbf{A}_p$ is time-invariant, and therefore does not require the time-step identifier (k).

The second element terms in the right-hand-side of (6.25) are obtained from

$$\frac{(N_p - i)}{N_p} y_v(k+1) = \frac{(N_p - i)}{N_p} \Big(\mathbf{A}_v(k)(2,j)\mathbf{x}_v(k) + \mathbf{B}_v(k)(2,j)\mathbf{u}(k) \Big) \tag{6.27}$$

Thus, the second terms in the right-hand-side of (6.25) can be obtained with

$$\mathbf{A}_f(k)\mathbf{x}_v(k) + \mathbf{B}_f(k)\mathbf{u}(k) \tag{6.28}$$

where

$$\mathbf{A}_f(k) = \begin{bmatrix} \frac{N_p-1}{N_p}\mathbf{A}_v(k)(1,j) \\ \frac{N_p-2}{N_p}\mathbf{A}_v(k)(1,j) \\ \frac{N_p-3}{N_p}\mathbf{A}_v(k)(1,j) \\ \vdots \\ \frac{1}{N_p}\mathbf{A}_v(k)(1,j) \\ 0 \\ 0 \end{bmatrix}_{(N_p+1 \times n)} \tag{6.29}$$

and

$$\mathbf{B}_f(k) = \begin{bmatrix} \frac{N_p-1}{N_p}\mathbf{B}_v(k)(1,j) \\ \frac{N_p-2}{N_p}\mathbf{B}_v(k)(1,j) \\ \frac{N_p-3}{N_p}\mathbf{B}_v(k)(1,j) \\ \vdots \\ \frac{1}{N_p}\mathbf{B}_v(k)(1,j) \\ 0 \\ 0 \end{bmatrix}_{(N_p+1 \times p)} \tag{6.30}$$

The preceding theory has considered the reference path defined only by the lateral position of the road path, but can be extended to include the yaw angle using a similar approach.

Extending the previous definition of the discrete-time state space system model (6.1) to include $(N_p + 1)$ preview points for a linear reference path, the whole process can, using the matrices defined above, be re-expressed again in the simple state space form using the matrices defined above:

$$\begin{bmatrix} \mathbf{x}_v(k+1) \\ \mathbf{y}_f(k+1) \end{bmatrix} = \begin{bmatrix} \mathbf{A}_v(k) & \mathbf{0} \\ \mathbf{A}_f(k) & \mathbf{A}_p \end{bmatrix} \begin{bmatrix} \mathbf{x}_v(k) \\ \mathbf{y}_f(k) \end{bmatrix} + \begin{bmatrix} \mathbf{B}_v(k) \\ \mathbf{B}_f(k) \end{bmatrix} \mathbf{u}(k) + \begin{bmatrix} \mathbf{0} \\ \mathbf{B}_p \end{bmatrix} \mathbf{y}_{rn}(k) \tag{6.31}$$

where $\mathbf{y}_{rn}(k)$ represents again the new preview point fed into the system, corresponding here to a point $N_p + 2$ steps ahead of the current motorcycle position, and $\mathbf{B}_p$ is the corresponding matrix to input this new information into the rider's preview as given in Chapter 4, (4.2). This matrix form therefore generates the future road path that the rider attempts to follow as a linear path between the motorcycle's current position and the actual road path information at the limit of the rider's preview horizon.

Linear Error Reduction Path

The previous reference path definition was for a linear reference path, going directly from the motorcycle's position to some target position at the limit of the rider's preview, taking no account of the path direction in between. Here, the definition is subtly different, with the linearity being in the reduction of the error between the set path and the reference path. Thus, if the set path curves, so too will the reference path, but the error between the two will be a linear function that will see the reference path gradually track back onto the set path by the limit of the preview horizon (Figure 6.6).

To achieve this, the reference path is taken as the set path less some multiple of the difference between the motorcycle and the relative set path position. This multiple is a linear function from one to zero, such that the error between the set path and reference path gradually and linearly reduces to zero also.

The preview horizon includes N_p preview points, where the first preview point is one step ahead of the motorcycle (Figure 6.6). Thus, there are N_p discrete steps between

the motorcycle and the limit of the preview.

The function that therefore gives the linear function from zero at the motorcycle to one at the limit of the preview horizon is, for the i^{th} preview point, given by $1-\frac{N_p-i}{N_p}$. Numerically then, the i^{th} point on the reference path is given by

$$y_{f_i}(k) = y_v(k) + (y_{r_i}(k) - y_v(k))\Big(1 - \frac{N_p - i}{N_p}\Big) \tag{6.32}$$

which can be simplified to

$$y_{f_i}(k) = y_{r_i}(k)\Big(1 - \frac{N_p - i}{N_p}\Big) + y_v(k)\Big(\frac{N_p - i}{N_p}\Big) \tag{6.33}$$

It is seen from this definition that, unlike the direct linear reference path, in this case the full set path information, i.e. $y_{r_i}(k)$ for $i = 1, \ldots, N_p$, is required. This naturally makes this approach more complicated, as the complete system state vector must now therefore include the motorcycle states, the set path road information *and* the reference path road information in the rider's preview horizon. Since the required format for the modelling is the state space representation, (6.33) must also be written in a discrete-time state space form, such that $y_{f_i}(k+1)$ can be obtained.

The set path information is updated by the simple shift-register matrix. Thus, $y_{r_i}(k+1) = y_{r_{i+1}}(k)$ as before.

The motorcycle lateral position $y_v(k+1)$ is also readily obtained by using the appropriate elements of the state space matrices for the motorcycle dynamics as seen previously, i.e. $y_v(k+1) = \mathbf{A}_v(k)(2,j)\mathbf{x}_v(k) + \mathbf{B}_v(k)(2,j)\mathbf{u}(k)$. Thus, the necessary complete system state space model can be achieved with

$$\begin{bmatrix} \mathbf{x}_v(k+1) \\ \mathbf{y}_r(k+1) \\ \mathbf{y}_f(k+1) \end{bmatrix} = \begin{bmatrix} \mathbf{A}_v(k) & \mathbf{0} & \mathbf{0} \\ \mathbf{0} & \mathbf{A}_p & \mathbf{0} \\ \mathbf{A}_s(k) & \mathbf{A}_r & \mathbf{0} \end{bmatrix} \begin{bmatrix} \mathbf{x}_v(k) \\ \mathbf{y}_r(k) \\ \mathbf{y}_f(k) \end{bmatrix} + \begin{bmatrix} \mathbf{B}_v(k) \\ \mathbf{0} \\ \mathbf{B}_f(k) \end{bmatrix} \mathbf{u}(k) + \begin{bmatrix} \mathbf{0} \\ \mathbf{B}_p \\ \mathbf{B}_p \end{bmatrix} \mathbf{y}_{rn}(k) \tag{6.34}$$

where the matrices $\mathbf{A}_v(k)$ and $\mathbf{B}_v(k)$ are as defined in 3.23, $\mathbf{A}_p$ and $\mathbf{B}_p$ are as in 4.2, and additionally,

$$\mathbf{A}_s(k) = \begin{bmatrix} \mathbf{A}_v(k)(2,j)\frac{N_p-1}{N_p} \\ \mathbf{A}_v(k)(2,j)\frac{N_p-2}{N_p} \\ \mathbf{A}_v(k)(2,j)\frac{N_p-3}{N_p} \\ \vdots \\ \mathbf{A}_v(k)(2,j)\frac{1}{N_p} \\ 0 \end{bmatrix}_{(N_p \times n)} \tag{6.35}$$

$$\mathbf{A}_r = \begin{bmatrix} 0 & \left(1-\frac{N_p-1}{N_p}\right) & 0 & 0 & 0 & 0 \\ 0 & 0 & \left(1-\frac{N_p-2}{N_p}\right) & 0 & 0 & 0 \\ 0 & 0 & 0 & 0 & 0 & 0 \\ \vdots & & & & & \\ 0 & 0 & 0 & 0 & 0 & \left(1-\frac{1}{N_p}\right) \\ 0 & 0 & 0 & 0 & 0 & 0 \end{bmatrix}_{(N_p \times N_p)} \tag{6.36}$$

$$\mathbf{B}_f(k) = \begin{bmatrix} \mathbf{B}_v(k)(2,j)\frac{N_p-1}{N_p} \\ \mathbf{B}_v(k)(2,j)\frac{N_p-2}{N_p} \\ \mathbf{B}_v(k)(2,j\frac{N_p-3}{N_p} \\ \vdots \\ \mathbf{B}_v(k)(2,j)\frac{1}{N_p} \\ 0 \end{bmatrix}_{(N_p \times p)} \tag{6.37}$$

Exponential Reference Path

The definition of the reference path as an exponential curve from the current vehicle state to the target vehicle state follows from the theory outlined for the linear error reduction case. To define an exponential path using the linear reference path theory would be incorrect, as highlighted by Figure 6.7. Rather than gradually recovering the set path, the reference path could potentially overshoot the set path and return to it non-tangentially.

Although the path is indeed an exponential path, no account is taken for the trajectory of the path, only the final target point. The proposed form is therefore to reduce exponentially the error between the motorcycle and the reference path, using the

method outlined for the linear error reduction approach above. This would lead to a path that may typically look something like the situation presented in Figure 6.8.

Specifically, an exponential growth from zero to one can be defined by

$$f(x) = 1 - \exp(-x/l_r) \tag{6.38}$$

where l_r is a value that defines the relaxation length of the exponential growth. Thus, modifying (6.33) to account for an exponential reduction results in

$$y_{f_i}(k) = y_{r_i}(k)\Big(1 - \exp(-(i-1)/l_r)\Big) + y(k)\Big(\exp(-(i-1)/l_r)\Big) \tag{6.39}$$

Comparing (6.39) with (6.33), it can be seen that by using the same approach as for the linear error reduction reference path, the state space matrices $\mathbf{A}_s(k)$, $\mathbf{A}_r$, $\mathbf{B}_f(k)$ and $\mathbf{B}_{fn}(k)$ for the exponential error reduction reference path will be the same as those for the linear error reduction case, modified only such that the terms $\frac{N_p - i}{N_p}$ are replaced by $\exp(1-i)/l_r)$.

6.2.4 MPC Optimal Gains

The optimal control approach formulated a cost function consisting of elements relating to the system's output accuracy and control effort input. Weighting parameters were included in the cost function, such that the relative contributions of each to the overall cost could be varied, and as such the controller's bias towards accuracy or control efficiency could be adjusted.

The MPC approach is very similar; the notable difference between the two is that for MPC, the output error penalised in the cost function is the error between the predicted future controlled system output and the reference path. The theory for the generation of the model predictive controller gains is as follows [11, 52].

Considering the lateral positions of the motorcycle and the path, the error function of an individual preview point is defined as

$$e_i(k) = \hat{y}_i(k) - y_{f_i}(k) \tag{6.40}$$

where $\hat{y}_i(k)$ the predicted output of the i^{th} preview point and $y_{f_i}(k)$ is the reference output at the k^{th} iteration step. Extending to the full system preview, the vector of all errors in the preview horizon is therefore defined by

$$\mathbf{e}(k) = \boldsymbol{\varphi}(k) - \mathbf{y}_f(k) = \Big(\mathbf{M}(k)\mathbf{x}(k) + \mathbf{N}(k)\boldsymbol{\Upsilon}(k)\Big) - \mathbf{y}_f(k) = \mathbf{N}(k)\boldsymbol{\Upsilon}(k) - \boldsymbol{\varepsilon}(k) \quad (6.41)$$

As with the optimal control cost function, the MPC cost function is formed by the weighted sum of squares of the path following errors and the control input costs, such that

$$J = \sum_{k=0}^{N-1} \Big(\mathbf{e}^T(k)\mathbf{Q}\mathbf{e}(k) + \boldsymbol{\Upsilon}^T(k)\mathbf{R}\boldsymbol{\Upsilon}(k)\Big) \quad (6.42)$$

where $\mathbf{Q}$ and $\mathbf{R}$ are again invariant weighting matrices on the system outputs and control inputs. Here, they take the form of diagonal matrices, where the elements on the diagonal correspond to the weightings on the outputs $[q_1, q_2, \ldots]$, repeating N_p times, and the weightings on the inputs $[r_1, r_2, \ldots]$ repeating N_u times.

The weighting vectors on the output and inputs are decomposed as

$$\begin{aligned} \mathbf{Q} &= \mathbf{S}_Q^T \mathbf{S}_Q \\ \mathbf{R} &= \mathbf{S}_R^T \mathbf{S}_R \end{aligned} \quad (6.43)$$

in which case the cost function (6.42) can alternatively be expressed as

$$J = \left\| \begin{bmatrix} \mathbf{S}_Q(\mathbf{N}(k)\boldsymbol{\Upsilon}(k) - \boldsymbol{\varepsilon}(k)) \\ \mathbf{S}_R\boldsymbol{\Upsilon}(k) \end{bmatrix} \right\|^2 \quad (6.44)$$

where $\mathbf{S}_Q$ and $\mathbf{S}_R$ are the square symmetric roots of the matrices $\mathbf{Q}$ and $\mathbf{R}$. In this case they are symmetric, diagonal matrices and the square root can readily be obtained as the squares of the individual terms on the diagonals. For more elaborate matrices, other methods such as single value decomposition or Choleski decomposition may be required.

Thus, the control input $\boldsymbol{\Upsilon}(k)$ that minimises the cost function J is obtained from the least-squares solution [52] of the equation

$$\begin{bmatrix} \mathbf{S}_Q(\mathbf{N}(k)\boldsymbol{\Upsilon}(k) - \boldsymbol{\varepsilon}(k)) \\ \mathbf{S}_R\boldsymbol{\Upsilon}(k) \end{bmatrix} = \mathbf{0} \tag{6.45}$$

The optimal gains for the controller can be obtained by making the substitution $\boldsymbol{\Upsilon}(k) = \boldsymbol{\kappa}(k)\boldsymbol{\varepsilon}(k)$

$$\begin{bmatrix} \mathbf{S}_Q\mathbf{N}(k) \\ \mathbf{S}_R \end{bmatrix} \boldsymbol{\kappa}(k)\boldsymbol{\varepsilon}(k) = \begin{bmatrix} \mathbf{S}_Q \\ \mathbf{0} \end{bmatrix} \boldsymbol{\varepsilon}(k) \tag{6.46}$$

and using QR decomposition, such that

$$\boldsymbol{\kappa}(k) = \begin{bmatrix} \mathbf{S}_Q\mathbf{N}(k) \\ \mathbf{S}_R \end{bmatrix} \backslash \begin{bmatrix} \mathbf{S}_Q \\ \mathbf{0} \end{bmatrix} \tag{6.47}$$

This then gives a full matrix of dimension $(N_u p) \times (N_p m)$ where p and m are respectively the numbers of control inputs and controlled outputs. Each row of the matrix $\boldsymbol{\kappa}(k)$ corresponds to the optimum gain multipliers for each of the N_u future control inputs. The optimum future inputs are obtained by multiplying each row of this matrix $\boldsymbol{\kappa}(k)$ with the vector of future errors, $\boldsymbol{\varepsilon}$, i.e. using the previous substitution $\boldsymbol{\Upsilon}(k) = \boldsymbol{\kappa}(k)\boldsymbol{\varepsilon}(k)$. At each iteration step of the program, it is only the first element $\mathbf{u}(k)$ in the future control input vector $\boldsymbol{\Upsilon}(k)$ that is used, and hence it is only the first row that is required to calculate the next control input. At the next iteration step, the problem is re-evaluated, a new matrix $\boldsymbol{\kappa}(k)$ calculated and hence the next new control input $\mathbf{u}(k)$ calculated. Thus, the optimal MPC input applied to the system can be defined as

about Δu

$$\mathbf{u}(k) = \mathbf{k}(k)\boldsymbol{\varepsilon}(k) = \mathbf{k}(k)[\mathbf{y}_f(k) - \mathbf{M}(k)\mathbf{x}(k)] \tag{6.48}$$

where $\mathbf{k}(k)$ refers to the first column of the gains matrix $\boldsymbol{\kappa}(k)$.

6.2.5 Application to Motorcycle Rider Modelling

The preceding section outlined the fundamental mathematical principles of the MPC theory, using generic states vector $\mathbf{x}(k)$ and generic input vector $\mathbf{u}(k)$. The specific application of the MPC technique to the motorcycle rider model is now explored.

In defining the theory of MPC, the discrete-time state space model of the system dynamics was given as

$$\mathbf{x}(k+1) = \mathbf{A}(k)\mathbf{x}(k) + \mathbf{B}(k)\mathbf{u}(k) \tag{6.49a}$$

$$\mathbf{y}(k) = \mathbf{C}(k)\mathbf{x}(k) + \mathbf{D}(k)\mathbf{u}(k) \tag{6.49b}$$

Equation (4.3) showed how the motorcycle dynamic response model was combined with a state space representation of the rider's road preview to develop the combined motorcycle–preview model given as

$$\begin{bmatrix} \mathbf{x}_v(k+1) \\ \mathbf{y}_r(k+1) \end{bmatrix} = \begin{bmatrix} \mathbf{A}_v(k) & 0 \\ 0 & \mathbf{A}_p \end{bmatrix} \begin{bmatrix} \mathbf{x}_v(k) \\ \mathbf{y}_r(k) \end{bmatrix} + \begin{bmatrix} \mathbf{B}_v(k) \\ 0 \end{bmatrix} \mathbf{u}(k) + \begin{bmatrix} 0 \\ \mathbf{B}_p \end{bmatrix} \mathbf{y}_{rn}(k) \tag{6.50}$$

where all terms have the same meanings as before; $\mathbf{x}_v(k)$ is the vector of the motorcycle states, $\mathbf{y}_r(k)$ the vector of the road preview information, $\mathbf{y}_{rn}(k)$ is the vector of the new road preview point information, and $\mathbf{A}_v(k)$ and $\mathbf{B}_v(k)$ are the state space matrices of the motorcycle dynamics, all at the k^{th} step. The matrices $\mathbf{A}_p$ and $\mathbf{B}_p$ are time-invariant state space matrices for the road preview shift-register algorithm. $\mathbf{u}(k)$ is the system input vector. Here, only a single input, steer torque, is present, and so $\mathbf{u}(k)$ can simplify to $u(k)$.

The control input has no effect on the approaching road path, it is a defined feature, and therefore to generate a prediction model for the road path would be unnecessary. Omitting the (k) for simplicity of presentation, the predicted future states that are generated in the MPC technique are therefore related to the motorcycle dynamics alone, and are given as

$$\begin{bmatrix} \hat{\mathbf{x}}_v(k+1) \\ \hat{\mathbf{x}}_v(k+2) \\ \hat{\mathbf{x}}_v(k+3) \\ \vdots \\ \hat{\mathbf{x}}_v(k+N_p) \end{bmatrix} = \begin{bmatrix} \mathbf{A}_v \\ \mathbf{A}_v^2 \\ \mathbf{A}_v^3 \\ \vdots \\ \mathbf{A}_v^{N_p} \end{bmatrix} \mathbf{x}_v(k) + \begin{bmatrix} \mathbf{B}_v & \mathbf{0} & . & \mathbf{0} \\ \mathbf{A}_v\mathbf{B}_v & \mathbf{B}_v & . & \mathbf{0} \\ \mathbf{A}_v^2\mathbf{B}_v & \mathbf{A}_v\mathbf{B}_v & . & \mathbf{0} \\ . & . & . & . \\ \mathbf{A}_v^{N_p-1}\mathbf{B}_v & \mathbf{A}_v^{N_p-2}\mathbf{B}_v & . & \mathbf{B}_v \end{bmatrix} \begin{bmatrix} \hat{u}(k) \\ \hat{u}(k+1) \\ \hat{u}(k+2) \\ \vdots \\ \hat{u}(k+N_p-1) \end{bmatrix} \tag{6.51a}$$

Similarly, for the system output

$$\begin{bmatrix} \hat{\mathbf{y}}_v(k+1) \\ \hat{\mathbf{y}}_v(k+2) \\ \hat{\mathbf{y}}_v(k+3) \\ \vdots \\ \hat{\mathbf{y}}_v(k+N_p) \end{bmatrix} = \begin{bmatrix} \mathbf{C}_v\mathbf{A}_v \\ \mathbf{C}_v\mathbf{A}_v^2 \\ \mathbf{C}_v\mathbf{A}_v^3 \\ \vdots \\ \mathbf{C}_v\mathbf{A}_v^{N_p} \end{bmatrix} \mathbf{x}(k) + \begin{bmatrix} \mathbf{C}_v\mathbf{B}_v & \mathbf{0} & . & \mathbf{0} \\ \mathbf{C}_v\mathbf{A}_v\mathbf{B}_v & \mathbf{C}_v\mathbf{B}_v & . & \mathbf{0} \\ \mathbf{C}_v\mathbf{A}_v^2\mathbf{B}_v & \mathbf{C}_v\mathbf{A}_v\mathbf{B}_v & . & \mathbf{0} \\ . & . & . & . \\ \mathbf{C}_v\mathbf{A}_v^{N_p-1}\mathbf{B}_v & \mathbf{C}_v\mathbf{A}_v^{N_p-2}\mathbf{B}_v & . & \mathbf{C}_v\mathbf{B}_v \end{bmatrix} \begin{bmatrix} \hat{u}(k) \\ \hat{u}(k+1) \\ \hat{u}(k+2) \\ \vdots \\ \hat{u}(k+N_p-1) \end{bmatrix} \tag{6.51b}$$

The prediction model for the motorcycle dynamics can be represented by

$$\chi_v(k+1) = \mathbf{F}_v(k)\mathbf{x}_v(k) + \mathbf{G}_v(k)\Upsilon(k) \tag{6.52}$$

$$\varphi_v(k) = \mathbf{M}_v(k)\mathbf{x}_v(k) + \mathbf{N}_v(k)\Upsilon(k) \tag{6.53}$$

If necessary, the rightmost $(N_p - N_u)$ columns of the matrix $\mathbf{G}_v(k)$ can be summed as shown for the generic controlled system (6.10). The control inputs from the limit of the control horizon (N_u) up to the limit of the preview horizon (N_p) are considered

invariant as the value $u(N_u)$ at the limit of the control horizon. Thus, all the rightmost columns of the matrix $\mathbf{G}_v(k)$ multiply by the same input $u(N_u)$, which can be achieved by summating the rightmost $N_p - N_u$ columns and multiplying singularly by $u(N_u)$.

The solution for the optimal steer torque input control follows the theory defined by equations (6.40) to (6.48).

If the reference path $\mathbf{y}_f(k)$ is defined as the actual road path $\mathbf{y}_r(k)$ that is stored in the combined motorcycle–preview state vector, then, from (6.48), the control input can be defined as

$$u(k) = \mathbf{k}_v\boldsymbol{\varepsilon}(k) = \mathbf{k}_v(k)[\mathbf{y}_r(k) - \mathbf{M}_v(k)\mathbf{x}_v(k)] \tag{6.54}$$

As both vectors $\mathbf{x}_v(k)$ and $\mathbf{y}_r(k)$ are combined in the motorcycle–preview state vector $\mathbf{z}(k)$, then equation (6.54) can be neatly written in the vector form

$$u(k) = -\begin{bmatrix} \mathbf{k}_v(k)\mathbf{M}_v(k) & -\mathbf{k}_v(k) \end{bmatrix} \begin{bmatrix} \mathbf{x}_v(k) \\ \mathbf{y}_r(k) \end{bmatrix} = -\begin{bmatrix} \mathbf{k}_v(k)\mathbf{M}_v(k) & -\mathbf{k}_v(k) \end{bmatrix} \begin{bmatrix} \mathbf{z}(k) \end{bmatrix} \tag{6.55}$$

Thus, by solving (6.47) as before for the motorcycle dynamics model to obtain $\boldsymbol{k}_v(k)$, the optimal control for the motorcycle following the road path can be readily obtained.

Noting the structure of (6.55), it can be seen that the controller gain elements applied to the motorcycle states and to the road states can be identified readily. The gains element $\mathbf{k}_v(k)\mathbf{M}_v(k)$ multiplies by the motorcycle states, while the element $-\mathbf{k}_v(k)$ multiplies by the road preview information. Consequently, $\mathbf{k}_v(k)\mathbf{M}_v(k)$ and $-\mathbf{k}_v(k)$ will henceforth be referred to as the state gains $\mathbf{K}_s$ and the preview gains $\mathbf{K}_p$ respectively.

6.2.6 MPC Theory Conclusions

The theory for the solution of a model predictive controller has been presented in some detail, including the freedom to select different reference paths, and with both linear and non-linear prediction models. Where appropriate, the theory has been compared and contrasted to the optimal control approach.

Based on the theory presented in this chapter, it is believed that the model predictive control approach may be a more realistic representation of a motorcycle rider's actions. A rider would certainly have some anticipation of how the motorcycle would respond to control actions, and would therefore have some subconscious planning of control actions based on knowledge of the approaching road path and likely system behaviour. Furthermore, the freedom to define a reference path that takes the rider from the motorcycle's instantaneous state to some target state in the future intuitively seems representative of the manner in which the motorcycle would move from one position, quite possibly off the target path, in a direction that will aim to regain the target path.

These observations on the theory of model predictive control and the requirements of a suitable model to replicate the actions of a motorcycle rider would appear to suggest that the former will adequately meet the requirements of the latter. The results of the application of model predictive control to the rider model will aim to answer this question more definitively.

6.3 Model Predictive Control Rider Model Results

The motorcycle–rider model is tasked with a simple single lane-change path to follow, comprising a lateral shift of the road path of 3.5 m over a forward distance of 20 m (Figure 6.9). Analysis of the controller's performance in attempting this task will be used to assess the appropriateness of using such a control strategy in modelling a human motorcycle rider and to discuss any rider control requirements that may transpire from the analysis.

Several parameters regarding the performance of both the motorcycle and the rider model can be varied, and their effect on the control task assessed. Concerning the motorcycle, the inherent physical properties of the motorcycle, such as geometric details or inertial properties, can be altered. Almost certainly these will influence the control task and hence the path following performance of the motorcycle–rider model. The scope for adjustment of the physical parameters is vast, ranging from the major influences such as steering geometry, to the more minor such as individual component inertias. The task here is to study and evaluate primarily the controller, and as such the motorcycle model remains fixed throughout all of the path following

simulations. Details of the motorcycle model used can be found in Chapter 3 and Appendix A.

Detailed analysis will therefore be limited to variation of the controller parameters alone, yet even here there remains still plenty of scope for adjustment. The trajectory-following performance of an MPC controller is primarily affected by the cost function (6.42) composed of accuracy and effort components with weightings applied to the individual components of each part. The controller then attempts to minimise this cost function, effectively a mathematical compromise between contributions made by the two components.

In this application the cost function penalises the lateral path and the yaw angle errors against the handlebar steer torque input. From a rider's perspective, the requirement to apply large steer torques is undesirable, so penalising this parameter is intended to keep steer torques to acceptable levels. Weighting factors are applied to all measured (simulation) values in the cost function, and so there exist m weighting parameters relating to the output accuracy and p weighting parameters applied to the control inputs.

The cost function weighting parameters therefore form the initial modelling variable, and secondly the horizons available to the rider model can also be varied. In the case of an MPC strategy, three horizons exist; the preview horizon T_p, the control horizon T_u, and the dead-zone horizon T_w. The dead-zone horizon was mentioned briefly in Section 6.2. The horizon represents a system lag between control input and system response. For systems with large response lags, particularly chemical processes for example, this can be a very useful feature. For the motorcycle, the effect of control input on the system's response is assumed instantaneous. Any response lag that may be experienced is assumed to be accounted for by the relaxation length property of the tyre's lateral force response (Chapter 3). The dead-zone horizon is not required here and is therefore always zero. The remaining horizons T_p and T_u can be varied independently with the proviso that the control horizon cannot exceed the preview horizon.

Finally, details of the simulation itself can be varied. The nature of the path to be followed in terms of both the geometric path and of the road surface can be varied, and the speed at which the motorcycle–rider attempts the manoeuvre changed. Variation

of the road geometry to be followed will naturally influence the control applied by the rider, however, the task here is to study the controller, and the fundamental influence of the controller settings upon the path following performance. These would be expected to remain broadly fixed regardless of the road geometry. Changes to the road surface, such as elevation and surface roughness, both factors in real-world riding scenarios, would similarly be expected to have minimal influence on the broad performance of the control strategy, and thus opening up the simulation parameters to include factors relating to changes in the road geometry and surface would complicate the analysis unnecessarily. The road path and surface will therefore be maintained constant throughout all parameter studies.

The parameter studies will therefore focus on four key variables; the lateral path error cost weighting q_1, the preview horizon T_p, the control horizon T_u and the forward speed v. In addition, the effect of non-linear prediction models will be evaluated. The results will be discussed in specific parts, with initially the controller performance analysed for a single set of controller parameters, such that the generic behaviour and characteristics of the MPC controller can be assessed and compared with the performance of an optimal control strategy using the same controller parameters. Following this, parameter studies will be made by progressively varying the four controller variables to draw further conclusions about the behaviour and suitability of MPC techniques to the task of motorcycle rider modelling.

6.3.1 Low Speed Baseline Prediction Model

This part of the results section is concerned with results generated using a linear prediction model, discussed in Section 6.2.1. The linear prediction model is a considerably more computationally efficient process, and therefore allows for a large range of results to be generated readily. This model is used to study the effects of the controller parameters for a range of settings, enabling the effects of individual parameters alone to be studied. The implications of the using the linear prediction model compared to the technically more accurate non-linear prediction model will be investigated later in the results, to determine how critical this aspect is in the overall performance of the model predictive control rider model.

In considering the performance of the controller with reference to the task, several

output variables will be analysed. Primarily, the path following performance of the controller is observed in attempting to follow the path, since this is the fundamental task for the controller. Additionally, the state and preview gains, and the steer torque generated, will be examined, with the results discussed both qualitatively and quantitatively.

Baseline Parameter Set

The initial simulation parameters, set to act as a baseline giving a simulation with moderate accuracy and preview levels at a low speed, are presented in Table 6.1 Set 1. This set of values will subsequently be extended to provide variation in all parameters, with the influence upon the controller's characteristics as a result of these changes analysed.

Figure 6.10 shows the path following performance of the controller with the initial baseline parameters. It is seen that the path following performance is good, with the model being able to track the target path with acceptable accuracy. There is an initial deviation away from the path where the motorcycle rider model initiates the manoeuvre with countersteer and there is a small overshoot at the end of the manoeuvre phase, after which the controller recovers the path and follows the straight-running section of the path exactly.

The controller gains are considered next. The state gains are presented in Figure 6.11, and are seen to be not dissimilar from those achieved using optimal control methods. As before, the largest state gain corresponds to the yaw angle, followed by the roll angle gain, and with all other gains of considerably lower significance. The yaw angle directly influences the errors between the predicted path heading for the rider and the target path, and so it is perhaps unsurprising that, as with the optimal control approach, this state is associated with the largest gains. With fixed rider, the cornering radius of a motorcycle is directly influenced by the roll angle of the motorcycle. The roll angle therefore has a direct bearing on the future path of the motorcycle, at least over the immediate preview distance, and thus the errors between predicted future path and target future path. It is therefore unsurprising that the roll angle of the motorcycle should also figure significantly in the rider's control task.

The preview gains are presented in Figure 6.12. As with the state gains, these show

considerable similarity to gains achieved using optimal control strategies, with the significant characteristics of a peak gain in the middle preview distance, decaying towards zero values at the limit of the available preview.

The steer torque that results using this controller is presented in Figure 6.13. It shows smooth development of the steer torque as might be expected of a real rider, and includes the necessary countersteer torque needed to initiate the manoeuvre. The path following of the motorcycle is also overlaid on this plot, allowing the path following that results from the steer torque to be seen.

Consideration of the gains and resulting control inputs suggests that the baseline parameters can represent a controller that appears to have sufficient knowledge of the approaching road path to make good judgement of control required to accomplish the task. The preview gains tend to zero, indicating that the information at the limit of the rider's preview has minimal significance, the steer inputs resulting are smooth, progressive and representative of the approach that may be expected of a real rider, and ultimately the path following ability of the controller is judged to be acceptable. The behaviour is not unlike the results achieved using optimal control methods, a technique that has previously been judged to represent well the control strategies of a motorcycle rider [94].

Cost Function Weighting

The baseline parameter set is extended to consider first three different values of lateral error cost function weighting, q_1. The initial value of q_1 was set at 5000 m^{-2} which gave rise to moderately close path following performance. Additionally values of 1,000 m^{-2} and 10,000 m^{-2} are now considered, which will aim to represent looser and tighter control respectively (Table 6.1, Sets 2 & 3).

The results of this are presented graphically. The path following is shown in Figure 6.14, and as may be expected, the higher weighting results in closer following of the path, showing reduced corner-cutting. Both controller weightings display qualitatively similar characteristics, and for both controller settings the motorcycle follows the path accurately after the manoeuvre has been completed (not explicitly shown).

The difference in the path following performance results from changes in the controller

gains that are generated. Figures 6.15 and 6.16 show the state gains and the preview gains respectively for all the path error weightings considered, with $q_1 = 1000$, 5000 and 10,000 m^{-2}.

It is seen that the state gains are increased as a result of an increase in the path-error weighting. All states are influenced, though the ratio of the magnitudes of the individual state gains remains constant for all values of q_1. The rate of change of the state gains is seen to reduce with the increase in the path error weighting.

In considering the preview gains, tight control implies that the rider is concerned with accurately following the path. Thus, during the simulation, the rider may be expected to place greater emphasis on the road immediately ahead of him, and ensuring that his trajectory will keep him on this path regardless of the control cost (Figure 6.17, left). The road some distance ahead of him is of less concern; he must ensure he tracks the path accurately, irrespective of whether this path is the most direct route between the start and finish points. Similar observations were made for the optimal control approach.

Conversely, lower values of q_1 result in the control input cost becoming more dominant in the overall cost function. Thus, a loose controller is concerned with minimising the control input effort, achieved by attempting to make the complete path easier to follow. The rider might therefore be expected to consider the whole road that he can see to evaluate the easiest path from his current position to his ultimate target at the limit of his visual preview. The rider is less concerned with the road immediately ahead of him, but is aiming instead to follow the road that can be seen ahead of him efficiently. As a result, a loose controller would be expected to cut corners more readily, in order to track the path globally yet efficiently.

If a controller is to model a human rider realistically, the controller must also reflect these characteristics. The preview gains achieved for the tight and loose control strategies are therefore considered.

It was expected, based on the literature, that the emphasis of a tight control strategy would be placed on road information in the rider's near preview, with less emphasis given to the road seen in the distance. Figure 6.16 showed the preview gains for all three path error weightings considered. The changes in the gains reflect the expected effects; higher error weighting q_1 resulting in tighter control stems from a shift of

emphasis towards the near preview distance. Conversely, loose control considers the observed path more broadly, with lower peak gain value and more evenly distributed gains over the entire preview distance.

Confirmation of the correct performance of the controller model is made by considering the steer torque that the rider applies to the motorcycle's handlebars. A loose controller would be expected to begin to steer well in advance of the turn, in order to make the turn progressive and minimise the control effort he is required to input, ultimately making the manoeuvre more efficient with regard to his control input. Conversely, tight control might be characterised by later steer control inputs, beginning closer to the turn, and correspondingly having to be larger in magnitude.

The steer torques for all three path error weightings are presented in Figure 6.18. The loose control displays the required early turn initiation, lower ultimate steer torques and a more gentle turn. Notable again is the countersteer applied at the beginning of the manoeuvre.

Thus far, the task of assessing the controller's performance has considered several aspects. These aspects have all suggested that the use of an MPC control strategy replicates well the behaviour that may be expected of a real rider. 3.0 s of visual road preview appears sufficient at this speed, showing good path following performance and with the preview gains diminishing to zero for all path error weighting values considered, with variations in the lateral path following error resulting from changes to the controller's behaviour in a manner that appear consistent with the behaviour expected of a human rider.

Preview Horizon

The influence of the controller cost function weighting parameters on the performance of the controller as a whole has been investigated. The fundamental input to the controller comes from the road information that the rider sees, and so logically the preview and control horizons would be expected to have a significant impact upon the controller's performance. The effects of both an increase and decrease in the available preview information afforded to the rider model therefore require investigation.

Considered first is the case for an increased preview horizon (Table 6.1, Set 4). As

the rider initially appeared to have sufficient preview information available to him at the forward speed of 10 m/s, it may be expected that additional preview information would have minimal significant impact on the controller's performance. T_p is increased from 3.0 s to 4.5 s, representing what is believed to provide excessive visual preview. The limited preview horizon case is also considered (Table 6.1, Set 5), for a reduction in the preview horizon from 3.0 s to 1.5 s. For both controller sets, the results will be analysed in the same manner as before, looking at path following performance, gain distributions and resulting control inputs.

For all three horizon lengths considered, the path following accuracy shows little difference (Figure 6.19); only when examining the data in detail for the loosest controller ($q_1 = 1000$) is there a discernable difference. In analysing the influence of the path error weighting function, it was seen that loose control was associated with fuller use of the available preview information, such that the extra preview information enabled the rider to improve the input-effort efficiency of his manoeuvre, consequently leading to the rider cutting the corner to a greater degree than previously. Conversely, tight control placed the emphasis on the road information close to the motorcycle's position. It may therefore be expected that for tighter control additional preview information in the far preview region would not significantly affect the control strategy applied during the manoeuvre.

The state gains for both $T_p = 1.5$ s and 4.5 s are compared with the baseline parameter set (Figure 6.20). Minimal difference is observed for the two horizon values considered compared to the baseline set. For the 4.5 s case, it appears that the increase in the amount of road information available to the rider model has, as predicted, had minimal influence upon the state gains. Likewise, the reduction in preview shows barely perceptible differences.

The preview gains show similar findings, with minimal differences between the gain values achieved with $T_p = 3.0$ s compared with $T_p = 4.5$ *s* (Figure 6.21). Again, this suggests that for the current level of path following accuracy a preview time of 3.0 s is sufficient, and any additional preview information would be of little use to the rider. The reduction in preview to 1.5 s again brings only subtle changes to the pattern of the gains, suggesting that the reduction has had only a minor effect on the rider's control.

As neither the state gains nor the preview gains are significantly affected by the increase in the preview distance available to the rider, the consequential effect on the steer torque is minimal (Figure 6.22).

It appears therefore that for the speed and path error weighting functions considered here, additional preview information has not affected the rider's control strategy significantly. For riding with these path following parameters, greater than 3.0 s of visual preview appears to have minimal benefit to the rider. Similarly, with a reduction in the preview horizon to 1.5 s, the effects on the controller and the path following performance appear to be of minor significance.

Control Horizon

The predictive control strategy also permits the control horizon to be set independently of the preview horizon. For restricted control horizons, the control input is assumed to be invariant from the limit of the control horizon up to the limit of the preview horizon, such that a control input for the full preview horizon is still available (Section 6.2.1). This is a standard practice when employing predictive control techniques [9, 35] A loose control strategy has been shown to favour a longer preview horizon, and so this limited control horizon case is tested against a loose control strategy in order to provide a more challenging test, comparing three cases; the preview horizon is fixed at 3.0 s, with initially a 3.0 s control horizon, then restricted to 1.5 s, and the last case with the control horizon reduced further to 0.5 s (Table 6.1, Set 6).

As may be expected, some change in the controller's performance is observed. Figure 6.23 shows the path errors between the three controller settings. The shortest control horizon case (0.5 s) displays the largest errors. Over approximately the first 40 m of the manoeuvre, the 1.5 s control horizon case displays the best performance. In the middle phase the 1.5 s and 3.0 s cases are very similar, while over the last phase of the manoeuvre, from approximately 55 m to 65 m, the 3.0 s case proves superior to the 1.5 s control horizon case.

The corresponding state and preview gains are given in Figures 6.24 and 6.25.

Low Speed Modelling Conclusions

Having conducting a parameter study for the motorcycle running at low speed, some conclusions can be made regarding the performance and characteristics of the control strategy for this application.

In line with what may intuitively be expected, changes to the required path following accuracy affect the way in which the modelled rider uses the road information available to him. A loose control strategy implies that the concern is biased towards minimisation of control effort, with accurate path following being less important. Consequently, the rider makes more use of the full picture of the road ahead, thereby allowing the most efficient route to be taken over the road that he can see. Conversely, tight control requires accurate path following, so regardless of where the road may go some distance in the future, the prime consideration is the immediate path that the rider is about to encounter, and ensuring that his motion tracks this road accurately. These characteristics for tight and loose control are thus reflected in the preview gains that represent the use that the rider makes of the observed road path.

If sufficient visual road preview is available in order to make the suitable compromise between path accuracy and control effort, then any additional road preview at the limit of the rider's preview appears to have no effect on the controller gains and hence the control actions of the rider model. Again, this characteristic would appear to be representative of the manner in which a human rider would operate.

Initial results for the application of the model predictive control strategy to motorcycle rider modelling therefore appear encouraging, and the analysis is extended for the motorcycle running at increased forward speeds.

6.3.2 High Speed Linear Prediction Model

Results presented thus far have been for one forward speed alone, $v = 10$ m/s, where it was observed that the controller produced good results for preview times T_p in excess of 1.5 s. Variation of the control parameters produced acceptable changes in the controller's gains and consequently control actions.

The forward speed was therefore increased in order to assess the implications that

forward speed has upon the controller's ability to guide the motorcycle along the target path.

Baseline Parameter Set

As for the model running at $v = 10$ m/s, the model has been run with a set of baseline parameters, but now at a forward speed of $v = 40$ m/s (Table 6.2, Set 7). The modelling parameters were varied as at the lower speed, with the results analysed and compared with the lower speed condition.

Examining first the path following capabilities of the controller (Figure 6.26), the motorcycle continues to follow the intended path, negotiating the manoeuvre section successfully, returning to follow the path accurately along the subsequent straight-running section. Compared with the lower speed case (Figure 6.10), the motorcycle was seen to overshoot at the turn exit to a greater degree than for the lower speed case, cut the corner much more significantly, but ultimately achieved the manoeuvre.

The controller gains essentially represent a mathematical balance between the cost associated with the output (path following) accuracy and the control effort (steer torque) input. Higher speeds lead to an increase in gyroscopic forces associated with the rotating wheels, and hence require a greater steer torque input effort to achieve similar steer angles and thus path following performance. Like for like, higher speeds lead to an increase of the contribution to the cost function made by the control input effort. The path following error becomes relatively less of a priority at higher speeds, and consequently the path following accuracy suffers. In this manner, the behaviour with increased speeds is not unlike setting the controller to operate in a looser manner, where the relative contribution to the cost function is reduced, and indeed this is reflected in the path following performance of the controller.

The state gains provide some interesting observations (Figure 6.27). The bulk of the states gains are not changed significantly with the increase in forward speed, except for the gain corresponding to the yaw angle, which sees an increase of nearly 250%. A yaw angle error implies that the motorcycle is heading away from the intended path. As the forward speed is increased, for a given iteration time step it is seen that doubling the forward speed will double the lateral path error that is generated over one iteration step (Figure 6.28). Perhaps then it is unsurprising that a 300% increase

in the forward speed and therefore the preview distance should result in a similar increase to the gain applied to the yaw angle of the motorcycle.

Comparing the preview gains (Figure 6.29), it appears that with $T_p = 3.0$ s the gains again come close to diminishing to zero, though perhaps not quite as completely as seen at the lower speed. Also of note is the oscillatory response of the gains for the higher speed. This condition is due to the minimal damping of the wobble mode at this forward speed (Figure 3.15), seen also for the optimal control approach (Figure 5.21). Although the gains at the higher speed are clearly tending to zero it appears that they have not yet reached a steady value, implying that a small increase in the preview horizon may be required to achieve this. At the increased speed, the peak gains obtained are smaller than had been seen for $v = 10$ m/s, with peak gains of less than 1.5 comparing with over 2.0 for the lower speed. This is an interesting result, since the higher speeds are seen to increase the magnitudes of the state gains, while seemingly reducing the magnitude of the preview gains. Considering again Figure 6.29, the trend seen here is again not dissimilar to that shown when the controller running at $v = 10$ m/s was set to operate in a loose manner; the peak gains are lower but the rider apparently is required to look further down the road to apply complete control.

The increased gyroscopic forces are in part suspected to account for this; at the raised speeds, the steer torques required to overcome the gyroscopics will increase, leading to an increase in the relative contribution to the cost function relating to the control effort. Consequently, since the ratio between the cost function's components is fixed, the cost contribution associated with the system output also increases. Thus, the errors associated with the path following also increase, and so the path following performance appears to deteriorate.

To confirm that the deterioration in path following accuracy is largely as a result of increased gyroscopics and hence increased cost function contribution due to the system inputs, the inertias of the wheels were reduced, thus decreasing the gyroscopic forces from the wheels that form a significant contribution to the stability and manoeuvrability of the motorcycle. If the hypothesis is correct, then the reduction in wheel gyroscopics should lead to an improvement in the path following performance achieved. The wheel moments of inertias were therefore halved, and the path following as a result is presented in Figure 6.30. Here, it is clearly seen that this reduction in

wheel inertia has had a significant impact on the path following accuracy. The path following errors are not halved, since the gyroscopic forces are not the only forces contributing to the steer torque required to steer the motorcycle, but it is apparent that the contribution is nonetheless a notable element.

As anticipated, at higher speeds the steer torques applied by the controller are seen to be significantly greater than had been seen at the lower speeds (Figure 6.31). Given, in part, the relationship between forward speed and wheel gyroscopic forces this result is perhaps not unexpected. The magnitudes of the steer torques generated in this simulation are likely to be greater than a rider would be capable of applying. The results here are a mathematical solution, and this result adds weight to the need for some form of limits or constraints that formed one of the motivations for using model predictive control techniques. In spite of the increased steer torques, the steer angles obtained are reduced compared with those achieved at lower speeds (Figure 6.32).

The comparisons drawn between the behaviour of the controller operating with the higher speed baseline set indicate that, for all other parameters fixed, the control behaviour resulting appears to exhibit a more loose manner than at the the lower speed. This agrees with the observation that increased speeds lead to higher control contribution to the cost function, and hence the controller must compromise path accuracy at high speeds in an attempt to contain the control input effort required.

Cost Function Weighting

The influence of the output error cost function weighting parameter is again analysed for the higher speed case (Table 6.2, Sets 8 & 9). It was observed that the influence upon the state gains, preview gains, steer torques and steer angles all showed comparable behaviour to the lower speed case.

Reducing the cost weighting results in lower state gains, while increased cost weighting results in higher state gains (Figure 6.33). For the looser control, the preview gains are lower in magnitude but biased further forwards and more evenly distributed over the visual preview horizon, comparable to a looser control strategy. However, it is noted that for the preview gains to diminish to zero, as had been achieved at the lower speed with $T_p = 3.0$ s, it becomes necessary to increase the preview horizon to achieve the same results. Figure 6.34 plots the preview gains against preview

distance allowing 4.5 s of visual preview, where the preview gain pattern with regard to the complete preview horizon is then comparable with Figure 6.16. Tighter control was seen to result in higher peak preview gain values, biased more towards the near preview.

The effects on the steer torques and hence steer angles are qualitatively similar to the effects seen at lower speed (Figure 6.35), and are consistent with the observations made regarding rider control for the lower speed case.

Preview Horizon

The influence of the preview horizon on the controller performance is again analysed, now at the higher speed (Table 6.2, Sets 10 & 11). As noted previously, to achieve comparable preview gain distribution at the higher speed it is seen to be necessary to increase the length of the preview horizon, with the increased preview horizon taken as 4.5 s. At the higher speed, comparison of the preview gains for the three preview horizon times (Figure 6.36) shows minimal difference between $T_p = 3.0$ s and $T_p = 4.5$ s. However, the lower preview horizon, $T_p = 1.5$ s, shows more notable difference to the other two settings. In contrast, at the lower speed (Figure 6.21), all three horizons gave very similar gain patterns.

These results appear to show that as the speed is increased an increased preview time is ideally necessary to maintain the control performance of the motorcycle, and as before, it is suggested that this is again the result of the increase in gyroscopic forces experienced as the speed increases (Figure 6.30). Consequently, and in order to maintain control torque effort, the rider must begin manoeuvres further in advance of the turn as the speed is increased, which therefore requires a greater preview horizon in order to facilitate this.

In spite of the apparent deterioration of the controller gains for higher speeds with short preview horizon, the model is still capable of negotiating the path competently. What this result would appear to suggest is that the rider model's control may be compromised by the limited preview, but this does not necessarily prevent successful riding, as may be expected of a real rider.

Control Horizon

Thus far, the control problem has dealt with the situation for which the rider's visual preview horizon and his control horizon are the same. In other words, the rider plans a control strategy for the full road picture that he has available. The MPC strategy enables the two horizons to be set independently, thus allowing the control horizon to be set shorter than the preview horizon. Relating this to a rider, this would imply that the rider has knowledge of the road a long way ahead, but plans his control for only a shorter time ahead of him.

It has been seen previously that for the low speed baseline parameter set (Table 6.1), the controller's performance was good, and a reduction in the preview and control horizon to 1.5 s did not adversely affect the overall ability of the controller to complete the task.

As the speed was increased, it was noted that the reduction in preview horizon from 3.0 s to 1.5 s did appear to have an effect on the preview gains. While the ultimate performance of the controller was not significantly degraded, the effect of the reduced preview horizon was apparent.

An appropriate point to begin to investigate the effect of a reduced control horizon is therefore with the higher speed baseline parameter set. The simulation is therefore run with a preview horizon $T_p = 3.0$ s, but with also a limited control horizons of $T_u = 1.5$ s and 0.5 s (Set 12). Selecting these values will allow the performance to be compared with earlier results with equal preview and control horizons.

The path following performance of all three control horizon settings was seen to result in very similar results which were difficult to discern from one another. The path errors, being the difference between the target path and the actual path achieved, are therefore plotted in Figure 6.37, where it is seen that overall the performances of the three controllers are similar. Only in the initial countersteer phase and at turn exit are there any notable differences.

The maximum error during the initial phase is seen for the shortest control horizon, as may be expected, but, interestingly, the best performance in this part is for the 1.5 s control horizon. The 3.0 s control horizon falls midway between the two. At turn exit, the roles are reversed; the shortest control horizon $T_u = 0.5$ s shows the

best performance, the 1.5 s case the worst, with again the 3.0 s case in between.

Both the state gains (Figure 6.38) and preview gains (Figure 6.39) show this similar interesting pattern, whereby the values of the 3.0 s control horizon case fall midway between the values of the 1.5 s and 0.5 s values.

High Speed Linear Prediction Model Conclusions

The analysis for the two different forward speeds considered has generated some interesting conclusions, indicating the requirement for greater preview information for complete control as the speed is increased.

A human rider is constrained by physical limits of strength which ultimately limit the magnitudes of steer torque that can be applied to the motorcycle. Higher speeds require higher steer torques due to the increase in gyroscopic forces (Figure 6.30), and so as the rider's physical limits become more heavily used, he must instead find ways to reduce this torque requirement. This is most readily achieved by commencing the turn earlier and more progressively, and essentially the rider may be forced to operate with a looser control strategy by limitations of physical strength.

In a real riding situation, there are additional steps that a rider can take in order to reduce the steer torque requirement in order to overcome the gyroscopic forces. Typical techniques include more emphasised countersteer to force the bike into the lean and movement of body weight, in order either to force the bike to lean into the turn or to reduce the angle to which the motorcycle itself must lean, by moving his own bodyweight to achieve the necessary balance between overturning moments and moments due to centripetal forces.

In performing a manoeuvre, a car is not required to lean into a turn in the manner that a motorcycle must. As such, the increased gyroscopic forces that result from higher speeds are inconsequential to a car driver. It may therefore be suspected that as speeds are increased a car driver has less requirement to increase his preview horizon for complete control in the manner that a motorcycle rider, it appears, would need to. It is widely regarded that motorcycle riders exercise much greater visual preview, examining the road ahead to a greater distance than a car driver might, and indeed the findings here would appear to support those beliefs and offer some feasible

explanation of why this needs to be so.

6.3.3 Non-Linear Prediction Model

The analysis conducted so far used a prediction model that employed a fixed state space model of the motorcycle for the entire prediction horizon, as discussed in Section 6.2.1. If a technically more correct prediction model were to be used, the technique to obtain the prediction element is essentially the same, albeit computationally more demanding. The theory of this approach was presented in Section 6.2.2. In regard of the additional computational load of the non-linear model, a typical simulation conducted here required several hours for the non-linear prediction as opposed to several minutes for the linear prediction. For off-line model simulation, this does not technically pose a problem. However for the processing of a significant number of modelling conditions, as considered within this thesis, the additional computational time becomes a more relevant consideration.

In order to assess how critical the choice of a technically more correct non-linear prediction model is to the modelling of the motorcycle rider, the full non-linear prediction model has been run for the set of low-speed baseline parameters presented in Section 6.3.1.

For the linear prediction model running at moderately low speeds, the path following performance was seen to be quite acceptable, with the motorcycle tracking the path well and with smooth progress during the manoeuvre (Figure 6.10) The control gains generated (Figures 6.11, 6.12) seemed consistent with what might logically be expected and the steer torque (Figure 6.13), while not completely smooth, also seemed consistent with the actions that may be expected of a human rider.

The full non-linear model was run using the same modelling parameters and over the same path. The path following performance of the model was examined first, and compared with the linear prediction model results obtained previously. The differences between the linear and non-linear prediction models are hard to discern; both models follow broadly the same path, and it is only when the performance is examined in detail that the differences become apparent. Figure 6.40 presents the final phase of the manoeuvre, as the motorcycle is exiting the turn phase and returning to straight running. By examination of this phase, it is apparent that the non-linear

model performs better, tracking the target path more closely, both during the turn and as the motorcycle begins to straighten its path.

The steer torques generated by the controller are also examined, and once again compared with the linear prediction model results obtained previously. For the linear prediction model, the steer torques appeared acceptable (Figure 6.13), albeit not entirely progressive over the course of the manoeuvre. Figure 6.41 presents the steer torques for both the linear and non-linear prediction models, and from this the superior performance of the non-linear prediction model is apparent, the steer torques generated using the full non-linear prediction model showing much smoother torque inputs without the transient oscillatory behaviour apparent with the linear prediction model.

The results of this are significant for two reasons. Primarily, it is apparent that the performance of the controller is superior when a more realistic prediction model is used. This result is not surprising, since the controller bases the control decision on the predicted output, and if the predicted output and the actual system output to a given control input differ, then clearly the system behaviour will suffer from less accurate performance.

Secondly, although the full non-linear prediction model *is* seen to provide superior performance, the difference in the resulting outputs are not so different as to call into question the validity of the results and observations made in assessing the MPC controller using the linear prediction model.

It is likely that for the higher speed case, the difference between the linear and non-linear models will be more distinct. At higher speeds, the lean angles required to negotiate turns are greater, and as such the change in lean angle over the manoeuvre in the prediction horizon could be expected to increase. Consequently, the dynamics of the motorcycle will change to a greater extent over the preview horizon, making the difference between the linear prediction model and the non-linear prediction model more marked. Additionally, at the higher speed the preview distance increases, meaning that a greater distance of road is seen in the rider's preview horizon, and therefore the manoeuvre planned for a greater length of the road path. The greater the length of the road path, the greater the potential changes in the road path that the rider will see. Correspondingly, the potential changes in the motorcycle's predicted future

trajectory may be greater, adding further to the differences between the linear and non-linear prediction models at the higher speed.

6.3.4 Reference Path Definition

The application of a reference path, often used in predictive control methods, concerns the definition of a target path to follow, different to the set path, that the system output will attempt to track. With this method, the intention is to take the system output from a position away from the ideal and guide it back onto track in some defined way.

The results presented so far have been for the case where the set path and reference path were equal. If the motorcycle were displaced from the target path, this would effectively result in a step path that the rider would attempt to follow. However, it was postulated that this may not be entirely realistic of a human rider, and that once displaced from the ideal path of the road, a rider may not attempt immediately to recover the road centreline, but will aim instead to gradually guide himself back onto the road path.

The manner in which the set path regains the target path can be defined in different ways. Here, three methods were considered: linear path, linear error reduction path, and exponential error reduction path. The performance of the controller using these modified path definitions will be compared with the original definitions using only the set path, to determine whether improved controller performance can be achieved.

Linear Set Path

The theory of the linear set path was covered in Section 6.2.3. Essentially, the linear set path defines a path that takes the system output state from the current position to the target position at the limit of the preview horizon. Making use of the motorcycle's current position and a target position given as the set path at the limit of the rider's preview horizon, the intermediate linear reference path is calculated. The theory of a linear prediction model is applied to the motorcycle model, and the controller then attempts to follow the single lane change manoeuvre as before.

The path following ability of the controller is assessed first. From the trace of the path

output (Figure 6.42), it is immediately apparent that this is not an entirely suitable manner in which to model the controller's actions. Essentially, by modelling the set path as a linear path from current position to final position, at each point during the simulation the rider is ignoring the road path in his preview horizon, focusing only on his distant target. For very gentle manoeuvres, this may be an acceptable approach, but realistically it is not suitable for the application here. Throughout the manoeuvre the rider is always attempting to cut the corner by the maximum amount, and hence the resulting performance is poor and unrealistic of the control actions of a motorcycle rider.

If a target point other than the final preview horizon point were chosen, say a point half way along the rider's preview horizon, then the path following performance of the rider would be expected to improve. However, the rider would still be aiming to follow a path that heavily cuts corners (Figure 6.43), and would therefore give inferior performance to the use of the set path. No further analysis was therefore conducted for this definition of reference path.

Linear Error Reduction Path

The definition of the reference path here is subtly different to the full linear reference path. There, the path was taken as a straight path between current position and a target position some way in the distance, with no consideration of the path information in between in the rider's preview horizon.

The reference path defined here is such that the error between the set path and the reference path is reduced linearly over the full preview horizon, from the current lateral error to zero at the horizon limit. This does not imply that the set path itself is linear, as was the case for the linear set path defined previously; if the road curves, so too will the set path, but it is the error between the two paths that will reduce linearly over the forward distance.

The theory of this model was discussed in Section 6.2.3. The performance of the controller using this strategy is again analysed by considering the path following performance and the controller's input actions. Displayed in Figure 6.44, the result is notably different to the linear reference path definition assessed previously. In this case, the rider model does not begin to cut the corner well in advance, and begins

the manoeuvre phase as the actual manoeuvre of the road set path begins.

However, beyond this point, the path following is again inferior to the performance when the set path and reference path were equal. Essentially, by defining the set path as a linear error reduction between current position and a target in the future, a weaker path following target is being set for the rider model to attempt to follow, and consequently the actual path following accuracy of the motorcycle, relative to the actual road defined by the set path, is reduced.

Exponential Error Reduction Path

The reference path is now defined in such a manner that the path error diminishes exponentially to the target path. The basic theory of this approach is similar to the linear error reduction path, except that now the reduction of the path error over the full horizon is an exponential decay.

The theory of this approach (Section 6.2.3) was not dissimilar to the theory for the linear error reduction case. Therefore, it is not surprising that the resulting performance shows similar characteristics to those of the linear error reduction method.

As with that method, the motorcycle does not begin the manoeuvre until the actual road path begins to deviate. However, once the path does begin to deviate, the path followed by the motorcycle does not track this path particularly closely, as before taking a more direct route towards the road path at the limit of the preview (Figure 6.45).

The magnitude of the path error is not as great as for the linear error reduction case, though this magnitude is dependent on the value of l_r, the exponential path relaxation length, set here at values of 20 m and 50 m. The smaller this value, the closer the exponential path comes to a step function, essentially the case when the set path and reference path are set equal. The shorter the value, the more the reference path tends towards the linear error reduction case. Here, the value of l_r is such that the exponential rise time is quite short, and consequently the path following appears to be quite promising. However, if a longer rise-time were used, then the results would tend more towards those seen for the linear error reduction case.

The conclusion for the use of an exponential error path reduction therefore must be

that, in line with the previous two approaches considered, an inferior path following results is produced compared with the use of the set path as the target path to follow.

6.4 Model Predictive Control Conclusions

This chapter has considered the modelling of the control actions of a motorcycle rider using the theory of model predictive control. Through the generation of a suitable cost function, a control input is generated that aims to theoretically minimise the combined costs associated with system output accuracy and system input effort required.

The method has been shown to be highly effective in replicating the control actions of a rider. The controller was tasked with a lane-change manoeuvre, for a variety of controller and task-dependent conditions. Variations in forward speed, rider preview allowances and cost function weighting parameters were all considered. Additionally, the possibility to define a reference path that the system may attempt to track instead of the actual road (set path) was explored.

On the whole, variations to the modelling conditions gave encouraging results. Increased weightings on path errors were seen to reduce the errors in the resulting path following of the motorcycle, sufficient rider preview was seen to result in the best path following performance, and increases to the forward speed of the motorcycle produced the sort of results that may be expected of a real motorcycle and rider.

Not all investigations were entirely successful. A distinct feature of predictive control concerns the ability to define a reference path, distinct from the set path. For some controlled systems, this feature may be able to provide an improvement in the required system response. However, when applied to the road path that the controlled motorcycle attempts to follow, the resulting performance was inferior. Such an approach would be worthy of further consideration only if the manner in which a rider may recover a target path can proved experimentally to be of a specific nature such as presented here. It is likely that riders would have subconscious strategies by which path errors would be corrected, but a firm answer as to what this strategy may be would not be easy to obtain. It may be the case that the choice of recovery strategy employed by the rider is dependent on a number of factors that may include the forward speed of the motorcycle, the nature of the road path and severity of his

departure from the target path, all of which would be very difficult to model. Further work may be able to address this area, though for now the availability of the reference path feature is considered superfluous.

Additionally, a full non-linear prediction model has been compared with the more computationally efficient linear prediction model. It was expected that this would provide superior path following performance, and the results confirmed this. Ideally then, modelling work of this nature should employ a full non-linear prediction model, though the comparison of the two approaches showed that for moderately severe manoeuvres the differences between the two were not so great as to consider the simpler, linear prediction model wrong.

The apparent suitability of the predictive control strategy with regard to replicating the control process of a motorcycle rider and the prediction element that his riding task may include was cited as a strong reason for exploring this control strategy. The aim was therefore to replicate the positive features of the optimal control approach and the apparent suitability to the application, while also correcting some of the limitations found. Both these goals appear to have been achieved, with the generic characteristics of the optimal control approach retained. Due to the strong similarity of the two methods, in order to provide a more detailed comparison of the two approaches Chapter 7 directly compares the two approaches resulting in more defined conclusions about the relative performances of the two approaches.

6.5 Tables

Parameter	Set 1 Baseline	Set 2 Loose Control	Set 3 Tight Control	Set 4 Long Preview	Set 5 Short Preview	Set 6 Short Control
v [ms^{-1}]	10	10	10	10	10	10
T_p [s]	3	3	3	4.5	1.5	3.0
T_u [s]	3	3	3	4.5	1.5	3.0, 1.5, 0.5
T_w [s]	0	0	0	0	0	0
q_1 [m^{-2}]	5000	1000	10000	5000	5000	1000
q_2 [rad^{-2}]	0	0	0	0	0	0
r [(Nm)$^{-2}$]	1	1	1	1	1	1

Table 6.1: Low speed controller parameter sets, model predictive control

Parameter	Set 7 Baseline	Set 8 Loose Control	Set 9 Tight Control	Set 10 Long Preview	Set 11 Short Preview	Set 12 Short Control
v [m/s]	40	40	40	40	40	40
T_p [s]	3	3	3	4.5	1.5	3.0
T_u [s]	3	3	3	4.5	1.5	3.0, 1.5, 0.5
T_w [s]	0	0	0	0	0	0
q_1 [m^{-2}]	5000	1000	10000	5000	5000	5000
q_2 [rad^{-2}]	0	0	0	0	0	0
r [(Nm)$^{-2}$]	1	1	1	1	1	1

Table 6.2: High speed controller parameter sets, model predictive control

6.6 Figures

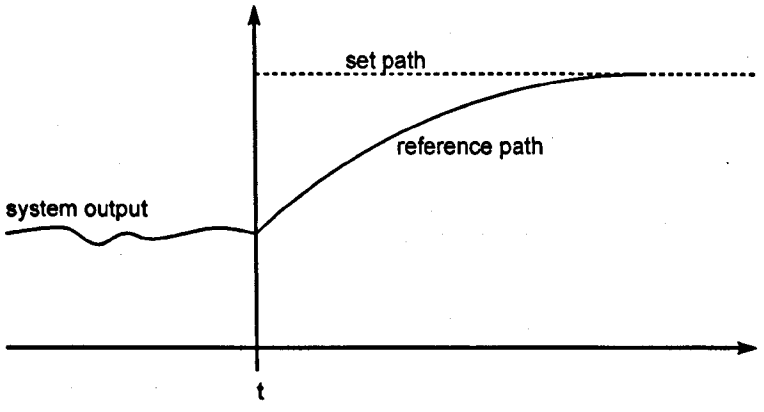

Figure 6.1: Path definition in Model Predictive Control, [9]

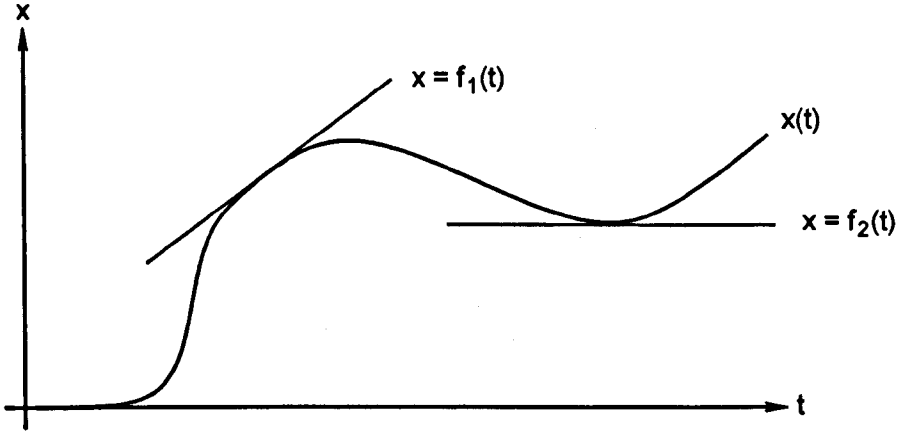

Figure 6.2: Linearisation of a non-linear system at two points

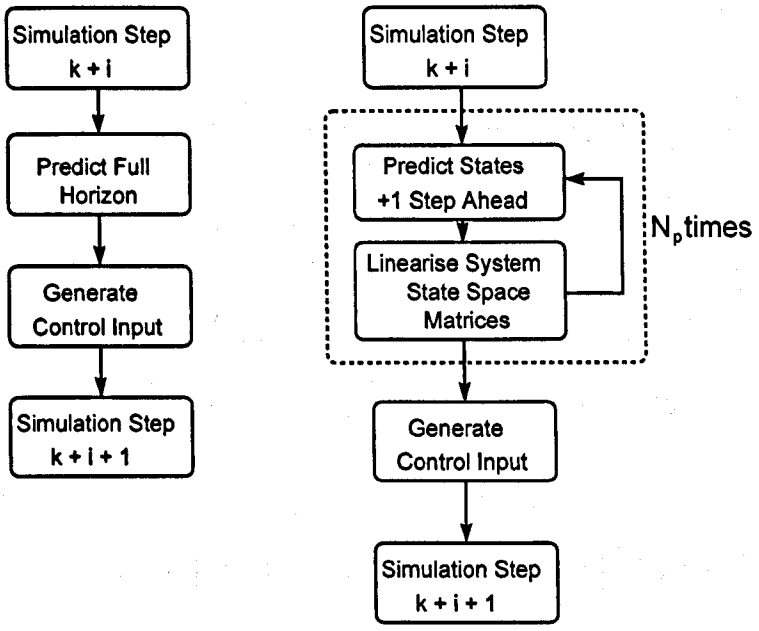

Figure 6.3: Added complexity of non-linear prediction model (right) against linear prediction model (left)

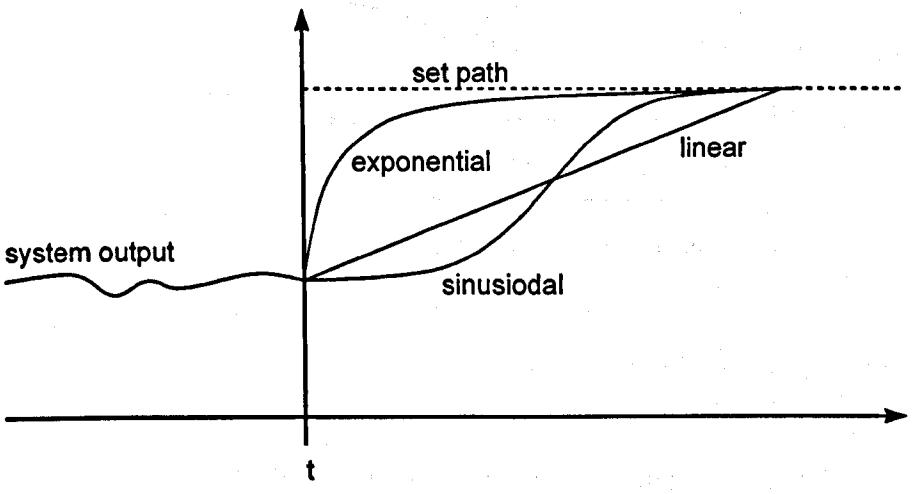

Figure 6.4: Typical reference path definitions in MPC systems

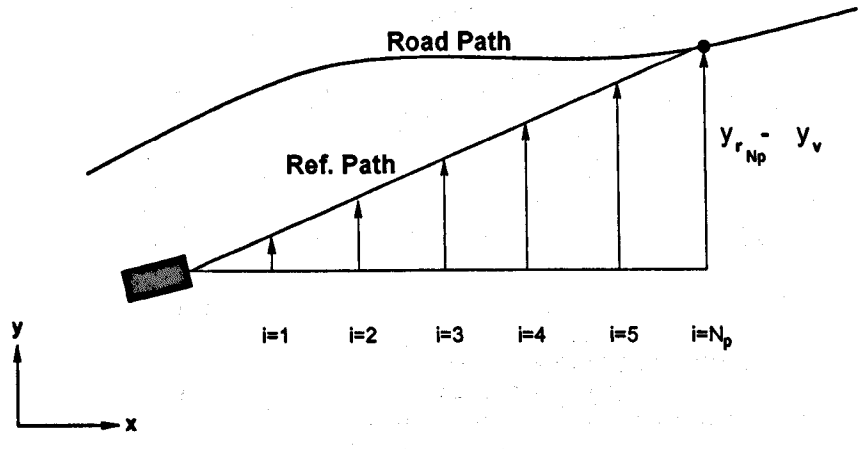

Figure 6.5: Definiton of a linear reference path, $N_p = 6$

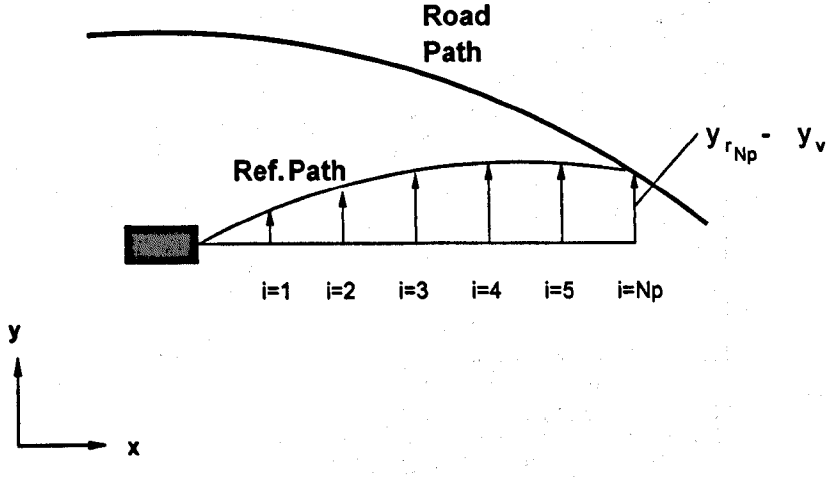

Figure 6.6: Definiton of a linear error reference path, $N_p = 6$

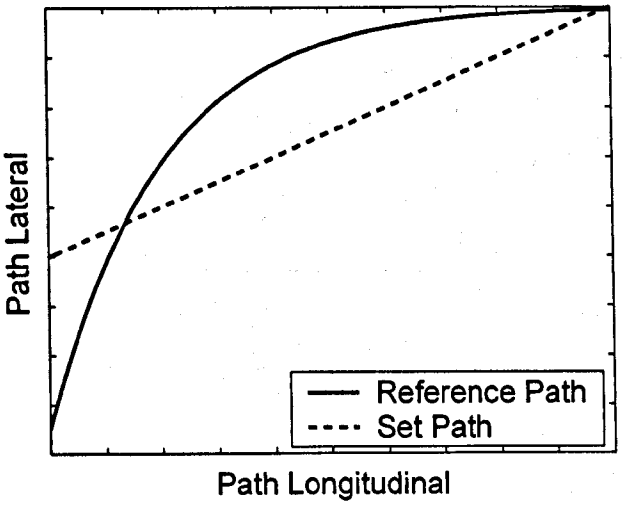

Figure 6.7: Exponential reference path definitions

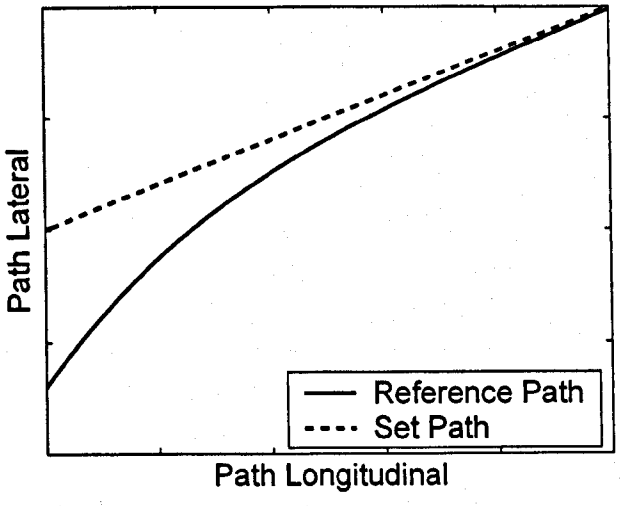

Figure 6.8: Exponential error reduction reference path definitions

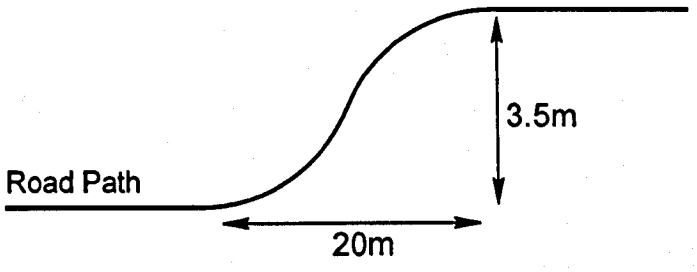

Figure 6.9: Single lane change path, not to scale

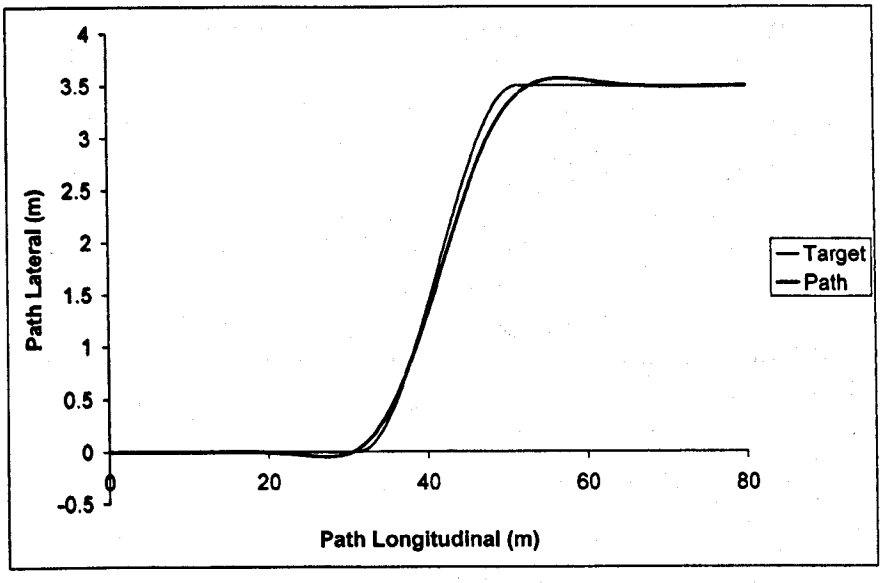

Figure 6.10: Path following, $v = 10$ m/s, $T_p = 3.0$ s, $q_1 = 5000$ m^{-2}

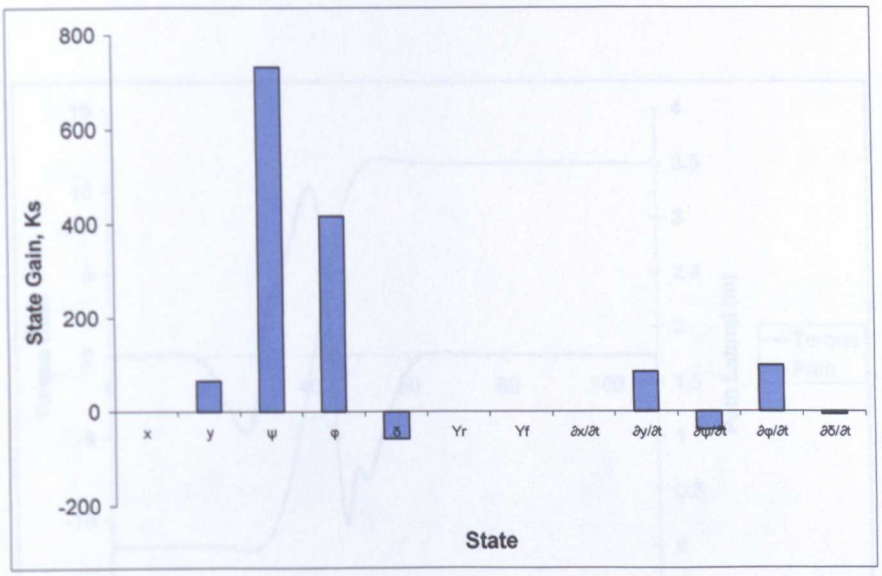

Figure 6.11: State gains, $v = 10$ m/s, $T_p = 3.0$ s, $q_1 = 5000$ m^{-2}

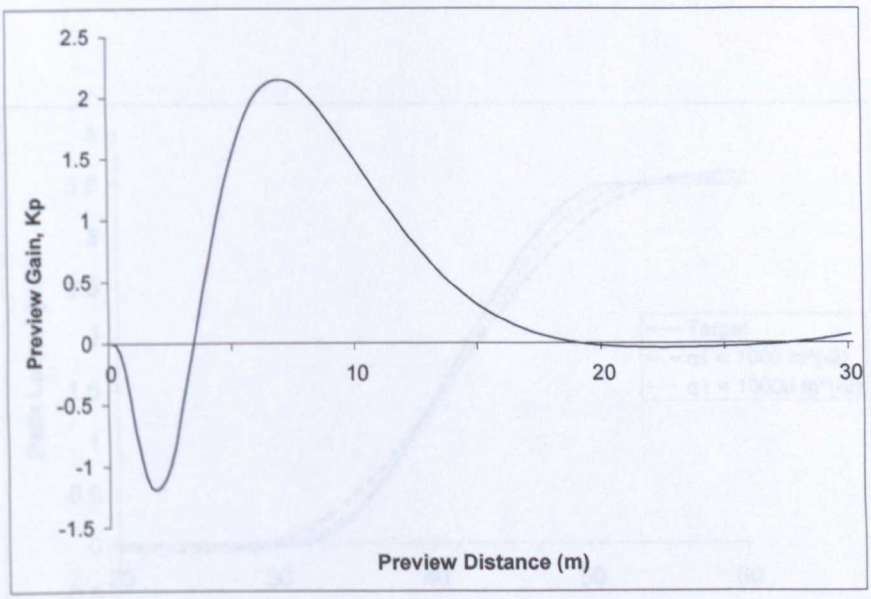

Figure 6.12: Preview Gains, $v = 10$ m/s, $T_p = 3.0$ s, $q_1 = 5000$ m^{-2}

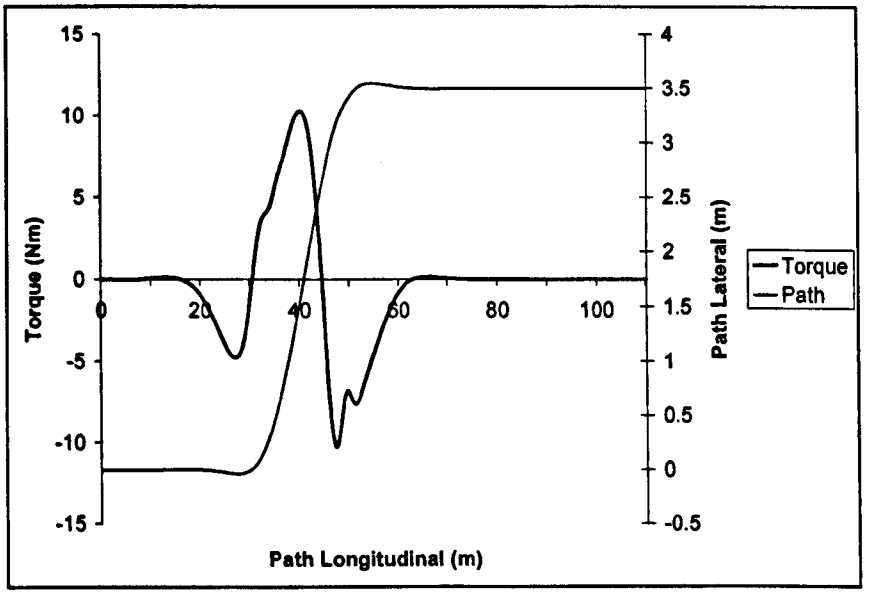

Figure 6.13: Steer Torque, $v = 10$ m/s, $T_p = 3.0$ s, $q_1 = 5000$ m^{-2}

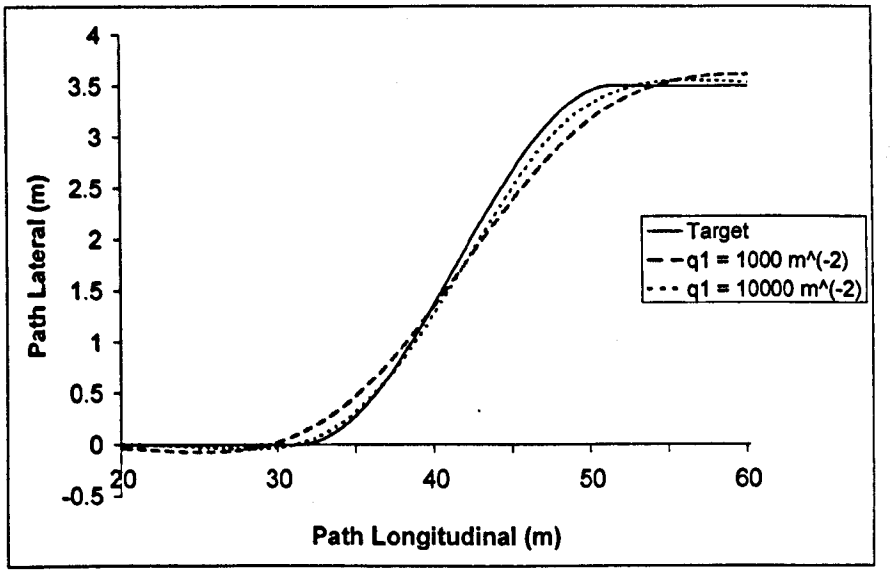

Figure 6.14: Path following, $v = 10$ m/s, $T_p = 3.0$ s, $q_1 = 1000$ & 10000 m^{-2}

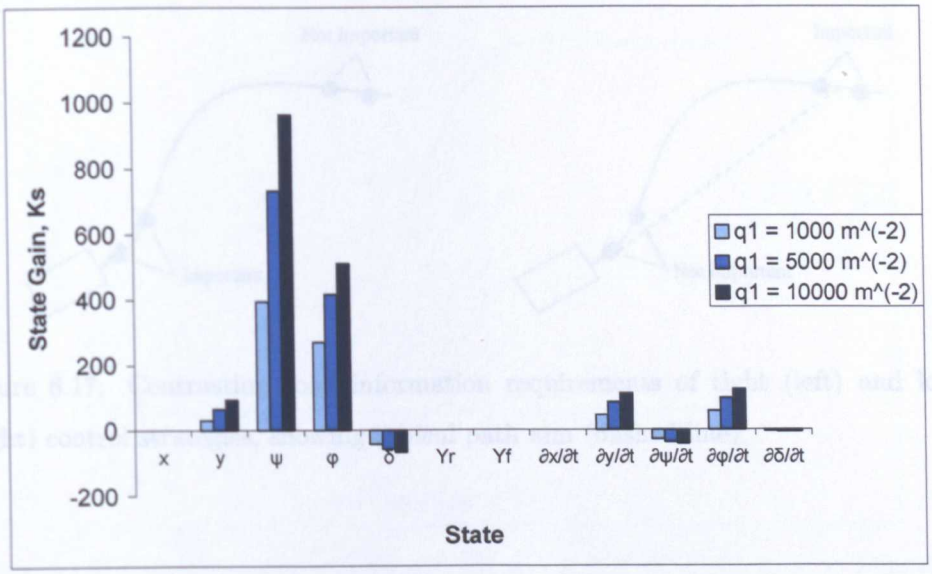

Figure 6.15: State gains, $v = 10$ m/s, $T_p = 3.0$ s, $q_1 = 1000$, 5000 & 10000 m^{-2}

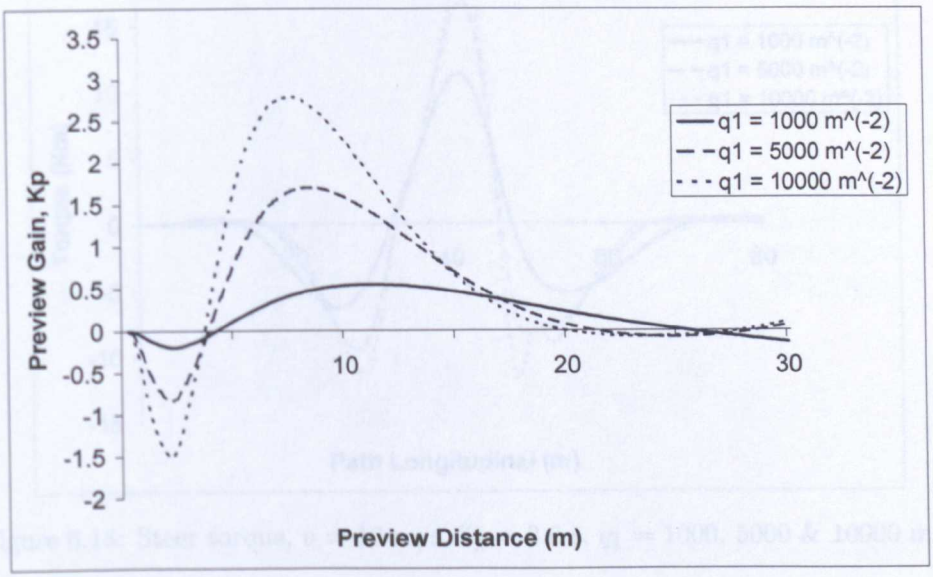

Figure 6.16: Preview gains, $v = 10$ m/s, $T_p = 3.0$ s, $q_1 = 1000$, 5000 & 10000 m^{-2}

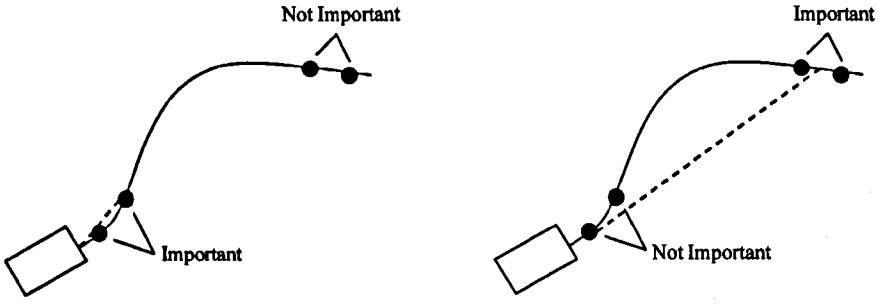

Figure 6.17: Contrasting road information requirements of tight (left) and loose (right) control strategies, showing typical path aim (dashed line)

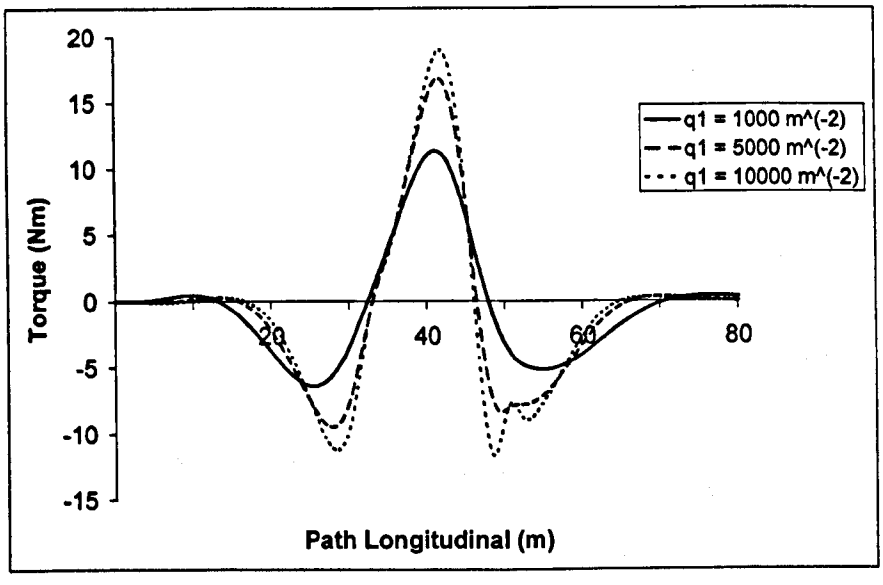

Figure 6.18: Steer torque, $v = 10$ m/s, $T_p = 3.0$ s, $q_1 = 1000$, 5000 & 10000 m^{-2}

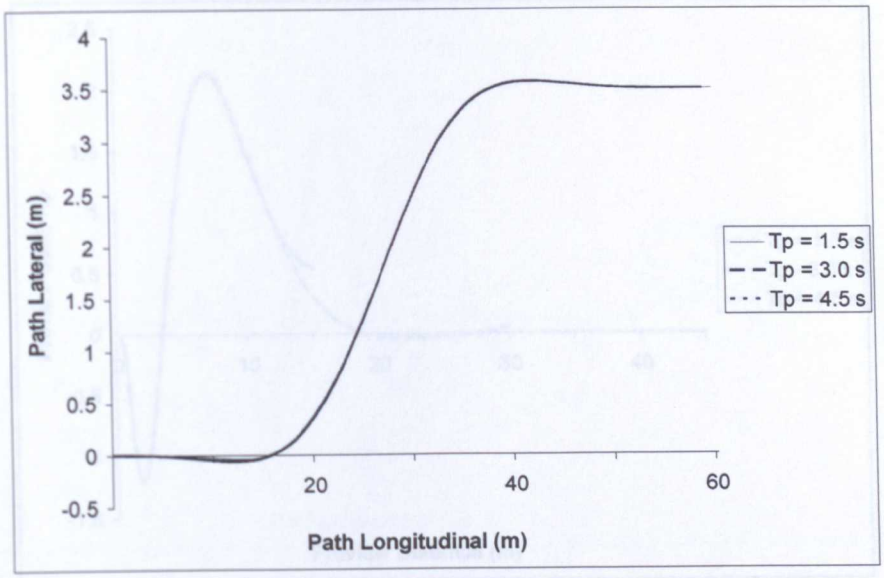

Figure 6.19: Path following, $v = 10$ m/s, $T_p = 1.5$ s, 3.0 s & 4.5 s, $q_1 = 5000$ m^{-2}, results overlapping

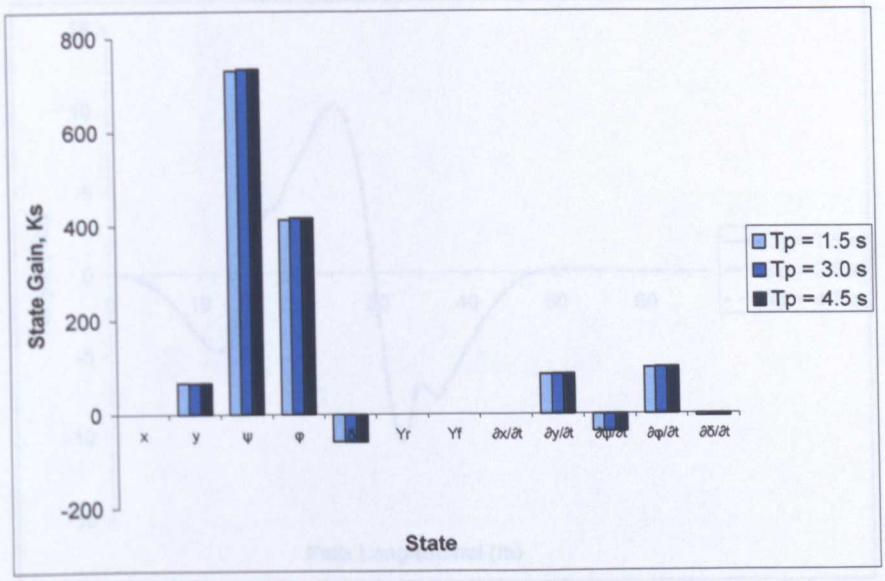

Figure 6.20: State gains, $v = 10$ m/s, $T_p = 1.5$ s, 3.0 s & 4.5 s, $q_1 = 5000$ m^{-2}

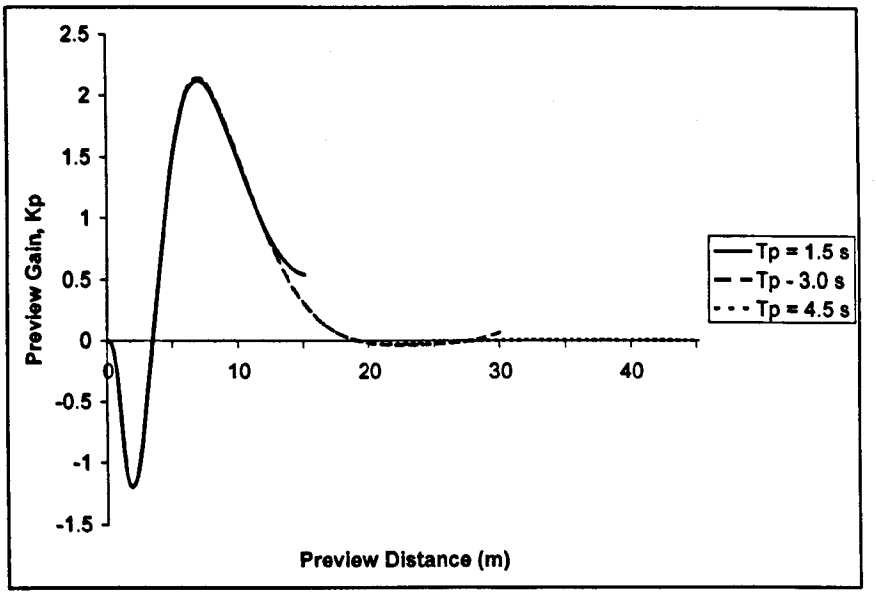

Figure 6.21: Preview Gains, $v = 10$ m/s, $T_p = 1.5$ s, 3.0 s & 4.5 s, $q_1 = 5000$ m^{-2}, paths coincident

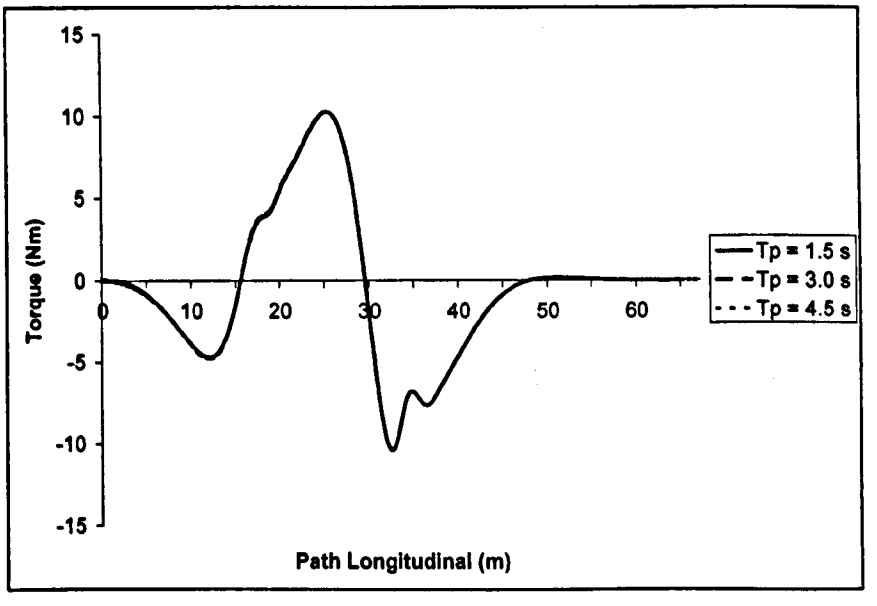

Figure 6.22: Steer Torque, $v = 10$ m/s, $T_p = 1.5$ s, 3.0 s & 4.5 s, $q_1 = 5000$ m^{-2}

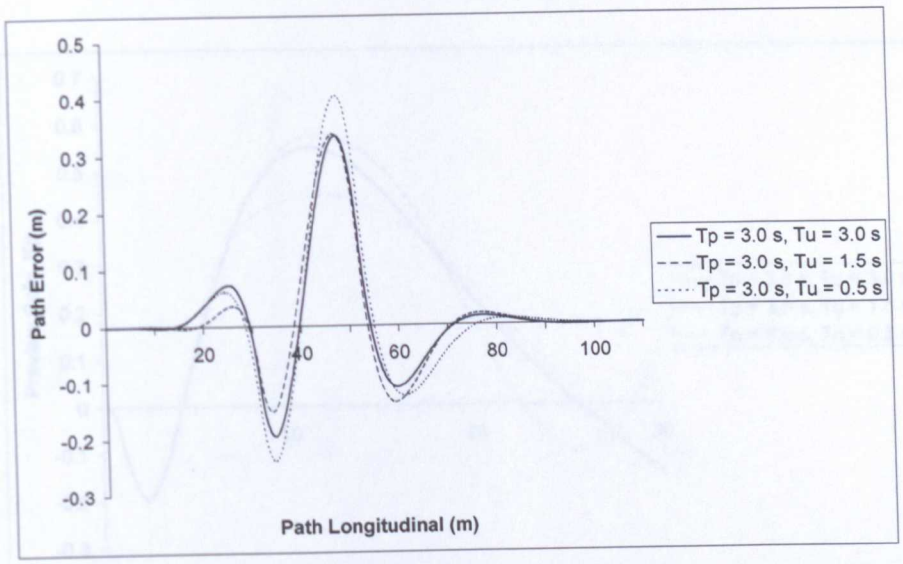

Figure 6.23: Path Errors, $v = 10$ m/s, $T_p = 3.0$ s, $T_u = 3.0$ s, 1.5 s & 0.5 s, $q_1 = 1000$ m^{-2}

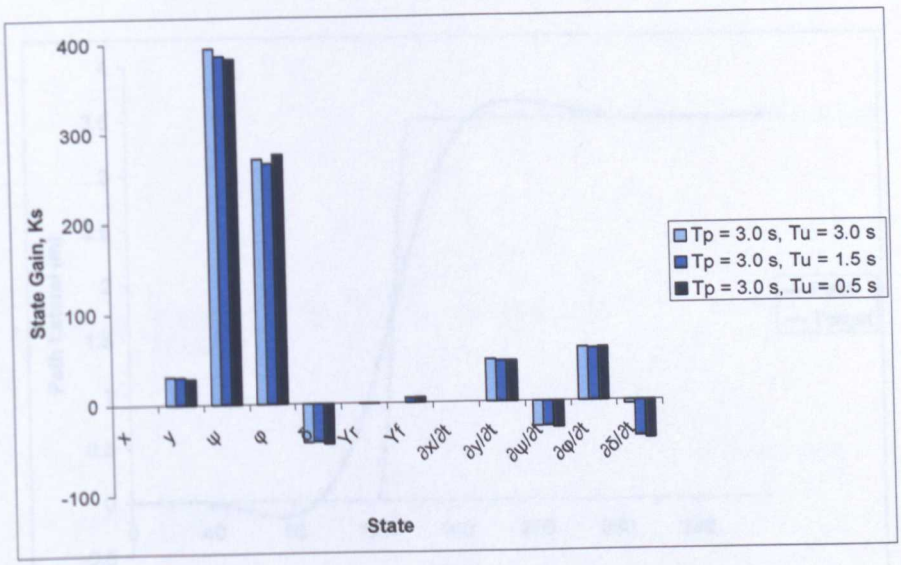

Figure 6.24: State Gains, $v = 10$ m/s, $T_p = 3.0$ s, $T_u = 3.0$ s, 1.5 s & 0.5 s, $q_1 = 1000$ m^{-2}

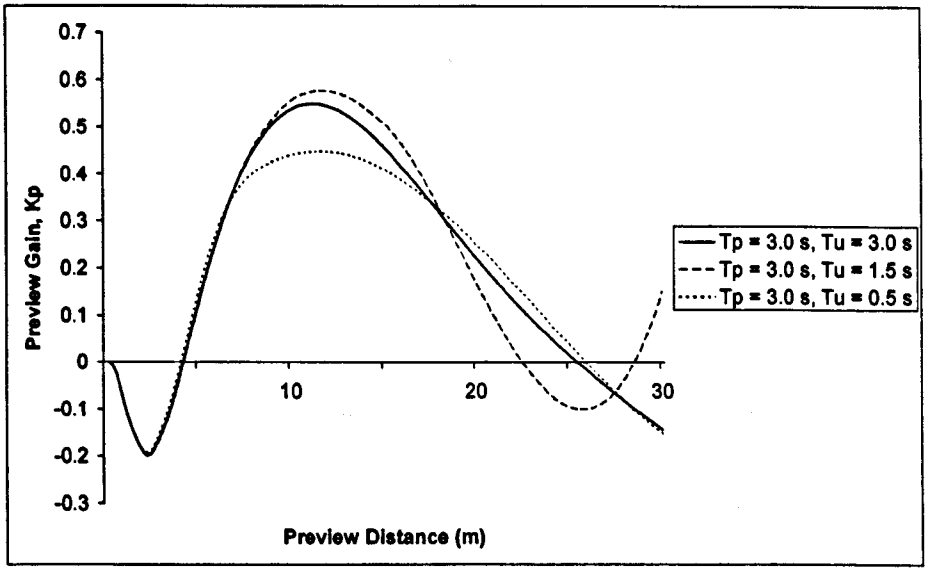

Figure 6.25: Preview Gains, $v = 10$ m/s, $T_p = 3.0$ s, $T_u = 3.0$ s, 1.5 s & 0.5 s, $q_1 = 1000$ m^{-2}

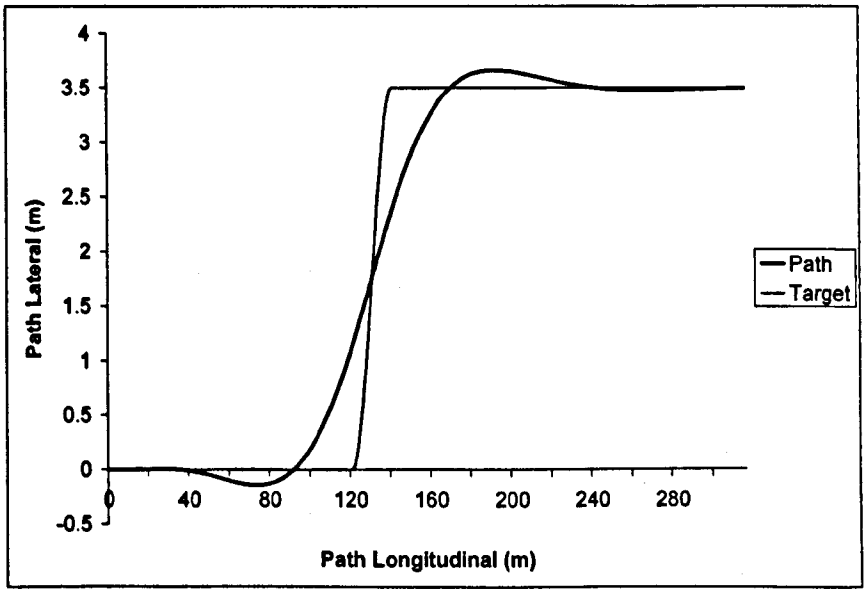

Figure 6.26: Path following, $v = 40$ m/s, $T_p = 3.0$ s, $q_1 = 5000$ m^{-2}

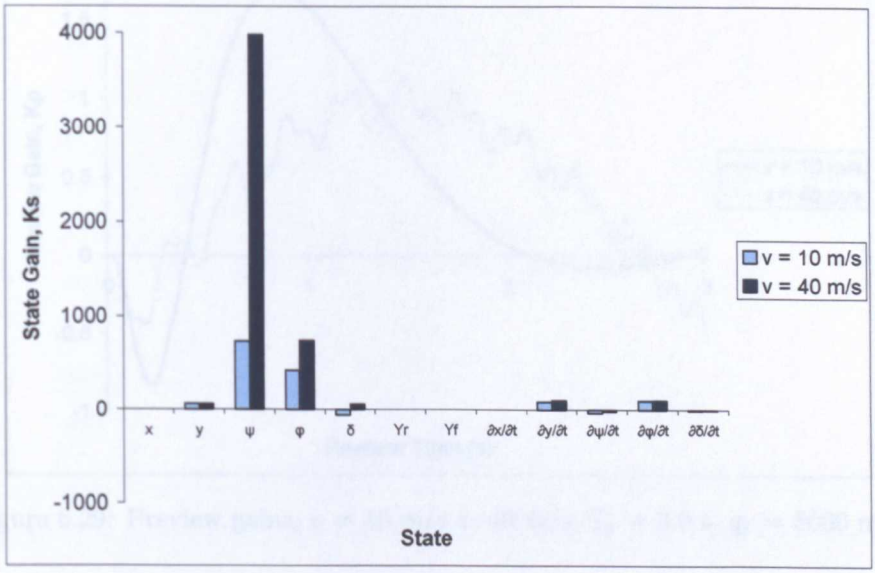

Figure 6.27: State gains, $v = 10$ m/s & 40 m/s, $T_p = 3.0$ s, $q_1 = 5000$ m^{-2}

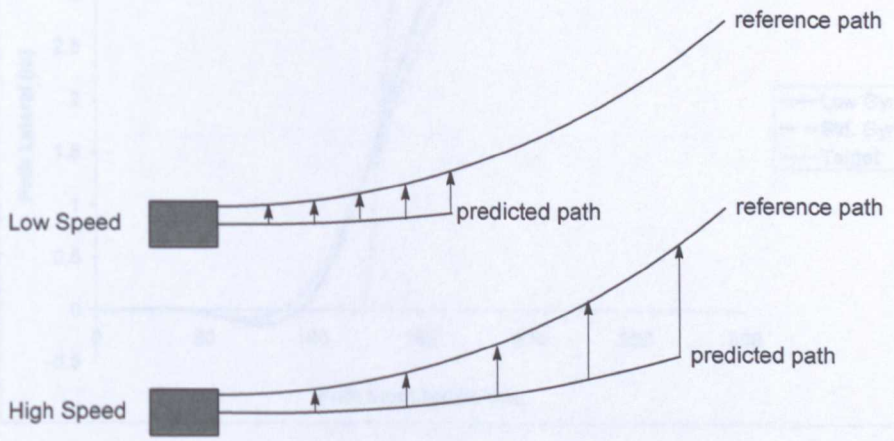

Figure 6.28: Total lateral preview error; effects of increased forward speed

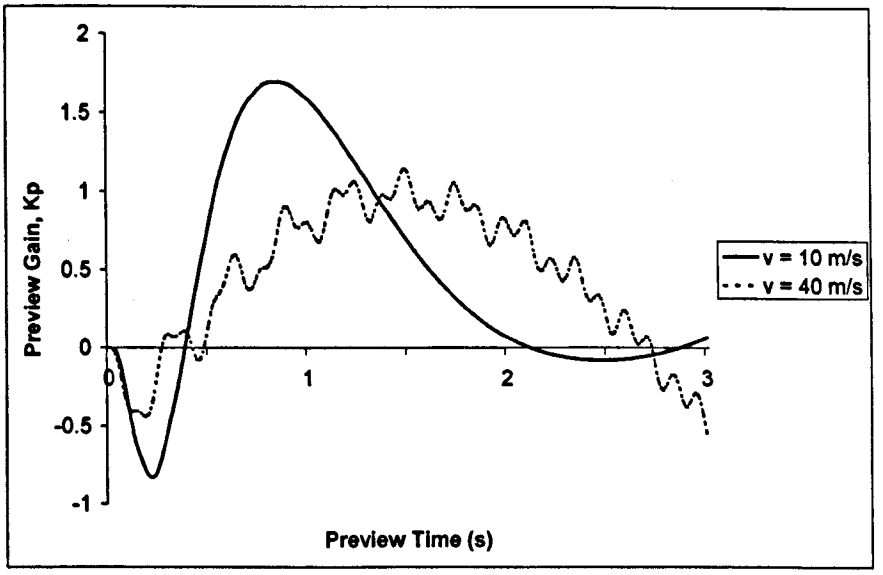

Figure 6.29: Preview gains, $v = 10$ m/s & 40 m/s, $T_p = 3.0$ s, $q_1 = 5000$ m^{-2}

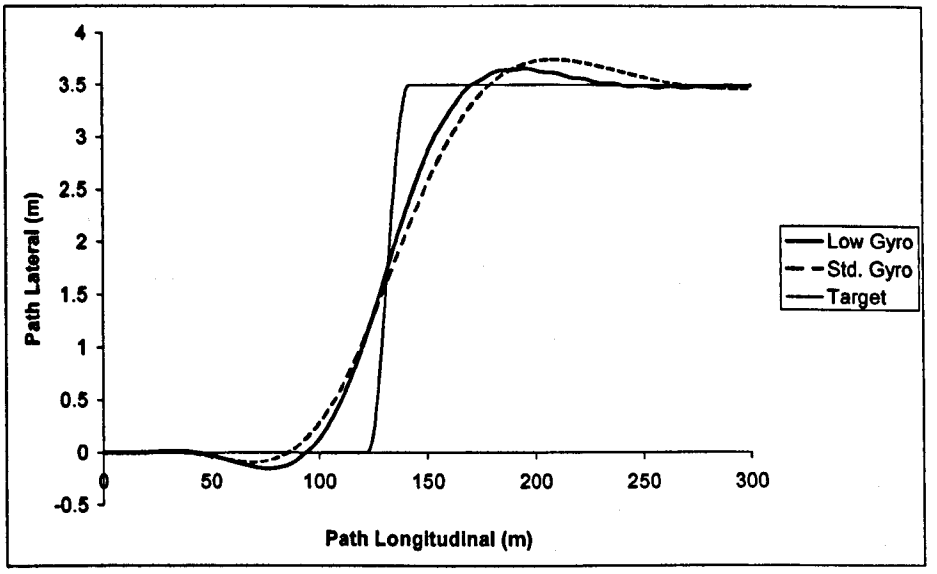

Figure 6.30: Path following performance with reduced wheel inertia, $v = 40$ m/s, $T_p = 3.0$ s, $q_1 = 5000$ m^{-2}

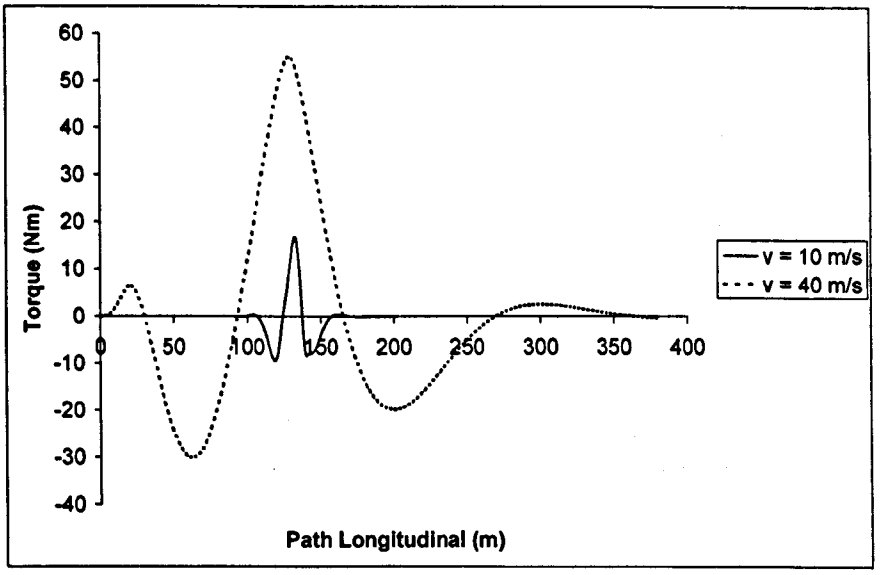

Figure 6.31: Steer torque, $v = 10$ m/s & 40 m/s, $T_p = 3.0$ s, $q_1 = 5000$ m^{-2}

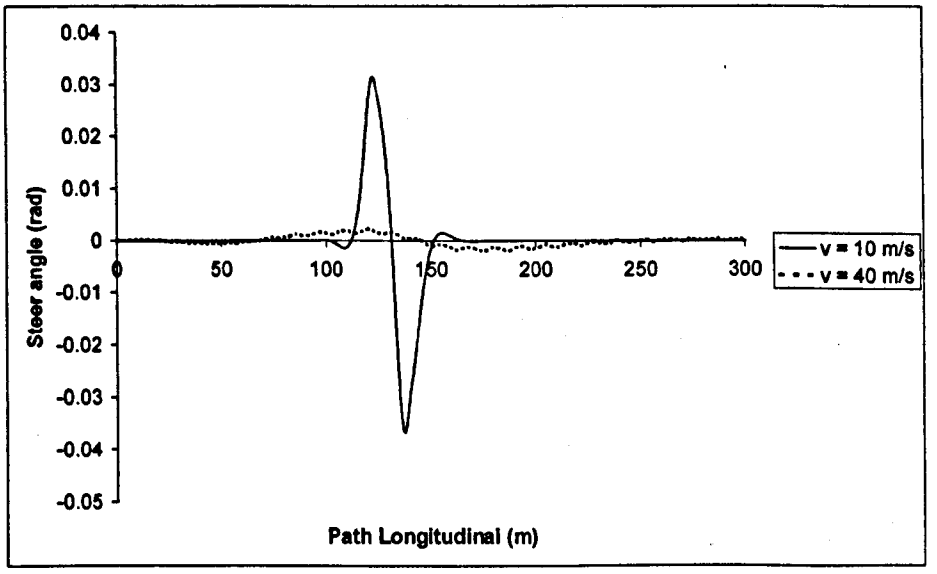

Figure 6.32: Steer angle, $v = 10$ m/s & 40 m/s, $T_p = 3.0$ s, $q_1 = 5000$ m^{-2}

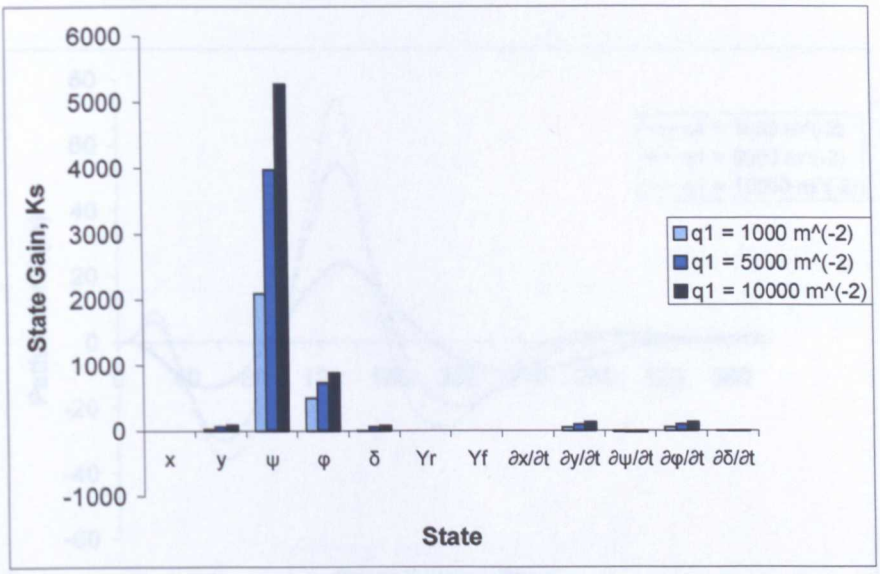

Figure 6.33: State gains, $v = 40$ m/s, $T_p = 3.0$ s, $q_1 = 1000$, 5000 & 10000 m^{-2}

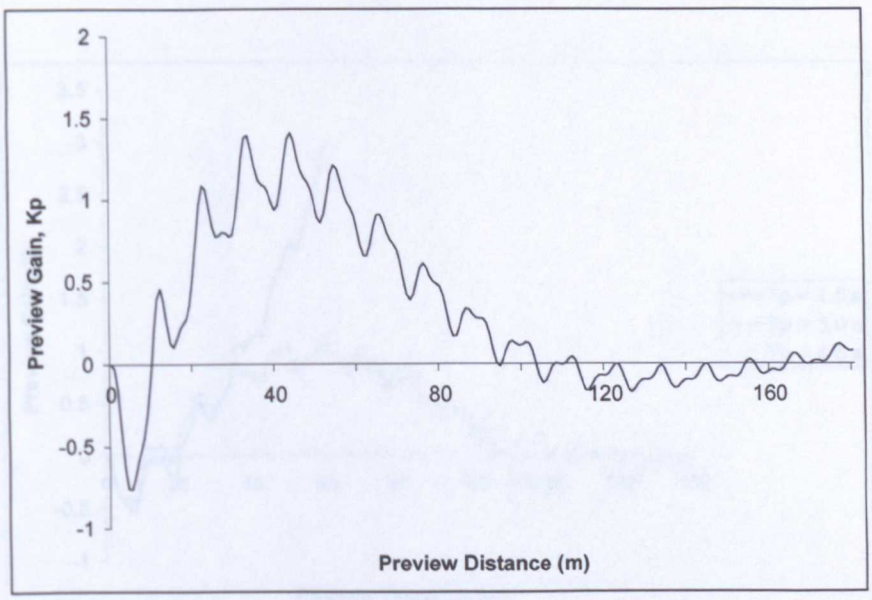

Figure 6.34: Preview gains, $v = 40$ m/s, $T_p = 4.5$ s, $q_1 = 5000$ m^{-2}

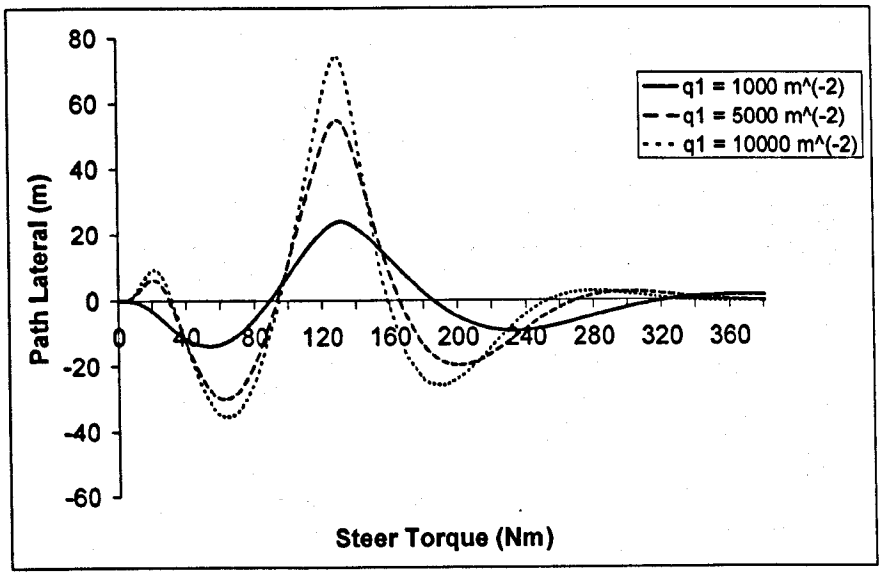

Figure 6.35: Steer torque, $v = 40$ m/s, $T_p = 3.0$ s, $q_1 = 1000$, 5000 & 10000 m^{-2}

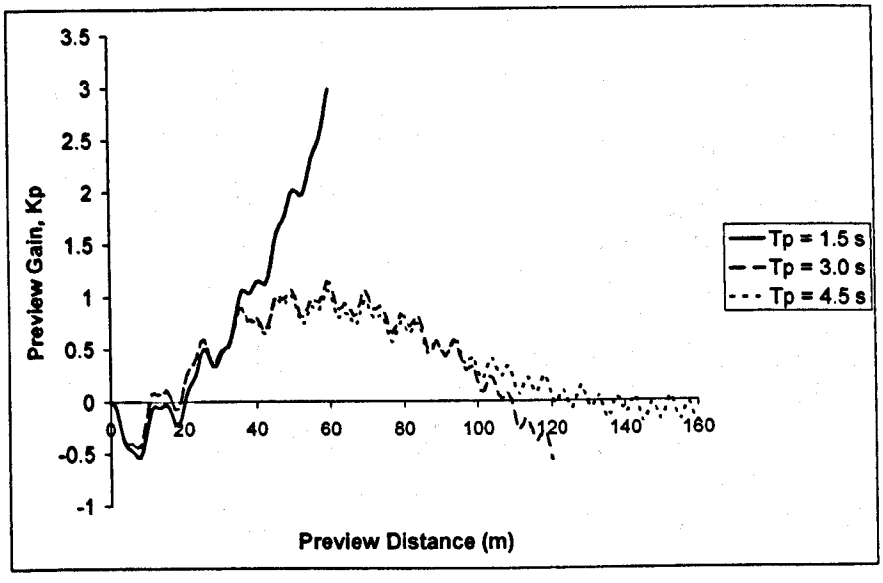

Figure 6.36: Preview gains, $v = 40$ m/s, $T_p = 1.5$ s, 3.0 s & 4.5 s, $q_1 = 5000$ m^{-2}

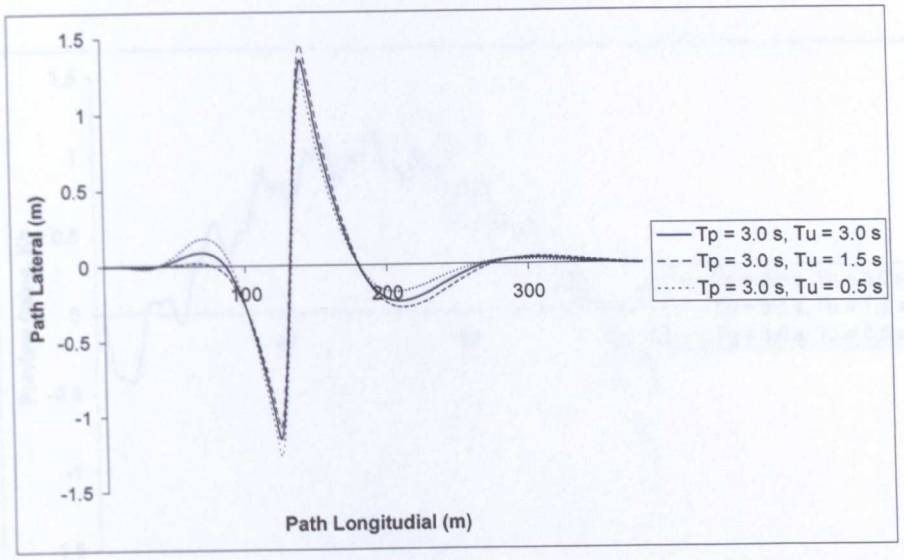

Figure 6.37: Preview gains, $v = 40$ m/s, $T_p = 3.0$ s, $T_u = 3.0$ s, 1.5 s & 0.5 s, $q_1 = 5000$ m^{-2}

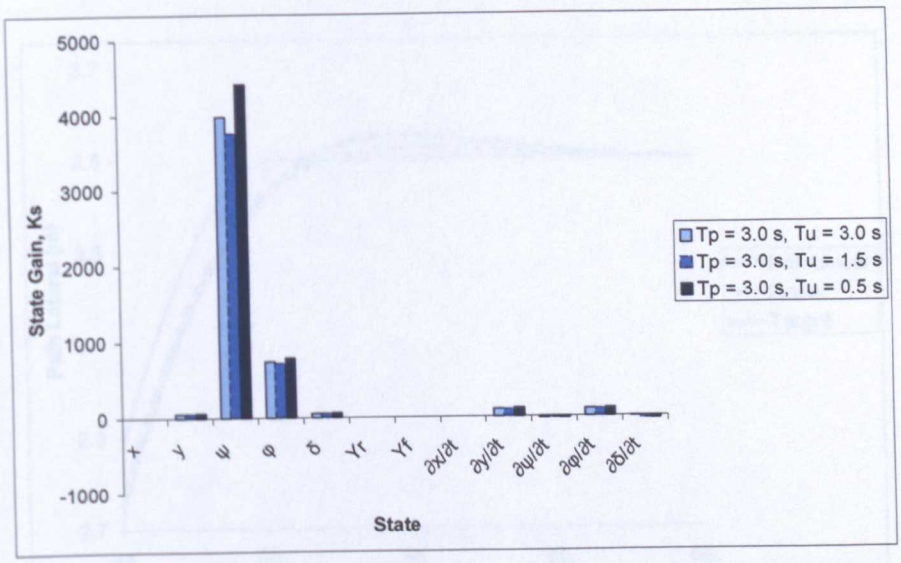

Figure 6.38: State gains, $v = 40$ m/s, $T_p = 3.0$ s, $T_u = 3.0$ s, 1.5 s & 0.5 s, $q_1 = 5000$ m^{-2}

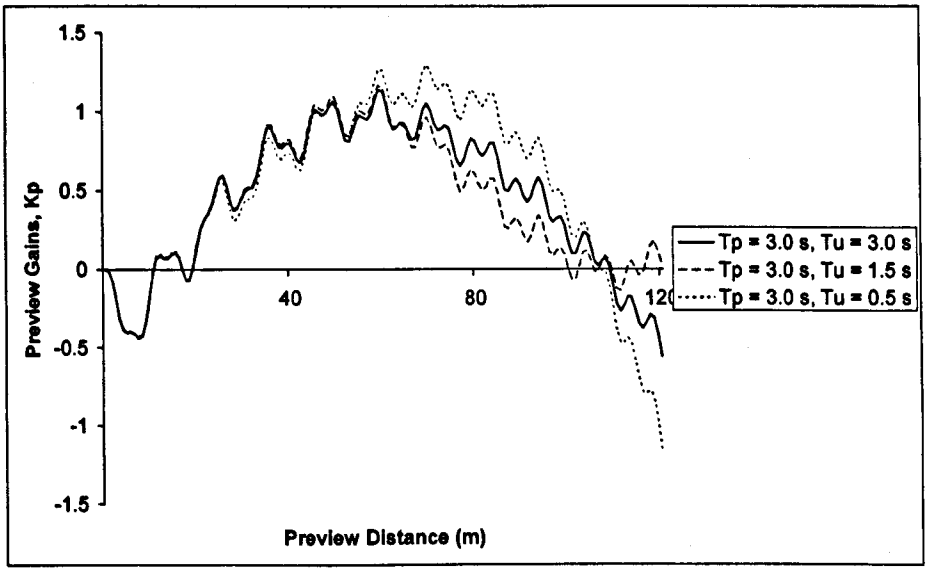

Figure 6.39: Preview gains, $v = 40$ m/s, $T_p = 3.0$ s, $T_u = 3.0$ s, 1.5 s & 0.5 s, $q_1 = 5000$ m^{-2}

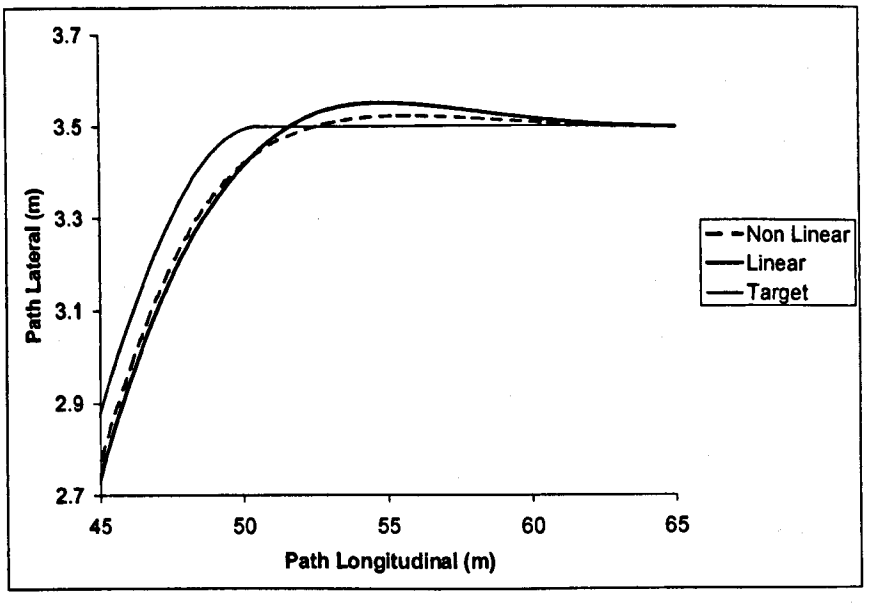

Figure 6.40: Path following, $v = 10$ m/s, $T_p = 3.0$ s, $q_1 = 5000$ m^{-2}

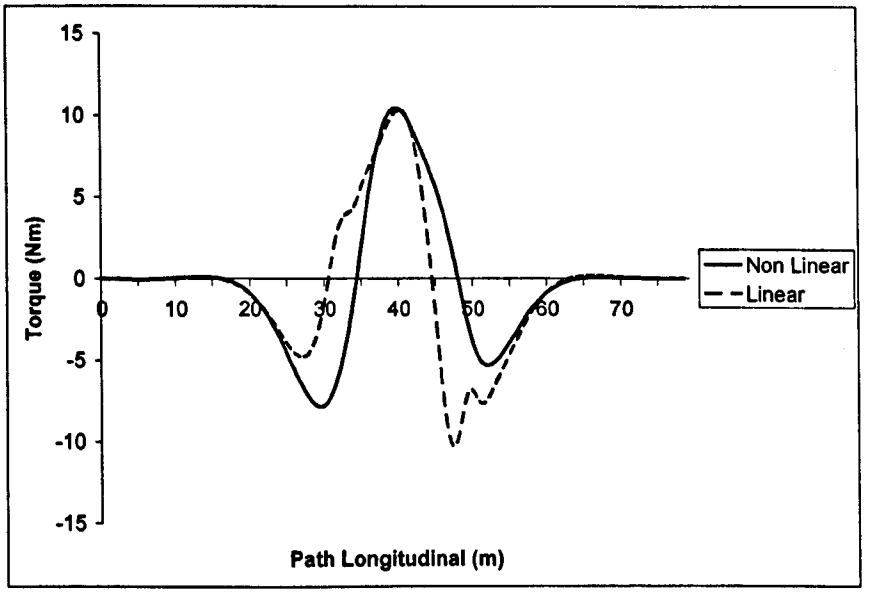

Figure 6.41: Steer torque, $v = 10$ m/s, $T_p = 3.0$ s, $q_1 = 5000$ m^{-2}

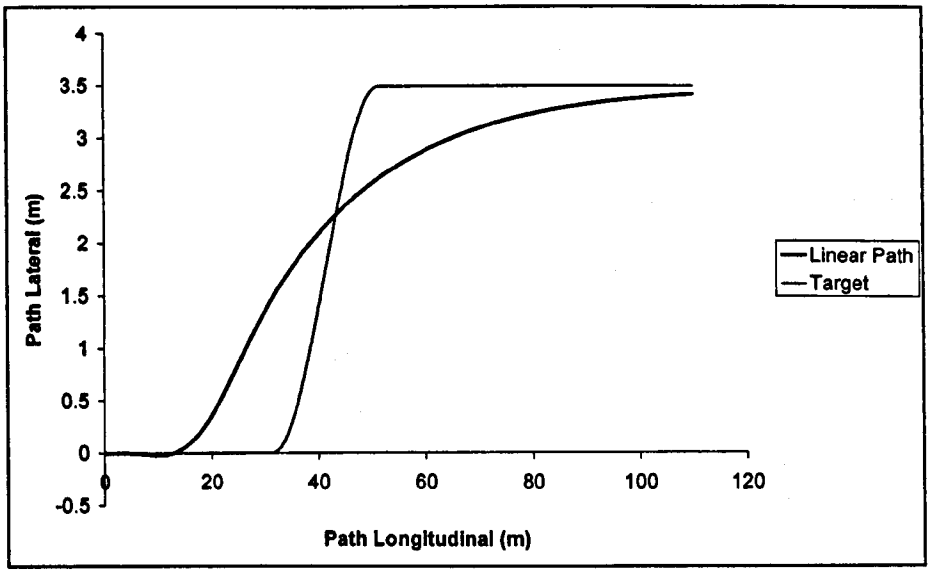

Figure 6.42: Path following, $v = 10$ m/s, $T_p = 3.0$ s, $q_1 = 5000$ m^{-2}, Linear reference path

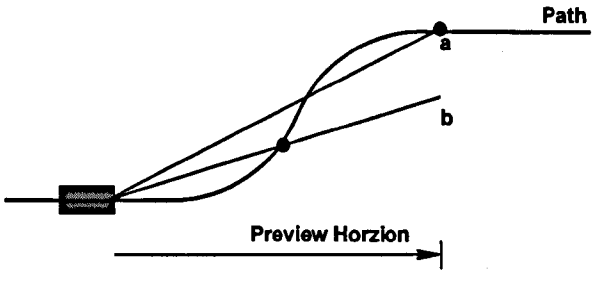

Figure 6.43: Linear reference path, showing alternative points of aim; limit of preview horizon (a), half way point of preview horizon (b)

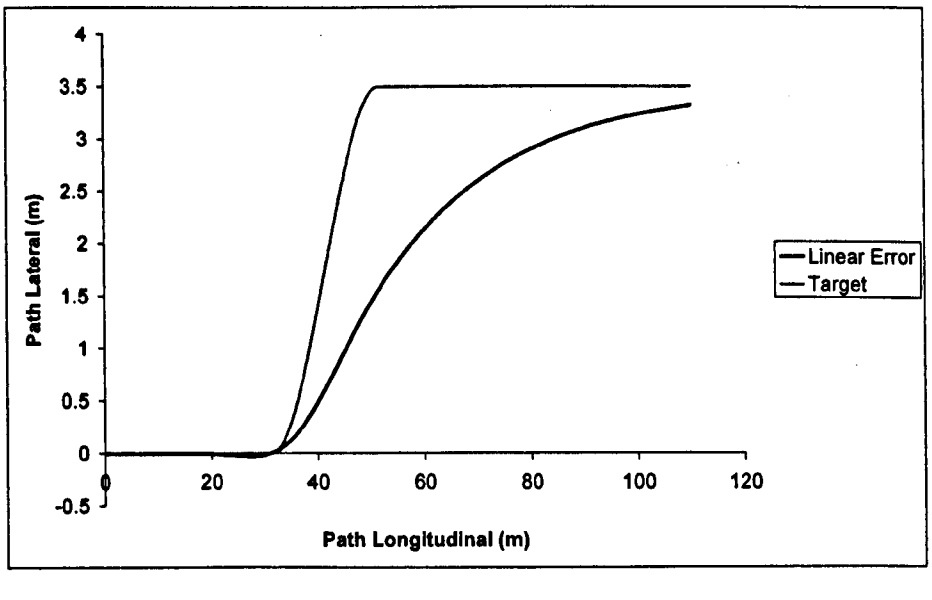

Figure 6.44: Path following, $v = 10$ m/s, $T_p = 3.0$ s, $q_1 = 5000$ m^{-2}, Linear error reduction reference path

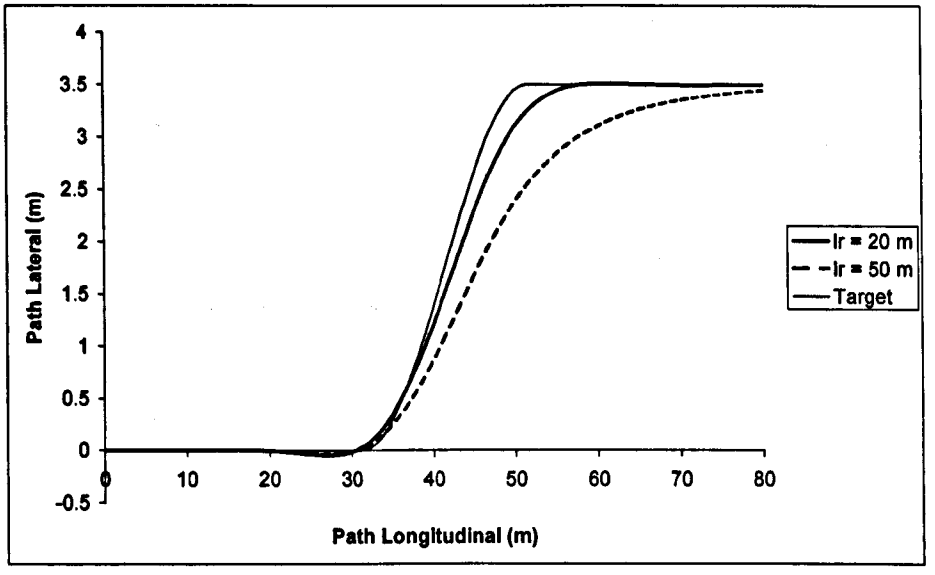

Figure 6.45: Path following, $v = 10$ m/s, $T_p = 3.0$ s, $q_1 = 5000$ m^{-2}, Exponential error reduction reference path

Chapter 7

Performance Comparisons of Control Techniques

7.1 Introduction

Two principal control strategies, optimal control and model predictive control, have been assessed for modelling the control actions of a human motorcycle rider. Both techniques have their roots in the solution of a quadratic cost function, but the formulation of the elements of the cost function, notably of the cost associated with the system output, varies.

Essentially, the mathematical difference between the two methods centres on the way in which the rider model determines the errors from the path that he is attempting to follow and the definition of the optimisation horizon. Additionally, predictive control offers further controller tuning options compared with optimal control, allowing the preview and control horizons to be set independently and with the option of a reference path that the system attempts to follow.

The results obtained in the preceding two chapters (Chapters 5 & 6) have shown that, on the whole, both techniques are capable of applying appropriate control to a motorcycle model when attempting a single lane change manoeuvre. Controller gains, indicative of the importance placed on the available system information by the controller, were seen to be similar for the two methods considered. The differences between the methods therefore lie in the details, and so this chapter will aim to

identify and explore the fundamental differences between the performances of the two approaches and the potential advantages that may be gained through the use of predictive control techniques.

The characteristics of the optimal control approach [94] were generally regarded to provide a good representation of the control actions of a motorcycle rider. For the model predictive control approach to be considered a more suitable alternative, the characteristics of the controller must therefore be similar, while also providing some useful advantage over the optimal control approach and correcting any identified weaknesses.

This chapter will therefore draw together the results of the optimal control (Chapter 5) and the predictive control (Chapter 6) approaches. Specific controller conditions, for example the short preview horizon case, will be examined and the direct comparisons of the two approaches compared. The results of these direct comparisons will enable the final conclusions of this research work, regarding the suitability of the model predictive control approach to the motorcycle rider task, to be made. These final conclusions are subsequently given in Chapter 8.

7.2 Comparison Results

Both control techniques have been applied to the motorcycle model, detailed in Chapter 3, combined with the road preview information, as shown in Chapter 4, for a range of controller parameters. For each control approach a number of elements of the controller's behaviour were analysed. A select range of these parameter sets will be directly compared, presented in Table 7.1.

7.2.1 Comparison 1 - Baseline Parameters, Low Speed

Both control techniques were applied to the motorcycle model using a baseline parameter set that permitted a moderate balance between path following accuracy and control cost. The low speed baseline parameter set is therefore used initially to compare the performances of the two techniques.

The paths of the two control approaches when using this baseline set are considered

first (Figure 7.1). The paths are very similar, with both approaches following the target path well. No obvious differences are initially apparent, and so to consider the performances in greater detail, the path errors for the two approaches are analysed, defined as the difference between the target (set) path and the actual path achieved by the motorcycle model. The results are presented in Figure 7.2 and again the results for the two approaches are not too dissimilar. Both show similar errors at similar points along the path, and in this example the optimal control model actually produces marginally lower total errors over the lane change phase. However, for the model predictive control case, the path error returns to zero after the manoeuvre, whereas for the optimal controller this is not the case, with a small steady error of -0.002 m resulting after the lane change.

The broad controller characteristics for the predictive control approach should be largely similar to those of the optimal control approach. The state gains and preview gains are compared in Figures 7.3 and 7.4, being almost identical and therefore suggesting that, if the controller gains for the optimal control approach were considered representative of a human rider's actions, then so too can the gains produced by the predictive controller.

7.2.2 Comparison 2 - Baseline Parameters, High Speed

The same comparison is drawn for the higher speed case, again using the baseline parameters, and again analysing the path differences that result for the optimal controller and the model predictive controller (Figure 7.5). At the higher speed, the relative performances of the two methods are again very similar to those seen at the lower speed. However, at the increased forward speed the steady state error of the optimal control model after the manoeuvre phase is more apparent.

The optimal controller has peak path following errors of 1.067 m and -1.509 m, and a steady state final error of -0.166 m. By contrast, the predictive controller has peaks of 1.357 m and -1.152 m, and a final error of zero.

7.2.3 Comparison 3 - High Speed, Loose Control

The previous analysis in Chapters 5 and 6 indicated that the both high speed and loose control conditions require greater levels of preview for good control. The combined case for high speed running with loose control is therefore considered. In line with the results of the previous two comparisons, the optimal controller again shows significant steady state errors (Figure 7.6). The point of note now is that the steady state path error of the optimal controller is positive, indicating that the lane change has fallen short of the 3.5 m lateral shift. For $q_1 = 5000$ (Figure 7.5), the error was negative, indicating that the motorcycle had overshot the lane change, and had settled to a steady state at a lateral path value greater than the target 3.5 m. This suggests the possibility for some value of q_1 which, although not resulting in preview gains that diminish to zero, may result in zero steady state errors and erroneously suggest a sufficiently long preview horizon that the gains to diminish to zero.

7.2.4 Comparison 4 - Limited Preview, Loose Control

The case for limited preview is a situation that should be considered important when assessing the applicability of the approach to the modelling of a human rider. It seems logical that a rider can still exercise accurate path following even given limited visual preview. If a rider were, for instance, following a large vehicle such as a lorry, due to restricted knowledge of the road some way in advance, it may be expected that his transient control behaviour would be compromised. However, for a steady, straight section of road, despite limited forward vision, the rider would still be expected to be able to adopt the correct position on the road. In essence, limited preview should not restrict the rider from eventually achieving the correct position-in-lane.

It has been seen in the earlier analysis of the control methods (Chapters 5 and 6) that a loose control strategy is in general associated with a greater emphasis on the distant road preview information. From a control perspective then, the worst case scenario would be a loose control strategy coupled with limited preview horizon.

The results would be expected to be similar to the high speed, loose control approach, since increased speed in general requires greater preview. Increasing the speed without increasing the preview horizon is therefore similar to keeping the speed the same but

reducing the preview horizon.

The two control methods are therefore analysed for the limited preview, loose control situation, with a preview horizon T_p of 1.5 s and a path error weighting q_1 of 1000 m^{-2}. The path error comparison is drawn in Figure 7.7, highlighting, in common with the previous analysis, the errors that can occur when the optimal control approach is employed with less than ideal levels of preview allowed. During the manoeuvre phase, the path errors for the predictive control approach peak at 0.25 m, decaying to zero after the manoeuvre section of the path. By contrast, the errors for the optimal control approach peak at 1.41 m, before settling to 1.17 m after the manoeuvre.

In such a situation, the knowledge that the rider has of the motorcycle does not change. A rider would still have full knowledge of the yaw angle, roll angle, steer angle and so on, and therefore it may be expected that the state gains would, qualitatively, not change significantly with a reduction in the preview horizon (Figure 7.8). However, the rider's knowledge of the approaching road, which is also used by the rider to determine his control inputs, does change significantly with a reduction in the preview horizon, and so it may be expected that the rider would need to re-evaluate the use that is made of this limited information. Figure 7.9 compares the preview gains for the limited horizon, loose control situation, and here a significant difference is seen between the two control approaches. The superior path following performance of the predictive controller has already been seen (lower path errors, Figure 7.7), and so the change in the preview gain is suggested to be representative of the change in emphasis that the rider places on the limited road path information available.

7.2.5 Comparison 5 - Yaw Error Minimisation

The vast majority of results presented in this thesis have concerned the rider model operating to minimise the lateral path error of his position relative to the target path. The capability to minimise the yaw angle of the motorcycle relative to the path also exists, and the comparison of the two control strategies operating in this manner are drawn.

In a similar way to the lateral path error minimisation analysis, the optimal control strategy results in a steady state error, this time between the heading of the target path and the heading of the motorcycle. Consequently, with forward motion the

motorcycle's lateral error progressively increases (Figure 7.10). Although yaw angle error minimisation is not considered as the primary way in which a motorcycle rider would assess his path following performance, it is nonetheless a strategy which could be adopted in conjunction with lateral error minimisation, and is therefore worthy of some consideration.

7.2.6 Comparison 6 - Short Control Horizon

One of the main features of model predictive control that distinguishes it from optimal control concerns the ability to set the control horizon shorter than the preview horizon. In the case of a limited control horizon, the model predictive control strategy assumes the control to be invariant from the control horizon up to the preview horizon, therefore providing the controller with a full control input up to the preview horizon. This strategy of control is therefore compared with the optimal control model, for which the preview and control horizons are intrinsically equal.

Figure 7.11 presents the path errors resulting from the path following task using the low speed baseline parameters, with the control horizon reduced to both 1.5 s and 0.5 s for the predictive controller. Even with limited control horizon, the predictive controller is still capable of generating appropriate controller gains, and hence the performance comparison between the limited control horizon predictive controller and the optimal controller is very close to the comparison with equal preview and control horizons (Comparison 1). The predictive controller with limited control horizon is still capable of completing the manoeuvre and returning to a zero steady state lateral path error condition despite the restricted control horizon. Although in some respects the reduced control horizon appears to deteriorate the controller's performance, the differences are not severe.

7.2.7 Comparison 7 - Very Low Speed

Above a forward speed of 10 m/s, the stability characteristics of the motorcycle are relatively invariant (Chapter 3, Figures 3.10, 3.15), but below this speed is notably different: the weave mode is an unstable low frequency oscillatory mode at low speeds, while the capsize mode is more stable at low speeds. As a consequence, the control required to stabilise and guide the motorcycle may change, and so the performance

of the two control approaches under such conditions is compared.

Miyamaru et al. [65] suggested that at moderate speeds and above, the rider's directional control is achieved by control of the roll angle of the motorcycle, while at low speed the primary control technique to influence the motorcycle's trajectory is through control of the steer angle of the motorcycle. Both the optimal and predictive control strategies were therefore tasked with the same path following task, but this time at a forward speed of only 4 m/s, with both strategies reflecting the change in the control technique suggested by Miyamaru et al. The state gains distribution is seen to change such that now the peak controller state gains are for the steer angle state (Figure 7.12).

Also of some significance in this figure is the state gains relating to the tyre lateral forces. For the optimal controller, these are minimal, while for the predictive controller they are not, with the front tyre gain being the more significant of the two by some margin.

These observations are worthy of some thought, and are believed to be due to the change in stabilities of the capsize and weave modes at low speeds. At low speed, as the motorcycle begins to capsize, the geometry of the steering system is such that a significant steer angle is generated, correcting the lean of the motorcycle [29]; it is this characteristic which gives the low speed capsize stability. However, this may then result in a lean to the opposite side, where the same effect results, consequently resulting in a low speed, low frequency weave behaviour. A number of movie clips are available in [26] and [78] that more clearly demonstrate this combined low speed capsize and weave. At low speeds, significant steer angles will therefore be expected, and consequently relatively large tyre forces. Furthermore, the weakness of the gyroscopic forces at low speeds also increases the relative contribution that the tyre lateral forces must provide in order to stabilise the capsize mode of the motorcycle.

For a low speed weave, the change in lateral position may be small, but the change in heading angle is relatively much larger, and will therefore have a significant impact on the predicted future path.

The optimal control strategy, for lateral path error control, bases the control decision on the motorcycle's current position relative to the target path alone. This, it is suggested, will not change significantly.

Predictive control bases the control decision on the predicted future path. Although the lateral deviation may be small, the heading angle change will not be, leading to a significant change in the motorcycle's trajectory and hence predicted future path.

The tyre forces influence the stability and the heading of the motorcycle. As the predictive controller would be expected to place more emphasis on reducing the change in heading angle (and consequently future predicted path) during a low speed weave, and the primary means of doing this is through the tyre lateral forces, then an increase in controller gains relating to the tyre forces may not be unsurprising. As the changes in the tyre lateral forces are dictated by the steer angle, itself dictated by the steer rate, it is also perhaps unsurprising to see that the gains on the steer rate for the predictive controller is larger in magnitude at these low speeds compared with the optimal controller.

7.3 Performance Comparison Conclusions

This chapter has brought together a detailed comparison of the two control strategies of optimal and predictive control. The results have largely confirmed the strong similarities of the two approaches for the majority of conditions, but importantly has drawn out the significant differences.

The inability of the optimal control approach to result in truly zero steady state errors following a manoeuvre was highlighted in Chapter 5, Section 5.3.1. Indeed, the steady state errors will only truly reach zero when the preview horizon distance is infinite. Cole et al. [11], with specific reference to a car steering task, investigated and presented the fundamental reasons behind these observations, and the potential benefits that predictive control could give for such a preview-limited case. Fundamentally, the optimal control theory employed here is based on the theory of an infinite horizon, whereas the predictive controller calculates gains based on a horizon only up to the preview horizon of the controller. Thus, provided that the optimal controller's gains have reached zero, then the numerical loss of information that results from this infinite horizon assumption is insignificant to the numerical result, and the two controllers essentially give the same results. When the preview horizon is shortened significantly, the predictive controller calculates a new set of gains based on this new limited horizon, while the optimal approach employs still an infinite horizon assump-

tion, with correspondingly inferior results in such a case. The results presented in this chapter have deliberately aimed to highlight this feature in a significant way, and the result that a predictive controller will, by contrast and regardless of the horizon length, result in a zero steady state error. Analysis in Chapter 5 showed how this path following error with limited horizon could be overcome with the use of a local coordinates approach. Similar observations were made by Cole et al. [11], though the two approaches differed subtly.

These results have been emphasised by the use of higher speed, tighter control weightings and limited preview horizons. With less than a finite preview horizon, the optimal control approach is not, in fact, able to seemingly apply an optimum control, as some steady state error will always result. However, it was shown in Chapter 5 that while a local coordinates approach does not, in theory, make a difference to the problem, in practice the steady state path errors are seen to be reduced to zero.

For the optimal control approach, variation of the speed and the cost function error weightings dictate the accuracy of the path following that results. Although the steady state values will never truly reach zero, sufficient preview length can result in steady state errors which are minimal, and so the speed, error weightings and preview horizon length are intrinsically linked in determining the magnitude of the final steady state errors.

The predictive controller's path following performance is also affected by the speed, error weightings and horizon lengths in a similar way to the optimal control method. However, the steady state error has no dependency on these, and thus the error will, given sufficient distance to reach the steady value, always be zero.

Important differences are also seen for the very low speed running condition of the two controllers. At low speed, the distribution of the state gains show some significant differences between the two approaches. For the low speed case, a human rider will sense the capsize of the motorcycle and apply a steering action to correct it. During a capsize, the heading angle of the motorcycle is also changed significantly, leading to a deviation from the target path. With low forward speed the lateral deviation that results from the heading angle change is small, and therefore does not significantly affect the optimal controller, which will aim mainly to stabilise the roll of the motorcycle. However, the predictive controller anticipates that, although the

current lateral deviation may be small, the resulting heading angle change has more significant consequences for the predicted future path, resulting in notably different state gains for the predictive controller.

7.4 Table

	Comparison 1		Comparison 2		Comparison 3		Comparison 4		Comparison 5		Comparison 6		Comparison 7	
Parameter	OC	MPC	OC	MPC	OC	MPC	OC	MPC	OC	MPC	OC	MPC	OC	MPC
v [ms^{-1}]	10	10	40	40	40	40	10	10	10	10	10	10	4	4
T_p [s]	3	3	3	3	3	3	1.5	1.5	3	3	3	3	3	3
T_u [s]	3	-	3	-	3	-	1.5	-	3	-	1.5,0.5	-	3	-
T_w [s]	0	-	0	-	0	-	0	-	0	-	0	-	0	-
q_1 [m^{-2}]	5000	5000	5000	5000	1000	1000	1000	1000	0	0	5000	5000	5000	5000
q_2 [rad^{-2}]	0	0	0	0	0	0	0	0	5000	5000	0	0	0	0
r [(Nm)$^{-2}$]	1	1	1	1	1	1	1	1	1	1	1	1	1	1

Table 7.1: Controller comparison parameter sets

7.5 Figures

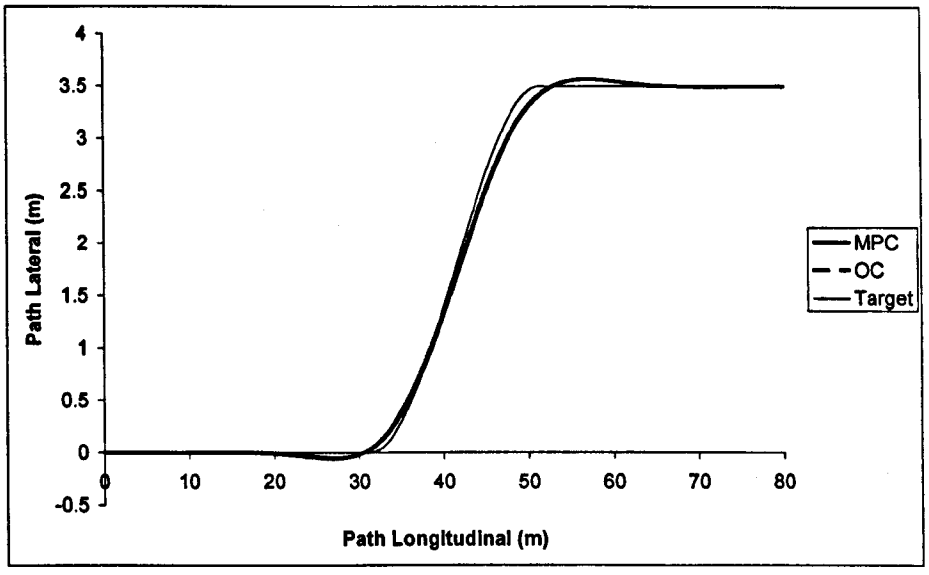

Figure 7.1: Path following, $v = 10$ m/s, $T_p = 3.0$ s, $q_1 = 5000$ m^{-2}

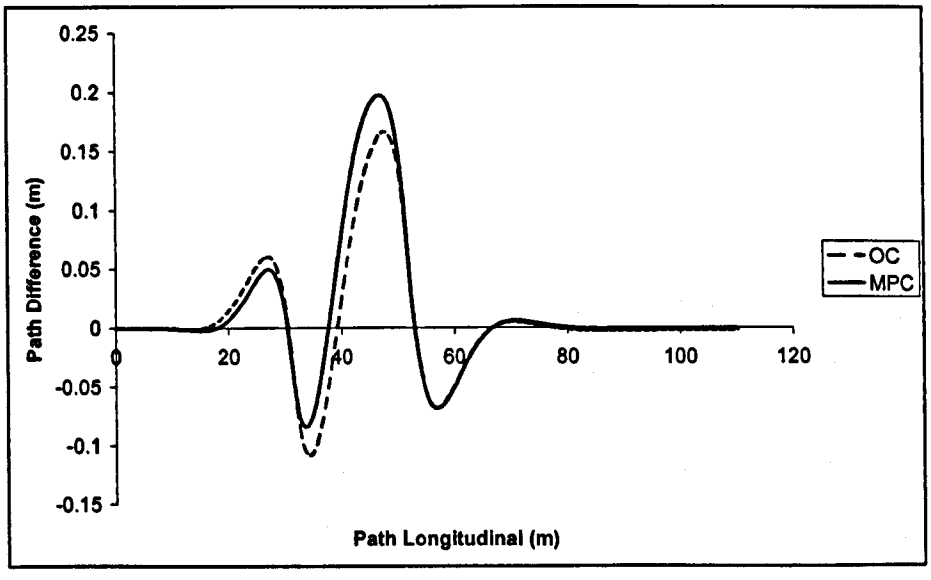

Figure 7.2: Path errors, $v = 10$ m/s, $T_p = 3.0$ s, $q_1 = 5000$ m^{-2}

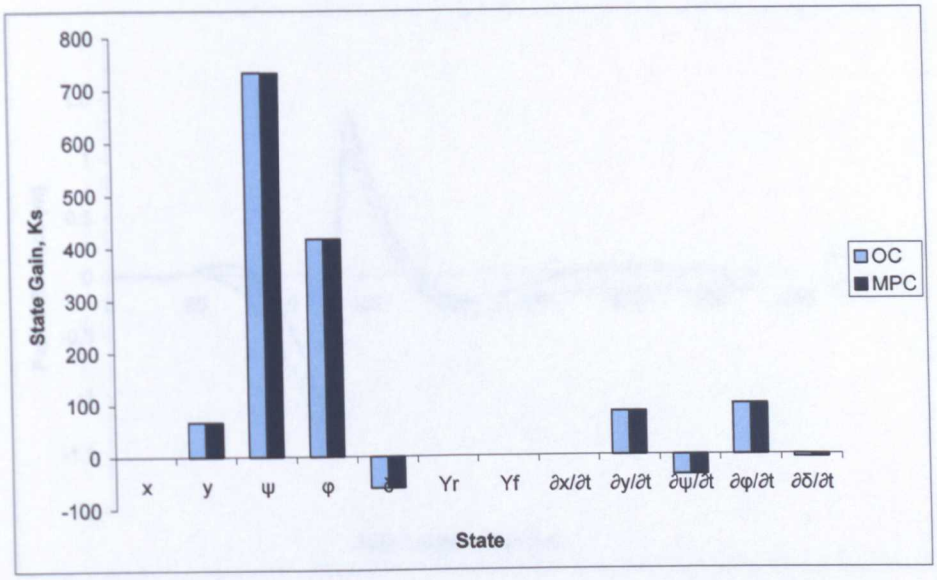

Figure 7.3: State gains, $v = 10$ m/s, $T_p = 3.0$ s, $q_1 = 5000$ m^{-2}

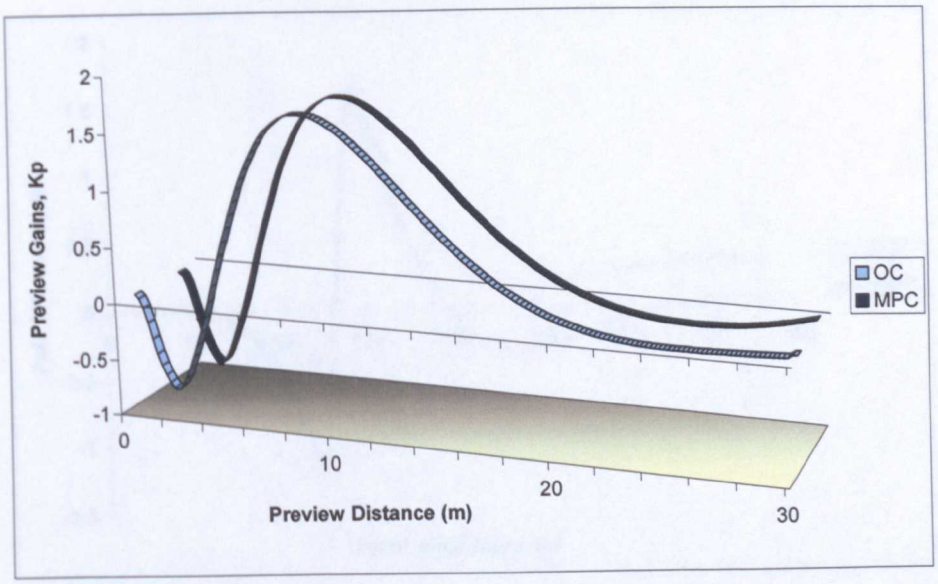

Figure 7.4: Preview gains, $v = 10$ m/s, $T_p = 3.0$ s, $q_1 = 5000$ m^{-2}

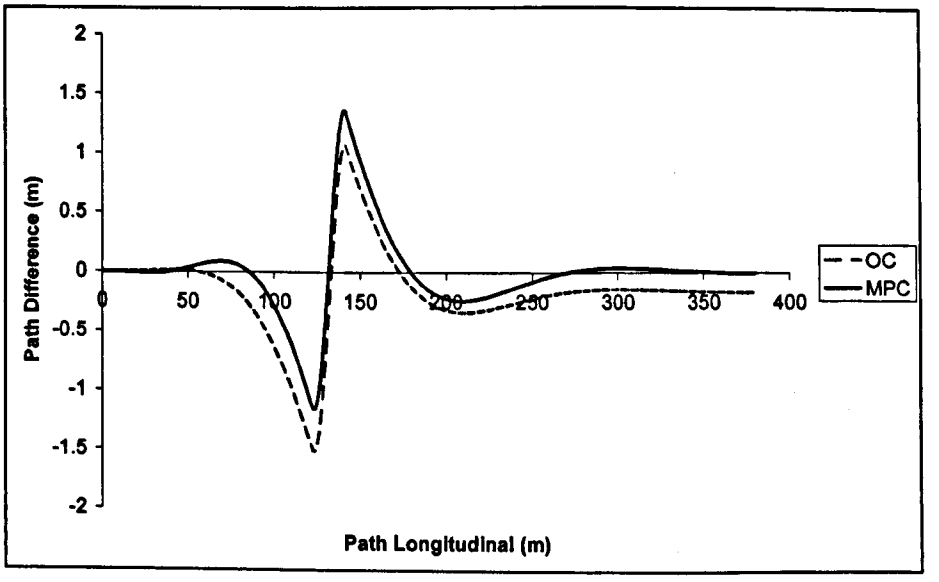

Figure 7.5: Path errors, $v = 40$ m/s, $T_p = 3.0$ s, $q_1 = 5000$ m^{-2}

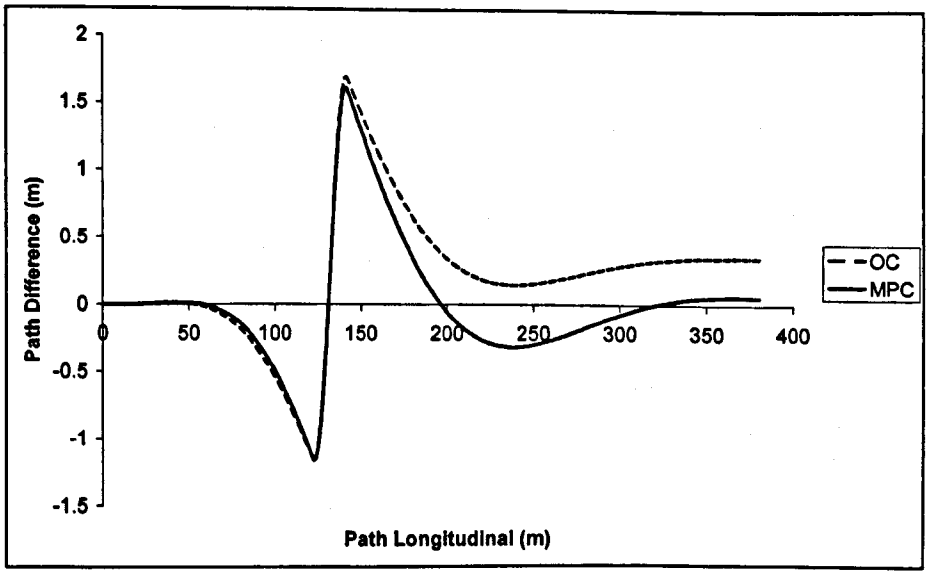

Figure 7.6: Path errors, $v = 40$ m/s, $T_p = 3.0$ s, $q_1 = 1000$ m^{-2}

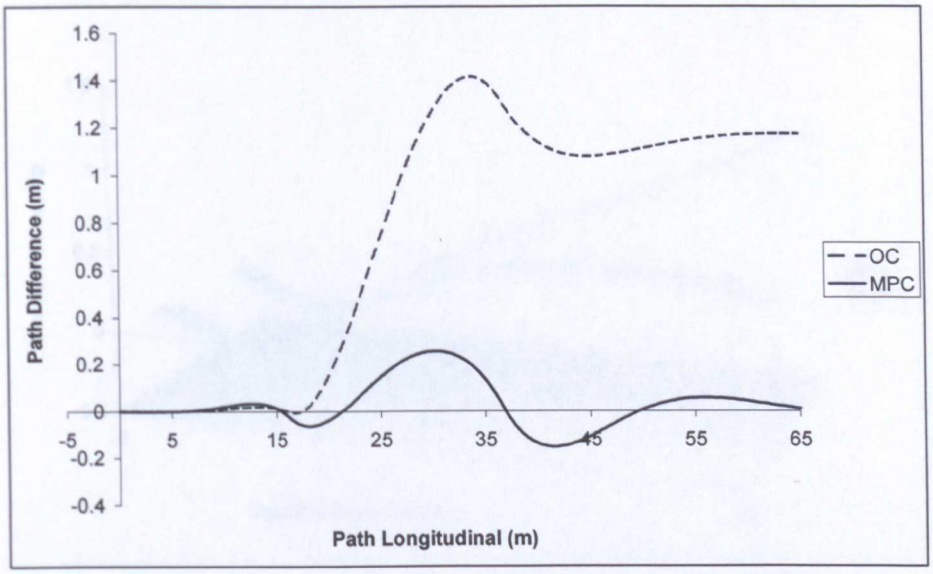

Figure 7.7: Path errors, $v = 10$ m/s, $T_p = 1.5$ s, $q_1 = 1000$ m^{-2}

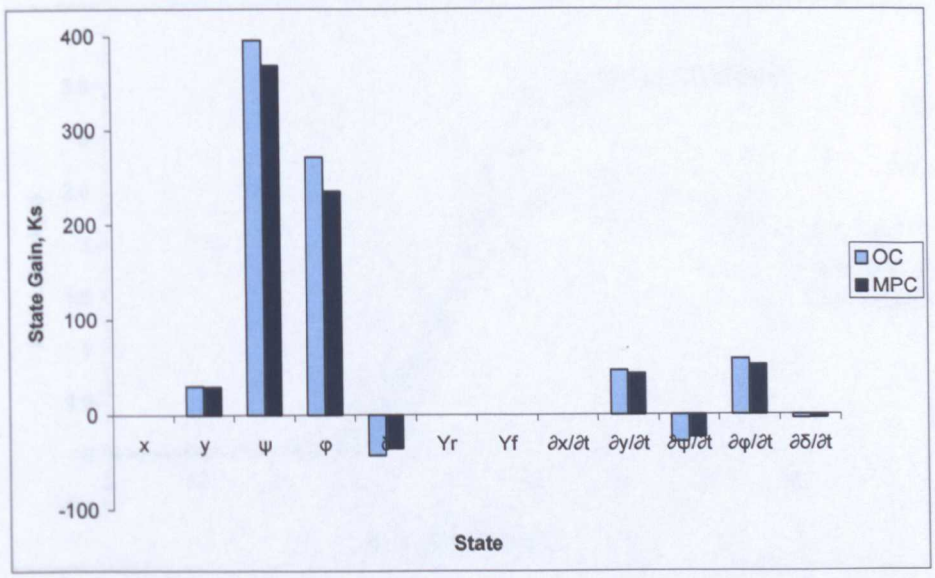

Figure 7.8: State gains, $v = 10$ m/s, $T_p = 1.5$ s, $q_1 = 1000$ m^{-2}

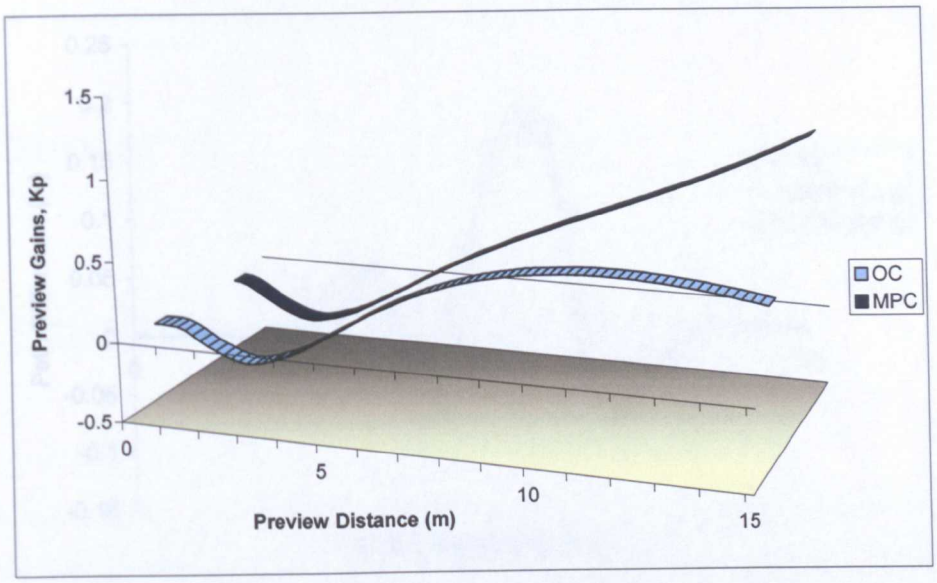

Figure 7.9: Preview gains, $v = 10$ m/s, $T_p = 1.5$ s, $q_1 = 1000$ m^{-2}

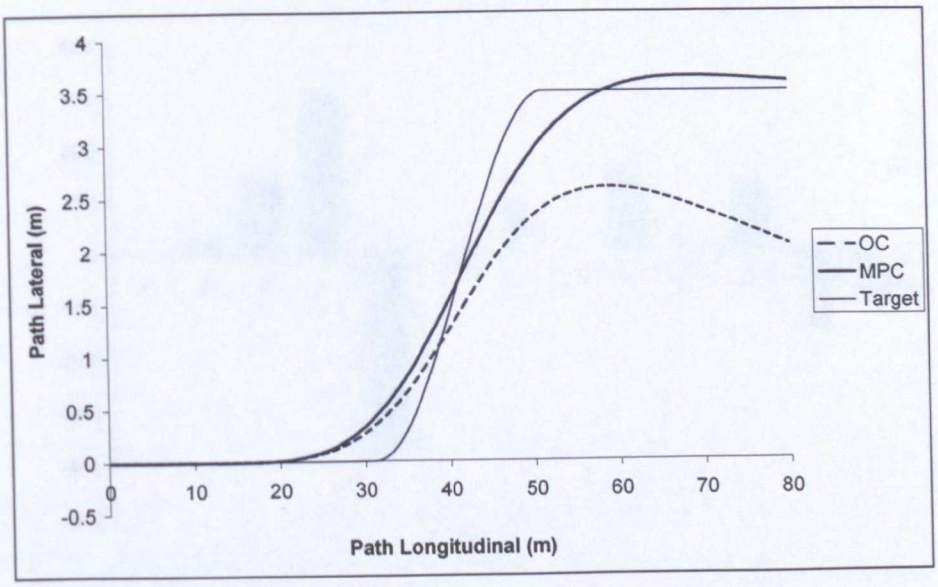

Figure 7.10: Path following, $v = 10$ m/s, $T_p = 3.0$ s, $q_2 = 5000$ rad^{-2}

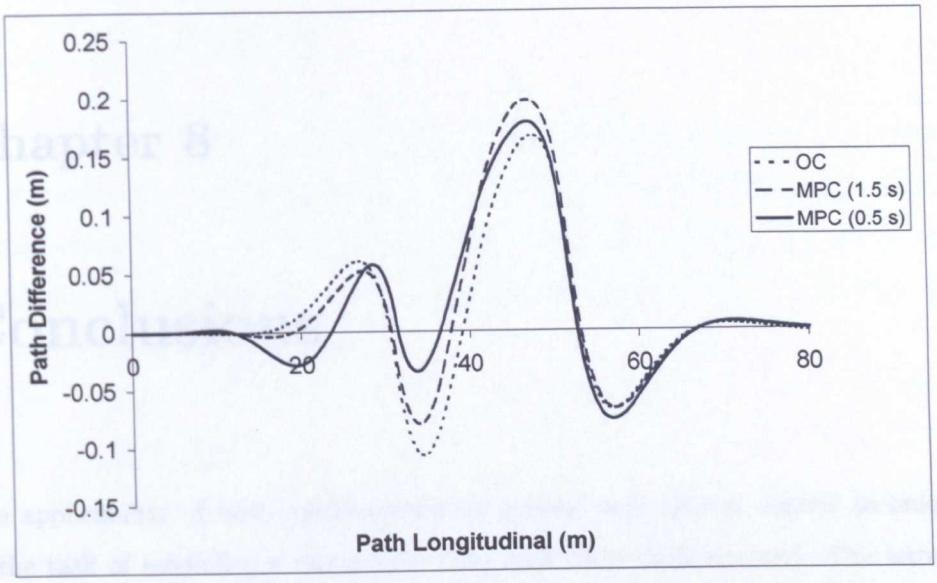

Figure 7.11: Path errors, $v = 10$ m/s, $T_p = 3.0$ s, T_u =1.5 s & 0.5 s, $q_1 = 5000$ m^{-2}

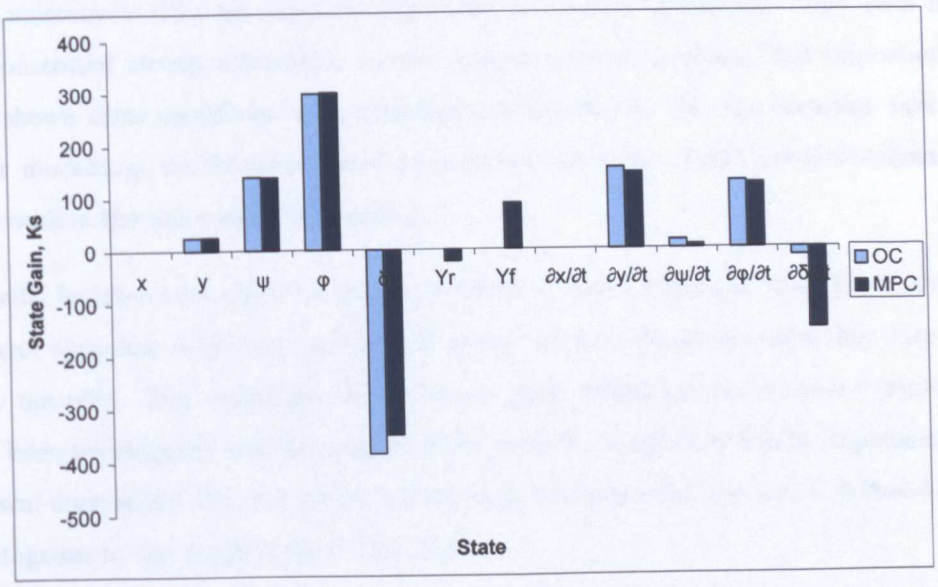

Figure 7.12: State gains, $v = 4$ m/s, $T_p = 3.0$ s, $q_1 = 1000$ m^{-2}

Chapter 8

Conclusions

The applicability of both model predictive control and optimal control techniques to the task of modelling a motorcycle rider have been demonstrated. The latter is not a new concept, having originally been presented by Sharp [94]. However, further parameter studies have been conducted to obtain more insight into the characteristics of the controller to assess some of the strengths and weaknesses of the approach.

Building on previous related work by MacAdam [51], Sharp [94], and Cole et al. [11] amongst others, the application of model predictive control to the modelling of a motorcycle rider presented in this thesis is a novel application. The work has demonstrated strong similarities to the optimal control approach, but importantly has shown some significant and advantageous differences. For the broadest task of rider modelling, the findings therefore suggested that the model predictive control approach is the more suitable approach.

Specific features that differentiate the predictive control approach from the optimal control approach have been assessed to determine the advantages that they may or may not offer. The availability of a reference path definition to the control problem has been investigated and the mathematical manner in which it can be implemented shown, concluding that the opportunities that this may offer are not considered advantageous to the application at this time.

Additionally, the implementation of a non-linear prediction model as opposed to the more common linearised prediction has been made. As may be expected the extra computational burden was shown to result in performance advantages as may be

expected for a non-linear plant model.

8.1 Model Analysis

The effectiveness of the model control strategy in replicating the control actions of a motorcycle rider can be assessed by consideration of a number of factors relevant to the controller, notably the controller gains, the performance of the controller in completing the task and the way in which the controller's behaviour changes with changes to the modelled riding task.

8.1.1 State Gains

The analysis of controllers of this nature usually focus primarily on the controller's gains, since these essentially determine the way in which control is applied to the system. The gains achieved here for both the optimal controller and the model predictive controller show good agreement to both experimental and anecdotal evidence of the motorcycle riding task achieved by previous authors.

A number of research works, some of which are covered in the literature review (Chapter 2), have sought to understand the important criteria that a vehicle driver or rider attempts to control. For motorcycle riding, Weir [102] identified the control link between roll angle and steer torque as the primary stabilising control loop, with a slightly weaker reliance on the heading angle and lateral position of the motorcycle. Miyamaru et al. [65] also concluded that for anything other than very low speed riding the control task was concerned with roll angle stabilisation, and that this would then dictate the trajectory, rather than the steer angle. This forms a distinct difference between single and twin vehicle track controllers.

A correct rider control model should therefore reflect this trend, placing the greater importance on controlling the roll angle of the motorcycle (which ultimately dictates the trajectory), followed by heading angle and lateral position. The results of both the optimal control and the model predictive control approaches have been shown to display these trends.

Although the state gains associated with the roll angle were not numerically the

largest, when the contribution of the roll angle gain to the total steer torque was assessed, it was shown that the roll angle provided the largest contribution, therefore appearing to have the most significant influence upon the rider's control as required. The yaw angle contribution formed the second largest contribution, again agreeing with Weir [102]. The contribution from the lateral position was low. The contribution made by the steer angle of the motorcycle was found to be significantly smaller, which is seen to be in agreement with the findings of Miyamaru et al. [65]. However, when both controller models were run at low speeds, the steer angle gains were seen to be notably greater, again in agreement with [65].

For the broad case of generous preview horizons and moderate path following task, both the optimal controller and the model predictive controller produced near identical state gains. In this sense, both control approaches appear equally capable of reflecting the control actions of the rider with reference to the motorcycle's states. Only when the preview horizon is notably restricted do any differences emerge, with the state gains of the predictive controller reduced compared with the optimal controller. We consider now why this may be and how it may reflect a motorcycle rider's control process.

Manoeuvrability and stability are generally regarded as conflicting goals. When operating in a limited preview condition, the rider will have only limited time to react to the road information presented to him that he is aiming to follow, and therefore it seems reasonable that in such a situation the rider may favour a manoeuvrable motorcycle. The motorcycle states are generally regarded as the meters by which the rider stabilises the motorcycle [102], while the preview is used for guidance control. A reduction in the gains applied to these states may suggest that the rider is operating in a manner in which the stabilisation of the motorcycle is of less concern, as may be the case for restricted preview when manoeuvrability is the more pressing requirement. In this sense, the predictive controller appears to be able to represent this shift in the rider's priorities, while the optimal controller does not.

8.1.2 Preview Gains

A number of publications have sought to determine the control actions of a road user with regard to the visual perception of the road available, with results obtained both

experimentally and theoretically [25, 47]. Both control strategies considered here were modelled for a wide range of controller parameters, with the results obtained here again giving good agreement with the previous literature. The model predictive control approach gives good agreement with the optimal control approach with regard to the preview gains when sufficient preview is permitted. With restricted preview, the gains pattern changes notably for the model predictive controller, leading subsequently to better controller performance.

In assessing a driver's use of preview information, Donges [25] observed the parallel features of guidance control based on the distant preview and position-in-lane control via the near preview, observations later agreed with by Land and Horwood [47]. These characteristics are reflected in the preview gains produced by both the optimal control and model predictive control strategies. The controllers were run for both tight and loose control strategies, the former defining accurate path following and hence accurate position-in-lane control, the latter defining efficient following of a more distant target, hence guidance control. The tight control resulted in a bias of the preview gains to the near preview distance, therefore operating with the required bias towards position-in-lane control, while loose control placed greater emphasis towards the more distant preview, hence biasing towards a guidance control strategy. MacAdam [51] also observed that a vehicle driver would have a natural tendency to utilise shorter preview times under manoeuvre-demanding conditions. Tight control can arguably be classed as a demanding manoeuvre when compared with a looser strategy. The agreement between the experimentally observed patterns concerning the use of road preview information covered by previous literature, and the results obtained when using both the optimal control and model predictive controllers, highlights the suitability of both approaches for this task.

In the main, both control approaches show similar preview gains. Crucially, as the preview horizon is reduced the gains for the predictive controller are modified, whereas for the optimal controller they are not. When the preview information available is reduced, it seems intuitive that the limited information remaining is more highly regarded; a driver or rider would realistically be expected to concentrate harder on the road far ahead when driving in thick fog compared with clear air, due largely to the restricted reaction time available. Thus it is expected that the preview gain values relating to the limited road information available would increase in recognition of the

higher attention placed on this limited road preview information. This characteristic is observed with the predictive controller, but not the optimal controller.

8.1.3 Reference Path

One of the features that differentiates the predictive controller from the optimal controller concerns the capability to identify a reference path, distinct from the set path. Previous authors have suggested the separate definition of a distinct reference path, including Guo and Guan [33], as potentially offering modelling advantages. The definition of a reference path distinct from the set path has therefore been investigated, specifically with the definitions of linear, linear error reduction and exponential error reduction reference paths for the model predictive control approach.

Universally, the results demonstrated that defining the target road path in this way was detrimental to the overall performance of the rider control model. While the fundamental behaviour of the controller was unaffected, the performance certainly was. The control model forms a measured balance between corner cutting, relative to the set path, and the control input effort required. By defining a reference path, a weaker trajectory, already accounting for a corner-cutting allowance, is presented to the controller. The controller then makes the same balance between path accuracy, this time against the weaker reference path, and the control inputs. This results in an actual trajectory which attempts to follow, to a tighter or looser extent depending on the controller settings, an already weaker target path.

Therefore, unless a more elaborate reference path definition can clearly be demonstrated to produce superior controller performance compared with common reference and set paths, then the recommendation is made that the concept of a separately defined reference path is not applied for the modelling of riding or driving tasks, instead leaving the controller strategy to make its own judgement with regard to the level of path simplification that it is prepared to tolerate. Ideally, future research work will investigate the manner in which a rider aims to regain a target path, such that the concept of the reference path can be employed more usefully.

8.2 Coordinate System

The modelling work conducted in this thesis has mostly been done using a global coordinate system. This approach employs a simple shift-register algorithm for the road preview [98], which is simple to employ, easy to understand and computationally relatively simple.

A local coordinates approach has also been presented here. Arguably, the rider operates in a local coordinates manner, and so if the task is to model the rider's control then it seems appropriate to consider the problem from the rider's perspective.

For the optimal control approach, the use of a local coordinate system showed clear advantages, especially when limited visual preview horizons were available. If an optimal control approach is to be used, the recommendation is therefore to employ a local coordinates approach.

Chapter 5 showed how the limitations of the infinite horizon optimal controller when using a short preview horizon were overcome if the problem were modelled using a local coordinates approach. The method shown here converted the shift-register algorithm to update the preview information of the road path in local coordinates, which corrected the errors seen when using a global coordinate system. Cole et al. [11] performed the similar process, but in their case modifying the controller's gains multiplied by the global road picture to achieve the same results.

For the model predictive control case, limited preview horizons did not result in any steady state errors of the kind seen for optimal control, and so the question of local or global coordinates is not as important. For simplicity, the global coordinates approach is preferable, though the use of local coordinates more intuitively captures the process from the rider's perspective. The selection of coordinate system may therefore be based on the relative importance of these merits as appropriate to the application.

8.3 Non-Linear Prediction

The majority of the results presented in this thesis have been obtained using a linear prediction model. The dynamics model of the motorcycle vary non-linearly with each

step of the motion simulation, but over the prediction horizon at each simulation step were assumed invariant. Use of this approach simplifies the procedure markedly and reduces computational requirements. The theory for a non-linear prediction model was covered (Chapter 6, Section 6.2.2).

The results showed that, when using a full non-linear prediction, the resulting control led to superior performance, suggesting that, ideally, this non-linear approach should be adopted for the best controller performance. However, the performance when using the linear prediction model also showed that the controller was still capable of applying a suitable control input to achieve the required lane change task.

The question of the importance of the linear or non-linear prediction model therefore depends upon the degree to which the model dynamic behaviour changes over the length of the prediction horizon. For relatively gentle manoeuvres of the motorcycle, the changes to the dynamics are not severe, and consequently the differences resulting from the use of a linear prediction model compared with a non-linear prediction are also not severe.

The suitability of the linear prediction model will therefore depend on the anticipated change in system behaviour of the prediction horizon, the accuracy of results required, and the computational processing capacity available.

8.4 Simulation Results

The performance of the controller, with regard to the controller's gains, suggests that both optimal control and model predictive control operate in a manner consistent with what may be expected of a real rider. The actual performance of the motorcycle that results from the riders control actions further confirms this.

The path following ability of both control models appear to accomplish the task, displaying the qualities of a human rider such as a countersteer manoeuvre in anticipation of the turn. Donges [25] identified the anticipatory element of a car driver's control strategy. The path tracking can be replicated by monitoring the lateral position of the motorcycle with regard to the intended path or by the yaw angle of the motorcycle relative to the path. The original optimal control work by Sharp [94] considered only lateral path error weightings, as the yaw angle error was considered

secondary to the control problem.

When the preview horizon is sufficient such that the preview gains settle towards zero, the performance of both approaches produce similar results. However, for limited preview horizons the model predictive control approach was shown to demonstrate clear advantages.

In the case of the optimal controller, mathematical analysis of a reduction of the preview horizon to any value below infinite was suggested to result in a steady state error between the target path and the actual path achieved; the magnitude of this error however only became significant as the preview horizon was significantly reduced, below the point at which the preview gains become close to zero.

For the case of the 10 m/s baseline modelling parameters considered in the analysis, following the manoeuvre the optimal control model tracked the path with a small steady lateral position error of 0.002 m. At the higher speed of 40 m/s, the lateral steady path tracking error increased to 0.165 m. As the preview distances were halved, these errors increased further, to 0.383 m and 1.813 m respectively.

By contrast, the preview horizon of the model predictive controller could safely be reduced without the introduction of steady state errors. Although the transient behaviour was deteriorated as a result of the limited preview, the steady state path of the motorcycle would still eventually return to the target path. For all modelling conditions considered for the model predictive controller, all lateral position errors would return to a steady zero. The behaviour of the model predictive controller would appear much more suitable and representative of a motorcycle rider in such a situation.

This feature of steady state errors is also notable when the controller is set to operate by minimisation of yaw angle errors. This aspect of control was considered in [94], but results were not presented as it was not considered representative of a motorcycle rider's actions. This case is, however, considered here for completeness. In the same way that steady state errors were observed for lateral position control of the optimal control approach, the same result is found for yaw angle control, except that in this case a steady state error is between the final yaw angle of the motorcycle and the path. Consequently the motorcycle follows a straight path but heading on a different angle to the intended path. For the 10 m/s baseline parameters, this resulted in a heading

error of 0.028 rad, and for the higher speed case a heading error of 0.074 rad. As with the lateral position control case, the model predictive controller results in zero steady state errors, and thus the actual and intended paths are parallel. Although the path does not exactly follow the intended path, the performance of the model predictive controller in this situation is clearly superior to that of the optimal controller.

8.5 Final Conclusions and Further Work

Thus far, the conclusions have been made that both optimal control and model predictive control appear to provide a control strategy that represents the rider's control actions well. Both approaches aim to minimise a cost function that includes the road path, and therefore both aim to provide the best, or optimal, control input to achieve this. While both approaches can therefore be considered as some form of 'optimal' control, the distinction is made between the mathematical approaches of optimal control and model predictive control, as given in Chapters 5 and 6.

While both approaches appear capable of generating appropriate control inputs to follow a target path, in specific cases, notably the case of restricted visual preview, the results that have been shown here demonstrate that the predictive control approach has clear advantages. Mathematically, the characteristic that a steady state error for the optimal controller is in fact always present has been shown. However, provided that sufficient preview is allowed such that the preview gains reach close to zero, this error becomes insignificant. Previous work [90] indicated the requirements for zero steady state errors by allowing sufficient preview, the analysis has been extended to show how those steady state errors arise, and how they can be overcome with a local coordinates controller definition.

A local coordinates approach was presented which was shown to be theoretically capable of correcting the steady state path following errors of a short preview horizon optimal controller. Similar findings had been made by Cole et al. [11]. Although the overall controller's strategies were comparable, the methods differed mathematically. In the method presented here, the road preview element of the state vector contains the road information explicitly in the rider's local preview, while the method of Cole et al. retains a global definition and essentially converts the preview to local coordinates implicitly.

Model predictive control also offers other advantages that have yet to be explored. One of the motivations for the use of model predictive control regarded the relative ease with which hard constraints can be included into the model. The reference texts provide greater detail on the possibilities available and the processes required [9, 52]. The modelling work revealed that, without constraints, the theory produces mathematical answers which may not represent physically achievable values, with the steer torques generated for the high speed running cases being a good example of such a case. In addition to limits on the steer torques, these hard constraints could be used to account for physical restrictions such as road boundaries, steer angle limits and acceleration and braking constraints if the modelling were extended to include forward speed control.

The controller gains for the optimal and predictive control approaches were seen to be close to identical when long preview horizons were permitted, but became significantly different as the horizon was reduced. The gains for the predictive controller were seen to change as the preview horizon was reduced, allowing the motorcycle to still follow the path correctly. This suggests that a motorcycle rider must modify his perception of the available road information in such limited preview conditions.

While the results presented here have included extensive parametric studies, they remain only theoretical. The rider's control strategy with regard to the use of road preview has been compared with experimental studies for twin-track vehicle driving [25, 47], and the experimental results for rider input control [74, 104]. Experimental evaluation of a motorcycle rider's use of road preview would provide a useful addition to enable validation of the results presented here, and to broaden the knowledge in the wider field of motorcycle rider control.

More specifically, the theoretical results that have been presented in this thesis have suggested that a non-linear prediction model is capable of superior path tracking abilities, and certainly strictly the more correct form of prediction. However, the ability of the rider to account for these non-linearities in the motorcycle's response is another unanswered question. It may be that a highly skilled and experienced rider is able to account for the non-linearities of the motorcycle's response in his output prediction, and can therefore optimise the performance of the motorcycle to a greater extent than a less skilled rider. This may somehow reflect the differences between, say, professional motorcycle racers and a more average rider. While this is only a

conjecture, it would be an interesting, although challenging, task to quantify more firmly to what extent a rider may be able to predict the non-linear behaviour of the motorcycle.

Overall, the applicability of model predictive control has been demonstrated using a somewhat simplified problem. The model was considered to run at a constant forward speed, and the motorcycle model itself was a relatively simple model. The initial implementation of a non-linear tyre model was hoped to provide the ability to model more complicated manoeuvre strategies to further investigate the characteristics and advantages of using predictive control for motorcycle rider modelling. It is hoped that the results found here will provide encouragement to develop more elaborate rider control models employing these techniques, ultimately leading to both a broader understanding of the rider's control strategies and also potentially as an advantageous tool for motorcycle design and analysis.

Bibliography

[1] Antos P. & Ambrósio J. A. C., A control strategy for vehicle trajectory tracking using multibody models, Multibody System Dynamics, 11(4), 2004, pp. 365 – 394.

[2] Aoki A., Experimental study on motorcycle steering performance, SAE Paper No. 790265, 1979.

[3] AutoSim, www.carsim.com. Accessed 23rd July 2007.

[4] Bertolazzi E., Biral F. & Lio M., Symbolic-numeric indirect method for solving optimal control problems for large multibody systems: The time-optimal racing vehicle example, Multibody System Dynamics, 13(2), 2005, pp. 233 – 252.

[5] BikeSim, www.carsim.com. Accessed 23rd July 2007.

[6] Biral F. & Da Lio M., Modelling drivers with the optimal manoeuvre method, 7th International Conference & Exhibition, Florence ATA (Associazione Tecnica dell'Automobile), Italy, 23 – 25 May 2001.

[7] Bortoluzzi D., Doria A., Lot R. & Fabbri L. Experimental investigation and simulation of motorcycle turning performance, 3rd International Motorcycle Conference, Munchen, Germany, 11 – 12 September 2000.

[8] Bower G. S., Steering and stability of single-track vehicles, The Automobile Engineer, 5, 1915, pp. 280 – 283.

[9] Camacho E. F. & Bordons C., Model predictive control, Springer, London, Great Britain, 2000. ISBN 3540762418.

[10] CarSim, www.carsim.com. Accessed 2rd July 2007.

[11] Cole D. J., Pick A. J. & Odhams A. M. C., Predictive and linear quadratic methods for potential application to modelling driver steering control, Vehicle System Dynamics, 44(3), 2006, pp. 259 – 284.

[12] Cooper K. R., The effect of aerodynamics on the performance and stability of high speed motorcycles, Proceedings of the Second AIAA Symposium on Aerodynamics of Sports and Competition Automobiles, Los Angeles, California, U.S.A., 11 May 1974, pp. 165 – 184.

[13] Cossalter V., Motorcycle Dynamics, Race Dynamics, Greendale, Wisconsin, U.S.A., 2002. ISBN 978-0972051408.

[14] Cossalter V., Da Lio M., Biral F. & Fabbri L., Evaluation of motorcycle maneuvrability with the optimal manoeuvre method, SAE Meeting; Motorsports Engineering Conference & Exposition, Dearborn, Michigan, U.S.A., 16 – 19 November 1998, SAE Paper No. 983022.

[15] Cossalter V., Da Lio M., Lot R. & Fabbri L., A general method for the evaluation of vehicle manoeuvrability with special emphasis on motorcycles, Vehicle System Dynamics, 31, 1999, pp. 113 – 135.

[16] Cossalter V., Doria A. & Lot R., Steady turning of two wheel vehicles, Vehicle System Dynamics, 31, 1999, pp. 157 – 181.

[17] Cossalter V., Lot R. & Maggio F., The influence of tire properties on the stability of a motorcycle in straight running and in curve, SAE Automotive Dynamics & Stability Conference (ADSC), Detroit, Michigan, U.S.A., 7 – 9 May 2002, SAE Paper No. 2002-001-014.

[18] Cossalter V. & Lot R., A motorcycle multi-body model for real time simulations based on the natural coordinates approach, Vehicle System Dynamics, 37, 2002, pp. 423 – 447.

[19] Cossalter V., Doria A., Lot R., Ruffo N. & Salvador M., Dynamic properties of motorcycle and scooter tyres: measurement and comparison, Vehicle System Dynamics, 39(5), 2003, pp. 329 – 352.

[20] Cossalter V., Lot R. & Maggio F., The modal analysis of a motorcycle in straight running and on a curve, Meccanica, 39, 2004, pp. 1–16.

[21] Cossalter V., Doria A., Basso R. & Fabris D., Experimental analysis of out-of-plane structural vibrations of two-wheeled vehicles, Shock and Vibration, 11, 2004, pp. 433 – 443.

[22] Department for Environment, Food and Rural Affairs, Passenger transport emissions factors, June 2007, www.defra.gov.uk. Accessed 15th July 2007.

[23] Department for Transport, Second Review of the Government's Road Safety Strategy, February 2007, www.dft.gov.uk. Accessed 15th July 2007.

[24] Dohring E., Stability of single-tracked vehicles, Forschung im Ingenieurwesen, 21(2), 1955, pp. 50 – 62 (Translation to English by J. Lotsof, Cornell Aeronautical Laboratory Inc., New York, U.S.A., March 1957).

[25] Donges E., A two-level model of driver steering behaviour, Human Factors, 29, 1978, pp. 691 – 707.

[26] Dressel A., Website of Andrew Dressel, http://audiophile.tam.cornell.edu/~ad29. Accessed 23rd July 2007.

[27] European Union Road Federation, 2007 Road Statistics, June 2007, www.erf.be. Accessed 15th July 2007.

[28] Evangelou S., The control and stability analysis of two-wheeled vehicles, PhD Thesis, Dept. Electrical and Electronic Engineering, Imperial College London, 2004.

[29] Fajans J., Steering in bicycles and motorcycles, American Journal of Physics, 68(7), 2000, pp. 654 – 659.

[30] Federation of European Motorcyclists Association, European agenda for motorcycle safety, February 2004, www.fema.ridersrights.org. Accessed 15th July 2007.

[31] Foale T., Motorcycle handling and chassis design, Tony Foale Designs, Spain, 2002. ISBN 84-933286-1-8.

[32] Genta G., Motor vehicle dynamics – modelling and simulation, World Scientific, Singapore, 1997. ISBN 9 810 22911 9.

[33] Guo K. & Guan H., Modelling of driver/vehicle directional control system, Vehicle System Dynamics, 22, 1993, pp. 141 – 184.

[34] Honda Motorcycles, www.honda.co.uk/motorcycles. Accessed 23rd May 2007.

[35] Huang S., Tan K. K. & Lee T. H., Applied predictive control, Springer, London, United Kingdom, 2002. ISBN 1852333383.

[36] Hucho W., Aerodynamics of road vehicles, Annual Review of Fluid Mechanics, 25, 1993, pp. 485 – 537.

[37] Huyge K., Ambrósio J. & Pereira M., A control strategy for the dynamics of a motorcycle, including rider, ENOC 2005, Eindhoven, Netherlands, 7 – 12 August, 2005, CD-ROM.Pa

[38] Jacobs O. L. R., Introduction to Control Theory (2nd Edition), Oxford Science, Oxford, United Kingdom, 1996. ISBN 0-19-856249-7.

[39] James S.R., Lateral dynamics of an off-road motorcycle by system identification, Vehicle System Dynamics, 38(1), 2002, pp. 1 – 22.

[40] Jennings G., A study of motorcycle suspension damping characteristics, SAE Paper No. 740628, 1974.

[41] Kamata Y. & Nishimura H., System identification and attitude control of motorcycle by computer-aided dynamics analysis, JSAE Review 24, 2003, pp. 411 – 416.

[42] Kane T. R., The effect of frame flexibility on high speed weave of motorcycles, SAE Paper No. 780306, 1978.

[43] Katayama T., Aoki A. & Nishimi T., Control behaviour of motorcycle riders, Vehicle System Dynamics, 17(4), 1988, pp. 211 – 229.

[44] Katayama T., Nishimi T., Okayama T. & Aoki A., A simulation model for motorcycle rider's control behavior, SAE Paper No. 972126, 1997.

[45] Koenen C., The dynamic behaviour of a motorcycle when running straight ahead and when cornering, PhD Thesis, Delft University of Technology, 1983.

[46] Kwakernaak H. & Sivan R., Linear Optimal Control Systems, John Wiley & Sons, New York, U.S.A., 1972. ISBN 978-0471511106.

[47] Land M. & Horwood J., Which parts of the road guide steering?, Nature, 377, 1995, pp. 339 – 340.

[48] Limebeer D. J. N., Sharp R. S. & Evangelou S., The stability of motorcycles under acceleration and braking, Proceedings of the IMechE, Part C, Journal of Mechanical Engineering Science, 215 (9), 2001, pp. 1095 – 1109.

[49] Lot R. & Da Lio M., A symbolic approach for the automatic generation of the equations of motion of multibody systems, Multibody System Dynamics, 12, 2004, pp. 147 – 172.

[50] MacAdam C. C., An optimal preview control for linear systems, Journal of Dynamic Systems Measurement and Control, 102(3), 1980, pp. 188–190.

[51] MacAdam C. C., Understanding and modelling the human driver, Vehicle System Dynamics, 40(1–3), 2003, pp. 101 – 134.

[52] Maciejowski J. M., Predictive control: with constraints, Prentice–Hall, London, 2002. ISBN 978-0201398236.

[53] Maple 9.5, Maplesoft, 2004. www.maplesoft.com. Accessed 23rd July 2007.

[54] MATLAB 7.0 (R14), MathWorks, 2004. www.mathworks.com. Accessed 23rd July 2007.

[55] Motor Cycle Industry Association, The motorcycle industry manifesto for motorcycling, 2005. www.mcia.co.uk. Accessed 15th July 2007.

[56] Meijaard J. P. & Popov A. A., Stability of braked vehicles with application to motorcycles, Braking 2004: Vehicle braking and chassis control, Leeds, United Kingdom, 7–9 July 2004, pp. 15 – 24.

[57] Meijaard J. P. & Popov A. A., Application of non-linear dynamics to instability phenomena in motorcycles, Vehicle System Dynamics, S41, 2004, pp. 567–576.

[58] Meijaard J. P. & Popov A. A., Tyre modelling for motorcycle dynamics, Vehicle System Dynamics, S43, 2005, pp. 187 – 198.

[59] Meijaard J. P. & Popov A. A., Practical stability analysis of multibody systems with application to the braking of a motorcycle, ENOC 2005, Eindhoven, Netherlands, 7–12 August 2005, pp. 541–548.

[60] Meijaard J. P. & Popov A. A., Numerical continuation of solutions and bifurcation analysis in multibody systems applied to motorcycle dynamics, Nonlinear Dynamics, 43(1), 2006, pp. 97 – 116.

[61] Meijaard J. P. & Popov A. A., Multi-body modelling and analysis into the non-linear behaviour of motorcycles, Proceedings of the IMechE, Part K, Journal of Multi-Body Dynamics, 221, 2007, pp. 63–76.

[62] Meijaard J. P., Papadopoulos J. M., Ruina A. & Schwab A. L., Linearized dynamics equations for the balance and steer of a bicycle: a benchmark and review, Proceedings of the Royal Society, A, 463, 2007, pp. 1955–1982.

[63] MD Solutions, MSC Software, www.mscsoftware.com. Accessed 23rd July 2007.

[64] Moon F. C., Applied Dynamics, John Wiley & Sons, New York, U.S.A., 1998. ISBN 0 471 13828 2.

[65] Miyamaru Y., Yamasaki G. & Aoki K., Development of a motorcycle riding simulator, JSAE Review 23, 2002, pp. 121 – 126.

[66] Nishimi T., Aoki T. & Katayama T., Analysis of straight running stability of motorcycles, 10th International Conference on Experimental Safety Vehicles, Oxford, United Kingdom, 1–4 July, 1985, pp. 1080 – 1094.

[67] Otto W. M., Effect of motorcycle accessories on stability, Proceedings of International Motorcycle Safety Conference, Washington DC, U.S.A., May 1980, pp. 1560–1581.

[68] Pacejka H. B., Tyre and Vehicle Dynamics (2nd Edition), Butterworth-Heinemann, Oxford, United Kingdom, 2002. ISBN 978-0750669184.

[69] Olsen J. & Papadopoulos J., Bicycle dynamics - The meaning behind the maths, Bike Tech, 7(6), December 1988, pp. 13–15.

[70] Prem H. & Good M. C., A rider–lean steering mechanism for motorcycle control, Proceedings of the 8th IAVSD Symposium on the Dynamics of Vehicles on Roads and on Tracks, Massachusetts Institute of Technology, U.S.A., 15–19 August 1983, pp. 422–435.

[71] Prokop G. & Sharp R. S., Performance enhancement of limited–bandwidth active automotive suspensions by road preview, IEE Proceedings, 142(2), 1995, pp. 140 – 148.

[72] Prokop G., Modeling human vehicle driving by model predictive online optimization, Vehicle System Dynamics, 35(1), 2001, pp. 19 – 53.

[73] di Puccio F., Forte P., Guiggiani M. & Rotti D., Modelling and simulation of driver's control on 4–wheeled vehicle dynamics, Proceedings of 4th International Conference on Control and Diagnostics in Automotive Applications, Sestri Levante, Switzerland, 2003, pp. 1 – 10.

[74] Rice R. S., Rider skill influence on motorcycle maneuvering, SAE Paper No. 780312, 1978.

[75] Roe G. E., Pickering W. M. & Zinober A., The oscillations of a flexible castor, and the effect of front fork flexibility on the stability of motorcycles, SAE Paper No. 780307, 1978.

[76] Rowell S., Popov A. A. & Meijaard J. P., Modelling the control tasks for riding a motorcycle, 19th Symposium of the International Association for Vehicle System Dynamics (IAVSD), Milan, Italy, 29 August - 2 September 2005, Poster Paper (CD-ROM), ISBN 88-901916-2-7.

[77] Rowell S., Popov A. A. & Meijaard J. P., Modelling the control strategies for riding a motorcycle, ISMA2006, Leuven, Belgium, 18–20 September 2006, CD-ROM.

[78] Schwab A. L., Website of A. L. Schwab, http://audiophile.tam.cornell.edu/~als93. Accessed 23rd July 2007.

[79] Seffen K., Parks G. & Clarkson P., Observations on the controllability of motion of two-wheelers, Proceedings of the IMechE, Part I, Journal of Systems & Control Engineering, 215(2), 10 April 2001, pp. 143 – 156.

[80] Sharp R. S., The stability and control of motorcycles, Journal of Mechanical Engineering Science, 13(5), 1971, pp. 316 – 329.

[81] Sharp R. S., The influence of frame flexibility on the lateral stability of motorcycles, Journal of Mechanical Engineering Science, 16(2), 1974, pp. 117 – 120.

[82] Sharp R. S., The influence of the suspension system on motorcycle weave mode oscillations, Vehicle System Dynamics, 5, 1976, pp. 147 – 154.

[83] Sharp R. S., A review of motorcycle steering behaviour and straight line stability characteristics, SAE Paper No. 780303, 1978.

[84] Sharp R. S., The lateral dynamics of motorcycles and bicycles, Vehicle System Dynamics, 14, 1985, pp. 265 – 283.

[85] Sharp R. S., Vibrational modes of motorcycles and their design parameter sensitivities, Vehicle NVH and Refinement, Mechanical Engineering Publications Limited, London, United Kingdom, 1994, pp. 107–121.

[86] Sharp R. S., Casanova D. & Symonds P., A mathematical model for driver steering control, with design, tuning and performance results, Vehicle System Dynamics, 33, 2000, pp. 289 – 326.

[87] Sharp R. S., Some contemporary problems in road vehicle dynamics, Proceedings of the Institute of Mechanical Engineers, Part C, 214, 2000, pp. 137 – 148.

[88] Sharp R. S., Stability, control and steering responses of motorcycles, Vehicle System Dynamics, 35(4), 2001, pp. 291 – 318.

[89] Sharp R. S. & Limebeer D. J. N., A motorcycle model for stability and control analysis, Multibody System Dynamics, 6, 2001, pp. 123 – 142.

[90] Sharp R. S. & Valtetsiotis V., Optimal preview car steering control, Vehicle System Dynamics Supplement, 35, 2001, pp. 101 – 117.

[91] Sharp R. S. & Bettella M., Tyre shear force and moment descriptions by normalisation of parameters and the "Magic Formula", Vehicle System Dynamics, 39(1), 2003, pp. 27 – 56.

[92] Sharp R. S., Evangelou S. & Limebeer D. J. N., Advances in the modelling of motorcycle dynamics, Multibody System Dynamics, 12, 2004, pp. 251 – 283.

[93] Sharp R. S. & Limebeer D. J. N., On steering wobble oscillations of motorcycles, Proceedings of the IMechE, Part C, Journal of Mechanical Engineering Science, 218(12), 2004, pp. 1449 – 1456.

[94] Sharp R. S., Optimal linear time-invariant preview steering control for motorcycles, Vehicle System Dynamics, S44, 2006, pp. 329 – 340.

[95] Strejc V., State space theory of discrete linear control, John Wiley & Sons, New York, U.S.A., 1981. ISBN 0 471 27594 8.

[96] Styles M. J., Predictive engineering processes for motorcycle dynamics, EngD Thesis, School of Mechanical Engineering, Cranfield University, 2004.

[97] Tezuka Y., Ishii H. & Kiyota S., Application of the magic formula tire model to motorcycle maneuvrability analysis, JSAE Review, 22, 2001, pp. 305–310.

[98] Valtetsiotis V., A discrete-time optimal preview control driver model, Master's Thesis, School of Mechanical Engineering, Cranfield University, 1999.

[99] Virtual.Lab, LMS, http://www.lmsintl.com. Accessed 23rd July 2007.

[100] de Vries E. J. H. & Pacejka H. B., The effect of tire modeling on the stability analysis of a motorcycle, Proceedings of 4th international symposium on advanced vehicle control, Nagoya, Japan, 14 – 18 September, 1998.

[101] Vu H. V. & Esfandiari R. S., Dynamic Systems – Modeling and Analysis, McGraw–Hill, New York, U.S.A., 1997. ISBN 0-07-021673-8.

[102] Weir D. H., Motorcycle handling dynamics and rider control and the effect of design configuration on response and performance, PhD Thesis, University of California, Los Angeles, U.S.A., 1972.

[103] Weir D. H. & Zellner J. W., Lateral–directional motorcycle dynamics and rider control, SAE Congress and Exposition, Michigan, U.S.A., 27 February – 3 March, 1978. SAE No. 780304.

[104] Weir D. H. & Zellner J. W., Development of handling test procedures for motorcycles, SAE No. 780313, 1978.

[105] Weir D. H. & Zellner J. W., Experimental investigation of the transient behavior of motorcycles, SAE Paper No. 790266, 1979,

[106] Whipple F. J. W., The stability of the motion of a bicycle, Journal of Pure and Applied Mathematics, 30, 1899, pp. 312–348.

[107] Wolfram Research, http://www.wolfram.com. Accessed 23rd July 2007.

[108] Yokomori M., Oya T. & Katayama A., Rider control behavior to maintain stable upright position at low speed, JSAE Review, 21(1), 2000, pp. 61 – 65.

List of Publications

- Rowell S., Popov A. A., Meijaard J. P., Modelling the control tasks for riding a motorcycle, 19th Symposium of the International Association for Vehicle System Dynamics (IAVSD), Milan, Italy, 29 August - 2 September 2005, Poster Paper (CD-ROM), ISBN 88-901916-2-7.

- Rowell S., Popov A. A., Meijaard J. P., Modelling the control strategies for riding a motorcycle, ISMA2006 Conference, Leuven, Belgium, 18 - 20 September 2006.

- Rowell S., Popov A. A., Meijaard J. P., Application of predictive control strategies to the motorcycle riding task, 20th Symposium of the International Association for Vehicle System Dynamics (IAVSD), Berkeley, California, U.S.A., 13 - 17 August 2007.

- Rowell S., Popov A. A., Meijaard J. P., Modelling the control tasks for riding a motorcycle, 5th IFAC symposium on advances in automotive control, Monterey, California, U.S.A., 20 - 22 August 2007.

Appendix A

Motorcycle Data

This Appendix section details the specific values for all necessary parameters of the motorcycle used to generate the results in this thesis. The motorcycle model is based on the simplified motorcycle model first presented by Sharp in [A1]. Additional parameter values, specifically for the more advanced tyre model introduced, were drawn from work by Meijaard and Popov [A2].

A.1 Motorcycle Data

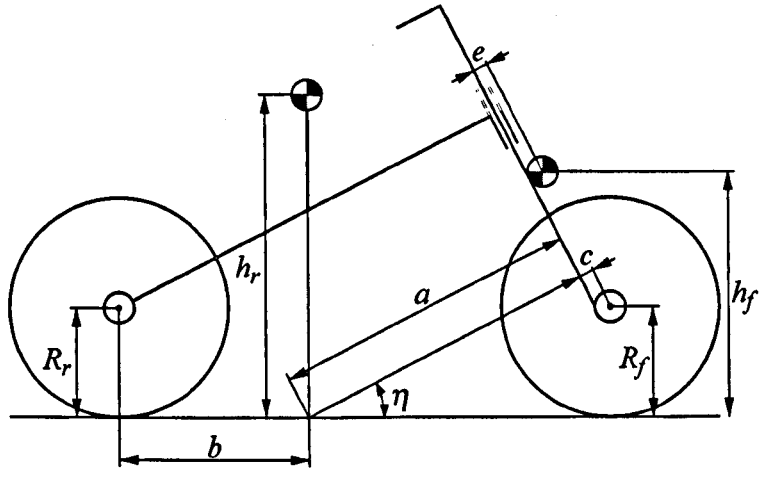

Figure A.1: Definitions of bicycle model dimensions

A.2 Geometric Details

$a = 0.9347$ m	$e = 0.0244$ m	$\eta = 0.4714$ rad
$b = 0.4798$ m	$h_r = 0.6157$ m	
$c = 0.0226$ m	$h_f = 0.4561$ m	

A.3 Inertial Properties

$I_{f,x} = 1.2338$ m^4	$I_{r,z} = 21.0694$ m^4	$I_{rw,y} = 1.0508$ m^4
$I_{f,y} = 0$ m^4	$I_{r,xz} = -1.7354$ m^4	$I_{rw,z} = 0$ m^4
$I_{f,z} = 0.4420$ m^4	$I_{fw,x} = 0.7$ m^4	$m_1 = 30.6472$ kg
$I_{f,xz} = 0$ m^4	$I_{fw,y} = 0.7186$ m^4	$m_2 = 217.492$ kg
$I_{r,x} = 31.1838$ m^4	$I_{fw,z} = 0$ m^4	
$I_{r,y} = 0$ m^4	$I_{rw,x} = 0$ m^4	

A.4 Tyre Properties

Simple tyre model:

$C_{\alpha,f} = 11174.38$ N/rad	$C_{\gamma,r} = 1326.6232$ N/rad	$R_r = 0.3048$ m
$C_{\gamma,f} = 938.6124$ N/rad	$r_t = 0$ m	$\sigma_f = 0.24$ m
$C_{\alpha,r} = 15831.8556$ N/rad	$R_f = 0.3048$ m	$\sigma_r = 0.24384$ m

Advanced tyre model:

$c_{r,f} = 0.2448$ m	$K_{n,r} = 142627$ N/m	$\sigma_f = 0.24$ m
$c_{r,r} = 0.2448$ m	$\mu_f = 1.0$	$\sigma_r = 0.24384$ m
$C_{l,f} = 11.096$	$\mu_r = 1.0$	$Ro_f = 0.3048$ m
$C_{l,r} = 11.096$	$\rho_f = 0.07$ m	$Ro_r = 0.3048$ m
$K_{n,f} = 100672.0\ 7$ N/m	$\rho_r = 0.07$ m	$r_t = 0$ m

References

[A1] Sharp R. S., The stability and control of motorcycles, Journal of Mechanical Engineering Science, 13(5), 1971, pp. 316 – 329.

[A2] Meijaard J. P. & Popov A. A., Numerical continuation of solutions and bifurcation analysis in multibody systems applied to motorcycle dynamics, Nonlinear Dynamics, 43(1), 2006, pp. 97 – 116.

Appendix B

VRML Simulation Model

B.1 Introduction

As an aid to the simulation work, and to obtain a clearer understanding of how the motorcycle was behaving during the simulated manoeuvre, a Virtual Reality Modelling Language (VRML) animation was generated, with the aim to produce a simple representation of the motorcycle such that the system output could be conveyed easily. VRML is a low-level code that allows simple shapes and forms to be drawn in three dimensions and, with suitable input data, freedoms and constraints placed upon the objects, motion to be simulated.

The intention of this Appendix is not to form a detailed guide for the programming of an animation using VRML; suitable texts on the subject can readily be found [B1]. The aim here is to provide a brief outline of the animation model generated to aid the understanding of the motorcycle and controller performance during this research work.

B.2 Coding

The code to draw and animate the motorcycle was written as a Matlab m-file, using a conversion program to convert the Matlab code to VRML code. This program was obtained from Schwab [B2].

B.2.1 Motorcycle Body

The preliminary task was to draw a simple motorcycle model in VRML. This did not require a intricately detailed model; in fact, the simpler the model the easier the behaviour would be to analyse. The model was therefore intended only as a representation of the simplified motorcycle model that was used to determine the motorcycle's dynamic response. This VRML model is shown in Figure B.1.

The VRML code allows simple three-dimensional objects to be drawn with relative ease. The frame was drawn as a series of cylinders, for which the two end points, the cylinder diameter and colour are defined. The rider's frame was drawn via a similar approach, with a simple sphere to represent the rider's head, defined by position, diameter and colour. Spheres were also used at the ends of the frame cylinders to provide a more aesthetically pleasing appearance. Specifically, spheres and cylinders are defined by entries of the following nature:

```
sphere(B,Dia,FrameColour)
cylinder(B,E,Dia,FrameColour)
```
(A-1)

where, here, `B` represents the centre of the sphere and is a 3×1 vector giving x-, y- and z-coordinates of the position, `Dia` is the diameter of the sphere and `FrameColour` is again a 3×1 vector giving the RGB ratios of the colour required. Additionally for the cylinder, a second x-y-z 3×1 vector `E` is defined; the two position vectors then define the centres of the ends of the cylinder.

The wheels were drawn as two-dimensional circles, extruded through a 360^o sweep about the centre of the tyre cross-section to obtain the toroidal shape of the front and rear wheels.

```
Shape {
  geometry Extrusion {
    crossSection [define cross – section shape ]
    spine [define extrusion spine ]
  }
}
```
(A-2)

The objects in the motorcycle model were constructed in a parent-child tree structure, such that, for instance, the front frame is a child of the rear frame, since any motion of the rear frame will influence the front frame, but a steer rotation of the front frame will not influence directly the rear frame.

A series of frames were defined, in which objects can be drawn. Any movement of these defined frames will move any objects drawn within and therefore attached to these frames. The structure of the frames was defined in such a way as to reflect the hierarchy of movement as defined by the coordinate system used. Thus, the first frame drawn was the global reference frame, in which the motorcycle frame was drawn, in which was drawn the yaw frame, then the roll frame, then the steer frame (Chapter 3).

Thus, the MOTORCYCLE frame is defined, which has the YAWFRAME as a child, which subsequently has the ROLLFRAME as a child, and so on:

```
DEF MOTORCYCLE Transform {
 children [
  DEF YAWFRAME Transform {
   children [                                    (A-3)
    ...
                ]}
              ]}
```

Thus, the order was: MOTORCYCLE → YAWFRAME → ROLLFRAME → STEERFRAME.

The rear frame and the rider were drawn in the ROLLFRAME and the front frame structure drawn in the STEERFRAME.

B.2.2 Animation

The results from the Matlab lane change simulations were exported to the VRML code, defining individually the lateral positions of the motorcycle frame, and the rotations of the yaw, roll and steer angles.

Each rotation was defined as a four-column vector, where each row entry corresponds

to one step of the iterative motorcycle simulation. The first three columns define the x-, y- and z-coordinates of the end of a vector from the origin. This vector forms the axis about which the rotation will occur. The fourth column defines the angle of the rotation. Thus, a rotation of 0.1 rad about the x-axis (roll) would be defined by [1 0 0 0.1], for example.

To fully simulate the motion, the individual frames defined when drawing the motorcycle (YAWFRAME, ROLLFRAME, STEERFRAME) are rotated by using the appropriate four-column rotation matrices. As the structure of the motorcycle is drawn in the ROLLFRAME and STEERFRAME, then as these frames are rotated the objects drawn within them also rotate, and hence the animation of the motion is obtained.

Further options exist for defining, for example, the cycle time of the simulation and the positions and orientations of camera angles. For the reader wishing to gain further insight into the possibilities offered by Virtual Reality Modelling Language, many suitable texts can be found than will provide a more detailed and specific introduction to the topic [B1].

Figures

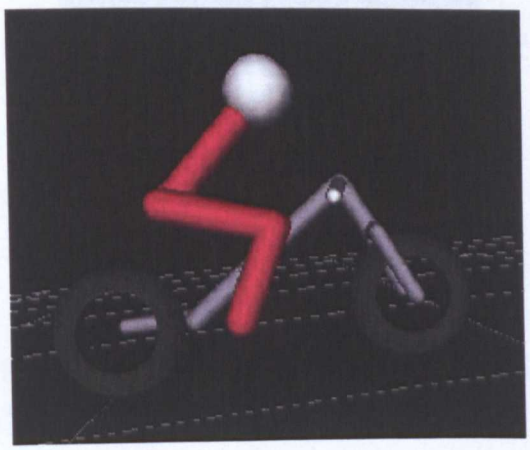

Figure B.1: VRML Motorcycle Model

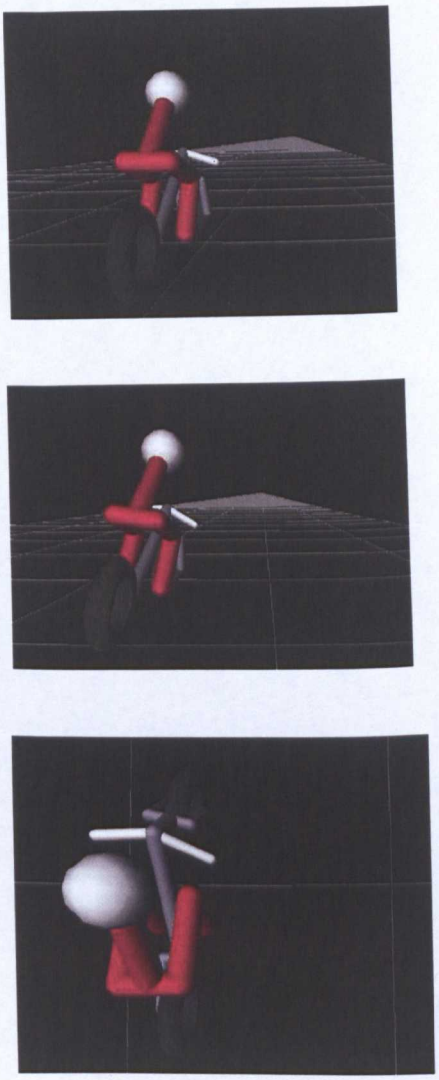

Figure B.2: VRML Animation snapshots

References

[B1] Ames A. L., Nadeau D. R. & Moreland J. L., VRML 2.0 Sourcebook, John Wiley & Sons, New York, U.S.A., 1997. ISBN 0-471-16507-7.

[B2] Schwab A. L., Website of Professor A. L. Schwab, http://audiophile.tam.cornell.edu/~als93/. Accessed 23rd July 2007.